

UNIVERSITY OF CALGARY

The Effects of Cholesterol on the Structure and Function of
Exogenous Pulmonary Surfactant and on Surfactant Inhibition

by

Lasantha Chandrajeewa Gunasekara

A THESIS

SUBMITTED TO THE FACULTY OF GRADUATE STUDIES
IN PARTIAL FULFILLMENT OF THE REQUIREMENTS FOR THE
DEGREE OF DOCTOR OF PHILOSOPHY

DEPARTMENT OF CARDIOVASCULAR /RESPIRATORY SCIENCES

CALGARY, ALBERTA

AUGUST, 2008

© Lasantha Chandrajeewa Gunasekara 2008



Library and
Archives Canada

Bibliothèque et
Archives Canada

Published Heritage
Branch

Direction du
Patrimoine de l'édition

395 Wellington Street
Ottawa ON K1A 0N4
Canada

395, rue Wellington
Ottawa ON K1A 0N4
Canada

Your file *Votre référence*
ISBN: 978-0-494-44353-8
Our file *Notre référence*
ISBN: 978-0-494-44353-8

NOTICE:

The author has granted a non-exclusive license allowing Library and Archives Canada to reproduce, publish, archive, preserve, conserve, communicate to the public by telecommunication or on the Internet, loan, distribute and sell theses worldwide, for commercial or non-commercial purposes, in microform, paper, electronic and/or any other formats.

The author retains copyright ownership and moral rights in this thesis. Neither the thesis nor substantial extracts from it may be printed or otherwise reproduced without the author's permission.

AVIS:

L'auteur a accordé une licence non exclusive permettant à la Bibliothèque et Archives Canada de reproduire, publier, archiver, sauvegarder, conserver, transmettre au public par télécommunication ou par l'Internet, prêter, distribuer et vendre des thèses partout dans le monde, à des fins commerciales ou autres, sur support microforme, papier, électronique et/ou autres formats.

L'auteur conserve la propriété du droit d'auteur et des droits moraux qui protègent cette thèse. Ni la thèse ni des extraits substantiels de celle-ci ne doivent être imprimés ou autrement reproduits sans son autorisation.

In compliance with the Canadian Privacy Act some supporting forms may have been removed from this thesis.

Conformément à la loi canadienne sur la protection de la vie privée, quelques formulaires secondaires ont été enlevés de cette thèse.

While these forms may be included in the document page count, their removal does not represent any loss of content from the thesis.

Bien que ces formulaires aient inclus dans la pagination, il n'y aura aucun contenu manquant.


Canada

Abstract

Pulmonary surfactant, a mixture of phospholipids, neutral lipids and proteins, controls the surface tension of the lung alveoli. Cholesterol is present in the natural surfactant as the major neutral lipid. To date, the physiological role of cholesterol in lung surfactant is uncertain.

The purpose of this study was to investigate the effect of cholesterol on the surface properties of the lipid extract surfactant. Previous work related to cholesterol and surfactant function showed variable results; in addition, the experimental conditions were mostly far from the physiological conditions. We used Captive Bubble Surfactometer (CBS), the best *in vitro* method currently available to evaluate surface properties of lung surfactant under condition close to those of healthy and diseased lungs. In order to investigate the structure of surface film we applied the most advanced methods available, including atomic force microscopy (AFM) and Kelvin probe microscopy (KPM).

Adding physiological amount of (5%, 10%) cholesterol to the bovine lipid extract surfactant (BLES) preparations, we discovered quick initial adsorption and very low surface tension during quasi-static and dynamic compressions of the surface film. However, when the cholesterol content was increased up to 20%, surfactant function was completely abolished. We propose this cholesterol mediated surfactant inhibition plays an important role during acute respiratory distress syndrome (ARDS). According to the AFM and KPM results, excess cholesterol clearly disrupts the normal surface film architecture and bilayer stack formation during film compression.

Methyl beta cyclodextrin (M β CD) has been known to act as a cholesterol-sequestering agent for decades. We were able to restore cholesterol-mediated surfactant dysfunction with M β CD very effectively, in a time-dependent manner. Hence, M β CD could be part of a potential treatment for cholesterol mediated surfactant dysfunction.

Finally we investigate plasma protein mediated surfactant inhibition *in vitro* using the CBS, with a new approach that better simulate physiological conditions in the lungs. We found that plasma protein mediated surfactant inhibition is transient and this inhibition disappears during continuous cycling. Furthermore, under the condition tested, our results indicate plasma protein mediated surfactant inhibition does not occur due to competitive adsorption at the interface as some studies observed previously.

Acknowledgements

There are many people to whom I owe my gratitude, love and appreciation. Without their encouragement and help, this work would never have been completed. I would like to dedicate my thesis to my former committee member Prof. Samuel Schurch, who is presently ill. He taught me how to work hard, and also enjoy my time in the laboratory. He had many innovative ideas, encouraged me to carefully try them, and made enquiries about our progress—until we had something interesting.

Special thanks to my supervisor, Dr. Matthias Amrein, who accepted me into his laboratory, and encouraged me to think rationally, and critically. He was always available to work with me when I needed help. He has been the best role model for me by his own hard work, and passion working in the laboratory. He imparted to me my knowledge of pulmonary surfactant, and provided me with many stimulating research ideas. In addition, he is a very supportive friend, generous, and superb person.

Also, my sincere thanks to my committee members Dr. Frances Green, S. Hasan and my external examiner Dr. R. Veldhuizen.

I also owe much appreciation to Dr. Michael Schoel. He kept me busy in the laboratory and taught me all about bubbles—captive bubble apparatus, and much more. He is a very resourceful person with knowledge in many fields. Our philosophical discussions about many things helped improve my life in many ways.

Sincere thanks go to the Canadian Institute of Health Research (CIHR) for funding my research project.

Other close friends—Deanna, Regina and Mia—helped me to edit my thesis and encouraged me all the way. My special friend, Rahini, has helped me from day one coming to Canada. She helped me in numerous ways, and I owe her much as it would have been much harder to come this far.

I would like to thank my parents Jinasoma and Malani Gunasekara.

Finally, my loving wife Sriya and my lovely son Harindu to whom I owe the most. We've had lots of really hard and happy times together. She has tolerated the hard time and helped me from the bottom of her heart. She worked very hard at work as well as at home when I was busy with my studies. She made many sacrifices, and handled many challenges to help me—I cannot say enough, so I say it here, “I love you.”

Table of Contents

Signature page	ii
Abstract	iii
Acknowledgements	v
Table of Contents	vii
List of Tables	x
List of Figures	xi
List of Abbreviations	x
Chapter 1: The Pulmonary Surfactant System	1
1.1 Overview to alveolar epithelial morphology and pulmonary surfactant system ...	1
1.2 Historical development of surfactant research	3
1.3 Overview of the composition of endogenous lung surfactant	5
1.4 Pulmonary surfactant synthesis	6
1.4.1 Intracellular sites of surfactant synthesis and processing	6
1.4.2 Synthesis of surfactant phospholipids and neutral lipids	7
1.4.3 Translocation of surfactant lipids across the LB limiting membrane ...	9
1.5 Secretion of lung surfactant	9
1.6 Recycling of lung surfactant	11
1.7 Lung surfactant subtypes in alveolar hypophase	12
1.7.1 Tubular myelin	13
1.8 The composition, structure, and function of the surfactant film at the air-water interface	14
1.8.1 Phospholipids	15
1.8.2 Surfactant-associated proteins	18
1.8.2.1 SP-A	19
1.8.2.2 SP-D	20
1.8.2.3 SP-B and SP-C	21
1.8.3 Neutral lipids	26
Chapter 2: Methods to Evaluate Surface Activity of Pulmonary Surfactant	30
2.1 Surface activity of lung surfactant	30
2.1.1 Introduction to surface tension	30
2.1.2 Surface properties of lung surfactant	31
2.1.2.1 Adsorption of surfactant	32
2.2 Techniques used to evaluate surface properties of lung surfactant	34
2.2.1 Wilhelmy Surface Balance (LWB)	34
2.2.1.1 Advantages of Langmuir-Wilhelmy balance	37
2.2.1.2 Limitations of Langmuir-Wilhelmy balance	37

2.2.2	Pulsating bubble surfactometer (PBS)	38
2.2.2.1	Advantages of pulsating bubble surfactometer	39
2.2.2.2	Limitations of PBS	40
2.2.3	Captive bubble surfactometer (CBS)	41
2.2.3.1	Surface activity parameters of CBS	44
2.2.3.2	Advantage of CBS	45
2.2.3.3	Limitations of CBS	46
2.2.4	Microbubble stability test	46
2.3	<i>In situ</i> measurement of surface tension	48
2.3.1	Pressure volume relations	48
2.3.2	Measurement of surface tension <i>in situ</i> – microdroplet method	49

Chapter 3: Effect of Cholesterol on Lipid Extract Pulmonary Surfactant- *in vitro* Study

	51
3.1	Background.....	51
3.1.1	General introduction to cholesterol	51
3.1.2	The origin and metabolism of alveolar cholesterol	53
3.1.3	Biophysical properties of cholesterol	55
3.2	Objectives of the study	59
3.3	General hypotheses	60
3.4	Specific hypotheses	60
3.5	Introduction	60
3.6	Materials and methods	63
3.6.1	Materials	63
3.6.2	Surface activity assessment	64
3.7	Results	66
3.7.1	Adsorption (film formation)	66
3.7.2	Quasi-static and dynamic compression and expansion of the pulmonary surfactant films	68
3.8	Discussion	72
3.8.1	Films, containing less than 20% cholesterol	72
3.8.2	Films containing 20% cholesterol	74
3.8.3	How cholesterol interacts with the molecular components of pulmonary surfactant	75
3.8.4	The role of physiological amounts of cholesterol	78
3.9	Conclusion	79

Chapter 4: Effect of Methyl Beta Cyclodextrin (M β CD) on Dysfunctional Surfactant Films due to Cholesterol

	81
4.1	Background	81
4.1.1	Cyclodextrins	81

4.1.2	Structure of cyclodextrins	82
4.1.3	Production of cyclodextrins	83
4.1.4	Cyclodextrin derivatives	84
4.1.5	Inclusion and non-inclusion complexes	84
4.2	Summary of the study	86
4.3	Introduction	87
4.4	Materials and methods.....	89
4.4.1	Representation of CBS results	91
4.5	Results	92
4.5.1	Adsorption/film formation	92
4.5.1.1	Control group 1 (BLES 27 mg/mL)	93
4.5.1.2	Control group 2 (BLES 27 mg/mL + 20mM of M β CD)	93
4.5.1.3	Test group (BLES 27mg/mL + 20% cholesterol) without M β CD in subphase	93
4.5.1.4	Test group (BLES 27 mg/mL + 20% cholesterol) with M β CD in subphase	94
4.5.2	Compression and expansion cycles	95
4.5.2.1	Control group (BLES 27 mg/mL) 1-area-surface tension isotherms	98
4.5.2.2	Control group (BLES 27 mg/mL + 20mM of M β CD) 2-area-surface tension isotherms	101
4.5.2.3	Test group (BLES 27 mg/mL + 20% cholesterol) – Area-surface tension isotherms	102
4.5.2.4	Test group (BLES 27 mg/mL + 20% cholesterol with 20 mM M β CD in subphase) – area-surface tension isotherms	103
4.6	Discussion	104
4.6.1.	Films containing BLES without cholesterol	104
4.6.2	Films containing 20% cholesterol	106
4.7	Conclusion	109

Chapter 5: Effect of Cholesterol on Structure of the Pulmonary Surfactant Film 111

5.1	Summary of the study	111
5.2	Introduction	112
5.3	Materials and methods	114
5.3.1.	Preparation of the surfactants	114
5.3.2	Film deposition.....	115
5.3.3	Microscopy	121
5.3.4	Quantitative image analysis	122

5.4	Results	123
5.4.1	Structure-function relationship of the surfactant films	123
5.4.2	The structure of the bilayer stacks as revealed by Kelvin probe force microscopy	125
5.5	Discussion	129
5.5.1	Sorting	130
5.5.2	Reinforcement	132
5.6	Conclusions	134
Chapter 6: A Comparative Study of Mechanisms of Surfactant Inhibition		135
6.1	Background	135
6.1.1	Surfactant inhibition and ARDS	135
6.1.2	Pathophysiology of ALI and ARDS	136
6.1.3	Cellular molecular mechanisms of injury	136
6.1.3.1	Endothelial injury	136
6.1.3.2	Epithelial injury	137
6.1.3.3	Neutrophil-mediated injury	137
6.1.3.4	Cytokine-mediated inflammation and injury	138
6.1.3.5	Oxidant-mediated injury	139
6.1.4	Mechanisms of surfactant alteration in ARDS	139
6.1.5	Mechanisms of surfactant inhibition	143
6.2	Introduction	143
6.3	Materials and methods	145
6.3.1	Surface activity assessment	145
6.3.2	Surfactant	146
6.3.3	The aqueous phase of the CBS	147
6.3.4	Representation of CBS results	147
6.3.5	Statistical analysis of CBS experiments	148
6.3.6	Electron microscopy	148
6.4	Results	149
6.4.1	Film formation	149
6.4.2	Film expansion and compression	154
6.4.3	Cryo-electron microscopy	158
6.5	Discussion	160
6.6	Conclusion	167
Chapter 7: Final Discussion		169
7.1	Conclusions	177
References		179
Appendix		

List of Tables

Table 4.1	Median Surface Tension Values for Quasi-Static and Dynamic Cycles	99
Table 4.2	Relative Area Change at the Surface Tension 10 mN/m	100
Table 6.1	Results Summary	151

List of Figures

Figure 1.1a	Composition of bovine pulmonary surfactant	27
Figure 1.1b	Composition of bovine pulmonary surfactant	27
Figure 1.2	Transmission electron micrograph from guinea pig lung showing some of the structures related to the surfactant film	28
Figure 1.3	Higher magnification of the alveolar surface film from a guinea pig lung showing that it is multilaminated	29
Figure 2.1	Langmuir-Wilhelmy Balance	36
Figure 2.2	Pulsating Bubble Surfactometer	40
Figure 2.3	Captive Bubble Surfactometer	43
Figure 2.4	Determination of alveolar surface tension <i>in situ</i> - Micro-droplet method ..	50
Figure 3.1	Illustration of the experimental procedure - Initial adsorption, quasi-static cycles and dynamic cycles	67
Figure 3.2	Surface tension-area isotherms for BLES films with different percentage of cholesterol	69
Figure 3.3	Surface tension-area isotherm of BLES containing 20% cholesterol after the addition of DPPC or DOPC	77
Figure 3.4	Surface tension-area isotherm of BLES films after the addition of DPPC or DOPC	78
Figure 4.1	Beta cyclodextrin molecular structure	81
Figure 4.2	γ -CD toroid structure showing spatial arrangement	82
Figure 4.3	Equilibrium binding of a guest molecule with cyclodextrin to form a 1:1 inclusion complex	86
Figure 4.4	Surface tension-area isotherms of BLES (27 mg/mL) control group 1	96
Figure 4.5	Surface tension-area isotherms BLES (27 mg/mL) + M β CD control group 2	96
Figure 4.6	Surface tension- area isotherms for BLES (27 mg/mL) + 20% cholesterol film	97

Figure 4.7	Surface tension-area isotherms for BLES (27 mg/mL) + 20% cholesterol with M β CD	98
Figure 5.1	Surface tension-area isotherm of BLES upon sample collection	116
Figure 5.2	AFM micrographs showing number of bilayers	117
Figure 5.3	AFM micrograph in three-dimensional representation of surfactant containing 5% w/w cholesterol	117
Figure 5.4	AFM topographies (20 μ m x 20 μ m) of BLES containing no cholesterol (A), 5% w/w cholesterol (B), and 20% w/w cholesterol (C)	118
Figure 5.5	(A) Overview of a film of BLES that contains no cholesterol, (B) BLES film at higher magnification	119
Figure 5.6	(A) Overview of a film of BLES that contains 20% cholesterol by weight protrusions in the topographical image (left) the potential map (right). (B) A high-resolution map of the topography (left) and potential (right) of the film containing 20% cholesterol	120
Figure 5.7	Mechanism explaining a positive surface potential on the large bilayer stacks	131
Figure 6.1	Adsorption of surfactant	150
Figure 6.2	Area-surface tension isotherms of BLES films exposed to plasma proteins	155
Figure 6.3	Area-surface tension isotherms of BLES films exposed to albumin (80 mg/ml)	157
Figure 6.4	Area-surface tension isotherms of BLES films containing 20% w/w cholesterol)	157
Figure 6.5	Cryo-electron micrographs of an aqueous suspension of BLES of 27 mg/ml BLES at 5 mg/ml and BLES at 5 mg/ml plus PEG	159

List of Abbreviations (in order presented)

ARDS	Acute Respiratory Distress Syndrome
RDS	Respiratory Distress Syndrome
ALI	Acute Lung Injury
PL	Phospholipid
PC	Phosphatidylcholine
DPPC	Dipalmitoylphosphatidylcholine
PI	Phosphatidylinositol
PG	Phosphatidylglycerol
SPH	Sphingomyelin
PS	Phosphatidylserine
PE	Phosphatidylethanolamine
SP-A	Surfactant protein A
SP-B	Surfactant protein B
SP-C	Surfactant protein C
SP-D	Surfactant protein D
VLDL	Very low-density lipoprotein
LDL	Low-density lipoprotein
HDL	High-density lipoprotein
LB	Lamellar body
ATP	Adenosine triphosphate
ABC family	ATP-binding cassette family
cAMP	Cyclic adenosine monophosphate
TM	Tubular myelin

PMPC	Palmitoylmyristol phosphatidylcholine
MPPC	Myristoylpalmityl phosphatidylcholine
PPoPC	Palmitoylpalmitoleoyl phosphatidylcholine
POPC	Palmitoyloleoyl phosphatidylcholine
ROS	Reactive oxygen species
ST	Surface tension
G min	Minimum surface tension
G max	Maximum surface tension
BLES	Bovine lipid extract surfactant
Π	Surface pressure
γ	Surface tension
LWB	Langmuir Wilhelmy balance
PBS	Pulsating bubble surfactometer
CBS	Captive bubble surfactometer
Q-stat cycle	Quasi-static cycles
P-V	Pressure-volume
TLC	Total lung capacity
LCAT	Lecithin cholesterol acyltransferase
HMGCoA	3-hydroxy-3-methylglutaryl coenzyme A reductase
Cho/PL	Cholesterol/phospholipid
AAP	4-aminopyrazolo(3,4d)-pyrimidine
T_m	Phase transition temperature
DOPC	Dioleoyl phosphatidylcholine
CGTase	Cyclodextrin glucosyl transferase

CD	Cyclodextrin
M β CD	Methyl beta cyclodextrin
chol-BLES	Cholesterol-bovine lipid extract surfactant
TNF α	Tumour necrosis factor α
IL	Interleukin
TGF	Transforming growth factor
CF	Cystic fibrosis
DSP	Disaturated phospholipid
DSPC	Disaturated phosphatidylcholine
HPLC	High performance liquid chromatography
ESI-MS	Electrospray ionization-mass spectrometry
AFM	Atomic force microscopy
KPFM	Kelvin-Probe force microscopy
sPLA ₂	Secretory phospholipase A ₂
Lyso-PC	Lysophosphatidylcholine
PEG	Polyethylene glycol

Chapter 1: The Pulmonary Surfactant System

1.1 Overview to alveolar epithelial morphology and pulmonary surfactant system

The lung alveolar system has a surface area of about 120 m^2 and is the second largest interface of the body to the environment (216,1). Although there are about 40 different cell types in human lungs, the alveolar epithelium is comprised of only two major types of cells, type I pneumocytes, and type II pneumocytes.

Type I pneumocytes are flattened cells that function as the major structural support cells in the epithelium. They cover about 97% of the alveolar surface area, but account for less than 10% of the distal lung cells (214). A human type I pneumocyte has an average volume of about $1800 \text{ }\mu\text{m}^3$ and covers an area of about $5100 \text{ }\mu\text{m}^2$ (2). These flattened cells are of low thickness ($<0.2 \text{ }\mu\text{m}$), and provide a structural lining with a short diffusion distance for gas exchange between alveolar air and capillary blood (214). Type I cells contain few organelles and are unable to divide. Recently, it was proposed that these cells are cation transporters (3).

Type II pneumocytes are cuboidal in shape and contain microvilli and specialized secretory organelles called lamellar bodies (4). These cells cover around 3% of the alveolar surface and account for up to 10-15% of the distal lung cells (214). Type II pneumocytes are the primary cells of surfactant synthesis, storage, release, and metabolism. They also have the capacity for *de novo* synthesis of all major phospholipids (PL) and the main surfactant associated proteins (5). In addition to surfactant synthesis, type II cells have other important roles. They participate in the lung cytokine/chemokines network by secreting and responding to a number of cytokines, growth factors, and other

varieties of mediators during lung growth, development, inflammation, injury, and repair. These mediators include TNF- α , IL-6,-8,-11, TGF- α and - β (214).

When type I pneumocytes are damaged due to many forms of lung injury, type II pneumocytes can proliferate and differentiate to replace type I cells (220). Such an alteration in type II cells can cause surfactant deficiency (214). Also, type II pneumocytes participate in defence responses by expressing various receptors, such as toll-like receptors (214).

Synthesized surfactant within type II cells is stored in lamellar bodies. Upon an appropriate signal, lamellar body membranes fuse with type II cell membranes and surfactant is exocytosed into the alveolar hypophase (6). Within the alveolar hypophase, the lamellae hydrate and unravel to form unique structures called tubular myelin (Fig 1.2). This process is facilitated by calcium ions and surfactant-associated protein A in the subphase. Tubular myelin is considered the precursor and source of the surface film in the air-liquid interface of the alveoli (214).

The surface film of surfactant in the air-liquid interface of the alveolar surface is responsible for alveolar stability and normal lung function. Lung surfactant reduces the work of breathing and prevents alveolar collapse during the end of the expiration by reducing surface tension at the air-liquid interface in the alveoli. Also, lung surfactant plays a vital role in protection against infection and oxidants (1).

Surfactant components are continuously recycled and cleared, with a long biological half-life of tens of hours in the alveolar lumen (208,209,210). Most of the surfactant components in the hypophase are endocytosed by type II cells and directly

incorporated into the surfactant secretory pathway, whereas the rest are broken down to precursors, which can be reused to synthesize surfactant components.

Studies have shown that a lack of functional surfactant is the main cause of a number of severe respiratory diseases, such as neonatal respiratory distress syndrome (RDS) (7). Impaired surfactant function is also the key pathophysiological feature of acute lung injury (ALI) and acute respiratory distress syndrome (ARDS), a devastating disease with multiple origins including tissue injury, inflammation, or sepsis (8). ARDS is a clinical syndrome associated with severe respiratory failure, which affects adults, children, and term infants. It affects about 50,000-150,000 patients in the United States alone each year (10,11,12,13).

1.2 Historical development of surfactant research

In 1929, Danish physician Kurt von Neergaard reported that the lung contained a surface-active material that facilitated lung expansion and stabilized the terminal airways (14). Observing air-filled and saline-filled excised lungs, von Neergaard determined that the difference between the pressures required to keep the lungs open with air compared to fluid arose from surface tension forces. Since the static retractive force of air-filled lungs is two to threefold greater than fluid-filled lungs, von Neergaard concluded that the surface forces were more important than the tissue elastic forces.

In 1955, Pattle reported more direct evidence to confirm the presence of a highly surface-active substance in the alveolus. He was interested in microbubbles formed in body fluids. Bubbles in water or serum normally collapse quickly due to the high-pressure difference across the air-fluid interface generated by surface tension. The

remarkable stability of bubbles produced from lung extracts led Pattle to conclude that they contained an insoluble material which reduced surface tension to near 0 mN/m at the air-liquid interface (15).

In 1957, using a Langmuir-Wilhelmy balance, Clements investigated the surface tension of lung extracts at different surface areas. Based on his results, Clements suggested that the surface films formed at air-water interfaces from surfactant extracts were the same as the alveolar surface film. He also reported that the surface tension in the lung reached values close to zero (16). In 1959, Avery and Mead (17) demonstrated that they were unable to find surfactant in lung extracts from infants who had died of hyaline membrane disease, and they hypothesized that prematurity and lack of surfactant were responsible for this condition.

Schurch and co-workers reported that surface tension within the alveoli at tidal volumes is operated within the range of zero to approximately 10 mN/m by a direct measurement in intact lungs using novel micropuncture technique (18,19,20). These results were confirmed by Bachofen (23) and Wilson (21,22) using isolated perfused lungs.

During 1985- 1995, four main surfactant-associated proteins and their respective genes were discovered. The sites of their synthesis, secretion, metabolism, and aspects of hormonal regulation have been reviewed thoroughly (4,45). The electron microscopic results have shown that the fluid lining layer covering the alveolar surface of the lung is continuous (24), and the film that is present in the air-liquid interface is often multilayered (25). Later, using fluorescence light microscopy, atomic force microscopy and Kelvin probe microscopy, Amrein and co-workers also suggested that the surface

lipid monolayer is attached to number of lipid bilayer stacks, scattered over the surface film (218,219,315,31).

1.3 Overview of the composition of endogenous lung surfactant

The composition of pulmonary surfactant is widely studied using bronchoalveolar lavage from the lungs of humans and several animal species (6,217). In order to prevent contamination from blood constituents, pulmonary surfactant is commonly separated from lung lavage by density gradient centrifugation.

Alveolar surfactant mainly consists of lipids (90% wt %) and surfactant-associated proteins (10% wt %) (Fig. 1.1a). Phospholipids (PLs) are the major lipid group and comprise 80-90% of the surfactant lipids. Phosphatidylcholine (PC) is the most abundant PL (70-85% by weight) (9,26) and, its disaturated version, dipalmitoyl phosphatidylcholine (DPPC) (C16:0, C16:0) (40-50% of PC), is the main surface tension reducing agent (14,27) in lung surfactant. In addition to saturated PLs, there are number of unsaturated PLs in lung surfactant which help to optimize surface activity of the surface film.

Phosphatidylglycerol (PG) (8-10% of lipids) and phosphatidylinositol (PI) (1-2%) that contain negatively charged head groups, are considered to be the next major PLs in lung surfactant. The ratio of PI/PG can vary throughout the development of an animal and between different mammalian and non-mammalian species (28,29). In addition to the aforementioned PLs, surfactant also contains about 1-7% of sphingomyelin (SPH), phosphatidylserine (PS), and phosphatidylethanolamine (PE) (6,26,4). PC, PE, and SPH are zwitterionic at a close-to-neutral pH, while PG, PI, and PS are anionic PLs.

Neutral lipids of pulmonary surfactant make up about 10% (mol 20%) of the total lipids. These lipids consist primarily of cholesterol, with lesser amounts of cholesterol esters, monoglycerides, diglycerides, and triglycerides.

In addition to surfactant lipids, there are four major surfactant-associated proteins: SP-A, SP-B, SP-C, and SP-D. These proteins are responsible for approximately 10% of the weight of lung surfactant. SP-A and SP-D are two large hydrophilic, multimeric proteins. The multidomain assembly of these proteins provides the ability to bind various types of ligands such as sugars, lipids, or calcium in a concerted manner (31). The binding ability of SP-A and SP-D allows these proteins to bind a range of pathogens that include bacteria, virus, and fungi; hence, they can play a major role in the innate immune system (34,32,33). SP-A is the most abundant surfactant protein (5-6% of total surfactant weight) and is highly conserved within vertebrates (35). In contrast, SP-D is present in lung lavage fluid in much lower amounts, about 0.5% with respect to total surfactant weight. There are two small hydrophobic surfactant proteins, SP-B and SP-C (36,37), each of which accounts for about 1-1.5% of surfactant weight (38). These two surfactant-associated proteins play a vital role in surfactant surface properties and are also important in surfactant biosynthesis (39).

1.4 Pulmonary surfactant synthesis

1.4.1 Intracellular sites of surfactant synthesis and processing

Surfactant-associated proteins and phospholipids are synthesized in the endoplasmic reticulum and are processed through the Golgi system. They are then transferred to the lamellar bodies. Lamellar bodies are specialized intracellular organelles

that regulate the storage and secretion of most surfactant lipids and some surfactant-associated proteins. A type II cell usually contains 100-150 membrane-bound lamellar bodies (146), which can differ in size between 0.1-2.4 μm in diameter (147). Under the electron microscope, lamellar bodies are filled with characteristic multilamellar and concentric swirls formed by phospholipid bilayers with little interlamellar space, surrounded by a limiting membrane. This interlamellar space is packed with electron-dense amorphous material that is probably proteinaceous in nature. SP-A, B, C have been demonstrated in lamellar bodies (148,149,150,151), while SP-D is absent (214).

1.4.2 Synthesis of surfactant phospholipids and neutral lipids

All lung surfactant phospholipids are synthesized in the endoplasmic reticulum of type II cells by pathways parallel to those seen in other cells in the body. However, these pathways in type II cells acquired some modifications in order to obtain the high content of disaturated and monoenoic phosphatidylcholines. In addition to *de novo* synthesis, the remodelling of unsaturated PL also gives rise to the high content of DPPC in lung surfactant. All diacyl glycerophospholipid synthesis starts with the acylation of glycerol-3 phosphate. Then, glycerol-3 phosphate reacts with different transferases to synthesize compounds that contain different head groups such as PC, PG, PI, and PE. The final mix of PCs consists mainly of disaturated PC and significant amounts of monoenoic species with a small amount of other compounds containing two or more double bonds in fatty acid chains (29,40,152,153,214).

Just prior to birth, Type II pneumocytes synthesize a massive amount of surfactant that is then secreted with the first breath during birth. After birth, most of the

surfactant components are continuously recycled, and the requirement for *de novo* synthesis is much lower (216).

In the neutral lipid compartment of the lung surfactant, cholesterol is the major component and is thought to be derived mainly from the serum lipoproteins such as VLDL, LDL, and HDL (221). Type II cells have receptors for these lipoproteins, which can be internalized using receptor-mediated endocytosis (222) and can use this cholesterol fraction to incorporate into surfactant. In addition to cholesterol from lipoproteins, type II pneumocytes are also capable of *de novo* synthesis (2% of total cholesterol which is present in alveolar surfactant (214)).

The surfactant-associated proteins are also synthesized in the endoplasmic reticulum and then transferred to the Golgi (45). It is believed that multivesicular bodies containing surfactant-associated proteins, SP-B and SP-C might fuse with the small, lipid-containing lamellar bodies (45), while SP-A and SP-D may be secreted independently. Analysis of composition of isolated lamellar bodies clearly demonstrates the presence of mature SP-B and SP-C with very little amount of SP-A (149) and no SP-D (214).

After being synthesized in the ER, the lipid components of lung surfactant have to first be transported to the lamellar bodies using a variety of multivesicular bodies (intermediate form of lamellar bodies) and then translocated across the LB membrane (29,40,152,153,216). The internal pathway for lipid delivery from ER to LB is not clear. The carriers involved in PC delivery from ER to the LB have also not been clearly identified yet. One potential candidate is a phosphatidyl transfer protein, which is

expressed in lung but its function in vivo, cannot be confirmed. Mice lacking this protein have normal LBs and normal surfactant composition (155).

1.4.3 Translocation of surfactant lipids across the LB limiting membrane

Translocation of surfactant lipids across the LB membrane is facilitated by transporters from the ATP-binding cassette (ABC) family (156,216), and mainly the by the ABCA sub family (157). Disruption of the gene responsible for the ABCA1 transporter in mice led to both multiple morphological defects in the lung and respiratory distress (158). It was also associated with type II cells hyperplasia with some unusually enlarged LBs, while most of the other LBs appeared normal (158,216). Among the ABCA transporters, ABCA3 seems to be the most important isoform. This isoform is highly expressed in the lung and especially in type II cells. ABCA3 transporters are mainly located at the limiting membrane of the LBs (159). Mutation in ABCA3 results in a lack of mature LBs (160,161,216). In another study, the down regulation of ABCA3 by siRNA in differentiated type II cells gave rise to immature and distorted LBs (162). Mutation in ABCA3 results in a low PC content in the lung surfactant and as a result elevated surface tension as determined by analysis of the BAL fluid (163) and also leads to abnormal processing of SP-B and SP-C (164).

1.5 Secretion of lung surfactant

Pulmonary surfactant is secreted by the exocytosis of the LBs from type II pneumocytes to the alveolar hypophase (Fig. 1.2). A basal secretion rate is range from 5-

40% of lamellar body surfactant per hour. Newborn animals usually have higher secretory rates on a weight-normalized basis compared to adults (214,216).

Lung surfactant lipids and proteins have long biological half-lives of up to tens of hours within the alveolar lumen (208,209). Slow clearance rate of the surfactant lipids and the proteins within the alveolar lumen give rise to these high turnover rates (214). Wright et al. determined the secretory path turnover time (the time needed to transfer surfactant material from the LB fraction to the alveolar lumen) to be between 4 to 11 hours. This is the time required to replenish the alveolar surfactant pool by continuous secretion and recycling (210).

The secretion of the lung surfactant seems to be regulated mainly at the local level by factors such as mechanical stretch, hyperventilation (165,166), signals from the autonomic nervous system (167), and chemical mediators like catecholamines, other β -adrenergic agents, ATP, protein kinase A, protein kinase C, cAMP, phorbol ester, prostaglandins, and leukotrienes. These factors tend to stimulate surfactant secretion from the type II cells *in vitro* (168,169,170,166,171,172,216). On the other hand, SP-A is considered a strong inhibitor of surfactant secretion from type II cells (173,174).

The secretion of surfactant-associated proteins is more complex than the secretion of phospholipids via lamellar bodies. Small hydrophobic SP-B and SP-C are localized in LBs and secreted with rest of the LB contents whereas the other two large hydrophilic surfactant proteins, SP-A and SP-D, are secreted in an LB-independent manner (216).

1.6 Recycling of lung surfactant

A significant proportion of lung surfactant (25-95%) is recycled by endocytosis (5,29,42,175). This greater proportion of internalized surfactant components are reutilized directly or indirectly to enhance intracellular surfactant stores rather than being lost from the alveolar compartment (214,177, 27). Approximately 10-15% of the alveolar surfactant components seem to be taken up by macrophages, and most of those are apparently degraded. This pathway is likely responsible for much of the loss from the alveolar compartment over time. In addition to these mentioned routes, a small fraction of 2-5% of the alveolar surfactant is cleared into the airways (214).

After internalization to type II cells, some surfactant lipids and proteins are transported to lamellar bodies without degradation. Once there, they are incorporated directly into newly synthesized surfactant, while the other components are catabolised to products that can be integrated into their synthetic pathways (214,1). Thus, LBs are at an intersection of secretory and endocytic pathways (180,181,1).

Turnover times for the lung surfactant lipids and proteins in the alveolar lumen vary from 1-24 hours in different animal models. These turnovers reflect the reuptake and reutilization of surfactant components in type II pneumocytes as well as loss from the alveolar compartment (214). Turnover rates for the alveolar surfactant are component-dependent as well as age-dependent. On a per weight basis, full-term newborn animals have larger intracellular and alveolar surfactant pools, higher rates of recycling, and a lower rate of synthesis compared to adult animals (214). Preterm animals usually have surfactant pools at or below the lower end of the pool size that is found in healthy adults. Alveolar turnover of surfactant-associated proteins is rapid. Receptor-mediated

internalization may be associated with the uptake of some of the surfactant proteins (178). SP-A promotes reuptake of phospholipids into type II pneumocytes. This is facilitated by high affinity SP-A receptors in type II cells (153). SP-A and phospholipids are transported together to early endosomes via clathrin-coated vesicles (179). SP-B, SP-C, and SP-D are also subject to recycling but so far, there is no evidence of the involvement of such receptors in this process.

1.7 Lung surfactant subtypes in alveolar hypophase

When phospholipid molecules are suspended in the bulk aqueous phase, they form different types of aggregates. This is due to the amphipathic nature of phospholipid molecules, which allows a different type of configuration to be organized in order to minimize free energy (182). Examples of such aggregates in water are multilayers (lamellae), unilamellar or multilamellar spheroidal vesicles (liposomes), and Hex I and Hex II cylindrical hexagonal phases. Sizes of these aggregates vary from the nanometer scale to the micron scale depending on the concentration, temperature, and composition of the lipids (214).

In lung surfactant, phospholipid aggregation is also significantly influenced by interactions with surfactant proteins. One such example of this is the formation of tubular myelin. In alveolar hypophase, pulmonary surfactant exists as a heterogeneous population of phospholipid rich aggregates that vary in size from the nanometer scale to micrometers. Standard or density gradient centrifugation of minced lung materials or suspensions of lavaged endogenous lung surfactant gives rise to different subpopulations of alveolar hypophase aggregates. These subpopulations are often termed as “subtypes”

or “subfractions” of lung surfactant (183,184,185,29,176). These subfractions of surfactant are different in their surface activity, composition and ratio of phospholipids to proteins. Large aggregate subfractions, which are denser, show higher surface activity compared to smaller aggregate subtypes (186,184,187,188,189,190,214). This may be due to the presence of a higher content of phospholipids and surfactant-associated proteins in the large aggregates (187,188,190,191). Studies have suggested that large aggregates may contain recently secreted materials that have high surface activity, whereas smaller aggregates may reflect “used” surfactant that has been shed from the interface after repetitive cycling. Also, small aggregates are considered to be surfactant aggregates that are present in the hypophase prior to reuptake by type II cells and alveolar macrophages. There is equilibrium between large and small aggregate subfractions in healthy lung surfactant present in the alveolar hypophase. Abnormal changes in lung surfactant subfraction can lead to lung surfactant inactivation during lung injury (192,184,193,185,214).

1.7.1 Tubular myelin

Tubular myelin (TM) is often considered the precursor of the surface film in the air-water interface of the lung (187,194,188). There is a correlation between the existence of TM and the capability of lung surfactant to adsorb very rapidly (123). Sen et al. showed continuity between TM and the surface film at the air-liquid interface, supporting the above assumption (211). In tubular myelin, the walls of the tubules have bilayers, and the corners either intersect or closely oppose bilayers with very high curvature (123). These tubules are nearly rectangular in cross-section (212). Under an electron

microscope, they appear as three-dimensional lattices made up of stacks of intersecting phospholipid bilayers with a repeat distance of about 50 nm (Fig. 1.3). There are particles aligned systematically along parallel phospholipid bilayers. The size and the structure of these particles imply that they are oligomers of SP-A. Even though SP-B is also required for the formation of tubular myelin, its location and distribution in tubular myelin is still unknown. SP-C is not essential for tubular myelin formation.

1.8 The composition, structure, and function of the surfactant film at the air-water interface

The surface film has long been considered to be a simple monolayer containing DPPC and non-DPPC lipids. Thus, repeated compression and expansion of the monolayer squeezes out fluid, non-DPPC lipids, and leads to enrichment of the film with DPPC (14,239,240). These squeezed-out surfactant materials, which are lost to the subphase during compression, need to be replaced with fresh surfactant material for optimal function of the surface film. This replenishment process is not well explained by monolayer theory.

However, recent experimental evidence clearly explained the above process as involving functional multilayers that closely associate with the surface film and supply surfactant phospholipids to the surface film (14,241,196). These multilayer structures can be described as adsorption reservoirs generated during film formation and compression reservoirs formed during compression of the surface film (14,196). These surface-associated surfactant reservoirs supply surfactant components during film expansion. The presence of multilayers has also been observed in recent electron microscopic and surface

activity studies (195,196,215). Furthermore, novel studies that were performed with atomic force microscope also confirm the existence of multilayers attached to the surface film (218,219,123,217).

During expiration, the lung alveoli become reduced in size, and unsaturated PL and neutral lipids present in the surface film are thought to be excluded from the surface film to surface-associated surfactant reservoirs. Also, some of the excluded materials can be lost to the hypophase, and may later be recycled or degraded under the influence of SP-A and possibly SP-D (27,197,215). Thus, at the end of the expiration, the remaining surface film at the interface could be highly enriched in disaturated phosphatidylcholine (especially DPPC). This can give rise to very low surface tensions close to 0 mN/m (5). When the lung expands (inspiration), unsaturated phospholipids and cholesterol are retrieved from surface associated surfactant reservoirs (respreading) or from tubular myelin, and are incorporated into the surface layer between DPPC rafts (6,215). SP-C and SP-B promote this rapid adsorption of lipids to the surface film of the air-water interface (198). These unsaturated phospholipids and cholesterol reduce the phase transition temperature of the saturated phospholipid film and as a result, enhance the fluidity of surfactant (14). This helps it to re-spread over the expanding alveolar surface (6).

1.8.1 Phospholipids

Lung surfactant PLs can be categorized as disaturated phospholipids (DSPs) and unsaturated phospholipids (USPs) depending on the presence (or absence) of double bonds in the fatty acyl chains. These hydrophobic fatty acyl chains are specifically important for biophysical behaviour. Fatty acyl chain length and saturation highly

influence the fluidity, film properties, and phase behaviour of surfactant PLs. Disaturated phospholipids (fatty acyl chains with no double bonds) such as DPPC have significantly higher melting points and phase transition temperatures (temperatures that changes gel phase lipids into liquid phase lipids) than otherwise similar monoenoic PLs (with one double bond). Even though there are some saturated PL compounds with different head groups present in the lung surfactant, the DSPs are commonly approximated by disaturated phosphatidylcholine (DSPC).

DPPC is the major disaturated PC present in lung surfactant with two C16:0 fatty acyl chains. The percentage of DPPC in lung surfactant varies from 40-70% of PC (29,40,41,42,43, 44,45). Recently, the amount of DPPC in pulmonary surfactant in calf lung has been carefully re-evaluated using new techniques such as high-performance liquid chromatography (HPLC) and electrospray ionization-mass spectrometry (ESI-MS). The new value is only about 40% of the total PC, and is therefore less than half of the total surfactant lipids (46,213). Although DPPC is an unusual PC in most mammalian tissues (in most mammalian tissue PC is unsaturated, as in the membranes of biological systems), very small amounts of DPPC can be present in other tissues such as the brain (214). Hence, it is not surfactant-specific, but the presence of very high amounts of DPPC in surfactant is unique (42).

In addition to DPPC, there are a few other disaturated PCs present in lung surfactant, such as palmitoyl-myristoyl-PC (PMPC C16:0/C14:0) and myristoyl-palmitoyl-PC (MPPC C14:0/C16:0). There are also a number of unsaturated phospholipids present in active isolates of lung surfactant with PC as the most abundant class. Other head groups such as PG, PE, and PS also have a number of unsaturated fatty acyl chains in

their sn-1 and sn-2 position, as well as saturated fatty acyl chains (29,40,43,44,45) that influence surface-active behaviour.

The characteristic biophysical properties inherent to DPPC are mainly determined by its two fatty acyl chains. With its ability to pack very tightly upon dynamic (in the sense of continuous) compression, DPPC is highly capable of lowering surface tension to very low values (<1 mN/m). Although DPPC films achieve very low surface tensions during dynamic compressions, they also exhibit poor adsorption (film formation) properties at the air-water interface (53, 54) and poor respreading (ability to re-enter the surface film from surface associated material while expanding the film) during successive cycles of compressions and expansions (55,56,57,58,59). Mixed films consisting of saturated and unsaturated PLs in lung surfactant are much better at respreading than pure DPPC films (59). Fluid unsaturated PLs in lung surfactant do not reduce surface tension to low values on their own during dynamic compression, but they make major contributions towards improving respreading. In addition, the neutral lipid component and surfactant-associated proteins in lung surfactant also facilitate rapid adsorption and better respreading (53, 60).

Unsaturated PLs consist of at least one fatty acyl chain with one or more double bonds. The most common unsaturated PC compounds in lung surfactant are palmitoyl-palmitoleoyl-PC (PPoPC C16:0/C16:1) and palmitoyl-oleyl-PC (POPC C16:0/C18:1). There are other unsaturated PC species present in small amounts. The composition of these surfactant lipids and the phase behaviour of simple lipid mixtures suggest that phase transition might occur in the lung. These unsaturated PCs are all in the liquid-expanded phase at 37°C, while disaturated PCs with at least 16 carbon atoms in length are

in the liquid-condensed phase. Disaturated PCs with shorter chains are in the liquid-crystal phase at 37°C (49,50,51) because their gel to liquid crystal transition temperatures (T_c) are 27°C and 35°C respectively (52). In comparison, gel to liquid phase transition temperature for DPPC is 41°C. Therefore, lung surfactant film has a rigid gel phase as well as liquid condensed phase coexistence which collectively determine the characteristic surface properties of lung surfactant. Body temperature, length of the fatty acyl chains, and the presence of double bonds influence the phase behaviour of lung surfactant film at the air-water interface.

The contribution of anionic phospholipids (PI, PG, and PS) to the surface activity of lung surfactant is not well understood but their presence (PG and PI) may be used as a developmental marker of surfactant in fetal lung fluid (61,62,63,64,65,66,67,68). The association of anionic phospholipids with surfactant-associated proteins has been well documented (69,70,71,72,73). Positively charged amino acids in surfactant proteins can associate with negatively charged PLs. The depletion of anionic PLs in lung surfactant gives rise to minor decreases in surface and physiological activity when the remaining PLs combine with SP-B and SP-C (74).

1.8.2 Surfactant-associated proteins

SP-A and SP-D are members of the collectin family of C-type lectins. These proteins have four functional domains:

1. N terminal region
2. Collagen like domain with Gly-X-Y repeats
3. Hydrophobic neck region

4. Carbohydrate recognition domain

SP-A and SP-D can form multimeric structures due to the presence of collagen-like domains and carbohydrate-binding domains. The multidomain character of these structures offers proteins the capability to associate with a variety of ligands such as sugars, lipids, or calcium in a concerted manner (75). The main functions of these lung collectin family proteins are pathogen clearance and involvement in inflammatory responses (76,77).

1.8.2.1 SP-A

There are two human SP-A genes coding for SP-A in chromosome 10. The molecular weight of the final form of the SP-A monomer is 26-35 kDa and it is first synthesized as a 248 amino terminal precursor peptide from which a 20 amino acid signal peptide is removed. After glycosylation and other post transitional modifications, SP-A is oligomerized to an octadecamer consisting of 6 sets of trimers that are held together with covalent and noncovalent bonds (78,79). Hydroxylation of proline residues in SP-A is vital for oligomerization (80).

The main biophysical action of SP-A is to enhance the aggregation and ordering of phospholipids in a calcium- and pH-dependent manner (81,82,83). SP-A can bind phospholipid aggregates and influence the exchange of phospholipids between them (84). Moreover, it interacts with anionic and zwitterionic phospholipids. SP-A facilitates the aggregation of phospholipids into different types of larger aggregates, of which tubular myelin is the most important (85). In tubular myelin, oligomeric SP-A is aligned at regular intervals along the phospholipid bilayers, projecting from their intersections

(86,87). SP-A also plays a role in surfactant turnover. Specifically, it stimulates the uptake of phospholipids by type II cells (88, 89) and inhibits surfactant secretion (90,91). SP-A knock-out mice were found to breathe normally, but were highly prone to developing infections (92). Under challenging conditions such as low surfactant concentration (93) or the presence of inhibitory plasma proteins (94) or oxidants (95), adding SP-A can improve the surface activity of SP-A deficient surfactant (217).

1.8.2.2 SP-D

The molecular weight of the SP-D monomer ranges from 39-46 kDa (96). SP-D differs from other surfactant-associated proteins, as it is not a functional biophysical constituent of lung surfactant. This hydrophobic C-type lectin is similar in structure to SP-A but it is much larger. SP-D has several isoforms and will undergo extensive post-translational glycosylation and other types of processing. SP-D oligomerizes into a dodecamer consisting of four sets of triplet chains arranged into 46-nm rods terminating in carbohydrate binding heads (97). SP-D is synthesized and secreted in different pathways; hence, it is not found in lamellar bodies or in tubular myelin (98).

The major function of SP-D is host defence, but it may also participate in surfactant metabolism (99,100). SP-D does not play any significant role in the surface activity of lung surfactant at the interface since it is not associated with the surface-active lipid-protein aggregates. However, SP-D seems to affect the physical structure of phospholipid aggregates in surfactant, as well as their uptake and catabolism by type II pneumocytes (101). SP-D knock-out mice demonstrate an accumulation of phospholipids

in both tissues and surfactant, and they also have increased numbers of activated macrophages that contribute to lung inflammation and emphysema (102,91).

1.8.2.3 SP-B and SP-C

SP-B and SP-C are hydrophobic, surfactant-associated proteins, but they differ markedly from each other in their amino acid sequences and secondary structures. These proteins undergo post-translational modification from larger precursors to form smaller, active final peptides that are highly conserved among animal species. SP-B and SP-C are transported from the endoplasmic reticulum through the Golgi and trans-Golgi network to the multivesicular bodies and then to LBs (105,103,83).

SP-B belongs to the family of saposin-like proteins (SAPLIP), which are characterized by a high content of alpha-helical secondary structures and by the presence of six cysteine residues. The relative positions of these cysteine residues in the amino acid sequence are highly preserved in order to form three intramolecular disulfide bonds (104,106,107,108,223). The SP-B monomer contains 79 amino acids and has a molecular weight of 8.7 kDa (109). A single human SP-B gene is located on chromosome 2, and consists of 10 exons (199). The final SP-B peptide is produced by the proteolytic processing of approximately 40-46 kDa glycosylated precursor containing 381 amino acids (109,200).

SP-B is the only surfactant-associated protein that seems to be vital for the initiation and maintenance of breathing. Homozygous mutations in the human SP-B gene lead to a lack of SP-B in the alveoli and result in death from respiratory distress soon after birth (110,111). Similar observations are also seen with SP-B knock-out mice (110).

A partial deficiency in SP-B may lead to moderate respiratory dysfunctions (112,113, 114). The phenotype of SP-B-deficient lungs shows normal lung structure, but is associated with a lack of functional lung surfactant. These lungs are characterized by a lack of lamellar bodies, an accumulation of aberrant multivesicular bodies within type II cells, a lack of tubular myelin, and the synthesis of an abnormal form of SP-C precursor. Thus, SP-B is not only a vital component for both intracellular and extracellular synthesis and routing of surfactant lipids and proteins (14), but it also plays a vital role in the biogenesis of lamellar bodies (117). Furthermore, SP-B seems to promote fusion of the internal vesicles of multi-vesicular bodies into the unique lamellar membranes of the LBs (201). Fusogenic properties of SP-B have also been reported *in vitro* (115). Targeted disruption of the SP-B gene *in vivo* resulted in accumulation of multi vesicular bodies, but no LBs were found in type II cells (116,117). These immature LBs can be secreted to the alveolar hypophase, but they fail to form a functional surfactant film. This leads to death in mice (117) and humans (118). Also, SP-B is tightly associated with surfactant phospholipids and is necessary for the formation of tubular myelin in the presence of phospholipids, SP-A, and calcium.

Studies done with organic extracts of natural lung surfactant have shown that it adsorbs quickly to the air-water interface. This can be attributed to the low molecular weights of hydrophobic proteins like SP-B and SP-C (14). Such preparations contain only SP-B and SP-C, but not SP-A. Individually or together, these two hydrophobic proteins greatly improve the adsorption of DPPC-containing mixtures to equilibrium surface tension values (23 mN/m) (234,235,109,236,237). SP-B seems to have a greater effect on phospholipid mixtures that are similar to natural surfactant (236,237,59,238). The

molecular mechanism behind the surfactant adsorption that is facilitated by this hydrophobic surfactant protein seems to be their ability to function as a bilayer breaker. Bilayer breakers disrupt the bilayer structures in a certain way that permits the cooperative flow of bilayer phospholipids to the surface film (14). Furthermore, SP-B plays potential roles in maintaining the stability of highly compressed films (127,225,226) and facilitating the respreading of surfactant components during expansion. This gives rise to minimum surface tension values after successive compression-expansion cycles (139,227,72,228,126,229). Some studies have proposed that SP-B can operate as a bridge between bilayers or between bilayers and monolayers (122,123,223,229). Thus, SP-B can keep both of the components (materials squeezed out from the interface during compression, and the new material reaching the interface “*de novo*”) close to the interface, during the time the monolayer has to support maximal pressures, just before expansion and re-spreading (230). This suggests that SP-B contributes to sustaining the surfactant-associated reservoir and keeping the material needed for surface film renewal attached to the interface upon dynamic compression-expansion cycling (230,231,127,228).

The amino acid distribution along the sequence of SP-B facilitates the formation of several amphipathic helical segments (119,120). The amphipathicity of these helical segments helps provide SP-B with a relatively superficial disposition in lipid bilayers and monolayers (121,122,123). These helical segments of SP-B can interact mainly with the polar head groups of phospholipids, and to a lesser extent with the fatty acyl chains in the hydrophobic region of surfactant structures (223). SP-B has a number of basic amino acid residues, which gives the protein a cationic character, and allows it to interact

preferentially with acidic phospholipids such as PG in monolayers (124) and bilayers (122,223). Specifically, interactions between SP-B and negatively charged phospholipids seem to be important for the generation of non-bilayer intermediates that are essential in bilayer-monolayer transitions (125). The interaction of SP-B with PG seems to promote the enrichment of the interfacial film with essential phospholipids (126,127).

During acute lung injury /acute respiratory distress syndrome, the increased production of reactive oxygen species (ROS) is detected by the inflammatory cells. Surfactant function and metabolism are altered by direct oxidative damaged by ROS. Possmayer and co-workers recently found that both SP-B and SP-C undergo changes during oxidation that significantly alter their biophysical properties. The surface activity impairment seen in these reconstituted mixtures suggests that protein oxidation is the main cause of the impaired activity of oxidized surfactants, whereas phospholipid oxidation has a minor effect. Although oxidation of either SP-B or SP-C can impede surfactant function, non-oxidized SP-B can improve samples with oxidized SP-C. The destruction of surfactant hydrophobic proteins may play a significant role in the surfactant dysfunction that occurs during lung oxidative stress-related disorders such as ARDS, cystic fibrosis, and asthma (232,439).

SP-C is the most hydrophobic surfactant-associated protein (202,175). It contains 35 amino acids and has molecular mass of 4 kDa. Most of its amino acids, which include valine, leucine and isoleucine, are hydrophobic (203). In humans, the SP-C gene is located on chromosome 8 and is expressed strictly in the pulmonary epithelium. The mature SP-C peptide is processed in between the Golgi and multi vesicular bodies (128,117) of type II cells from its precursor, Pro-SP-C. Pro-SP-C has a molecular mass of

21 kDa (204) and contains 381 amino acids. Two-thirds of the mature SP-C sequence forms a very regular hydrophobic alpha helix with a length that is equal to the thickness of a fluid lipid bilayer (205). It also has a cationic N terminal tail that bears two cysteine residues, which are usually palmitoylated (206,223). This post-translational modification further stabilizes the alpha helical conformation of SP-C (207). Due to its hydrophobicity, SP-C seems to be located mainly in the interior of the phospholipids bilayer with its helical axis aligned parallel to the acyl chains (129,104,223).

SP-C is the only surfactant-associated protein without any known structural homology, and it is exclusively expressed in the pulmonary epithelial cells (38,223). Several studies of SP-C gene mutations that give rise to chronic familial respiratory diseases have been reported (111,130). For example, Belgian blue calves with a complete lack of SP-C gene, develop neonatal respiratory syndrome (131). On the other hand, SP-C knock-out mice breathe normally after delivery (132), but develop respiratory dysfunction later in life (133). This shows that deletion of SP-C is non-lethal but SP-C still plays a vital role in surfactant function. Both animal and human patient studies suggest that SP-C deficiency can lead to different forms of pulmonary diseases in different individuals (133,134,111). Mutations of the SP-C gene in humans are implicated in various acute and chronic lung diseases including acute respiratory distress syndrome and idiopathic pulmonary fibrosis (130,233). SP-C gene knock-out mice survive perinatally, but show abnormalities in the stability of the surface film, which demonstrates the possible role of SP-C in recruiting phospholipids to the monolayer/multilayer (133). Thus, SP-C is necessary for the stability of phospholipid films during dynamic compression (133). Using atomic force microscopy Amrein and

co-workers observed that SP-C facilitates the association of membrane patches with interfacial phospholipids films, and they proposed that the N-terminal segment of SP-C acts as a bridge between bilayers and monolayers (218,315,316,356,245). Thus, SP-C can promote the formation of surface-associated reservoirs (217).

SP-C mainly interacts with phospholipids via hydrophobic interactions, although its two positively charged amino acid residues can also interact with phospholipid head groups (135,122,223). Additionally, SP-C can facilitate the fusion of some phospholipids vesicles (136,137) and can enhance lipid vesicle binding and insertion into the surface film (138,139).

1.8.3 Neutral lipids

Neutral lipids account for 10% of surfactant weight (20 mol%) but they are probably the least understood component of pulmonary surfactant (140,141). The neutral lipid fraction consists mainly of cholesterol (80-90%), with lesser amounts of cholesterol esters, diacylglycerol, triacylglycerol and free fatty acids (14). The amount of cholesterol expressed as weight percentage of total phospholipids differs among various animal species, ranging from as high as 30% in Australian lung fish to as low as 7% in humans (141). Surfactant cholesterol seems to have a different origin compared to surfactant phospholipids and surfactant-associated proteins (141). Studies have shown that the cholesterol/phospholipid ratio in lung surfactant slightly increases as a result of exercise (143), and increases by 1.5-fold in heterothermic mammals undergoing torpor (144). The cholesterol/phospholipid ratio also increases several folds during lung injury (145,224).

The role of cholesterol for the surface activity of surfactant is discussed in greater detail in Chapter 3.

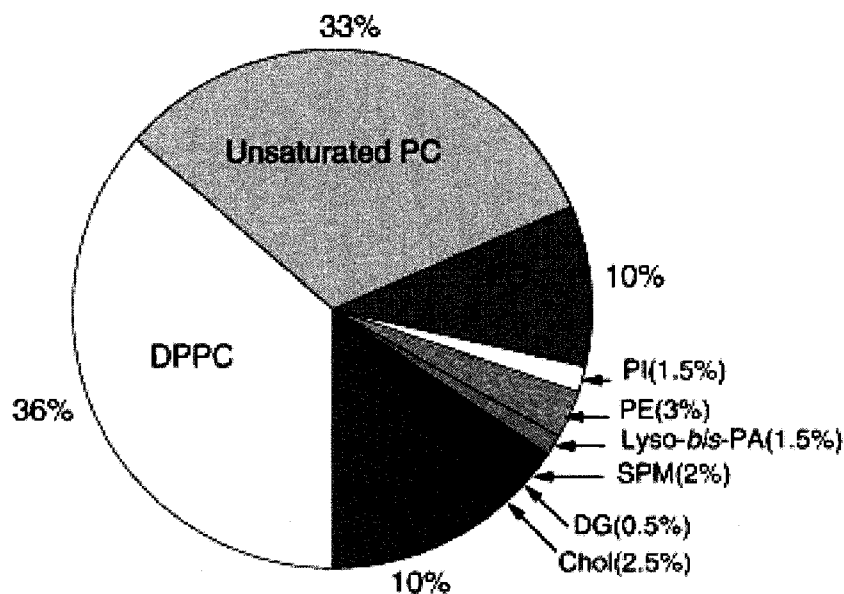


Figure 1.1a The composition of bovine pulmonary surfactant. DPPC: dipalmitoyl phosphatidylcholine; PC: phosphatidylcholine; PG: phosphatidylglycerol; PI: phosphatidylinositol; PE: phosphatidylethanolamine; Lyso-*bis*-PA: lyso-*bis*-phosphatidic acid; SPM: sphingomyelin; DG: diacylglycerol; Chol: Cholesterol. From Zuo et al.2008. (251).

Lipid class analysis

	Phospholipids - 97 ± 0.34, Neutral lipids - 3 ± 0.5
1. Neutral lipid composition	
Cholesterol -	89 ± 1.9
Diacylglycerol -	9.8 ± 0.2
Monoacylglycerol -	<1.0
Cholesterol esters -	<1.0
2. Phospholipid composition	
Phosphatidylcholine -	79 ± 1.6
Phosphatidylglycerol -	11 ± 0.5
Phosphatidylinositol -	1.8 ± 0.3
Phosphatidylethanolamine -	3.5 ± 0.5
Lyso- <i>bis</i> -phosphatidic acid -	1.5 ± 0.4
Sphingomyelin -	2.6 ± 0.5

Figure 1.1b Lipid composition of Bovine Pulmonary Surfactant (% Total \pm SEM)(Adopted from Yu et al 1983(295))

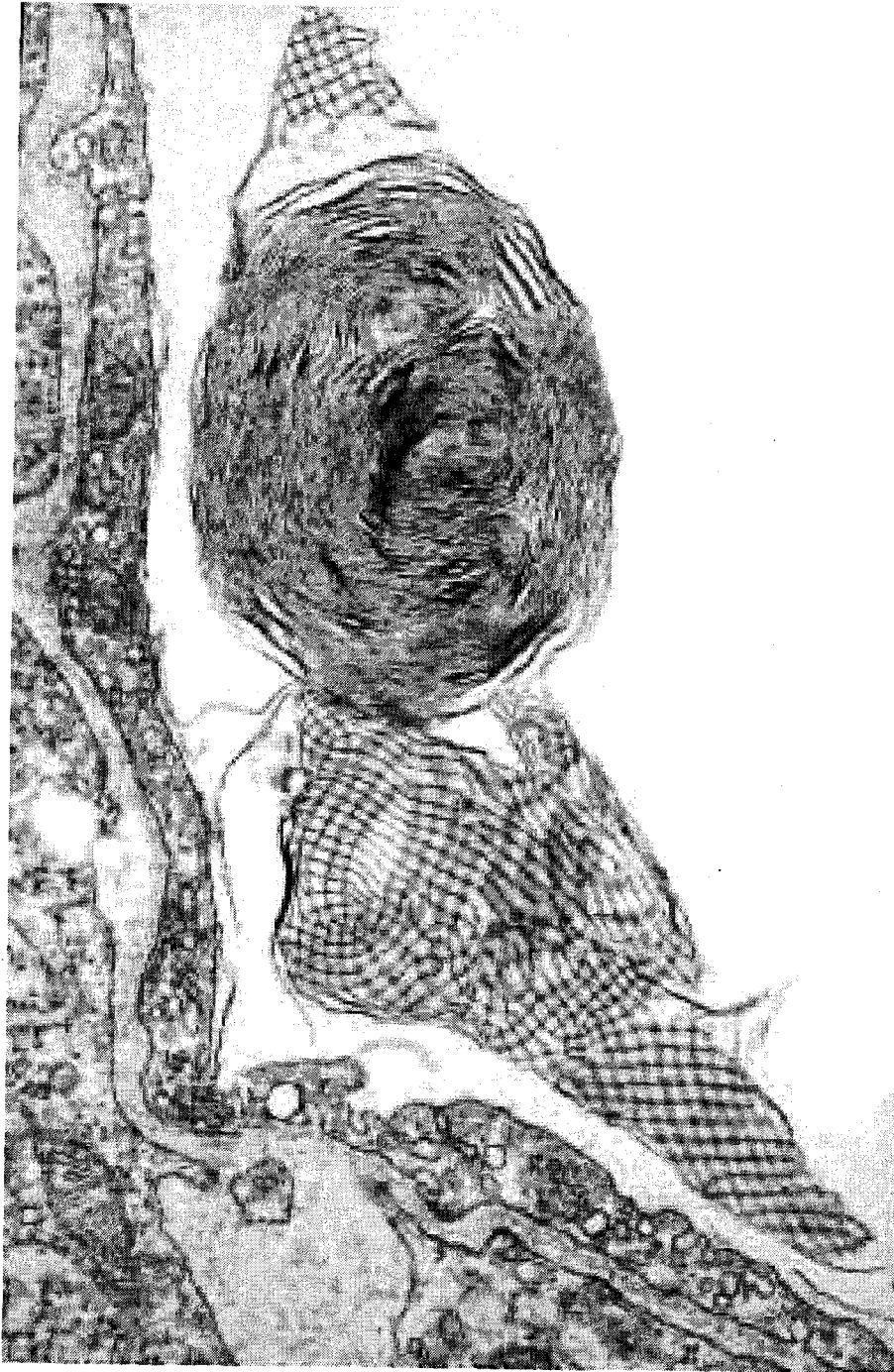


Figure 1.2 Transmission electron micrograph from guinea pig lung showing lamellar bodies, tubular myelin and some of the structures related to the surfactant film. From Schurch et al. 2001 (314).

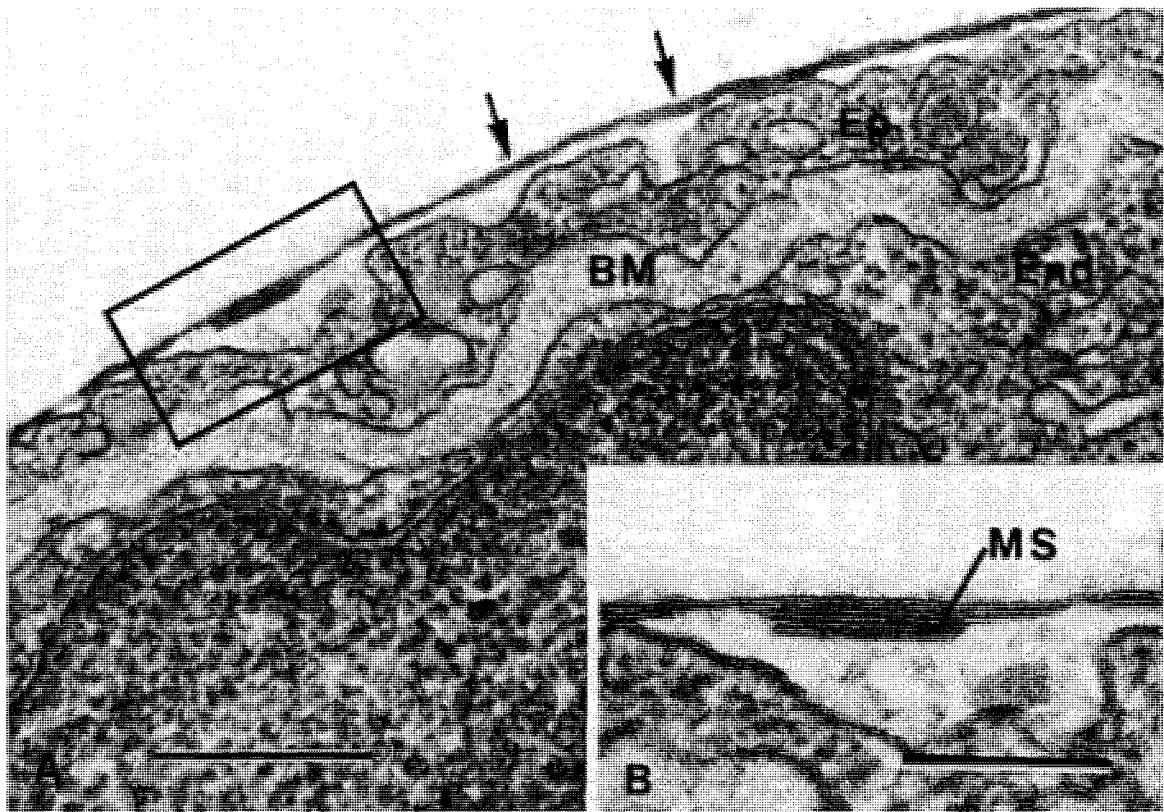


Figure 1.3 (A) Higher magnification of the alveolar surface film from a guinea pig lung showing that it is multilaminated. Bar=0.3 μm . (B) Close-up of alveolar surface film over type I pneumocyte showing variations in the number of lamellae from 2 to 7. A multilamellar structure (MS) resembling a disk-like vesicle is partially incorporated into the surface film. Bar=0.6 μm . (Adapted from Schurch et al.2001 (314)).(BM)- basement membrane, (EP)- epithelium. From Schurch et al.2001 (314).

Chapter 2: Methods to Evaluate Surface Activity of Pulmonary Surfactant

2.1 Surface activity of lung surfactant

2.1.1 Introduction to surface tension

Surface tension occurs as a result of unbalanced attractive forces between molecules (14,49,214). A typical molecule in the bulk phase of a liquid is attracted evenly in all directions by its surrounding molecules, and the net force exerted on it is zero. In contrast, the molecules below attract molecules at the surface, but they suffer from a relative lack of attraction from the dilute gas phase. Thus, there is an unbalanced attraction of the molecules in the interfacial region towards the bulk phase of a liquid. This creates an inward force towards the bulk phase called surface tension, which leads to minimized area at the interface (14).

The surface tension of a clean air-water interface is approximately 73 mN/m at 25°C. Water has a high surface tension due to the presence of hydrogen bonds between its molecules. Surface tension can be modified by the presence of another substance in the liquid. Phospholipids are integral components of lung surfactant, which are amphipathic in nature. These molecules are essentially insoluble, and are present in aqueous dispersion as aggregates, like liposomes (14). When phospholipids are added to the bulk solution of water, they form a surface film at the air-liquid interface. The polar head groups interact with water molecules whereas the hydrophobic fatty acyl chains extend towards the gas phase. Thus, the displacement of water molecules from the interface by these phospholipid molecules gives rise to low surface tension.

2.1.2 Surface properties of lung surfactant

Surface activity is dependent on the lipid-protein composition of surfactant. The accumulation of surfactant molecules at the interface and the resulting film formation is usually referred to as adsorption. The ability of lung surfactant to form a surface-active film at the air-liquid interface is indicated by its quick adsorption rate and the reduction of surface tension to an equilibrium surface tension (ST_{eq}). The rate of adsorption of lung surfactant from the aqueous hypophase to the air-liquid interface represents its ability to spread to the newly formed interface during the first breath, and to replenish the interfacial film whenever the matter has been inactivated or lost from the interface after birth. Natural surfactant shows very quick adsorption to the air-liquid interface in order to form a tightly packed surface film. This quick adsorption is highly facilitated by surfactant-associated proteins SP-B and SP-C, as well as by unsaturated phospholipids. As the area of the alveolar interface decreases during expiration, the molecular film packs even more tightly and the surface tension decreases to a minimal value (ST_{min}) <1 mN/m. The percentage of area compression ($\% SA_{comp}$) required to reach ST_{min} is an indicator of how rapidly and efficiently surfactant reduces surface tension under dynamic compression. Normal, healthy lung surfactant shows low film compressibility. Also, efficient replenishment occurs in the surface film upon expansion by the reinsertion of surfactant material (including squeezed-out materials) from a surface associated reservoir (243). *In situ* measurement demonstrated that the actual surface tension of the lung changes from 30 mN/m at total lung capacity to 20 mN/m at 80% of total lung capacity, and close to 0 mN/m at residual at residual lung capacity (19). The film is also distinct for its high-mechanical strength (244).

2.1.2.1 Adsorption of surfactant

Adsorption is a process by which surfactant molecules in the subphase enter the air-liquid interface and form a surface film. During adsorption, molecules move either individually or as a group into the interface. Particularly in lung surfactant, the adsorption of a group of molecules (aggregate) is thought to happen to form a surface film. This surface film reduces surface tension to a value called equilibrium surface tension, which is usually 25 mN/m for DPPC at 37°C at a concentration of 5 mg/mL in the aqueous subphase (245). Above a certain subphase concentration, ST_{eq} becomes independent of concentration and is approximately 23 mN/m for surfactant. Although all surface active material demonstrates positive net adsorption (214), they vary extensively in the rates at which they adsorb. Differences in the lipid species, the specific compositions of mixed substances, and the molecular organization of these substances in the aqueous subphase are the factors that influence adsorption rate (245,246). During the equilibrium state, there is balance between molecular adsorption into the interface and molecular desorption from the surface film. This is so that no net new matter moves into the interface, as it becomes energetically too costly to squeeze itself into the surface film that has already formed (245). Diffusion and convection in the bulk liquid assist to transport molecules from within the bulk phase into a region very close to the interface (subsurface region). Adsorption then involves the entry of molecules into the interface from the subsurface region to form a surface film (246). However, in the lung, diffusion might play a minor role as the aqueous lining is very thin (in the micrometer range). During alveolar inflation, this layer is stretched out. Surfactant aggregates in the aqueous phase are

comparable in size to the thickness of the aqueous lining. Thus, the aggregates may be forced into close contact with the interface rather than diffuse into it (245).

There are different types of surfactant aggregates in the alveolar hypophase, such as unilamellar vesicles, multilamellar vesicles, or the unique tubular myelin. All of these aggregates are based on lipid bilayers, but depending on the composition of the lipids, the nature of the bilayer can differ. Unsaturated lipids form fluid bilayers, whereas fully saturated phospholipid such as DPPC forms bilayers that are in a more condensed gel-phase at physiological temperatures. Adsorption of DPPC bilayers to the interface is a very slow process when compared with bilayers composed of unsaturated lipids, since DPPC bilayers are less likely to break up and rearrange in a monolayer than unsaturated bilayers, which are usually in a fluid state. Therefore, adding unsaturated lipids to DPPC increases the rate of adsorption (245).

Furthermore, the zwitterionic head group of a DPPC molecule has a strong hydration shell, and it prevents the fusion of two adjacent layers of DPPC (52). Thus, there is a high potential energy barrier to overcome, before the materials from the bulk aqueous phase can adsorb to the interface. This slows down the adsorption of DPPC. On the other hand, charged lipid layers of PG and PI repel each other when they come closer. Their head group charge attracts counter ions to form a diffuse layer of increased ion strength closer to them (electric double layer). When two electric double layers of two proximate bilayers start to overlap, they will repel due to osmotic stress. This can easily be overcome by the presence of divalent ions. A physiological amount of divalent cations is enough for these interfaces to come into close contact (245). Thus, adding charged phospholipids augments the rate of adsorption of surfactant at the air-liquid interface. The presence of

non-gel phase phospholipids and cholesterol in lung surfactant results in increased fluidity, which in turns causes rapid adsorption. However, this overall effect is relatively small (14). This leads to the conclusion that the capability of natural and modified lung surfactant to adsorb extremely rapidly can be attributed to the low molecular weight hydrophobic surfactant proteins SP-B and SP-C (14). Alone or together, these two proteins greatly enhance the adsorption of DPPC-containing mixtures to equilibrium surface tension (247,237). The mechanism by which these proteins promote adsorption of surfactant phospholipids is not clear. However, these hydrophobic proteins can be thought of as bilayer breakers, which disrupt the bilayer structures in such a way that they allow cooperative flow of bilayer phospholipids to the surface film (14,248). Schurch and coworkers reported that porcine lipid extract surfactant (Curosurf) adsorbs in discrete, sudden bursts corresponding to approximately 10^{14} phospholipid molecules (248).

2.2 Techniques used to evaluate surface properties of lung surfactant

A variety of methods are used to investigate the surface properties of surfactant and surfactant films. The main experimental methods that are commonly used with surfactant are:

1. Wilhelmy Surface Balance (LWB)
2. Pulsating Bubble Surfactometer (PBS)
3. Captive Bubble Surfactometer (CBS)
4. Microbubble Stability Test

2.2.1 Wilhelmy surface balance (LWB)

The classical Langmuir trough was invented by Langmuir in the early part of the 20th century. Subsequently, Agnes Pockels showed that the film area on the surface could be adjusted by means of barriers. In the classical Langmuir's trough, the surfactant film is confined by a rigid, movable barrier on one side and by a floating barrier on the other side. The force acting on the floating barrier can be measured directly to obtain the film pressure:

$$\Pi = \gamma_0 - \gamma$$

(γ = surface tension of the surface containing film and
 γ_0 = surface tension of the clean substrate)

In the classical Langmuir balance, the liquid subphase extends over the trough walls while a mechanically driven barrier lying across the top of the trough compresses the surfactant film. However, at minimal surface tensions, the subphase in a Langmuir trough wets and flows over the walls, and film leakage occurs as the water level drops. These design features are unfavorable to the study lung surfactant films that reach very low surface tensions during compression.

Therefore, the Langmuir-Wilhelmy balance (LWB) (Fig. 2.1) was invented to overcome the above limitations. The Langmuir-Wilhelmy method was applied to study surfactant films by Clements in his pioneering work on pulmonary surfactant extracts (249). The LWB provides surface tension-area isotherms (σ -A) or surface pressure-area (Π -A) behaviour in compressed surfactant films.

A modern Langmuir-Wilhelmy balance usually has a trough of metal that is coated with a hydrophobic material like Teflon or solid Teflon and a tightly fitting Teflon barrier. This modified balance has a liquid subphase that does not reach the top of the trough wall,

and a recessed barrier system that limits and compresses the surface film systematically using an external motor. Surface tension of the surface film is determined from the force that pulls down the Wilhelmy plate dipped into the liquid subphase. A force transducer, which is, attached to the Wilhelmy dipping plate measures the value of particular force. Subphase volume in the Wilhelmy balance ranges from 50 to 1000 ml. A rectangular or otherwise shaped trough holds the liquid subphase. A surfactant film can be formed at the air-liquid interface either by spreading surfactant from an organic solvent or by adsorption from the subphase. A pause of 5-10 minutes is allowed for solvent evaporation, prior to cycling of the film. Subsequently, the film is compressed and expanded using one or more barriers that confines the interface and creates a known change in surface area. The surface area during cycling is usually expressed as either a percentage of the fully expanded trough area or an inverse surface concentration in $\text{A}^{0.2}/\text{molecule}$, based on the amount of surfactant initially spread. While cycling (continuous reduction and expansion of the film surface area), measurements of the surface tension are obtained and then plotted as a function of surface area to define σ -A or Π -A isotherms at desired temperatures.

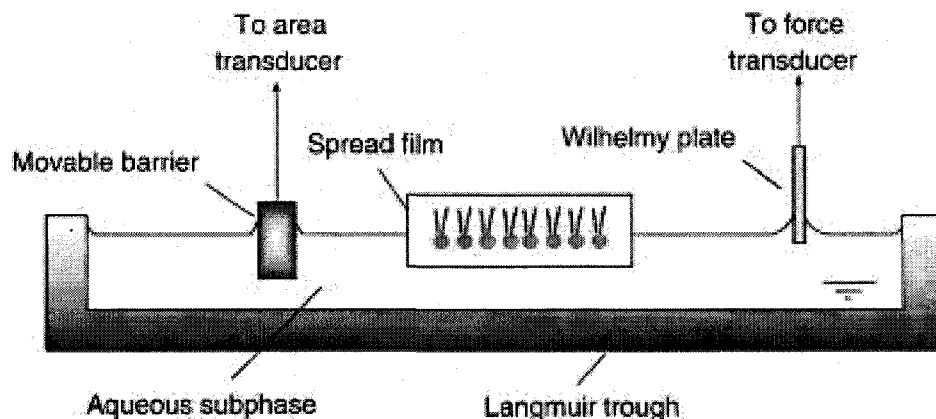


Figure 2.1 Langmuir Wilhelmy Balance (from Zuo et al. 2008 (251))

2.2.1.1 Advantages of the Langmuir-Wilhelmy balance

Langmuir-Wilhelmy balance provides valuable information such as surface tension lowering ability, respreading, and hysteresis (difference in surface tension-area behaviour between compression and expansion) properties of surfactant films during compression and expansion at the air-liquid interface. Further, the LWB technique can be combined with other techniques such as fluorescence microscopy, Brewster angle microscopy, x-ray diffraction techniques and spectroscopic techniques that are used to investigate surfactant film behaviour. Also, by drawing mica sheets, glass slides, or cover slips perpendicular to the plane of the surface film one can create Langmuir-Blodgett films, which can readily be used for atomic force microscopy. This combination of techniques allows examination of molecular structure, molecular orientation, domain formation, topography, and electrical surface potential of the pulmonary surfactant at the air-water interface or films transferred to a solid support. Finally, it is an excellent method to investigate spread films because the amount of material deposited and the compression of the film can be controlled accurately (214,241,246).

2.2.1.2 Limitations of the Langmuir-Wilhelmy balance

The major limitation of the LWB is “film leaking.” In the Langmuir-Wilhelmy balance, high surface pressure is needed to achieve surface tensions approaching 0 mN/m, when the film material “creeps” on to the Teflon walls and barriers (250). This is quite problematic for the spread films containing cholesterol or films containing higher amounts of unsaturated phospholipids, and is also more significant at physiologic temperatures. Furthermore, possible compression-expansion rates of the LWB (1-10 minutes/cycle) are not close to physiological values (20 cycles/minute). The LWB is time

consuming, and it requires considerable expertise and meticulous cleanliness of the equipment.

As the surface area of the Langmuir-Wilhelmy balance is large, relatively large amounts of surfactant sample is required to conduct such experiments. Furthermore, there can be a problem with the measurement accuracy of the Wilhelmy dipping plate since it needs a 0° contact angle between the vertical dipping plate and the adherent fluid layer (251).

Several modifications were introduced to the Langmuir-Wilhelmy balance to overcome these limitations. In order to minimize “leaking,” new LWB is equipped with continuous Teflon ribbons or bands standing on the edge with a suitable shaped frame (249) and tight fitting barriers. To prevent the film from occupying interfacial areas (wall-liquid or barrier-liquid interfaces) other than the air-water interface, the walls can be primed with long chain di-saturated phosphatidylcholine and a solution of lanthanum chloride (252). This makes Teflon walls more hydrophilic below the water line.

2.2.2 The pulsating bubble surfactometer (PBS)

To overcome the limitations of the Langmuir-Wilhelmy balance, the PBS was invented by Enhorning and Adams in 1977 (253,254). A commercial version of the PBS is made by General Transco Cooperation, Lancaster, NY. The main component of the PBS is a small cuvette, in which a bubble communicating with the atmosphere is drawn into the surfactant suspension to be evaluated (214,246). In PBS (Fig. 2.2), a small air bubble is formed at 37°C in an aqueous suspension of surfactant held in a disposable polyacryamide sample chamber. The chamber holds only $20\ \mu\text{L}$ of the sample fluid and it

is immersed in a temperature-control bath. Then the pulled bubble diameter is maintained for 10 seconds to measure adsorption. The bubble is subsequently oscillated at a known rate between a minimum (0.4 mm) and maximum (0.55 mm) radius by means of a precision pulsator that moves sample fluid back and forth from the sample chamber. The cycling frequency is usually 20 cycles/minute, which is close to the normal breathing cycle rate, but PBS also has the flexibility to change the cycling frequency. During cycling, the maximum and minimum radii (R) of the bubble are monitored by a microscope. As the bubble communicates with the atmosphere, pressure gradient across the bubble (ΔP) is continuously measured with a pressure transducer. Using the Laplace equation, surface tension is calculated for a spherical interface:

$$\Delta P = 2\sigma/R$$

(ΔP = pressure difference across a spherical interface,
 σ = surface tension, R = radius of the bubble)

2.2.2.1 Advantages of the pulsating bubble surfactometer

The PBS is relatively easy to learn, simple to use, and a small amount of surfactant sample is needed (20 μL) compared to the Wilhelmy surface balance. It is very efficient and less time-consuming. One measurement can be obtained within 5 minutes. Therefore, the PBS has been commonly used for the quality control of clinical surfactants. In the PBS, experimental conditions (cycling rate, temperature, and humidity) can be adjusted to mimic the existing conditions found in lung alveoli. Also, the PBS can be used in static mode to measure adsorption of the surface film. In this case, surface tension is measured as a function of time immediately after formation of an air bubble. The PBS is a useful method to screen animal and clinical surfactant samples since it needs less sample.

2.2.2.2 Limitations of the PBS

Even though the PBS is superior to the LWB, it still has some limitations. A major disadvantage of PBS is that sample fluid can remain in the capillary when the bubble is formed, which leads to variable increases in effective surface area (255). During cycling, when the surface tension is close to 0 mN/m, the bubble deforms and loses its spherical shape. This is a source of error when calculating surface tension (256). Furthermore, surface leakage can occur in the inner surface of the tube at the plastic-air interface as well as in the outer surface of the tube at the plastic-fluid interface. Leakage in the inner surface of the tube can be minimized by keeping the tube dry (249). Another problem with the PBS is the lack of flexibility in assessing the surface activity. For example, the time set for adsorption is 10 seconds. Thus, clinical samples are subjected to cycling (contraction-expansion) before equilibrium surface tension value is attained (251).

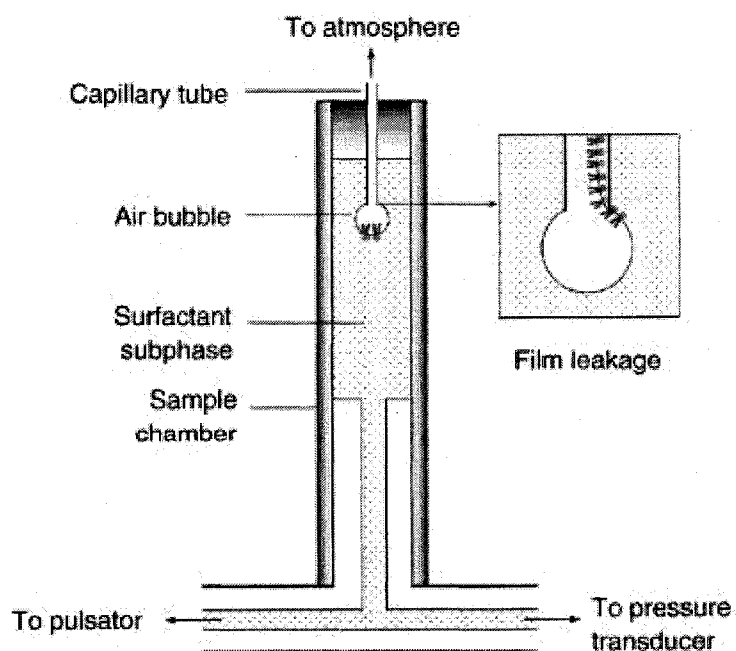


Figure 2.2 Pulsating Bubble Surfactometer (from Zuo et al. 2008 (251))

2.2.3 The captive bubble surfactometer (CBS)

The captive bubble surfactometer (CBS) (Fig. 2.3) was introduced by Schurch and coworkers in 1989 (243,250,244). The CBS is used for measuring surface activity, since *in situ* surface tension in the lung can be closely mimicked in this device (20). As the surface film is not interrupted by plastic walls, barriers, or outlets, the CBS is a leak-proof system. The CBS consists of a chamber, filled with buffered saline, and an air bubble floating against a convex agarose ceiling. Varying the volume in the chamber controls the volume of the bubble (243,250). As the volume is reduced, the surface area reduces and the surface tension of the bubble surface falls in the presence of a surfactant at the interface. Alterations in the surface tension at the air-liquid interface are visualized as a change in bubble shape, from nearly spherical at high surface tension to more flat as the surface tension falls. Unlike that of any other surface balance, the air-water interface in a CBS acts like a continuous surface. As a result, the interfacial film cannot escape the interface as long as the film does not collapse. The shape of the bubble is imaged over time by a video camera; the video frames are digitized by a frame grabber and saved to the computer's hard disk. The surface tension, area, and volume can be calculated from bubble height and diameter (260) using digital image processing based on the methods of Malcolm and Elliott (261) and Schoel et al. (260). Also, the axisymmetric drop shape analysis (ADSA-P) method can be used to obtain more accurate surface tension measurements (262). Furthermore, the CBS system can be used to conduct experiments in a quasi-static fashion similar to the procedures followed in the Langmuir-Wilhelmy balance. In addition, dynamic cycling frequencies can be chosen from extremely slow rates to very high rates such as 60 cycles/min.

A temperature-controlled jacket filled with water surrounds the sample chamber so that experiments can be performed at different temperatures.

Unlike other approaches, the CBS is able to obtain extremely low surface tensions with minimal area reduction on first compression using minimal amounts of surfactant. These stable, close-to-zero minimum surface tensions are consistent with those determined directly *in situ* in excised lungs (18,257).

In a CBS, surfactant film can be formed at the air-water interface of the bubble by two methods.

1. Adsorption from bulk suspension:

Adsorption from the bulk phase involves the formation of surfactant film at the air-liquid interface by surfactant molecules that are suspended in bulk liquid phase. The sample chamber is filled with a solution of known concentration of surfactant suspended in buffer. Then, an air bubble is formed in the sample chamber and left for 5 minutes until surface film forms at the air-liquid interface. The volume of the sample chamber in CBS is usually 0.5-1 mL. Surfactant concentrations used for this approach usually vary from as low as 50 $\mu\text{g/mL}$ or less to a maximum of 3 mg/mL (249). Usually surfactant samples are suspended in modified HEPES buffer (140 mM NaCl, 10 mM HEPES, and 2.5 mM CaCl_2 , pH 6.9). This method is suitable to investigate surface properties of surfactant samples with low concentrations. When the surfactant concentration increases, the subphase in the chamber becomes less translucent, making it difficult to detect the edge of the bubble. This leads to errors in bubble dimensions and as a result, errors in surface tension measurements as well. The surfactant concentrations, which are used in this technique, are much lower than the surfactant concentrations thought to be found in

lung alveoli (189). Thus, film formation in this approach is not closely reflecting surface film, which is present in lung alveoli.

2. Spreading of surfactant as a highly concentrated bolus:

This is a novel way to administer surfactant to air-water interface. This technique was developed by Dr.S.Schurch and first employed in a study of bat surfactant (263). Briefly, the sample chamber is filled with buffer and a small air bubble is introduced in to the chamber. next the bubble's air-liquid interface is brought into contact with a small but highly concentrated aqueous bolus of exogenous or endogenous surfactant using small Teflon tubing attached to a 10- μ L syringe (set up on a micromanipulator) (264). Then, approximately 0.05 μ L of concentrated surfactant is injected very close the air bubble interface. Higher surfactant concentrations that are closer to physiological conditions found in the lung alveoli can be investigated using this technique.

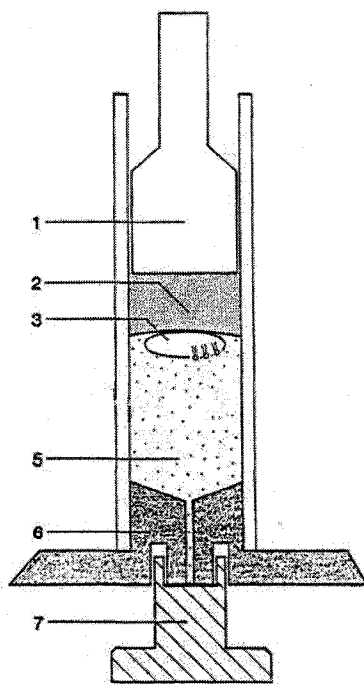


Figure 2.3 Captive Bubble Surfactometer: 1- Pressure tight piston, 2- Agarose gel, 3- Air bubble with surfactant, 5- Buffer, 6- Stainless-steel base, 7- Pressure tight plug

2.2.3.1 Surface activity parameters of CBS

1. Adsorption of surfactant film:

Depending on the concentration of phospholipids and the presence of surfactant proteins (SP-B, C), the rate of adsorption varies. Surfactant samples with high phospholipid concentrations reaches equilibrium surface tension (23-25 mN/m) within a few seconds. Quickly adsorbed surfactant films are of higher quality and stability, and have less compressibility.

2. Quasi-static cycles:

Quasi-static cycling commenced in the quasi-static portion of the experiment, in which the bubble can be compressed and expanded in a in a stepwise fashion by altering the hydraulic pressure in the chamber. This pressure can be changed by varying the chamber volume. Each step has two components: a 3-second change in volume followed by a 4-second delay where the chamber volume remains unchanged and the film is allowed to “relax.” There was a 1-minute inter-cycle delay between each of the four quasi-static cycles and a further 1-minute delay between the quasi-static and dynamic cycles.

3. Dynamic cycling:

In the dynamic cycle portion of the experiment, the bubble volume is smoothly varied for 20 cycles at a rate of 20 cycles/minute using the limits set (minimum and maximum bubble volume) in the last quasi-static cycle. Using dynamic data, the characteristics of dynamic surface tension-area isotherms, minimum and maximum surface tensions, and surfactant film compressibility can be obtained.

4. Assessment of film stability:

In the CBS, there are several methods to evaluate film stability at values of minimum surface tension near zero. Firstly, one can assess film stability by observing the “bubble clicking” at low surface tensions between 1 mN/m to 15 mN/m (265). Bubble clicking refers to a spontaneous and rapid increase in surface tension accompanied by a decrease in surface area. This indicates film instability, and is visualized as a rounding of the bubble (243). Based on Pattle’s pioneer observation (15), this phenomenon can be reproduced using the CBS.

Film stability can also be assessed by holding the captive bubble at minimum volume (minimum surface tension) and monitoring the bubble shape during a particular time period (i.e., 30 minutes). Then the surface tension vs. time graphs can be plotted. A stable film is able to maintain the minimum surface tension (γ_{\min}) without returning towards the equilibrium for a prolonged period (251).

2.2.3.2 Advantage of the CBS

Unlike the LWB and the PBS, the CBS is a leak-proof system (243). The CBS can be used to investigate the adsorption, quasi-static, dynamic behaviour of the surface film as well as its stability over time. In a CBS, the cycling rate, temperature, and surfactant concentration can be modified acutely to mimic conditions found in the lung alveoli. The CBS provides surface tension measurements that are very accurate.

Since a CBS can handle extremely small sample volumes (less than 1 μ L), it is ideal for investigating clinical samples and for studying surfactant inhibition.

Additionally, the CBS can be used to investigate the surface behaviour of surface associated surfactant reservoirs (243).

2.2.3.3 Limitations of the CBS

The CBS technique is time-consuming and the operation of a captive bubble surfactometer requires special training. Furthermore, data acquisition and analysis is more complex than in other techniques.

2.2.4 Microbubble stability test

The microbubble stability test is a reliable method to evaluate film stability at very low surface tensions. It was developed based on Pattle's observation of the unusual stability of microbubbles from the alveolar surface layer (15). Bubbles in water or serum normally collapse quickly due to the high-pressure difference across the air-fluid interface generated by surface tension. The remarkable stability of bubbles produced from lung extracts led Pattle to conclude that they contained an insoluble material which reduced surface tension to near 0 mN/m at the air-liquid interface (15).

In 1979, Pattle and his colleagues invented a method (microbubble stability test) to investigate the quality of pulmonary surfactant using human amniotic fluid. During the gestation of a fetus, components of the pulmonary surfactant, such as surfactant phospholipids and some surfactant proteins can be detected in human amniotic fluid. Pulmonary surfactant in amniotic fluid can generate microbubbles, which are less than 15 μm in diameter (266).

In this test, an aliquot (about 40 μL) of amniotic fluid or gastric aspirate is placed on a 76 mm x 38 mm microscope slide. A Pasteur pipette, with its tip touching the slide, is held almost vertically with the drop. The drop is sucked into and expelled from the pipette 20 times in rapid succession within a period of 6 seconds. This produces a good crop of bubbles. An aliquot of bubbles is immediately positioned onto a hollow slide, which is inverted so that a hanging drop is formed (266). Then, the slide is examined under a microscope and the number (n) of micro bubbles ($<15 \mu\text{m}$ in diameter) that are found in a 1-mm^2 field are counted. According to Pattle, if $n > 20$, respiratory distress syndrome (RDS) will not occur; however, if $n = 2-10$ or especially if $n = < 2$, there is a high risk of RDS (266, 249).

After the original works of Pattle, few refinements were added to the original method. Chida and Fujiwara reduced the bubble counting time to 2 minutes and then the test results could be provided within 10 minutes. The diagnostic accuracy of the test on amniotic fluid appears to be match favorably with that of biochemical and immunological tests. However, the test results rely on counting the absolute number of bubbles below a certain size, and this number also depends on the way the bubbles are produced (267). Subsequently, Berggren et al. (268) introduced a computer aided image analysis to evaluate the size distribution of microbubbles that can determine the median bubble diameter. According to his method, the samples were vortexed to generate microbubble. Using rabbit amniotic fluid, he observed that the median bubble diameter for the immature rabbit fetus at 27 days of gestation was $135 \mu\text{m}$, whereas samples from rabbits at 29 days of gestation were $76 \mu\text{m}$. This method is quicker and less time-consuming, so

it can be used for quick evaluation of the influence of different inhibitory substances on the surface activity of lung surfactant.

Fiori and colleagues extensively applied microbubble stability test with amniotic fluid, gastric aspirates, and tracheal aspirates (269,270,271). They too found accurate predictability for RDS.

2.3 *In situ* measurement of surface tension

2.3.1 Pressure volume relations

In 1929 von Neergaard demonstrated the importance of surface tension forces in lung mechanics (214). He compared the pressure-volume (P-V) relations of animal lungs inflated with air and with isotonic saline. Neergaard showed that the pressure required to inflate the lung to a fixed volume was greater when they it was filled with air than with saline. Inflating the lung with air at a fixed volume requires to work against tissue forces and surface tension forces. However, by filling the lung with saline removes the air-liquid interface that generates surface tension forces, leaving only lung tissue forces. The difference between pressure-volume (P-V) loops for saline and air thus reflects the contribution of surface tension forces to lung mechanics (214).

Due to the complexity of the alveolar lining, studying the P-V behaviour of an air-filled lung is quite complex. Tissue forces of the lung and surface tension forces act together under these conditions. Thus, it has been difficult to isolate the contribution of the tissue forces of the lung from the contribution made by surface forces. This surface forces directly contribute to the recoil forces of the lung and indirectly alter the configuration of the peripheral air space and the alveolar surface area. This increases the tissue forces of the lung (23).

Bachofen and co-workers compared the *in situ* P-V data and Langmuir-Wilhelmy surface balance data side by side. They observed some important aspects of P-V data that are not reflected in surface film data. Mainly, the hysteresis found in P-V data is not affected by cycling rate or by temperature as it does *in vitro* surface balance study. Also, the initial reduction of surface tension with change in area is much higher *in situ* compared to *in vitro*. Furthermore, they found that the film lining *in situ* is much more stable than the film in surface balance (249).

2.3.2 Measurement of surface tension *in situ* – microdroplet method

This method allows direct measurement of surface tension in an intact lung (18,20,243,86). A fluid droplet of known surface tension (fluorocarbon or silicon oil) can be placed onto the alveolar surface using micropipettes. Droplet shape is defined by the surface tension of the fluid lining of the alveolar surface. Such droplets spread to form a thin lens when their surface tension is similar to that of the underlying phase. Then the surface tension can be calculated from the relative diameter (d) of the droplet (Fig. 2.4) on the alveolar surface, divided by the diameter of the droplet in its spherical shape (d_0). Calibration of the test droplet with surfactant film on the Langmuir-Wilhelmy balance is pursued to accurately estimate the surface tension of the alveolar lining layer *in situ* (243). Under static conditions at a given lung volume, equal surface tension can be detected in all alveoli regardless of their sizes (243).

These microdroplet studies revealed that lung volume fluctuations during tidal breathing (e.g., between 40% and 50% of total lung capacity) were associated with only a slight increase in surface tension from 1 mN/m to 5 mN/m. They also showed that a large

inflation to total lung capacity resulted in alveolar surface tension values close to 30 mN/m which is slightly higher than equilibrium surface tension. When lung volume was reduced to functional residual capacity, or 40% of TLC, surface tension fell to less than 1 mN/m. This value was stable for a few minutes when the lung was held at this volume before rising gradually. Even after one hour, surface tension was less than 10 mN/m at residual lung capacity. This data shows that the surface film covering the alveolar surface is very stable (243).

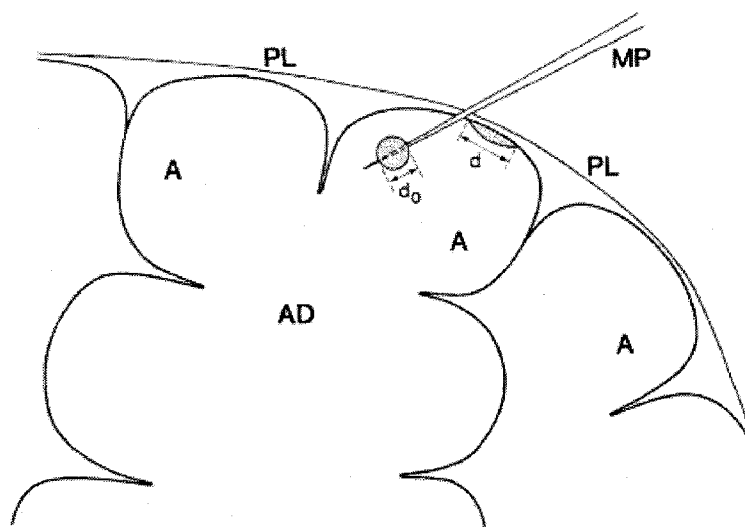


Figure 2.4 Determination of alveolar surface tension *in situ*. A test fluid droplet (e.g., perfluorocarbon fluid) is formed at the tip of a micropipette inside an alveolus. The diameter of the drop before deposition is d_0 . After deposition onto the alveolar surface, the drop spreads to a diameter d which is characteristic for the alveolar surface tension (From Schurch et al., 2001).

Chapter 3: Effect of Cholesterol on Lipid Extract Pulmonary Surfactant- *In Vitro* Study

3.1 Background

3.1.1 General introduction to cholesterol

Cholesterol is an important lipid molecule in animals, as it is both an essential constituent of the cell membrane and a precursor of many important biomolecules in the body. The liver is the major site of cholesterol biosynthesis in vertebrates, but all other cells in the body are capable of synthesizing cholesterol up to a certain extent. In contrast, complete cholesterol catabolism is limited to only a few organs, such as the liver and steroidogenic cells, in which cholesterol is converted to bile acid and steroid hormones respectively. Due to this, excess cholesterol molecules in other tissues must be removed and transported either to the liver or steroidogenic cells (272).

Extracellular cholesterol transport is usually done by plasma lipoproteins. The delivery of cholesterol from the liver to the peripheral cells is mainly performed by low-density lipoproteins (LDLs) via receptor-mediated endocytosis of the lipoprotein (273). However, a small proportion of cholesterol delivery is performed by high-density lipoproteins (HDLs) via the selective uptake of their cholesterol esters in certain organs (141,274). The release of cellular cholesterol also seems to be mediated by HDL. Thus, HDL is suggested to mediate “reverse cholesterol transport.” This pathway must exist since the cholesterol in most somatic cells cannot be degraded, and must instead be sent to the liver for conversion to bile acids. The most important step in this pathway is the release of cholesterol from the cells, which is vital for cellular cholesterol homeostasis.

There are two suggested mechanisms, which are responsible for this step. One is a non-specific cholesterol “efflux” from the cellular surface mediated by the physiochemical diffusion of cholesterol molecules via the aqueous phase, where net discharge of cellular cholesterol is governed by extracellular cholesterol esterification by lecithin cholesterol acyltransferase (LCAT) (272). The other mechanism is an assembly of new HDL particles with cellular phospholipids and cholesterol upon the interaction of helical apolipoproteins, which are present in HDL particle, with the cellular surface. A variety of specific cellular functions are needed in the cellular surface, including a cellular interaction site for apolipoprotein and specific intracellular cholesterol trafficking for this HDL assembly. This pathway seems to be the major source for plasma HDL (272).

Cholesterol is the major neutral lipid in lung surfactant with a concentration ~ 5-10 % by mass of surfactant (14-20 mol %) (141,214). It is responsible for 80-90 wt % of the neutral lipid compartment in pulmonary surfactant (141,214). Most vertebrates that are ectothermic (animals whose body temperature is not internally regulated) have variable body temperature (usually much lower) than eutherian mammals (warm-blooded mammals having a placenta). An ectothermic animal’s surfactant mixture needs more fluidity in order to compensate for its varying body temperature (141). Thus, its lungs are unlikely to be able to support a surfactant that is highly enriched in saturated fatty acids. Cholesterol seems to be the crucial lipid in lung surfactant that implicates these functions (274,275) in an ectothermic animal’s surfactant system. Thus, throughout the vertebrates, the cholesterol/phospholipid ratio is markedly variable (26). This variation is apparently due to the significant influence of temperature on lipids and lipid-lipid interactions (274,275).

3.1.2 The origin and metabolism of alveolar cholesterol

All mammalian cell cholesterol is derived from both serum lipoproteins and by *de novo* synthesis. Each cell might have a mechanism to sense the adequacy of the intracellular supply of cholesterol and adjust accordingly the activity of the regulatory step of *de novo* synthesis, which involves 3-hydroxy-3-methylglutaryl coenzyme A reductase (HMGCoA) (276).

Hass and Longmore (221) showed that 1% of surfactant cholesterol originates from *de novo* synthesis in the lungs, with the rest being derived from serum lipoproteins. Also, they found out that most, if not all, of alveolar surfactant cholesterol is derived through the lamellar bodies within type II pneumocytes. Finally, they reported that receptors for LDL and HDL were present in the lung and proposed that cholesterol metabolism in the lung may be regulated by serum lipoproteins (277). Later, Voyno-Yasenetskaya reviewed the role of lipoprotein using isolated alveolar type II cells and proposed that LDL and HDL affect the assembly and secretion of lung surfactant. Furthermore, he suggested LDL as the main cholesterol supplier to type II cells (276,278).

It is generally accepted that almost all surfactant components, including cholesterol, are secreted together when lamellar bodies are exocytosed. This notion is partly based on the observation that the lipid composition of a lamellar body is very similar to that of the alveolar surfactant fraction (279). Also, the turnover rates of the various phospholipids have been found to be very similar (280), implying that bulk uptake could be the mechanism accountable for surfactant turnover and recycling. However, the rapid

alterations that have been observed in the Cho/PL ratio suggest that alveolar cholesterol and DSP pools differ in their relative turnover rates.

Balasubramaniam and co-workers (281) administered an adenine analog, 4-aminopyrazolo(3,4d)-pyrimidine (AAP), to rats for 3 days and found that it could depress the hepatic secretion of the three main lipoproteins (LDL, HDL, VLDL). This in turn reduced serum cholesterol by >90%. Furthermore, they observed a 9-fold increase in cholesterol synthesis within the whole lung (276). Suzuki and Tabata (282) also treated rats with AAP for 3 days and observed the surfactant extracts of their lung homogenates. In these particular extracts, they found decreased amounts of PC and PG. However, they did not see any reduction in the amounts of cholesterol and other phospholipids.

Perrenazzo and co-workers (283) observed the rates of cholesterol clearance relative to phosphatidylcholine (PC) from the lung alveolar compartment. According to them, the clearance rates of both components are similar in the alveolar compartment, but PC clearance from lung tissue is higher than that of cholesterol. In contrast, by administering labelled cholesterol and DPPC, which were incorporated into lamellar bodies, Jones et al. investigated the rate of appearance of labelled cholesterol and DPPC in various lung fractions. From this, they reported that the turnover rate of cholesterol is much slower than that of DPPC (284).

Orgeig and co-workers (141,285) infused [^3H] cholesterol into the rat-tail vein and investigated the accumulation of labelled cholesterol in lamellar bodies and in the tubular myelin enriched fraction of the alveolar compartment. They observed that plasma-derived labelled cholesterol was very quickly incorporated into lamellar bodies, but very little was secreted into the alveolar compartment. In addition, they isolated

labelled lamellar bodies, ruptured them, and then separated the limiting membrane from the core of the lamellar body. Surprisingly, the limiting membrane comprised 76% of labelled cholesterol and the core contained the rest. As exocytosed, of lamellar bodies involve the fusion of the limiting membrane with the type II pneumocyte plasma membrane, the majority of the cholesterol in the lamellar body would remain with the type II cell and would not be secreted into the alveolar hypophase. Thus, cholesterol only in lamellar body core would secrete into the alveolar compartment. Therefore, although lamellar body cholesterol seems to be derived from serum cholesterol, most of it is not available for secretion into alveolar compartment. The cholesterol that is associated with the cell membrane may help with the processing and packing of phospholipids into lamellar bodies, as well as assist with their secretion (26). Therefore, in addition to lamellar bodies, there might be some other intracellular storage organelles for surfactant cholesterol. However, it is likely that most cholesterol is derived to type II cells via the LDL-receptor pathway (278). Although the type II cells are capable of *de novo* synthesis of cholesterol, it is unknown whether any of it is contributed to the surfactant system (26).

3.1.3 Biophysical properties of cholesterol

Cholesterol is a major neutral lipid, although small amounts of cholesterol esters, diglycerides, and triglycerides are also present in the lung surfactant. While the neutral lipids comprise a significant amount of surfactant weight, their function in surfactant is still uncertain. However, neutral lipids do influence overall system behaviour (214).

In most of the earlier studies, the biophysical properties of cholesterol were mainly focused on cell membrane function. Interaction between cholesterol and phospholipids is vital for cell membrane function and stability, and as such, these functions are applicable for pulmonary surfactant as well. The main effect of cholesterol on phospholipids seems to be through interactions involving fatty acyl regions. In surface films, the compact structure of cholesterol permits it to pack well between phospholipids molecules, especially between fatty acyl chains with kinks (unsaturated) (214). However, cholesterol can interrupt the tight packing in surface films composed of disaturated fatty acyl chains at high degrees of compression (214). One major property of cholesterol is its capability to reduce the phase transition temperature of lipids (286,141). This temperature-dependent phase transition generates changes in the physical state of lipids molecules and changes in the organization of the lipid molecules.

The transition temperature (T_m) is dependent on the degree of saturation, the chain length of the fatty acyl chains, the nature of the polar head groups of the phospholipid molecules, the hydration status of the membrane, and the presence or proportion of cholesterol (141,288). Adding cholesterol to the phospholipids reduces the T_m , a process that depends on the relative concentration and composition of the phospholipids (289). Increasing cholesterol concentration reduces the enthalpy change of the transition and it becomes less defined; later, it completely vanishes (141,288). The particular concentration of cholesterol where the transition vanishes is dependent mainly on the degree of saturation of the phospholipid acyl chains. This phase transition disappearance in the phospholipid-cholesterol mixture is associated with the formation of an intermediate state of fluidity in either the gel or the liquid-crystalline phase; at lower

temperatures, this occurs over a much broader range (141,288). Therefore, cholesterol has a profound effect on fluidity. Adding cholesterol to a phospholipid mix at below and above the transitional temperature gives rise to almost opposite effects on film fluidity. Adding cholesterol to phospholipids below T_m fluidizes the lipids, whereas adding it above T_m increases the rigidity of the film (141,290). Therefore, cholesterol tends to contribute to the balance of fluid and rigid lipids in lipid mixtures. However, Biophysical properties such as phase transition of cholesterol in simple lipid mixtures cannot apply directly to cholesterol association with lung surfactant since lung surfactant is a complex mixture consisting of a number of lipids and four surfactant-associated proteins.

Cholesterol esters also can affect bilayer and surface film behaviour, but they are less miscible with phospholipids than cholesterol. Hence, they have a lesser influence on biophysical behaviour (214).

In addition to the effects of cholesterol on fluidity, more recent biophysical studies on cholesterol have been focused on different aspects such as phospholipid film adsorption and film respreading. Using Langmuir films, Notter et al. showed that cholesterol enhances the adsorption of DPPC films and improves film respreading after collapse. Simultaneously, they reported that cholesterol also prevents archiving at very low surface tensions during film compression (214). Yu and Possmayer suggested that this negative effect of cholesterol could be due to the increase in the fluidity of the mixture and the ability of cholesterol to resist squeeze-out upon film compression (291,292,293).

Langmuir-surface films, which contain surfactant-associated proteins, phospholipids, and cholesterol form more complex films, thus giving very inconclusive

results. Taneva and Keough observed poor adsorption, respreading, impairment of surface activity, and less stability of these complex films (294). Yu and Possmayer obtained similar results with Langmuir films consisting of BLES and cholesterol (295). Note that BLES is a cholesterol-depleted commercial surfactant. Based on those results, cholesterol is removed from BLES and many clinically used surfactant preparations. However, it is obvious that cholesterol is endogenously present in surfactant and that very low surface tensions are obtained in the healthy lungs (19), which suggest that physiological amounts of cholesterol do not interfere with lung function *in vivo*. It is possible that the results, which were obtained in the Wilhelmy-Langmuir balance at 37°C and, with cholesterol, were influenced by film leakage (26).

Palmer et al. reported that there is a minimal negative effect on surface tension reduction when cholesterol is incorporated into BLES films (296). Similar results were obtained by Diemel using the captive bubble surfactometer. He concluded that adding a physiological amount of cholesterol has a very limited negative effect on adsorption and surface tension reduction in model surfactant (297).

Recently, Serna et al. demonstrated that a physiological amount of cholesterol is vital for organizing the lateral structure of membranes and surface films in lung surfactant (298). Furthermore, such lateral structures have the most favourable amount of surfactant-associated proteins needed in order to function optimally during dynamic lung functions. This result favours the notion that physiological amounts of cholesterol in endogenous lung surfactant play a physiological role.

A few other studies that used different animal models have shown that the amount of cholesterol in lung surfactant seems to be under dynamic regulation in response to

environmental conditions, such as body temperature or breathing regime (299,300). Different species carry a different proportion of cholesterol relative to phospholipids in their lung surfactant. Fascinatingly, cholesterol levels in pulmonary surfactant can vary very quickly. For instance, the hyperventilation induced in swimming rats lowers the cholesterol/disaturated PC ratio. An isolated perfused lung model reveals that there may be an alternate source of cholesterol other than the usual lamellar body mediated source of cholesterol, and that it can rapidly be mobilized by hyperventilation (301). Also, a decreased cholesterol/disaturated PC ratio can be seen in trained athletes during intense activity as compared to less fit individuals who showed an increase in this ratio (143).

Recently, several animal studies of lung injury models and a few human studies with ARDS have reported a high proportion of cholesterol in alveolar lavage (224,145,302), and alteration of intracellular cholesterol metabolism in type II pneumocytes and accumulation of cholesterol in the lung that is also seen in patients with cystic fibrosis (439).

Lipid-lipid interactions and lipid-protein interactions in lung surfactant are very complex, making them very difficult to study. Other important factors like the techniques that are used to investigate different experimental conditions, including temperature, concentrations of lipids and proteins, and the nature of the surfactant sample, also make the picture more complex to draw any firm conclusions about the functions and effects of cholesterol. Thus, we still do not have a clear picture of the biophysical role of cholesterol in lung surfactant. Further research is essential to unravel potential cholesterol-dependent mechanisms that modulate surfactant activity in a physiological context.

3.2 Objectives of the study

1. To investigate the role of cholesterol on surface properties of lipid extract surfactant *in vitro*.
2. To investigate the effects of cholesterol on the structure of the surface film of lipid extract surfactant at the air-liquid interface.

3.3 General hypotheses

1. There are no detrimental effects of physiological amount (5%-10% wt %) of cholesterol on surface properties of clinically used surfactants. Current removal of cholesterol from these surfactant preparations is at least unnecessary.
2. Excess amount of cholesterol (20% by mass) in pulmonary surfactant may affect negatively towards its function.

3.4 Specific hypotheses

1. Physiological amount of cholesterol does not destabilize the surfactant surface film at air-water interface.
2. Physiological amount of cholesterol reduces the surface tension during compression and does not increase the maximum surface tension during expansion.

3.5 Introduction

Cholesterol is present with 5-10% by mass (10-20 mol %) and comprises the major fraction of the neutral lipids. The role of cholesterol has remained controversial. In

a number of earlier studies, very low surface tension was not obtained in the presence even of physiological amounts of cholesterol (303,55,304,295,306,307,308,234,294). These studies for the most part used incomplete surfactant mixtures or less than optimal test procedures. However, based on these findings, cholesterol is currently eliminated from most of the clinically used surfactant extracts through acetone extraction and not added to artificial exogenous surfactants. But the stable near zero minimum surface tension has been found in the lung (20) and (18) , showing that cholesterol at physiological proportions does not interfere with surfactant function in the healthy lung. In accordance with these findings, Diemel et al. (297) showed no effect of cholesterol on the surface activity of an artificial surfactant of close-to-natural composition. More recently, others have observed similar results (298) and suggest that physiologically relevant amounts of cholesterol play essential role in surfactant function and should be investigated further.

To re-evaluate this disagreement on the functional role of cholesterol in physiological proportion, we investigated the effect of cholesterol on the surface activity of pulmonary surfactant by adding cholesterol to a clinically used exogenous surfactant. BLES is a hydrophobic extract of bovine lung lavage, which differs from natural surfactant in the absence of SP-A and -D and cholesterol (295). To better evaluate the role of cholesterol *in vitro*, an experimental protocol was followed that more closely resembles conditions in the lung. The captive bubble surfactometer (CBS) was used for measuring the surface activity; in that device; in situ surface tension in the lung can be closely mimicked (20). The CBS consists of a chamber filled with buffered saline and an air bubble floating against a convex agarose ceiling. Changing the volume in the chamber

controls the volume of the bubble. As the volume is reduced, the surface area reduces and the surface tension of the bubble surface falls in the presence of a surfactant at the interface. Variations in the surface tension at the air-liquid interface in the CBS are visualized as a change in the bubble shape from nearly spherical at high surface tension to more flat as the surface tension falls. Unlike in any other surface balance, the air-water interface in a CBS acts like a continuous surface. As a result, the interfacial film cannot escape the interface as long as the film does not collapse. This is important because surfactant films containing cholesterol have been shown to leak over barriers or spread along the restraining walls in other surface balances at high film pressure (i.e., low surface tension) (250) and (265). The pulsating bubble surfactometer can experience film leakage as well, though special measures can be employed to minimize this problem (255) and (310). Thus, it is difficult to distinguish the effect of film leakage from that of dysfunctional surfactant when either technique is employed.

We also studied whether cholesterol interferes with surfactant function at higher-than-physiological proportions. Such interference has so far been investigated mainly with regard to serum proteins (for reviews, see 311,312). But proteins alone have been found to have a very limited inhibitory effect on surfactant function (310,313). Observing at the very early stages of acute lung injury, Davidson et al. (302) reported a number of very rapid changes in the lung starting immediately after injury. These changes included increases in protein and significant increases in cholesterol. Panda et al. (145) also reported an enhanced level of not just serum protein but cholesterol as well with respect to phospholipids in acutely injured lungs, as compared to normal lungs. The injured lungs were also distinct by a marked decrease in compliance indicating most likely a

dysfunctional surfactant. Though the authors attribute this impairment primarily to blood serum proteins, they do note the possibility that the decrease in lung compliance could be due to excess cholesterol or to the action of proteins in combination with cholesterol. Lewis and Veldhuizen (312) also indicated the possibility that the role of cholesterol in surfactant inhibition when they note that “Changes to neutral lipids have not been studied extensively to date.”

In this study, surfactants were administered to the air-water interface in a novel manner, developed in our lab and first employed in a study of bat surfactant (263). The bubble’s air liquid interface was brought into contact with a small but highly concentrated aqueous bolus (27 mg/ml phospholipids with 0%, 5%, 10% or 20% by mass cholesterol added). The lower cholesterol amounts of cholesterol represent healthy lung levels and 20% cholesterol is the amount reported for injured lungs. We monitored the change in the surface tension upon spreading and then upon a slow (quasi-static) change in area. Finally, the area was cycled as in normal breathing.

3.6 Materials and methods

3.6.1 Materials

BLES (BLES Biochemicals Inc., London ON; see Yu et al. (295 and Fig.1.1b) for analysis of BLES composition) in non-buffered normal saline (pH 5-6) with a phospholipid concentration of 27 mg/ml was a kind gift by the manufacturer (BLES Biochemicals Inc., London, ON). Cholesterol was purchased from Sigma Chemicals, St. Louis, MO. A 1:1:1 ratio solution of methanol, chloroform, and BLES by volume was first vortexed and then spun at 100×g for 5 min. The bottom BLES/chloroform phase was

removed and saved. Then a second volume of chloroform was added to the methanol/water phase, which was then vortexed and spun like previously. The methanol/water phase was discarded and the BLES in chloroform was removed and added to the saved BLES in chloroform, and then 0, 5, 10 or 20% of cholesterol (by mass) with respect to phospholipids in chloroform was added. Each solution was then dried under N₂ and re-suspended in known volume of buffer (140 mM NaCl, 10 mM HEPES and 2.5 mM CaCl₂; pH 6.9) to obtain an aqueous suspension of BLES and cholesterol at a concentration of 27 mg/ml phospholipids. The samples with no extra cholesterol added were treated in the same way except that the final addition of chloroform before drying contained no cholesterol. Thus, the treatment required to add extra cholesterol would not likely be responsible for the differences found between samples with different amounts of added cholesterol. This same procedure was also employed to add DPPC or DOPC to the BLES.

3.6.2 Surface activity assessment

The surface activity of the BLES mixture was determined using a laboratory-built, fully computer controlled CBS evolved from the apparatus described earlier (314). The chamber of the CBS was filled with a buffer solution (140 mM NaCl, 10 mM HEPES, and 2.5 mM CaCl₂, pH 6.9) containing 10% (by mass) sucrose, to increase the density of the buffer solution (1.04 g/ml) above that of the surfactant (1.01 g/ml). Approximately 0.05 μ l of BLES-cholesterol mixture (27 mg/ml in buffer) was deposited at the concave agarose ceiling of the chamber by means of a transparent capillary. This allowed

depositing a precise volume of surfactant under visual control. The surfactant remained at the ceiling due to the density difference between it and the buffer solution in the chamber. It has been shown previously that sucrose has no effect on the surface activity of pulmonary surfactant (263). To exclude a specific interaction of glucose with the surfactants used in the current study, the buoyancy of the subphase was altered by the addition of cesium chloride instead of sucrose as a control. Both ways of changing the density produced the same result (these results not shown).

After introducing the surfactant into the chamber, a bubble 2-3 mm in diameter was allowed to float up to the ceiling. The shape of the bubble was imaged over time by a video camera (Pulnix TM 7 CN), and the video frames were then digitized by a frame grabber and saved to the computer's hard disk. During the experiment, the chamber was kept at 37°C. Prior to evaluation of each sample, the chamber was cleaned thoroughly by the combination of water and methanol and tested to ensure that no surface-active contaminants were present.

A 5-min adsorption (film formation) period followed the introduction of the bubble in to the sample chamber during which the bubble was not manipulated and the change in surface tension over time was monitored. The chamber was then sealed and the bubble was expanded to a volume of 0.15 ml. Five minutes after the bubble was expanded, quasi-static cycling commenced in the quasi-static portion of the experiment, in which the bubble size was first reduced and then enlarged in a stepwise fashion by changing the internal volume of the chamber. Each step had two components: a 3-second change in volume followed by a 4-second delay when the chamber volume remained unchanged and the film was allowed to "relax." There was a 1-min inter-cycle delay

between each of the four quasi-static cycles and a further 1-min delay between the quasi-static and dynamic cycles. In the dynamic cycle portion of the experiment, the bubble size was smoothly varied over the same range as the last quasi-static cycle for 20 cycles at a rate of 20 cycles/min. Bubble volume, interfacial area, and surface tension were calculated using height and diameter of the bubble as described (260). Tests were done with the quasi-static cycles omitted and the dynamic cycle results for samples with 0%, 10% or 20% cholesterol were unaffected by this omission.

3.7 Results

3.7.1 Adsorption (film formation)

Reduction of surface tension upon the adsorption of a surfactant is a measure of how fast this substance forms an effective film at the interface and so lowers its surface tension. With sufficient material, an equilibrium value will then be reached. Exogenous surfactant must be incorporated efficiently in the interface of a patient's lung to ensure structural stability of the lung's alveolar system and prevent lung injury. All samples studied here spread efficiently in accordance with this requirement. The bubbles rapidly assumed a new shape after they rose to make contact with the surfactant at the agarose ceiling of the chamber. An equilibrium surface tension of approximately 23 mN/m was reached within a few seconds at most (Fig. 3.1). There was no difference in the behaviour of surfactant samples with different amounts of cholesterol. In an effort to avoid an unphysiological large excess of material at the interface, the volume of the bolus placed in the chamber was kept very small (~0.05 μ l). Due to the small volumes involved, it was difficult to consistently place exactly the same amount of material at the agarose ceiling.

Thus, the amount of matter deposited varied slightly from sample to sample. Furthermore, at the concentration chosen, the samples of surfactant formed granules, 20-150 μm in diameter. A variety of phenomena suggest that these granules are particularly effective in film formation and that the surrounding matrix is minimally surface active. The small volume deposited contained only a small and likely variable number of these surfactant granules. This variability in the deposited amounts of surfactant became apparent upon compression and expansion cycles and is described below.

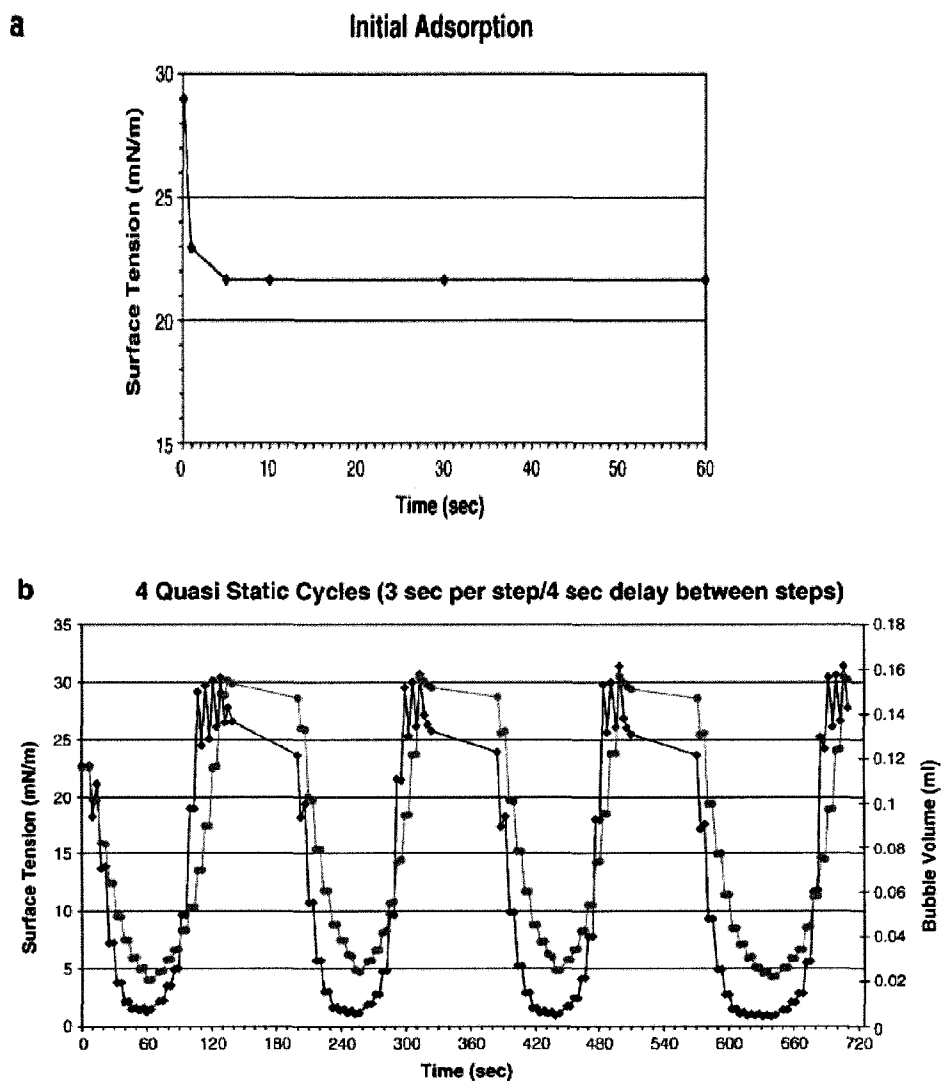


(Figure 3.1 cont'd ...)

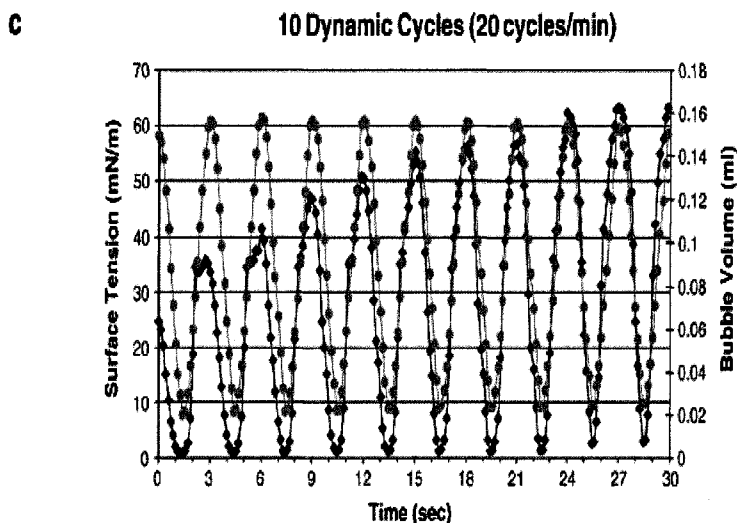


Figure 3.1 Illustration of the experimental procedure. Plots of the typical changes in surface tension over time in the *adsorption* (a), *Quasi-Static Cycle* (b) and *Dynamic Cycle* (c) phases of a sample test (BLES 27mg/mL). Measured bubble volume (grey lines) is plotted along with surface tension (black lines) in these last two graphs so that the changes in volume and the resulting changes in surface tension may be compared.

3.7.2 Quasi-static and dynamic compression and expansion of the pulmonary surfactant films

In the lung, the surfactant film at the air-water interface must reduce the surface tension to almost zero upon expiration. During tidal breathing, the change in relative interfacial area is small and the surface tension varies between almost zero and certainly less than 20 mN/m. (296). Hence, a functional surfactant must achieve a surface tension close to zero upon compression *in vitro* and must not return to equilibrium when kept compressed. We found that surfactant films formed from BLES containing 0%, 5%, and 10% cholesterol by mass all fulfilled these requirements and did so both under quasi-static and dynamic compression and expansion. No significant difference in the behaviour between these samples has been observed with respect to the minimal surface

tension achieved (see Fig. 3.2; Note: for simplicity the 5% cholesterol curves are not shown, as they are indistinguishable from the 0% curves).

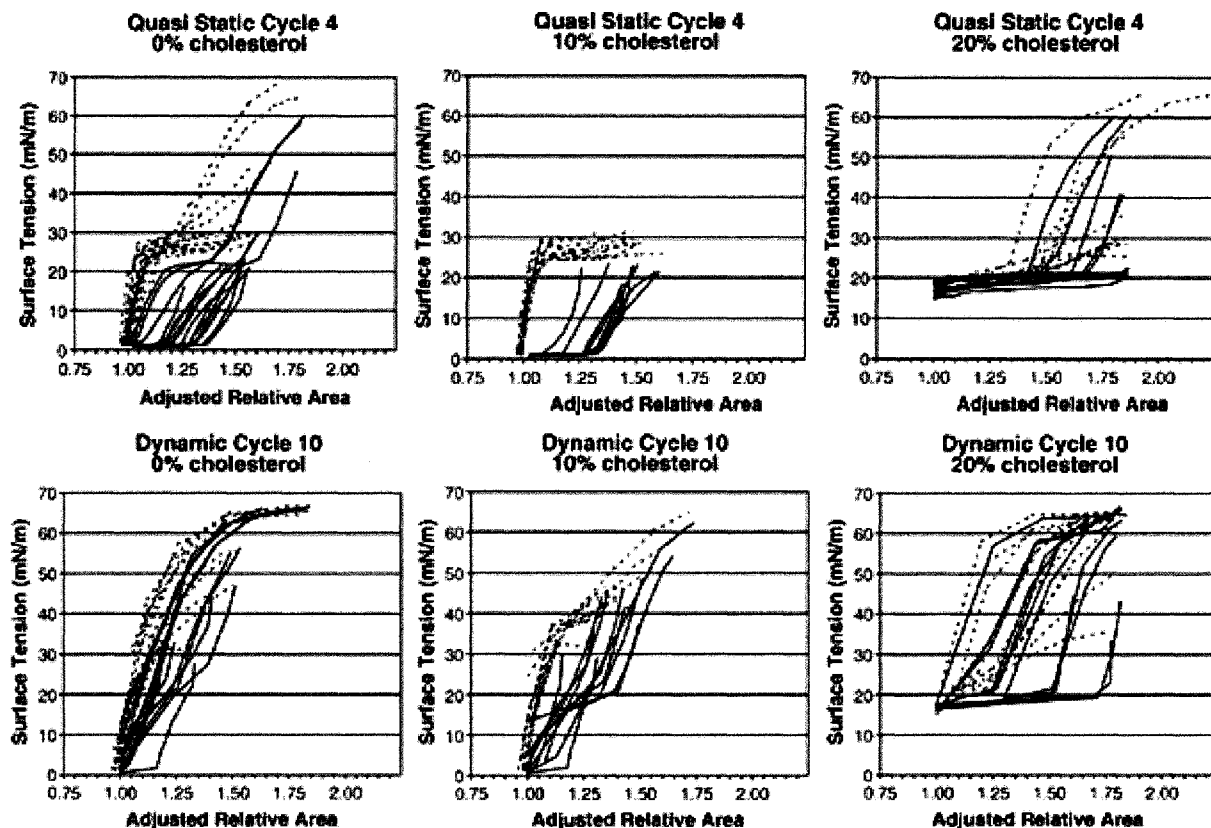


Figure 3.2 The compression phase (solid line) and expansion phase (dashed line) of quasi-static and dynamic cycles are plotted for the samples having either 0%, 10% or 20% cholesterol by mass. In the top row, the fourth of the repetitive quasi-static cycles (Q-stat) is shown (no significant difference between cycles occurred). The relative area has been normalized to be 1 at the end of the compression of the cycle. The bottom row shows the 10th of the series of repetitive dynamic cycles (no significant difference between cycles occurred). Each individual curve represents an individual sample.

Under quasi-static conditions, the films were compressed stepwise and allowed to equilibrate between each step (Fig. 3.2 top).

All samples containing less than 20% cholesterol achieve a surface tension close to zero. A few samples show a highly compressible region of the area-surface tension isotherm at a surface tension of about 23 mN/m (plateau region of the area-surface tension isotherm) and then the isotherm dropped steeply to the near zero minimum values (<2 mN/m). For the majority of these samples the isotherm first fell rapidly to the near zero value and declined only slightly with further reduction in area. Upon expansion, the surface tension rises with little increase in area to just above the equilibrium value. A plateau where surface tension increases only slightly with increased area follows this rise. For some samples, this plateau is relatively short and is followed by a relatively steeply rising segment in the isotherm to well above equilibrium values.

During dynamic conditions, the films were compressed and expanded at a rate that reflected normal breathing (20 cycles per minute; Fig. 3.2 bottom). Under these conditions, the samples containing less than 20% cholesterol all attained the near zero minimum surface tensions achieved when compressed in a Quasi-static manner. Some samples' isotherms declined steeply from maximum to minimum surface tension while a number showed an inflection near equilibrium surface tension. In some cases, the inflection was followed by a less pronounced compression plateau, while in the remainder the surface tension dropped smoothly though less steeply to the near zero minimum. For a limited number of samples, the isotherm showed a small inflection near 23 mN/m and a truncated and slightly steeper plateau near minimum surface tension than

was seen during quasi-static cycles. During dynamic expansion the isotherms rose rapidly to above equilibrium surface tensions with very small increases in area.

The films containing less than 20% cholesterol could sustain a very low surface tension for a long time. Following quasi-static and dynamic cycles, some of the samples were compressed to near zero surface tension and allowed to remain in that state for hours. During this time the surface tension did not rise, no matter whether the samples contained 0%, 5% or 10% cholesterol.

Samples containing 20% cholesterol did not achieve a low surface tension during compression. Those samples with above-equilibrium maximum surface tension behaved like the samples with lesser amounts of cholesterol when their surface tension was in this higher range. However, once the equilibrium surface tension of about 23 mN/m was reached, further film compression produced only a minimal reduction in surface tension below the equilibrium value for all samples. A minimum surface tension of about 16-20 mN/m was reached even after extensive compression. The minimum surface tension was not different for quasi-static and dynamic cycles.

In summary, 5% or 10% cholesterol by mass did not affect the most basic of pulmonary surfactant functions, that is, to reduce surface tension effectively and stably to a very low value. These samples behaved similar to samples containing no cholesterol. Samples containing 20% cholesterol did not reach low surface tension and so surfactant function was effectively abolished. In the following section, we discuss possible molecular mechanisms underlying the isotherms obtained with these samples and talk about the implications to human physiology and pathophysiology.

3.8 Discussion

3.8.1 Films, containing less than 20% cholesterol

Most samples reached equilibrium surface tension upon adsorption. A limited number of the samples showed maximum surface tensions well above equilibrium values. This indicated that the initial amount of surfactant, which was deposited, was insufficient for a full coverage of the interface. Interestingly, most of these samples showed a plateau near equilibrium surface tension during quasi-static compression. Amrein and coworkers have shown earlier that a plateau in this region of the isotherm may be due to the formation of lipid double-layer structures adjacent to a molecular monolayer at the interface (315,316). These surface associated structures have proven important to the stability of the interfacial film and are apparently a property of all functional pulmonary surfactant films (317,316). That is, only after the interfacial film of pulmonary surfactant has developed the specific molecular architecture of planar regions, interrupted or surrounded by areas consisting of stacks of multi-layers, does it become incompressible down to a very low surface tension and achieve its unique mechanical stability. Since we adsorbed a minimal and variable amount of surfactant, in some cases, the surfactant film was initially in the low-compressibility region of the isotherm (a sufficient amount of surfactant was initially adsorbed to the interface), whereas in other cases, the distinct architecture of the film first had to be created by compression (in the case when an insufficient amount had been adsorbed). These findings are in line with some earlier findings that multi-layers may form either during the adsorption of the matter to the interface or later, upon compression of the film, if an insufficient amount has been adsorbed to the interface in the first place (315). Whether the multilayer stacks have

formed upon adsorption or upon the first compression had no influence on the function of the films and all films showed comparably low compressibility below equilibrium regardless of their behaviour during the initial phase of the compression cycle. All but a few isotherms showed a plateau at low surface tensions and all showed a plateau in quasi-static expansion after first showing a very steep rise at the start of expansion. This plateau again reflects the formation (compression) and unfolding (expansion) of multiple lipid stacks adjacent to a planar film and the width of the plateau regions of the isotherm was variable from sample to sample (see Fig. 3.2). The variability in the plateau width was not correlated to the amount of cholesterol present in the sample. Rather, it was most likely caused by the variability in the amount of material, spread to the interface as described above. Despite there being some rather large area reductions after some of the samples reached near zero (<2 mN/m) surface tension values, this “over-compression” had no detrimental effect during the following cycles of expansion and compression. Rather, the slopes of the isotherms between the plateaus are quite similar both in the compression and expansion phase of the quasi-static cycle and show no relation to the length of the plateau.

All samples containing less than 20% cholesterol also achieved the same near zero surface tensions during dynamic cycles but generally achieved much higher surface tension levels in expansion than found in quasi-static expansion. The plateaus seen in quasi-static cycles were either absent in dynamic cycles or mostly replaced by more steeply sloped portions in the isotherm. Our explanation of the attenuated or missing plateaus is that during the more rapid dynamic cycles, there is insufficient time for a complete unfolding of multi-layers into a simple film at the air-liquid interface. As a

consequence, a very high surface tension occurs at the end of the expansion cycle. It is notable that in the lung, such unphysiologically high surface tensions will not occur because the area change during normal breathing is much less than employed here.

3.8.2 Films containing 20% cholesterol

Samples with 20% cholesterol by mass behaved similarly to those with less or no cholesterol during the initial part of bubble compression when surface tension was above equilibrium. However, after achieving equilibrium, there was limited reduction in surface tension. During expansion, any increase in surface tension that did occur was observed only after notably greater increments in surface area. No restoration of the low-compressibility region of the isotherm was achieved with samples containing 20% cholesterol even after spreading a large excess of matter to the interface or compressing the film over a very large range (data not shown). In a physiological sense, this surfactant was dysfunctional. The isotherms imply a continuous transition of a planar film into a multi-layered film upon compression and an unfolding upon expansion, without ever reaching a conformation, where the film becomes incompressible. Alternatively, multilayers may not have formed in the first place and matter was lost from the interface upon compression and then reabsorbed upon expansion.

Films containing 20% cholesterol would not allow for structural stability in the lung because of the insufficient reduction of surface tension. This breakdown of surfactant function at a higher proportion of cholesterol is very intriguing both for its implication for diseases and with respect to the molecular mechanism behind this phenomenon. Correlating our findings to the observations made by Panda et al. (145) strongly suggests that cholesterol is a contributing factor for surfactant inhibition in

acutely injured lungs. Similar to the current study, approximately 10% cholesterol (mass) with respect to total surfactant lipids was associated with normal lung compliance and approximately 20% cholesterol was associated with low lung compliance after acute lung injury. Panda et al. found protein level with respect to lipids was also increased in surfactant recovered from injured lungs. This leaves the possibility that proteins possibly in conjunction with cholesterol, originating most likely from blood plasma, were contributing to the inhibitory effect. There is reason to believe that plasma proteins by themselves may not have as marked an inhibitory effect on surfactant function as cholesterol alone (e.g., 313) though elevated amounts of proteins in combination with cholesterol may also be potent inhibitors of surfactant function.

3.8.3 How cholesterol interacts with the molecular components of pulmonary surfactant

Surfactant functions in the current study deteriorated in an all- or non-fashion with increased amount of cholesterol. Films containing 10% by mass of cholesterol or less all reached a very low surface tension (<2 mN/m), while all films containing 20% of cholesterol, in contrast, did not drop below 16 mN/m. To explain this behaviour at the molecular level one needs to take into account the way cholesterol is incorporated within the molecular architecture of the surfactant film at a physiological level and at an elevated level. Cholesterol has a very distinct effect on the molecular arrangement of surfactant films even at a low concentration as revealed by atomic force microscopy and fluorescence light microscopy (293,297,319). For example, compression of films of purified calf surfactant phospholipids caused phase separation with large circular

condensed domains of DPPC (318). When cholesterol was added to these films, the size of the domains decreased and with further compression, apparent phase separation vanished and the films appeared homogeneous under a fluorescence light microscope. This major influence of the lateral distribution of surfactant components brought about by cholesterol was attributed to the reduction in line tension of the dividing line between the DPPC domains and the fluid matrix (318). In their study, Discher et al. predicted from theoretical considerations that cholesterol should associate with DPPC rather than the more fluid matrix. This is highly plausible, as the planar cholesterol molecules of the plasma membrane are known to associate with the aliphatic groups of saturated lipids in sphingolipid cholesterol rafts. Tolerance of up to 10% cholesterol for functional surfactant and a breakdown of function above that proportion might be related to the saturation of the DPPC domains with cholesterol, i.e., cholesterol might not degrade the ability of the interfacial film to withstand a high film pressure as long as it is intercalated in-between the aligned, saturated aliphatic tails of DPPC. However, once exceeding the maximum possible stoichiometry of this complex and being forced to interact with unsaturated lipids or the surfactant protein C and/or surfactant protein B, cholesterol might abolish the ability of the film to withstand compression. To test the plausibility of this hypothesis, we increased the amount of DPPC in BLES containing 20% cholesterol such as to restore a physiological ratio of DPPC to cholesterol. As a result, the adverse effect of the high proportion of cholesterol was indeed reversed and 8 out of 10 of these samples reached a surface tension < 2 mN/m upon compression but with high film compressibility (Fig. 3.3). To ensure that restoration of surfactant function was not because cholesterol was now merely diluted in a proportionally larger phospholipid fraction, we substituted the

additional DPPC with DOPC as a control. Adding the same amount of DOPC to BLES containing 20% cholesterol did not restore surfactant function (Fig. 3.3) as only one sample reached near zero surface tension though three other samples did reach substantially lower levels than seen in samples with 20% cholesterol added. Note that DOPC, while otherwise identical to DPPC, has two unsaturated aliphatic tail and should therefore prevent efficient intercalation of cholesterol in the aliphatic tail region. Still, these materials did have some effect on surface activity of their own which affected a small proportion of the samples in each case. de la Serna et al. (298) provide suggestions as to possible mechanisms for these effects. As another control, increasing the proportional level of DPPC or DOPC in BLES without the addition of cholesterol did not affect surface activity of BLES in any way (Fig 3.4). Together, these findings suggest that a physiological proportion of cholesterol is indeed accommodated in the surfactant film by forming a complex with DPPC. Assuming the correctness of this interpretation, it still remains an open question why cholesterol in a complex with DPPC should be benign with respect to surfactant function, whereas cholesterol not associated with DPPC abolishes surfactant function.

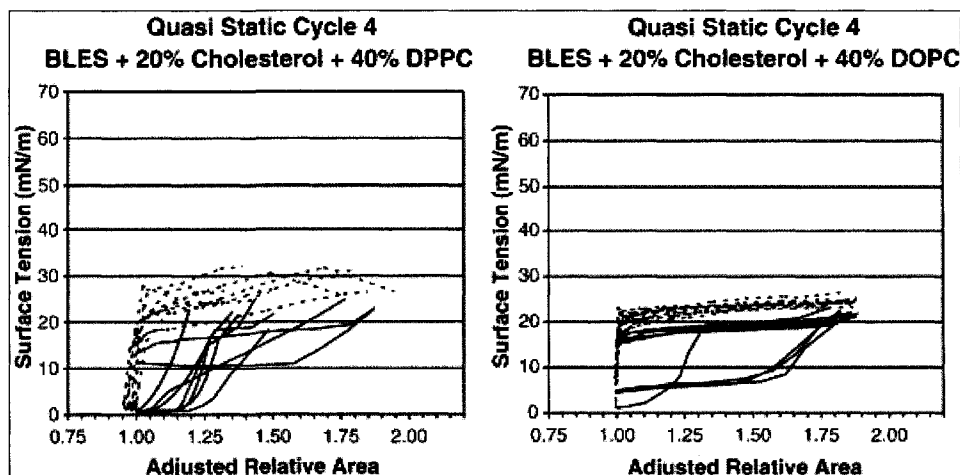


Figure 3.3 Surface activity of BLES containing 20% cholesterol by mass after the addition of DPPC or DOPC. The amount of DPPC or DOPC added corresponded to 40% of the mass of the cholesterol-containing sample. The maximum natural molar ratio of approximately 1:2 (cholesterol/DPPC) has therefore been reestablished for these samples. The fourth of the repetitive quasi-static cycles (Q-stat) is shown. The relative area has been normalized to be 1 at the end of the compression of the cycle. Each individual curve represents an individual sample.

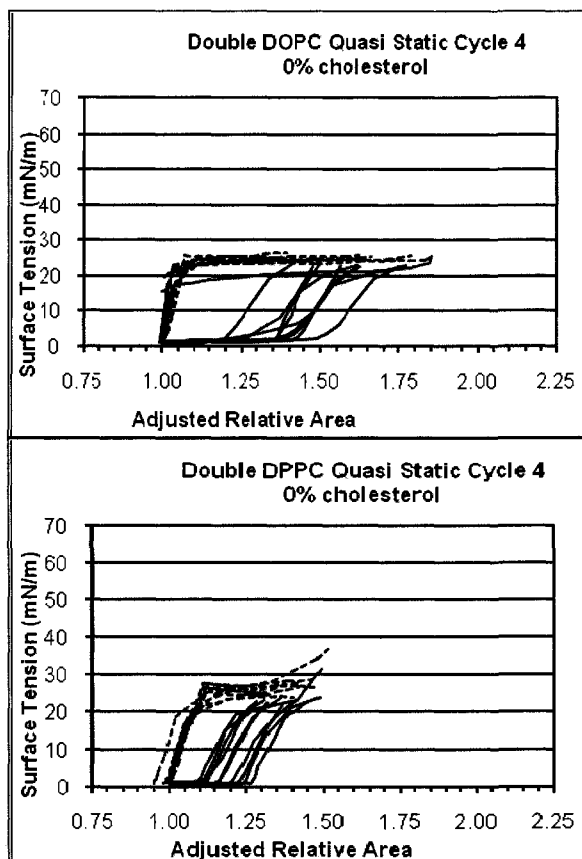


Figure 3.4 Surface activity of BLES after addition of DPPC or DOPC. The amount of DPPC or DOPC added corresponded to 40% of the mass of the BLES sample. The fourth of the repetitive quasi-static cycles (Q-stat) is shown. The relative area has been normalized to be 1 at the end of the compression of the cycle. Each individual curve represents an individual sample.

3.8.4 The role of physiological amounts of cholesterol

While no detrimental effect of physiological amounts of cholesterol has been found in this study, a beneficial function of physiological cholesterol levels within

surfactant has not been identified, except for some special cases. Indeed, such function has been established for animals such as bats and dunarts whose body temperature may change rapidly. For these animals, the level of cholesterol optimises surface activity of surfactant for strongly changing body temperatures down of low values to approximately 15°C (263,320,321). Cholesterol also has a function in pinniped lungs'to accommodate the special requirements of deep diving (322). It appears that results, which showed a deleterious effect of cholesterol on surfactant surface activity, in which low minimum surface tensions were not achieved, were often obtained with simplified surfactant mixtures and almost always obtained in the Langmuir troughs or in the pulsating bubble surfactometer without taking measures to minimize film leakage. It is conceivable that in these devices the cholesterol-containing films were able to spread along the restraining walls and barriers (film leakage) while similar films with no cholesterol did not. It should be noted that a difference in film leakage would not be due to a mere difference in surface viscosity. Films of BLES with physiological amounts of cholesterol added to them are not different with respect to surface viscosity from films containing no cholesterol (145,323). Nevertheless, an increased ability of cholesterol-containing surfactant films to spread over restraining walls in the Langmuir trough might reflect a property related to the spreading of surfactant films evenly across the highly structured lung with its tiny cavities and narrow airways.

3.9 Conclusion

The current study establishes that cholesterol at physiological proportions has no detrimental effect on the surface activity of pulmonary surfactant, notwithstanding its

marked influence on the molecular architecture of the interfacial films formed. A beneficial function of physiological amounts of cholesterol in the human lung, however, has yet to be discovered. However, recent studies have indeed established a role for cholesterol in several mammalian species such as bats (321), pinnipeds (322), and other species (323).

At an elevated level, cholesterol abolishes one of the lung surfactant's most important functions, that is, the ability to reach near zero surface tension. This finding may bring about a change in the paradigm how surfactant inhibition is explained and, eventually, treated in the case of acutely injured lungs and possibly in other conditions with impaired surfactant function as well. Until now, surfactant inhibition has largely been attributed to factors other than cholesterol. Clearly, the role of cholesterol in normal lung function and in conditions where surfactant function has been compromised requires careful re-evaluation with the best methodologies currently available.

Chapter 4: Effect of Methyl Beta Cyclodextrin (M β CD) on Dysfunctional Surfactant Films due to Cholesterol

4.1 Background

4.1.1 Cyclodextrins

Cyclodextrins (also known as as cycloamylose) belong to a family of cyclic oligosaccharides. They are composed of 5 to 8 α -D-Glucopyranoside (dextrose) units linked by 1 \rightarrow 4 linkages, as in amylose (325).

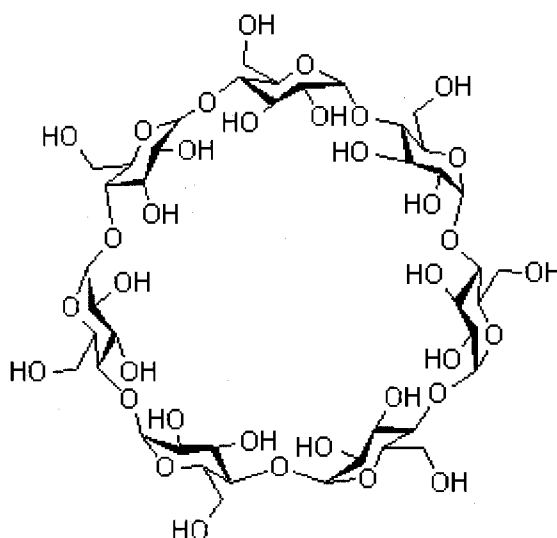


Figure 4.1 Beta cyclodextrin molecular structure (adopted from <http://www.chemblink.com/products/68168-23-0.htm>)

Cyclodextrins are produced from the enzymatic degradation (fermentation) of starch. This process leads to the formation of a mixture of monosaccharides, disaccharides, and various oligosaccharides, such as linear and branched dextrans (324). Under certain conditions, small amounts of cyclic dextrans (cyclodextrins) are also formed during this degradation process. The first written record on cyclodextrin was

published in 1891 by the French scientist A. Villiers. He isolated 3 g of crystalline substance from the bacterial degradation of 1000 g of starch, and named this crystalline substance “cellulosine” (324). It is now believed that he found a mixture of α - and β -cyclodextrins. However, it was F. Schardinger who specifically identified, α , β , cyclodextrins, which are the two naturally occurring cyclodextrins. Later, Freudenberg discovered the γ - cyclodextrin (324). It was discovered that a certain type of amylase known as, cyclodextrin glucosyl transferease (CGTase), was involved in the production of these cyclic dextrans (324). Certain microorganisms such as *Bacillus macerans* can produce CGTase (324). Pringsheim then demonstrated that cyclodextrins can form stable complexes with a number of chemicals. From the 1970s onwards, Szejtli and others could utilize cyclodextrins and their derivatives for many industrial and pharmacologic applications (324,325).

4.1.2 Structure of cyclodextrins

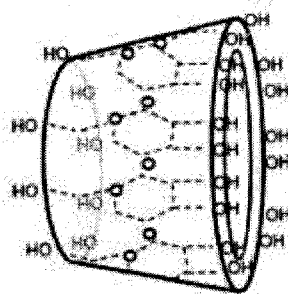


Figure 4.2 γ -CD toroid structure showing spatial arrangement (adopted from <http://en.wikipedia.org/wiki/Cyclodextrin>).

Cyclodextrin molecules are topologically represented as toroids, with the larger and the smaller openings of each toroid exposing secondary and primary hydroxyl groups

to the solvent respectively (326). Due to this arrangement, the inner core of the toroid is not hydrophobic, but it is still considerably less hydrophilic compared to the aqueous environment. Thus it is able to host other hydrophobic molecules (guest molecules) and form complexes with them. On the other hand, the exterior is sufficiently hydrophilic to impart cyclodextrins (or their complexes) water solubility. The formation of inclusion complexes greatly modifies the physical and chemical properties of the guest molecules, mainly in terms of their water solubility. On account of this, cyclodextrins have attracted much interest in the food and pharmaceutical industries, as well as many other industries. In the food industry, cyclodextrins are used for the preparation of cholesterol free products. The bulky hydrophobic cholesterol molecule is easily accommodated inside the cyclodextrin ring, which can then be removed. Also, inclusion complexes of cyclodextrins with hydrophobic molecules are able to penetrate body tissue; these can be used to release biologically active compounds under specific conditions. Some cyclodextrins are biocompatible, and can thus, be used readily in pharmaceutical applications (324,325,326).

4.1.3 Production of cyclodextrins

Amylase enzymes from *Bacillus macerans* react with starch to give rise to a crude mixture of α -cyclodextrins (~ 60%), β -cyclodextrins (~20%), and γ -cyclodextrins (20%) (309). With the biotechnological advances made in 1970, M β CD production was dramatically improved. Genetic engineering techniques allow for the production of more active and specific types of CGTases, which can in turn produce more purified versions of α -, β -, and γ -cyclodextrins than previously used enzymes (324).

4.1.4 Cyclodextrin derivatives

The aqueous solubility of α -, β -, γ -cyclodextrins is much lower than that of comparable linear dextrans (324). This is due to the relatively strong binding of cyclodextrin molecules in crystal states. Also, β -cyclodextrin molecules possess intramolecular hydrogen bonds that weaken their ability to form hydrogen bonds with the neighbouring water molecules. In order to overcome this limitation, some chemical modifications were introduced to water-soluble cyclodextrin derivatives. The substitution of any of the hydroxyl groups, even by hydrophobic moieties such as methoxy functions, resulted in a marked increase in their aqueous solubility. Thus, increasing the degree of methylation enables the solubility of β -cyclodextrin to increase until about 2/3 of all the hydroxyl groups have been methylated, whereupon solubility decreases upon further methylation (332). The methylated derivative of β -cyclodextrins (M β CD) is widely used as a cholesterol-sequestering agent in many clinical applications. M β CD removes cholesterol from cultured cells, and it is also employed to disrupt lipid rafts by removing cholesterol from the cell membrane. Furthermore, Atger and co-workers used cyclodextrins as catalysts for the removal of cholesterol from macrophage foam cells (324).

4.1.5 Inclusion and non-inclusion complexes

Aqueous solutions of cyclodextrins can form inclusion complexes in which water molecules located within the lipophilic central cavity are replaced by lipophilic guest molecules or lipophilic moieties. The guest molecule within the CD (cyclodextrin) forms a complex with CD by van der Waals interactions, and occasionally by hydrogen bonds. Different types of CD molecules have cavities of different sizes and axial lengths.

Thus, a given guest molecule can complex with the most appropriate host CD molecules (324,325,326).

The hydroxyl groups on the outer surface of the cyclodextrin molecule are able to form hydrogen bonds with cyclodextrin and other molecules (non inclusion complexes). They form water-soluble complexes with lipophilic water-insoluble compounds (333,334). For example, α -cyclodextrin forms both inclusion and non-inclusion complexes with dicarboxylic acids, and the two complexes coexist in aqueous solution (335). In saturated aqueous solutions guest/cyclodextrin complexes often consist of a mixture of inclusion and non-inclusion complexes. This could explain why the value of the equilibrium constant for complex formation is sometimes concentration dependent (324,336). For a number of reasons that include toxicological considerations and production costs it is important to use the smallest amounts of cyclodextrins possible in biological and pharmaceutical formulations (324). Therefore, a number of methods have been introduced to enhance the complexation efficiency (or rather the solubilization efficiency) of cyclodextrins. The formation of cyclodextrin complexes is an equilibrium process where free guest molecules are in equilibrium with molecules in the complex (324). Increasing the solubility of the guest molecule via ionization, salt formation, and the addition of organic co-solvents to the aqueous complexation will lead to enhanced complexation efficiency in aqueous cyclodextrin solutions saturated with the guest molecules (324).

This formation of an inclusion complex, which is usually a 1:1 interaction, is often described by the following equation:



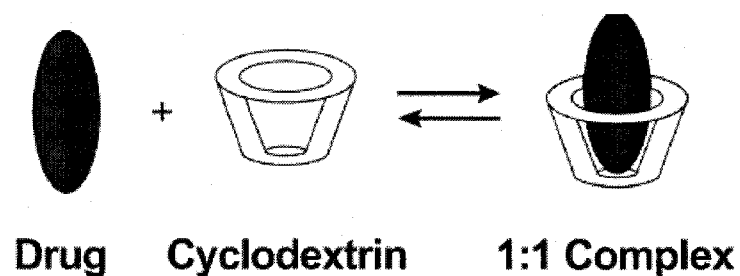


Figure 4.3 Equilibrium binding of a guest molecule with cyclodextrin to form a 1:1 inclusion complex (adopted from Stella et al., 2008 (325)).

In forming the complex, the physiochemical and biological properties of the guest molecule can be altered to create an advantage. If the guest is poorly soluble in water, and if it is able to form a complex with the CD, then its solubility in most cases will change as a function of CD concentration (325).

4.2 Summary of the study

The primary function of pulmonary surfactant is to reduce the surface tension of the air-lung interface to values that are close to zero. However, this is impaired in adult respiratory distress syndrome (ARDS), which results in diminished lung compliance, decreased lung volume, severe hypoxemia, and the release of inflammatory mediators by the lung. Such dysfunction coincides with a two- to five-fold increase in cholesterol in the surfactant of patients with ARDS. The increased level of cholesterol on its own or together with other factors causes surfactant failure. In our current study, we investigated whether inhibition by cholesterol can be reversed *in vitro* by exposing the dysfunctional surfactant to methyl- β -cyclodextrin (M β CD). We used bovine lipid extract surfactant (BLES) as the model of functional surfactant, and BLES with 20% w/w cholesterol added

(chol-BLES) to model surfactant found in ARDS. To test for function, the surfactants were spread at the air-buffer interface of a captive bubble surfactometer (CBS) and the surface tension was measured as a function of interfacial area. In the absence of M β CD, chol-BLES was dysfunctional and a value of surface tension below 16 mN/m could not be obtained. However, in the presence of 20 mMol M β CD in buffer, chol-BLES immediately regained partial function. Surface tensions close to 0 mN/m were now achieved, albeit only upon an abnormally large area reduction. After three hours of exposure to M β CD, the films eventually exhibited lowered surface tension without any signs of functional inhibition, indicating that cholesterol had been effectively sequestered by M β CD in buffer. When complexed with cholesterol, M β CD could also be used to deliver cholesterol to BLES in the buffer (“water soluble cholesterol”) and render it dysfunctional, similar to the effect of chol-BLES. We discuss the use of M β CD as a diagnostic substance and whether M β CD or its functional or structural analogues are amenable as therapeutic substances in ARDS.

4.3 Introduction

Acute respiratory distress syndrome (ARDS) is a common and devastating spectrum of disease that has a high overall mortality rate. The published, population-based incidence of ARDS ranges from 1.5 to 5.3/10⁵ population/year with a mortality rate of 36% to 60% (328,329,330,331). Since surfactant impairment is a major factor in the morbidity and mortality of ARDS, it has been targeted by replacement surfactant therapy. However, success has been minimal (for a review, see 312). This is likely because the exogenous surfactant also becomes inactivated in the affected lung. It is now generally

believed that successful treatment will depend on an in-depth understanding of the mechanisms of surfactant impairment.

In a recent comparative study on the causes of surfactant impairment, considering published alterations of surfactant in ARDS, we found an increased level of cholesterol as being particularly inhibitory (264). Cholesterol in surfactant is elevated from a physiological level of 5% to 8% w/w to about 20% w/w in animal models of lung injury (145) and 16% to 40% w/w in human ARDS (224). For a cholesterol level of 20% w/w surfactant was not functional in that surface tensions below 16 mN/m were not achieved (145). Dysfunction coincided with a distinct change in the molecular architecture of the film as seen with AFM (337). Functional surfactant assembled into a film with lipid bilayer stacks, cross-linked to a lipid monolayer. However, an elevated level of cholesterol inhibited the monolayer-bilayer conversion.

In our current study, which was performed *in vitro* under close-to-physiological conditions, we investigated whether impairment of surfactant films could be reversed by exposure to methyl- β -cyclodextrin (M β CD) in buffer. High concentrations of M β CD can extract substantial amounts of cholesterol from membranes and surfactant monolayers into a soluble cholesterol-cyclodextrin complex (327,298). On the other hand, an M β CD cholesterol-complex (“water soluble cholesterol,” molar ratio: cholesterol/M β CD \approx 1/7) is also commonly used to deliver cholesterol to the plasma membrane in cell cultures. This indicates that cholesterol in the plasma membrane and cholesterol in complexes with M β CD establish equilibrium.

The captive bubble surfactometer (CBS) was used for measuring surfactant function (surface activity), because it comes closest to mimicking lung function as

determined *in vivo* from pressure-volume studies (20). We investigated films formed from clinically used bovine lipid extract surfactant (BLES) (295). BLES contains all of the lipids of natural surfactant with the exception of cholesterol. In our experiments, we used BLES to reflect normal surfactant (control). We also added 20% w/w cholesterol to BLES (chol-BLES) in order to model the elevated amount found in diseased lungs (224).

4.4 Materials and methods

Surface activity assessment: The surface activity of the surfactant was determined using a laboratory-built, fully computer-controlled CBS evolved from the apparatus described earlier (244). The chamber of the CBS was filled with buffer solution (140 mM NaCl, 10 mM Hepes and 2.5 mM CaCl₂, pH 6.9), with or without M β CD as described below. Sucrose (10% w/w) was added to the buffer to increase its density so that the surfactant suspension would float and remain in contact with the bubble upon injection. Adding sucrose does not affect the surface activity of surfactant (264). Then, a small (0.035-0.040 ml) bubble was allowed to float up to the chamber's concave agarose ceiling, and ~0.05 μ l of surfactant was deposited at the air-buffer interface by means of a transparent capillary. This allowed a precisely defined volume of surfactant to be deposited under visual control. The bubble was imaged by a video camera (Pulnix TM 7 CN) and recorded for later analysis. The chamber was kept at 37°C during the experiment. Following the introduction of surfactant into the chamber, a 5-minute adsorption (film formation) period was carried out during which the bubble was not manipulated and the change in γ was monitored. The chamber was then sealed and the bubble was rapidly (1 sec) expanded to a volume of 0.13 ml. Five minutes after the

bubble was expanded, quasi-static cycling commenced. In the quasi-static portion of the experiment, the bubble size was first reduced and then enlarged in a stepwise fashion by altering the internal volume of the chamber. Each step had two components: A 3-second change in volume followed by a 4-second delay when the chamber volume remained unchanged, allowing the film to “relax.” There was a 1-minute inter-cycle delay between each of four quasi-static cycles, and a further 1-minute delay between the quasi-static and dynamic cycles. In the dynamic cycle portion of the experiment, the bubble volume was smoothly varied over the same range as the last quasi-static cycle for 20 cycles, at a rate of 20 cycles/minute. Bubble volume, interfacial area, and γ were calculated using height and diameter of the bubble as described in a previous study (260).

Surfactant: BLES (a kind gift from the manufacturer BLES Biochemicals Inc., London, ON. See Yu et al. (295 and fig. 1.1b) for an analysis of BLES composition) in non-buffered normal saline (pH 5-6) with added calcium and at a phospholipid concentration of 27 mg/ml was used with or without the addition of 20% w/w cholesterol (Sigma Chemicals, St. Louis, MO). Cholesterol cannot be added quantitatively to BLES while in aqueous suspension. Therefore, BLES was first taken up in organic solvent, cholesterol was added, and the mixture was returned into an aqueous solution as follows. A 1:1:1 solution of methanol, chloroform, and BLES by volume was first vortexed and then spun at 100 g for five minutes. The chloroform phase contained most of the BLES and was saved. For complete recovery of BLES, the water/methanol phase was extracted a second time with chloroform, and the two fractions of BLES in chloroform were pooled. Cholesterol in chloroform was added to this pool to a final concentration of 20% w/w with respect to BLES phospholipids. The solution was dried under N_2 and

re-suspended in buffer (140 mM NaCl, 10 mM Hepes and 2.5 mM CaCl₂; pH 6.9) to obtain an aqueous suspension of BLES and cholesterol at a phospholipid concentration of 27 mg/ml. Normal BLES (i.e., without cholesterol) underwent the same extraction procedure, but without the addition of cholesterol. This was to ensure that differences in the experimental findings between normal BLES and chol-BLES were solely due to differences in cholesterol content.

To probe the effects of M β CD, M β CD (Sigma Aldrich, Catalogue-No. C4555) was added to buffer in the CBS to a final concentration of 20 mM M β CD. Functional testing commenced immediately after spreading chol-BLES containing 20% w/w cholesterol and was repeated after a 1-3 hour waiting period. We also tested normal BLES against the buffer containing M β CD as a control. Under this condition, M β CD had no effect on BLES function.

4.4.1 Representation of CBS results

For quasi-static and dynamic cycles, surface tension (γ)-bubble area (A) isotherms were plotted and the film's relative area change (RA) change for $\gamma = 10\text{mN/m}$ during volume reduction was also calculated, according to the following equation, to further describe the surfactant films' surface activity.

$$RA_{\gamma=10} = (\Delta A_{\gamma=10})/A_{\gamma=10}$$

Where A is bubble surface area calculated by linear interpolation from measured values bracketing gamma (γ) = 10mN/m.

4.5 Results

We tested the following sample groups:

1. BLES (27 mg/mL) - control group - 4 samples
2. BLES (27 mg/mL) with 20mM M β CD in subphase - 4 samples
3. BLES (27 mg/mL) with 20% cholesterol (wt%) and 20mM M β CD in subphase - 4 samples

4.5.1 Adsorption/film formation

The samples were introduced into the air-buffer interface of a captive bubble surfactometer (CBS), and the subsequent drop in surface tension was observed over time as the first measure of surfactant function (film formation). The reduction of surface tension upon the adsorption of surfactant is a measure of how fast this substance forms an effective film at the interface, which results in a decrease in surface tension.

4.5.1.1 Control group 1 (BLES 27 mg/mL)

Spreading BLES onto buffer caused γ to drop to values between 35.0 and 30.0 mN/m within 0.15 s for all the samples. Thereafter, γ dropped further to reach a value of 23.5 (\pm 0.05) mN/m within 30 s). The equilibrium surface tension obtained with BLES is \sim 23 mN/m. Reaching this surface tension indicates that the process of film formation is complete. Hence, film formation can be seen as two processes with an initial extremely fast drop in γ that reflects surfactant material spreading from the point of contact to cover the interface. The following slower drop in γ to equilibrium values may reflect alterations in surfactant film architecture after the surface has been covered.

4.5.1.2 Control group 2 (BLES 27 mg/mL + 20mM of M β CD)

Spreading BLES onto a 20 mM M β CD-containing buffer was chosen for testing as a second control group. In the presence of M β CD in the subphase, the initially surface tension dropped to 47 mN/m. Following BLES injection surface tension further dropped down until it reached to equilibrium surface tension value (23 mN/m). Despite this initial drop in surface tension due to M β CD, the times taken by these samples to reach equilibrium were not significantly different from those of the controls without M β CD in the buffer. Hence, surface coverage by surfactant appeared to have been slightly affected by the presence of M β CD at the interface, but after initial coverage, film refinement progressed rapidly enough to obscure the effect by the time equilibrium was reached. This observation was consistent with all the samples in this control group.

Interestingly, M β CD had only limited effects when present at the time of film formation. Thus, both controls groups reached to equilibrium surface tension values (23 mN/m) at the end of film formation phase of the experiment.

4.5.1.3 Test group (BLES 27mg/mL+20% cholesterol) without M β CD in subphase

In these samples, equilibrium surface tension value was reached at the end of initial adsorption. The presence of cholesterol does not significantly affect the ability to attain neither equilibrium surface tension values, nor the time that taken to reach equilibrium values.

4.5.1.4 Test group (BLES 27 mg/mL + 20% cholesterol) with M β CD in subphase

The initial adsorption observed in this group is quite similar to that seen in control group 2. With the presence of M β CD in the subphase, the surface tension of the air-water interface initially dropped down to 47mN/m. After injection of the test sample (BLES + 20% cholesterol), surface tension decreased to equilibrium surface tension values by the end of the initial adsorption. However, the time taken to reach to equilibrium surface tension was not significantly different from the control groups.

For all three conditions tested, the surface tension of the surface film readily dropped to ~23 mN/m (equilibrium surface tension of BLES) (264). This indicated that the process of film formation was not affected by the presence of cholesterol in surfactant or by M β CD in the buffer.

Next, the bubble was rapidly expanded to approximately double the size of the air-water interface and γ was observed for another 5 minutes. Surfactant not only forms a single layer, but also spreads to the interface with patches of multiple surface associated layers when prepared as in the current study (264) and (196). Adsorption of additional surfactant from this surface associated reservoir to the interface was thus observed upon rapid expansion. For films devoid of cholesterol, surface tension peaked at similar levels after rapid expansion both in the presence and absence of M β CD where films containing 20% w/w cholesterol reached significantly higher surface tensions. Hence, insertion of new material from the surface associated reservoir was less efficient for films containing excess cholesterol than for films without cholesterol. However, by 60 s after the completion of expansion, all films had returned to equilibrium values. In our

experimental protocol, rapid expansion followed by a 5-minute waiting period concluded the assessment of film formation.

4.5.2 Compression and expansion cycles

After the film formation, the volume of the bubble was slowly decreased stepwise and then increased (quasi-static cycles). When the area decreases, the molecules at the interface become densely packed, film pressure builds up, and the surface tension drops below equilibrium values. Functional films can withstand the increasing film pressure, but dysfunctional films mechanically fail and material is removed from the interface. Quasi-static cycles reveal whether a surfactant film is able to sustain low surface tensions over time. This is an important parameter of surfactant function. A large proportion of the lung experiences minimal to no area change during tidal breathing and these parts of the lung too require stable near-zero surface tension to maintain the alveolar structure.

After completion of the quasi-static cycles, the samples were tested under dynamic conditions aimed to simulate lung inflation and deflation during normal breathing. Quasi-static and dynamic cycles were repeated (different series of quasi-static and dynamic cycles) in order to see whether the impaired surfactant regained function or whether the functional surfactant become impaired upon further cycling. In this study, four individual tests were carried out for each of the control and test groups. In the figures below, for the sake of clarity, only one representative case for each and for the different experimental condition is shown. For the test groups, multiple quasi-static and dynamic cycles were performed during regular time intervals after exposure to M β CD

(just after MBCD exposure, after 30 minutes, 60 minutes and 180 minutes). For the two control conditions, four individual tests were carried out.

Figures 4.4, 4.5, 4.6, and 4.7 represent surface tension-area isotherms (quasi-static and dynamic cycles). X and Y axes represent surface area (cm²) and surface tension (mN/m).

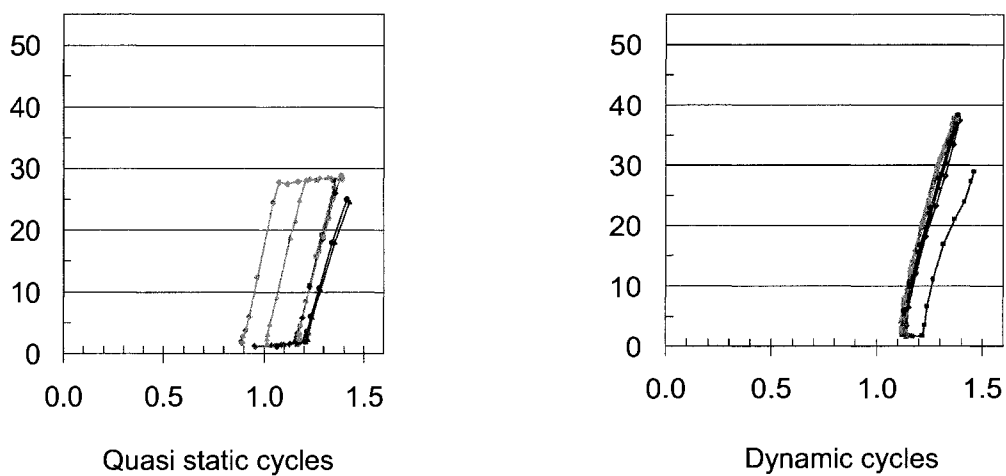
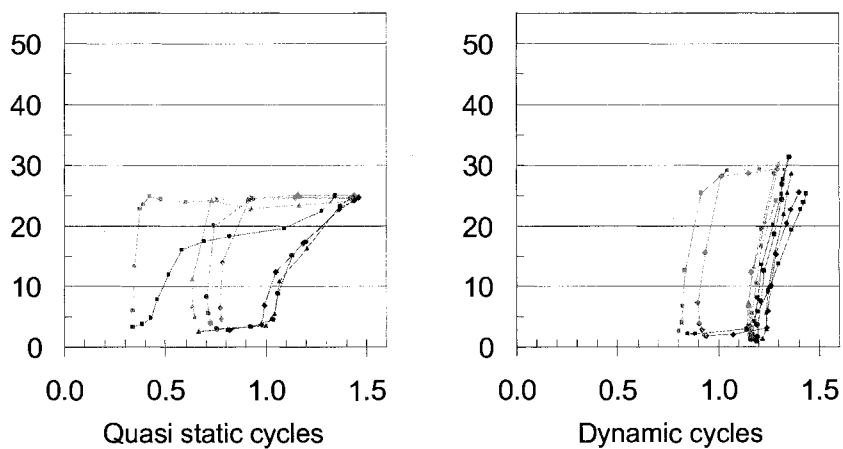


Figure 4.4 BLES (27 mg/ml) control group 1, surface tension-area isotherms

Just after MBCD exposure



(Fig. 4.5 cont'd ...)

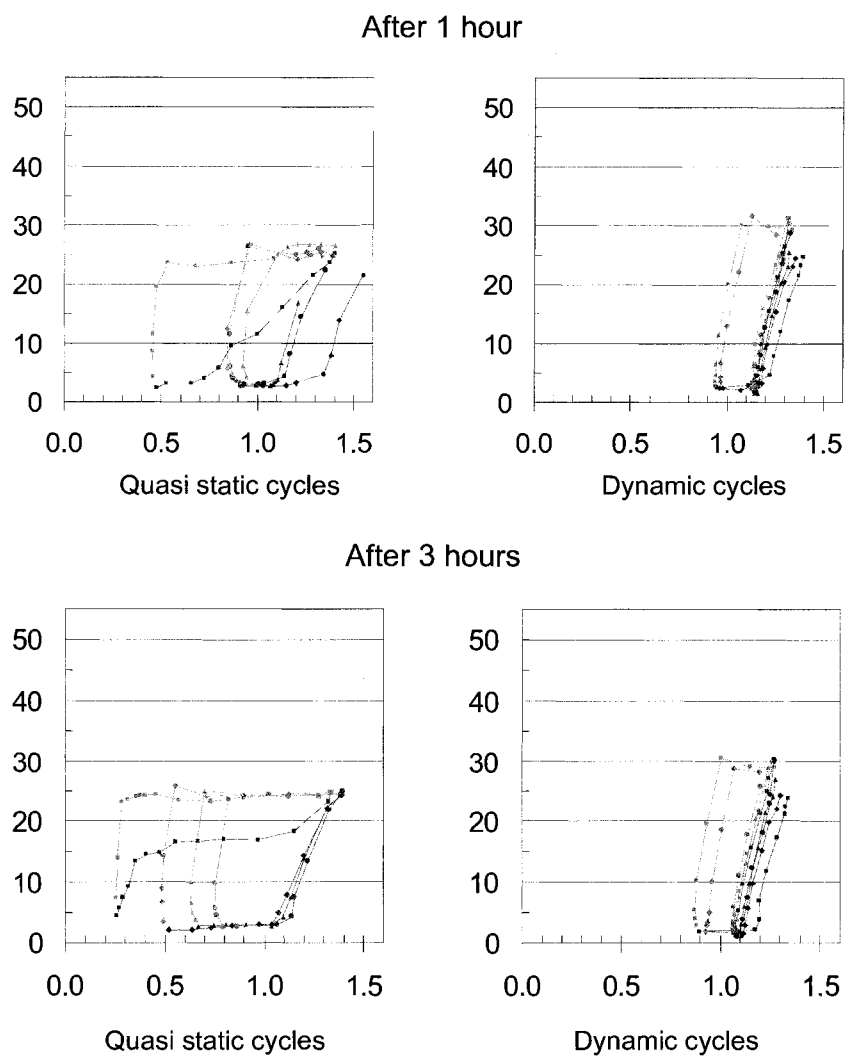


Figure 4.5 BLES - 27 mg/mL + M β CD control group 2, area-surface tension isotherms

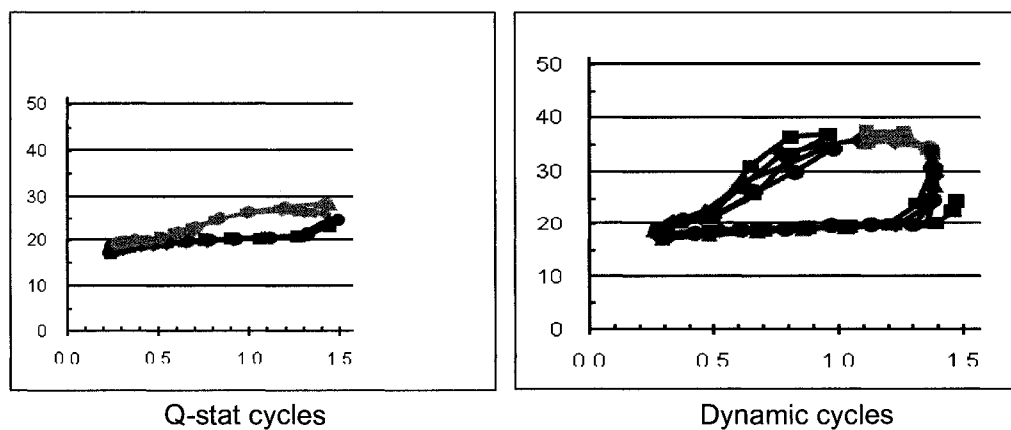


Figure 4.6 BLES+ 20% cholesterol area-surface tension isotherms

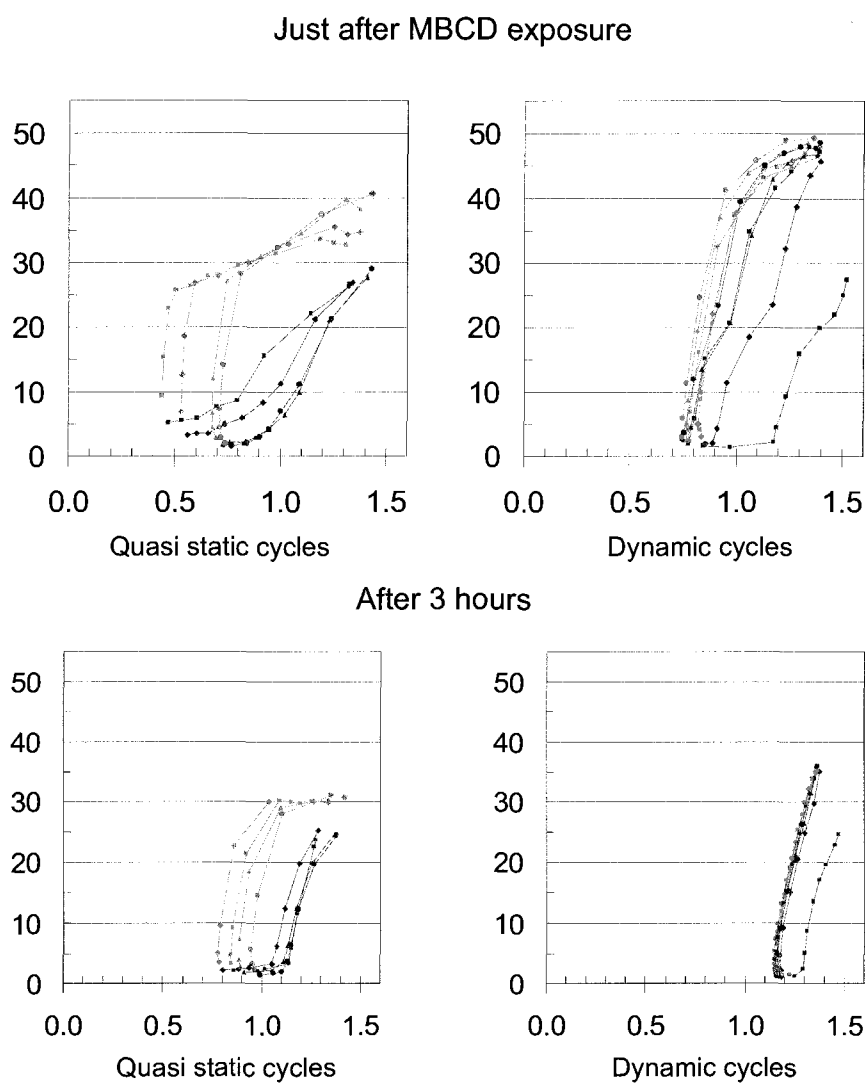


Figure 4.7 BLES + 20% cholesterol + MBCD isotherms

4.5.2.1 Control group (BLES 27 mg/mL) 1-area-surface tension isotherms

BLES samples (Fig. 4.4 above) lowered the surface tension to values close to 1 mN/m during compression (Tables 4.1 & 4.2). It also required minimal area reduction to bring about this low surface tension. This is consistent with a layer of already tightly packed molecules becoming even more compacted at the air-water interface. Upon

Table 4.1 Median Surface Tension Values for Quasi-Static and Dynamic Cycles

Sample		Q stat cycles (median surface tension values mN/m)				Dynamic cycles (median surface tension values mN/m)						
Control 1 (BLES)	0 hrs	Cycle	1	2	3	4	Cycle	1	2	5	10	20
		GMin	1.97646	1.81383	1.77929	1.64526	GMin	1.56151	1.69436	1.55888	1.57938	1.64648
		GMax	29.44242	30.26771	30.21022	30.21243	GMax	34.69505	34.87345	35.28378	35.28378	34.21822
Control 2 (BLES + MBCD)	0 hrs	Cycle	1	2	3	4	Cycle	1	2	5	10	20
		GMin	1.97646	1.81383	1.77929	1.64526	GMin	1.56151	1.69436	1.55888	1.57938	1.64648
		GMax	29.44242	30.26771	30.21022	30.21243	GMax	34.69505	34.87345	35.28378	35.28378	34.21822
Control 3 (BLES + 20% Cho)	3 hrs	Cycle	1	2	3	4	Cycle	1	2	5	10	20
		GMin	3.29514	2.92833	2.34999	2.56215	GMin	2.29101	1.86055	1.16334	1.12437	1.20248
		GMax	25.30280	26.24206	26.30576	25.18898	GMax	29.89894	29.43769	28.99338	28.27180	24.85958
Test (BLES + Cho + MBCD)	0 hrs	Cycle	1	2	3	4	Cycle	1	2	5	10	20
		GMin	18.87927	19.11501	19.21585	19.29023	GMin	14.64324	17.17542	17.93005	18.20986	18.52318
		GMax	27.45581	27.28704	27.19996	27.27647	GMax	36.94714	37.32957	37.62662	37.36769	40.91980
Test (BLES + Cho + MBCD)	3 hrs	Cycle	1	2	3	4	Cycle	1	2	5	10	20
		GMin	19.14365	19.20757	19.54858	19.41575	GMin	18.27235	18.80463	18.83613	18.60760	19.02881
		GMax	29.71236	31.06349	27.27347	27.03232	GMax	39.93597	36.70509	36.27107	36.63079	26.45200
Test (BLES + Cho + MBCD)	16 hrs	Cycle	1	2	3	4	Cycle	1	2	5	10	20
		GMin	8.70233	7.76907	6.89193	5.82344	GMin	1.23233	1.56971	1.77714	2.52714	2.32282
		GMax	33.17396	34.35155	34.86219	40.10074	GMax	48.15173	48.75661	49.84162	49.44976	48.97163
Test (BLES + Cho + MBCD)	3 hrs	Cycle	1	2	3	4	Cycle	1	2	5	10	20
		GMin	2.25143	2.31433	2.64976	2.50125	GMin	2.21809	2.49474	2.44798	2.46271	2.31862
		GMax	36.55304	39.60776	42.31973	45.50632	GMax	49.50950	49.70541	50.16705	49.55623	49.95815
Test (BLES + Cho + MBCD)	16 hrs	Cycle	1	2	3	4	Cycle	1	2	5	10	20
		GMin	1.73497	2.14951	2.23406	2.18055	GMin	1.89505	1.88593	2.05986	2.15087	2.19028
		GMax	35.78915	35.43757	36.32120	38.17552	GMax	46.55409	48.39293	48.25177	49.21009	48.40320

Table 4
1.2 Relative Area Change at the Surface Tension 10 mN/m

Sample	Q stat cycles (median surface tension values mN/m)				Dynamic cycles (median surface tension values mN/m)								
	0	1	2	3	4	1	2	3	4	5	10	20	
Control 1 (BLES)	Cycle	1				Cycle	1	2	3	4	5	10	20
	GMin	0.00456	0.00597	0.00607	0.00529	GMin	0.00465	0.00443	0.00506	0.00484	0.00511		
	GMax	0.00998	0.00837	0.00832	0.00773	GMax	0.00642	0.00595	0.00622	0.00629	0.00654		
Control 2 (BLES + MBCD)	Cycle	1	2	3	4	Cycle	1	2	3	4	5	10	20
	GMin	0.01648	0.00517	0.00751	0.00710	GMin	0.00279	0.00457	0.00390	0.00207	0.00361		
	GMax	0.04898	0.00898	0.00833	0.00769	GMax	0.00672	0.00719	0.00556	0.00727	0.00672		
3 hours	Cycle	1	2	3	4	Cycle	1	2	3	4	5	10	20
	GMin	0.01378	0.00757	0.00629	0.00748	GMin	0.00584	0.00136	0.00548	0.00353	0.00272		
	GMax	0.02904	0.01132	0.00925	0.01062	GMax	0.00829	0.00571	0.00658	0.00577	0.00686		
0 hours	Cycle	1	2	3	4	Cycle	1	2	3	4	5	10	20
	GMin	0.02234	0.03103	0.01769	0.02013	GMin	0.00647	0.00612	0.00659	0.00686	0.00756		
	GMax	0.29140	0.05142	0.03502	0.02091	GMax	0.01202	0.01269	0.01555	0.01559	0.01312		
Test (BLES + Cho + MBCD)	Cycle	1	2	3	4	Cycle	1	2	3	4	5	10	20
	GMin	0.00497	0.00608	0.00592	0.00538	GMin	0.00475	0.00430	0.00433	0.00467	0.00431		
	GMax	0.01200	0.01488	0.01298	0.01189	GMax	0.00957	0.01056	0.00975	0.00930	0.00859		
16 hours	Cycle	1	2	3	4	Cycle	1	2	3	4	5	10	20
	GMin	0.00307	0.00473	0.00562	0.00624	GMin	0.00407	0.00437	0.00483	0.00529	0.00465		
	GMax	0.02258	0.01326	0.01656	0.01580	GMax	0.01718	0.01637	0.01317	0.01066	0.01177		

expansion, the surface tension increased to above equilibrium value (30 mg/mL), with little increase in area. During the dynamic cycling of these samples, very low surface tension values (<2 mN/m) were reached during each compressions, and the film compressibility is very low. There were no signs of film deteriorations during dynamic cycling, so the minimum surface tension during the 20th cycle was <2 mN/m. During dynamic expansion, the isotherms rose rapidly to above equilibrium surface tensions, with very small increases in area.

4.5.2.2 Control group (BLES 27mg/mL + 20mM of M β CD) 2-Area-surface tension isotherms

Area-surface tension isotherms of the BLES films (Fig. 4.5 above) exposed to M β CD were acquired during film compression and expansion. Very low surface tension values were reached during compression in all of the quasi-static cycles (Fig. 4.5, Table 4.1). There was a transient increase in film compressibility during the first quasi-static cycle. However, this was completely recovered during the rest of the quasi-static cycles. Thus, these films regained full function with respect to the film compressibility starting from second quasi-static cycle. The maximum surface tension during expansion of the cycles was below 30 mN/m. The dynamic cycles were similar to those of the first control group, and the minimal and maximal surface tension values were also similar to those of the first control group. Thus, all the samples that were exposed to M β CD showed no evidence of impairment of surface activity during the course of the quasi-static cycles and dynamic cycles. In summary, BLES exposure to M β CD had no unfavourable effects

overall on function under the conditions tested. An effect (high compressibility), when present, was only observed in the first quasi-static cycling but not in dynamic cycles.

Figure 4.5 shows the time dependence of M β CD treatment in the control group (BLES without cholesterol). These results indicate that there is no significant difference in surface activity overtime in this control group during quasi-static and dynamic cycles. It is clearly seen that the first quasi-stat cycle in each series exhibited enhanced compressibility compared to the rest of the q-stat cycles, but the rest of the cycles regained low compressibility. However, there was no significant difference among the dynamic series that we tested in different timelines.

4.5.2.3 Test group (BLES 27mg/mL + 20% cholesterol) – Area-surface tension isotherms

Under these conditions, all the films (Fig 4.6 above) showed severe inhibition during the course of quasi-static and dynamic cycles. Once the equilibrium surface tension of about 23 mN/m was reached, further film compression produced only a minimal reduction in surface tension below this equilibrium value for all samples. A minimum surface tension of about 16-20 mN/m was reached even after extensive compression (264). The isotherms show an extended plateau at $\gamma \approx 20$ mN/m, which indicates continuous film collapse (264). This minimum surface tension was not different for the quasi-static and dynamic cycles. Function was also not regained upon a later series of compression-expansion cycles (results not shown). Furthermore, even after a waiting period of 12 hours, we did not observe any recovery of the function of BLES containing 20% cholesterol. Note that in chart 4.2 we could not calculate relative area

change at 10mN/m for this group as they did not reach 10mN/m during quasi static and dynamic compressions. Minimum surface tensions obtained with these samples during compression were close to 17mN/m.

4.5.2.4 Test group (BLES 27 mg/mL + 20% cholesterol with 20 mM M β CD in subphase) – area-surface tension isotherms

Immediately after spreading 20% cholesterol-BLES on the M β CD-containing buffer, the surfactant showed signs of inhibition. During the first quasi-static compression, surface tension dropped below 14 mN/m, but the film underwent continuous collapse as indicated by the plateau in the area-surface tension isotherm. This indicates that the stability of this film was improved over cholesterol-BLES, but not to the level of unimpaired surfactant. Although the first series of quasi-static cycles showed incremental improvements in surface activity, we could not completely restore it in terms of minimal surface tension and low film compressibility (Fig. 4.7a, Table 4.1, Table 4.2).

However, dynamic cycling initially brought about a drop in surface tension to value close to 2 mN/m. Moreover, the compressibility of the film was also very low, and was similar to that seen with normal surfactant. However, after a few initial cycles, minimal surface tension began to increase with subsequent cycles. This indicates that the cholesterol levels in the surface film are still higher than physiological levels immediately after exposure to M β CD, and the surfactant function is therefore not completely recovered.

After waiting for three hours, we performed another series of quasi-static and dynamic cycles. Surface tension values reached 2 mN/m in all the quasi-static cycles, and the film compressibility was markedly decreased (Tables 4.1 & 4.2). This confirms that

the function of cholesterol-BLES films was fully restored with respect to both of the important aspects of surfactant function, low compressibility and low minimum surface tension. Very low surface tension values were reached during the dynamic cycles, and the film compressibility was again similar to that of controls. However, the maximum surface tension values were increased (about 50 mN/m) during expansion of the film in the quasi-static and dynamic cycles. Even though, this maximum surface tension are high, surface tension values still reached <2 mN/m with very low compressibility during the compression followed.

During this *in vitro* study, control samples (BLES 27 mg/mL) showed all the the basic pulmonary surfactant functions, as expected. Samples containing 20% cholesterol did not reach low surface tension values and surfactant function was thus effectively abolished. When M β CD was added to the subphase, surfactant function was fully restored with respect to both of the important aspects of surfactant function: low compressibility and low minimum surface tension. This M β CD mediated surfactant restoration is time dependent, as a fully functional surface film was gained within 3 hours.

4.6 Discussion

4.6.1 Films containing BLES without cholesterol

During initial adsorption of the BLES films (control group 1), equilibrium surface tension values (23 mN/m) were reached very quickly. We have already observed the same results on a number of occasions with BLES (27 mg/mL) (264). In the presence of M β CD in the subphase (control group 2), the initial accumulation of M β CD may have

occurred at the air-water interface, before the introduction of the BLES sample. This led to a reduction in surface tension from 70 mN/m to 47 mN/m. Following the BLES injection, surface tension was further reduced from 47 mN/m to equilibrium surface tension (23 mN/m). However, at the end of the initial adsorption, all the samples reached equilibrium surface tension. The total time taken to reach equilibrium surface tension (23 mN/m) was not significantly altered by the presence of M β CD.

In the lung, the surface film of pulmonary surfactant must reduce surface tension to almost zero upon expiration. Hence, functional surfactant must reach a surface tension value close to zero upon compression *in vitro*, and must not return to equilibrium when kept compressed. Surfactant films of the control group 1 (BLES 27 mg/mL) and control group 2 (BLES 27 mg/mL and 20 mM of M β CD in subphase) agreed with the above conditions during quasi-static and dynamic cycling, and there were no signs of film inhibition due to the presence of M β CD in subphase. During compression, surface tension values close to 2 mN/m were reached in both quasi-static and dynamic cycles. However, enhanced film compressibility was observed in the control group 2 (M β CD in subphase), only during the first quasi-static cycle. This was probably due to the initial presence of M β CD molecules at the interface. However, this effect disappeared due to film refinement during cycling. From the second quasi-static cycle onwards we observed a fully functional BLES film with respect to both of the important aspects of surfactant function: the low compressibility and low minimum surface tension.

In order to observe any deterioration/improvement of the BLES films in the presence of the M β CD, we performed a multiple series of quasi-static and dynamic cycles on control group 2 (for surface tension values see Table 4.5). These extra series of quasi-

static and dynamic cycles were performed at different time intervals (60, 180 minutes). Our results showed that M β CD did not have negative effects on the surface tension lowering ability of BLES. However, in each series of quasi-static cycles, the first compression cycle showed increased film compressibility, an effect that disappeared during the rest of the quasi-static cycles (Fig 4.5, Table 4.2). During dynamic cycling, minimal surface tension values close to 2 mN/m were achieved with very low film compressibility. Thus, these results suggest that the presence of M β CD in subphase does not significantly affect surface properties of BLES.

4.6.2 Films containing 20% cholesterol

Films containing BLES and 20% cholesterol (wt %) were not significantly different the control groups in terms of the initial adsorption phase of the experiment. These samples reached equilibrium surface tension values during the initial adsorption phase of the experiment. Thus, the presence of cholesterol does not significantly affect initial adsorption. Test samples with BLES-20% cholesterol behaved similarly to those with no cholesterol during the initial portion of bubble compression, when the surface tension was above equilibrium. However, after achieving equilibrium, there was a limited reduction in surface tension. This resulted in an extended plateau in the surface tension-area isotherms for the cholesterol-inhibited films. No restoration of the low-compressibility region of the isotherm was achieved with samples containing 20% cholesterol. Below equilibrium surface tension, an interfacial film is metastable by definition (i.e., once matter has left the film, it can no longer return). It is a unique mechanical property of pulmonary surfactant to not collapse under this condition. This

property has been associated with the specific film architecture of a monolayer and dispersed multilayer patches (316,317) and excess cholesterol has been shown to disrupt this structure (337). In a physiological sense, this surfactant was dysfunctional. Films containing 20% cholesterol would not allow for structural stability of the lung because of the insufficient reduction of surface tension. This breakdown of surfactant function at a higher proportion of cholesterol is very intriguing, both for its implication for diseases and with respect to the molecular mechanism behind this phenomenon. The presence of cholesterol in the lung has long been identified. Recently we and others recognized excess cholesterol as an inhibitor of surfactant function (264,251). Elevated levels of cholesterol have been observed in animal models of lung injury, as well as in human studies of patients who have ARDS (145,224). ARDS patients are treated with a combination of treatment strategies including surfactant replacement. However, the inhibition of replaced surfactant is also observed in patients with ARDS, and treatment failure is common. It is possible that this inhibition can be due to the presence of excess cholesterol in the lung alveoli. Therefore, finding new strategies to overcome this cholesterol- mediated surfactant inhibition is essential for treating ARDS successfully.

Previously, we increased the amount of DPPC in BLES containing 20% cholesterol to restore the physiological ratio of DPPC to cholesterol. As a result, the adverse effect of the high proportion of cholesterol was partly reversed (264). However, the film compressibility during quasi-static and dynamic cycling was markedly increased. Also, at the end of the dynamic cycling we observed film deterioration, which reflected as increased minimal surface tension. Therefore, we decided to explore whether the M β CD has a recovery effect on cholesterol mediated surfactant dysfunction. Previously,

M β CD have been shown to extract membrane cholesterol selectively from the cell membranes of a variety of cell types, as well as from artificial membranes (259, 258,242). M β CD has the capacity to sequester lipophiles such as cholesterol in their hydrophobic core (305). This mechanism is time dependent. Thus, we allowed surface film to react with M β CD for 3 hours.

The initial adsorption of the BLES-20% cholesterol samples that were exposed to M β CD was similar to that of control group 2. Surface tension values of 47 mN/m were initially reached after exposure to M β CD. Subsequent injection of the sample (BLES+ 20% cholesterol), surface tension values further dropped down to the equilibrium surface tension (23 mN/m). However, there is no significant difference in the time taken to reach equilibrium surface tensions in comparison to the control group. Thus, for all three conditions tested, the process of film formation was not affected by cholesterol in surfactant or by M β CD in the buffer.

After post expansion adsorption, we performed a series of quasi-static and dynamic cycles at different time intervals (just after exposure to M β CD, after 60 minutes, 120 minutes, and 180 minutes). The aim of performing multiple series was to see whether there was any time-dependent improvement in the surface activity of films consisting of BLES-20% cholesterol in the presence of M β CD.

During different series of cycling, we observed an incremental recovery of surface activity. Although we observed signs of inhibition during the first q-stat cycle after exposure to M β CD, the first dynamic cycle showed significant recovery with minimal surface tension close to 2 mN/m. However, towards the end of the first series of dynamic cycles (10th to 20th cycle), we observed film deterioration that was reflected as an

increase in the minimal surface tension. This suggests that the surface film still carries an excess amount of cholesterol. However, during the waiting period, M β CD reacts with most of the cholesterol that was present in the surface film and formed inclusion complexes. The formation of M β CD-cholesterol complexes reduced the amount of cholesterol in the surface film, thus giving rise to an improvement in surface activity. After three hours, we observed maximum recovery from inhibition with respect to minimal surface tension and low compressibility. Specifically, all the test samples (BLES-20% cholesterol) reached surface tension values close to 2 mN/m during the quasi-static and dynamic compressions with very low film compressibility after 3 hours' exposure to M β CD (Fig 4.7). However, maximum surface tension during expansion was elevated (50 mN/m). This value is much higher than physiological maximum surface tension (20 mN/m) value that occurs during expansion at total lung capacity (18). Even though this maximum surface tension is significantly high, very low surface tensions (close to 2 mN/m) with low film compressibility were reached during subsequent compressions. This suggests that maximum surface tensions achieved during the expansion cycles do not negatively affect surface activity during compressions. These current findings indicate that under the experimental conditions we tested, cholesterol-mediated surfactant dysfunction can be recovered by M β CD *in vitro* in a time-dependent manner.

4.7 Conclusion

Previously, we and others reported that elevated amounts of cholesterol can inhibit surfactant function *in vitro*. Elevated levels of cholesterol have been observed in

animal models of lung injury, as well as in human studies of patients who have ARDS (145,224). The identification of the relevant mechanisms of surfactant impairment in ARDS is important for devising new strategies to counter surfactant inhibition and overcome the current lack of success with exogenous surfactant treatment.

Our current study showed that BLES inhibition due to excess cholesterol could be recovered by M β CD *in vitro*. However, it is important to investigate this concept in animal models of the lung injury in order to see if M β CD can be used as an adjunct to surfactant replacement therapy. If M β CD and BLES treatment can improve the conditions of such animals, they may be used as a potential treatment for ARDS after performing human trials.

Chapter 5: Effect of Cholesterol on Structure of the Pulmonary Surfactant Film

5.1 Summary of the study

In adult respiratory distress syndrome, the primary function of pulmonary surfactant to strongly reduce the surface tension of the air-alveolar interface is impaired, resulting in diminished lung compliance, a decreased lung volume, and severe hypoxemia. Dysfunction coincides with an increased level of cholesterol in surfactant which on its own or together with other factors causes surfactant failure. In the current study, we investigated by atomic force microscopy and Kelvin-probe force microscopy to see how the increased level of cholesterol disrupts the assembly of an efficient film. Functional surfactant films underwent a monolayer-bilayer conversion upon contraction and resulted in a film with lipid bilayer stacks, scattered over a lipid monolayer. Large stacks were at positive electrical potential while small stacks were at negative potential with respect to the surrounding monolayer areas. Dysfunctional films formed only few stacks. The surface potential of the occasional stacks was also not different from the surrounding monolayer. Based on film topology and potential distribution, we propose a mechanism for formation of stacked bilayer patches whereby the helical surfactant-associated protein SP-C becomes inserted into the bilayers with defined polarity. We discuss the functional role of the stacks as mechanically reinforcing elements and how an elevated level of cholesterol inhibits the formation of the stacks. This offers a simple biophysical explanation for surfactant inhibition in adult respiratory distress syndrome as well as possible targets for treatment.

5.2 Introduction

Lung compliance is dominated by the surface tension of the hydration layer covering the lung epithelium to the air (338). The air-water interface is covered by a tightly packed molecular film of pulmonary surfactant. The film hinders the interface from contracting under the influence of the surface tension. It thus reduces the surface tension from ~ 72 mN/m of a bare air-water interface to <1 mN/m once the air-lung interface is at its minimum size at end expiration (19). The surface tension likely always remains <10 mN/m during tidal breathing in the healthy lung (339). A low surface tension is required to reduce the Laplace pressure, which would otherwise cause the alveoli to collapse into the small airways.

In adult respiratory distress syndrome (ARDS), pulmonary surfactant function is inhibited. As a result, the surface tension is elevated and the lung function substantially impaired. ARDS is a common and devastating condition with 150,000 cases per year in the US and a mortality rate of $\sim 30\%$. Because surfactant impairment is likely a major factor for the morbidity and mortality of ARDS, it has been targeted by replacement surfactant therapy. However, success has been minimal (for a review, see (312)) because the exogenous surfactant apparently became inactivated as well. A better understanding of the cause and mechanism of the inactivation may therefore be required to address this more specifically.

Until recently, surfactant inhibition in ARDS has been investigated mainly with regard to serum proteins, which are highly elevated in the alveolar space in the case of ARDS (e.g., 312,311,340) and oxidative inactivation by reactive oxygen species (232,341,342,343). This study focuses on the role of cholesterol in surfactant. Karagiorga

et al. (224) recently reported an increase of cholesterol in surfactant from ARDS patients over control ($8.5 \pm 5\%$ w/w) from $15.6 \pm 2\%$ w/w up to $43 \pm 22\%$ w/w. Cholesterol in surfactant is also increased to 20% w/w in animal models of lung injury (145). For such elevated levels of cholesterol, the lowest surface tension observed *in vitro* is 16 mN/m (264). At a surface tension of 16 mN/m, the alveoli recede from a spherical shape into shallow cavities in the terminal airways and the gas exchange area is reduced to less than one-half of its normal value (339). It was therefore concluded that an elevated level of cholesterol abolishes surfactant function.

This study shows by atomic force microscopy (AFM) and Kelvin probe force microscopy (KPFM) that failure of surfactant function in the presence of 20% w/w cholesterol coincides with a distinct change in the molecular architecture of the interfacial film. KPFM is an imaging mode of AFM and produces a map of the local electrical surface potential in addition to a topographical AFM image. For films of amphiphilic molecules, the electrical surface potential is a footprint of the molecular species and/or their molecular order under the tip (344,345,346,347) and arises from the alignment of molecular dipoles μ , upon packing of the film (348). More specifically, the surface potential is a function of the component of μ normal to the interface, the dielectric constant ϵ of the environment of the dipoles, and the packing density of molecules (dipoles) or surface area A occupied by each molecule. For phospholipids, contributions have been ascribed to various regions of the molecules, each in its own dielectric environment the headgroup region, the aliphatic tail, and the terminal methyl group (348). For example, dipalmitoylphosphatidylcholine, the most abundant of the surfactant components, has been reported to give rise to a surface potential of ~ 500 mV, at the

surface tensions used in this study (26 mN/m) (349). In a film composed of many components like pulmonary surfactant, the local differences in electrical surface potential reflect not only the differences in local sample composition, but also the packing and ordering of the molecules in an area (219).

Films for this study were formed from bovine lipid extract surfactant (BLES). BLES is a clinically used replacement surfactant. BLES differs from natural surfactant in the lack of the hydrophilic surfactant-associated proteins SP-A and SP-D as well as cholesterol. It consists of 80% by weight of phosphatidylcholines, with dipalmitoylphosphatidylcholine (DPPC) and 1-palmitoyl-2-oleoyl-phosphatidylcholine being the major molecular species and dipalmitoylphosphatidylglycerol and 1-palmitoyl-2-oleoyl-phosphatidylglycerol being present at significant levels. It also contains phosphatidylethanolamine, phosphatidylinositol, sphingomyelin, trace amounts of lyso-phosphatidic acids, and vitamin E as well as the small hydrophobic surfactant-associated proteins SP-B and SP-C (350). Cholesterol, which is removed from BLES, is the major neutral lipid in mammalian surfactant at 5–10% w/w. In the current study, films were prepared from unaltered BLES, from BLES with 5% w/w cholesterol added (reflecting normal surfactant), and BLES with 20% w/w cholesterol added (reflecting surfactant in ARDS).

5.3 Materials and methods

5.3.1 Preparation of the surfactants

BLES in nonbuffered normal saline (pH 5-6) with a phospholipid concentration of 27 mg/ml was kindly donated by the manufacturer (BLES Biochemical, London, ON).

Cholesterol was purchased from Sigma Chemicals (St. Louis, MO). A solution of 1:1:1 ratio of methanol, chloroform, and BLES by volume was first vortexed and then centrifuged at 100 g for 5 min. The methanol/water phase was discarded and the BLES in chloroform was retained and none, 5% w/w, or 20% w/w of cholesterol, with respect to phospholipids, was added. Each solution was then dried under N₂ and resuspended with buffer (140 mM NaCl, 10 mM HEPES, and 2.5 mM CaCl₂; pH 6.9) to obtain an aqueous suspension of BLES and cholesterol at a concentration of 27 mg/ml phospholipids.

5.3.2 Film deposition

For the microscopy, the films were deposited onto freshly cleaved mica (ruby, ASTMV-2 quality, Asheville-Schoonmaker Mica, Newport News, VA) by the Langmuir-Blodgett technique. Surfactant suspensions were spread at the air-buffer interface (750 cm²) of a Langmuir trough (Nima Technology, Coventry, England) at room temperature. The film area was reduced or expanded at a rate of 100 cm²/min, the surface tension continuously monitored, and area-surface tension isotherm recorded (Fig. 5.1). For results shown in Figures 5.2-5.5 and 5.6, films were expanded or contracted before deposition by defined amounts as described in the following section. For deposition, a mica support was first lowered across the interface at a speed of 45 mm/min and then retracted at 25 mm/min. A film was deposited upon the upstroke while the surface tension was kept constant.

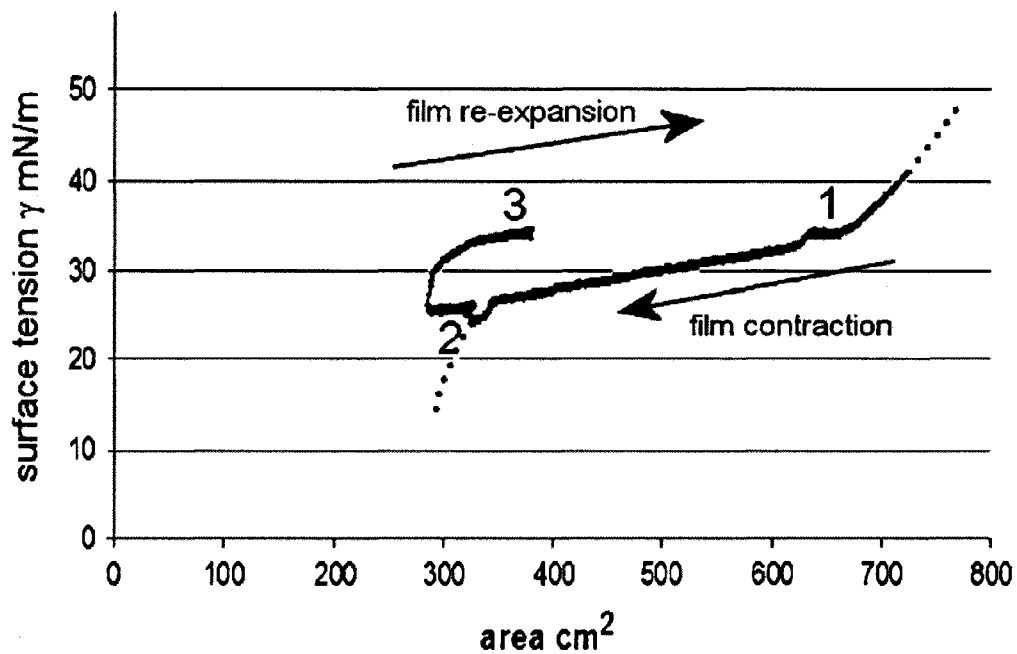


Figure 5.1 Surface tension-area isotherm of BLES upon sample collection. The solid black line denotes the isotherm. Upon contraction of the film, the surface tension first dropped steeply before flattening into a shoulder of the isotherm. At the inflection point, a first sample was collected (denoted by 1). The film transfer is visible as a short horizontal stretch in the isotherm. The film area was then further reduced until the surface tension started to drop more steeply again, at which point a second sample was collected (2). After transfer of the second sample, the film was re-expanded and a third sample collected (3). Dotted lines denote the likely progression of the isotherm in the absence of sample collection. The expected progression was deduced from an isotherm of this film acquired before collection of the samples.

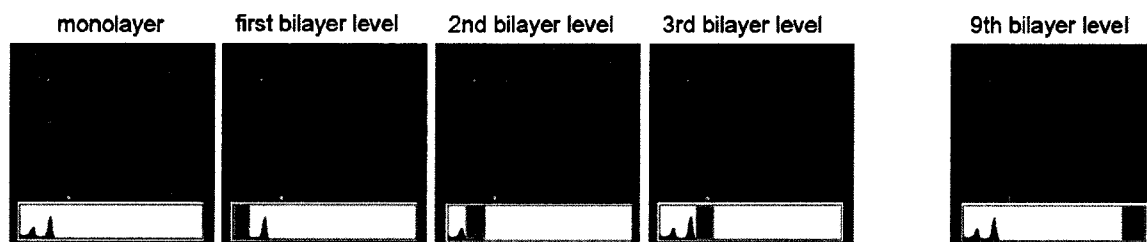


Figure 5.2 The discrete levels of lipid bilayer patches on top of each other were identified in each AFM micrograph in the histogram of the area count over topographical height using ImageJ (Wayne Rasband, National Institutes of Health, Bethesda, MD). In this example, a maximum of nine discrete levels of bilayers were identified.

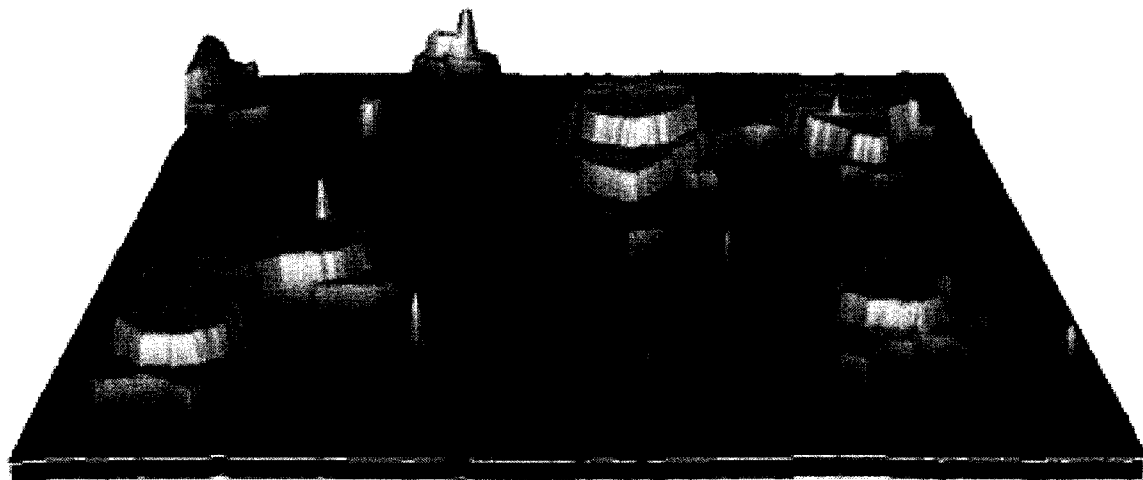


Figure 5.3 AFM micrograph in three-dimensional representation of surfactant containing 5% w/w cholesterol ($5\ \mu\text{m} \times 5\ \mu\text{m}$). The film shows stacks of bilayers up to three layers high. Each layer is five nanometers high.

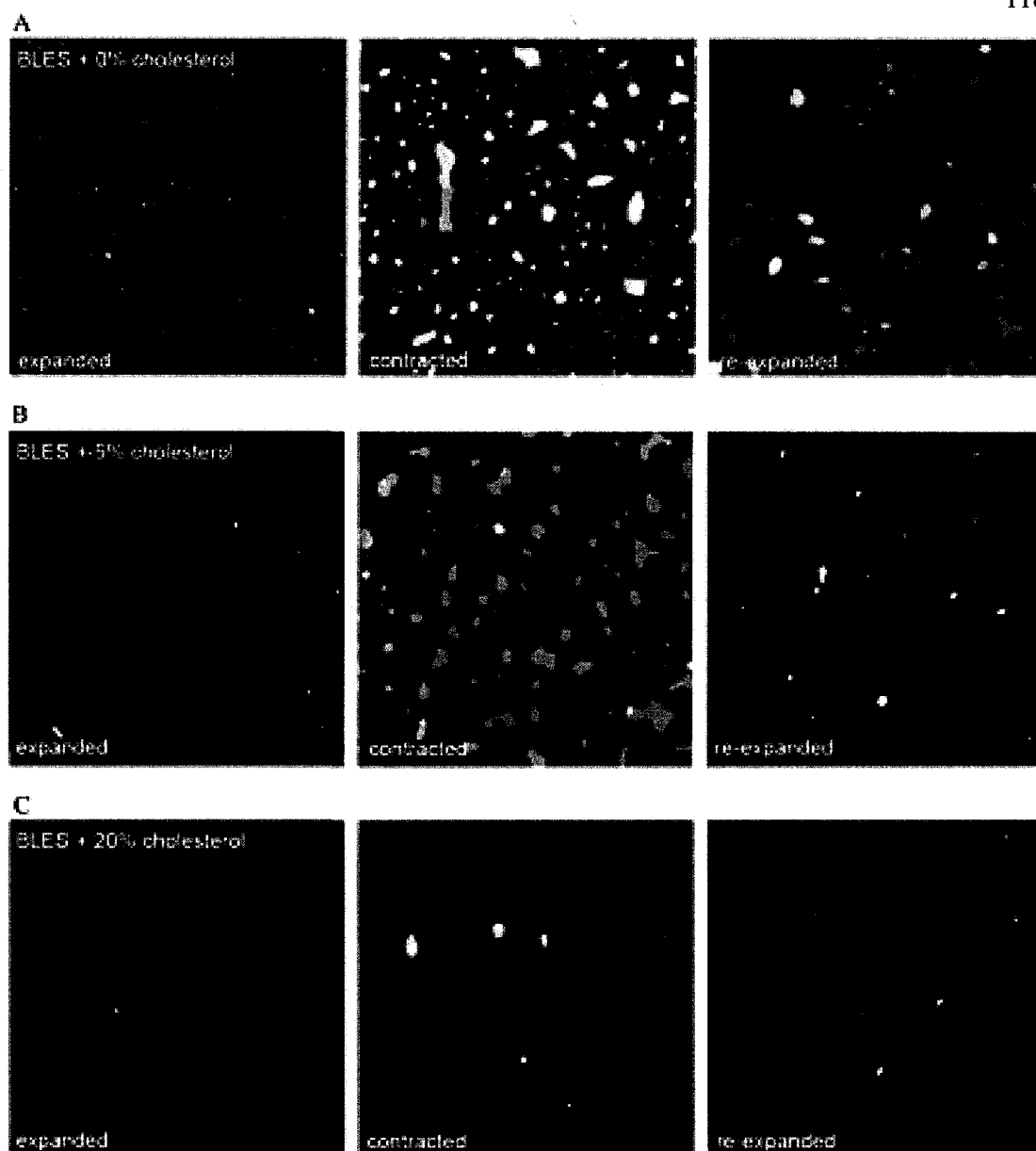


Figure 5.4 AFM topographies ($20\ \mu\text{m} \times 20\ \mu\text{m}$) of BLES containing no cholesterol (A), 5% w/w cholesterol (B), and 20% w/w cholesterol (C). The films denoted “expanded” have been collected from the Langmuir trough after the film was spread and allowed to contract up to the onset of a shoulder in the area-surface tension isotherm ($\gamma = 34\ \text{mN/m}$, see Fig.5.1). Then, the film area was further reduced and another sample collected (denoted contracted; ($\gamma = 26\ \text{mN/m}$)). The images in the right column have been acquired from films after a partial reexpansion ($\gamma = 34\ \text{mN/m}$). Films containing no or 5% cholesterol formed stacks of lipid bilayer patches, attached to the monolayer. The bilayer patches reintegrated in the monolayer when the film was re-expanded. Note that the re-expanded films of panels A and B still show some bilayer stacks because the area was only partially re-expanded. Films with 20% cholesterol formed almost no lipid bilayer stacks and continuously collapsed during contraction (C).

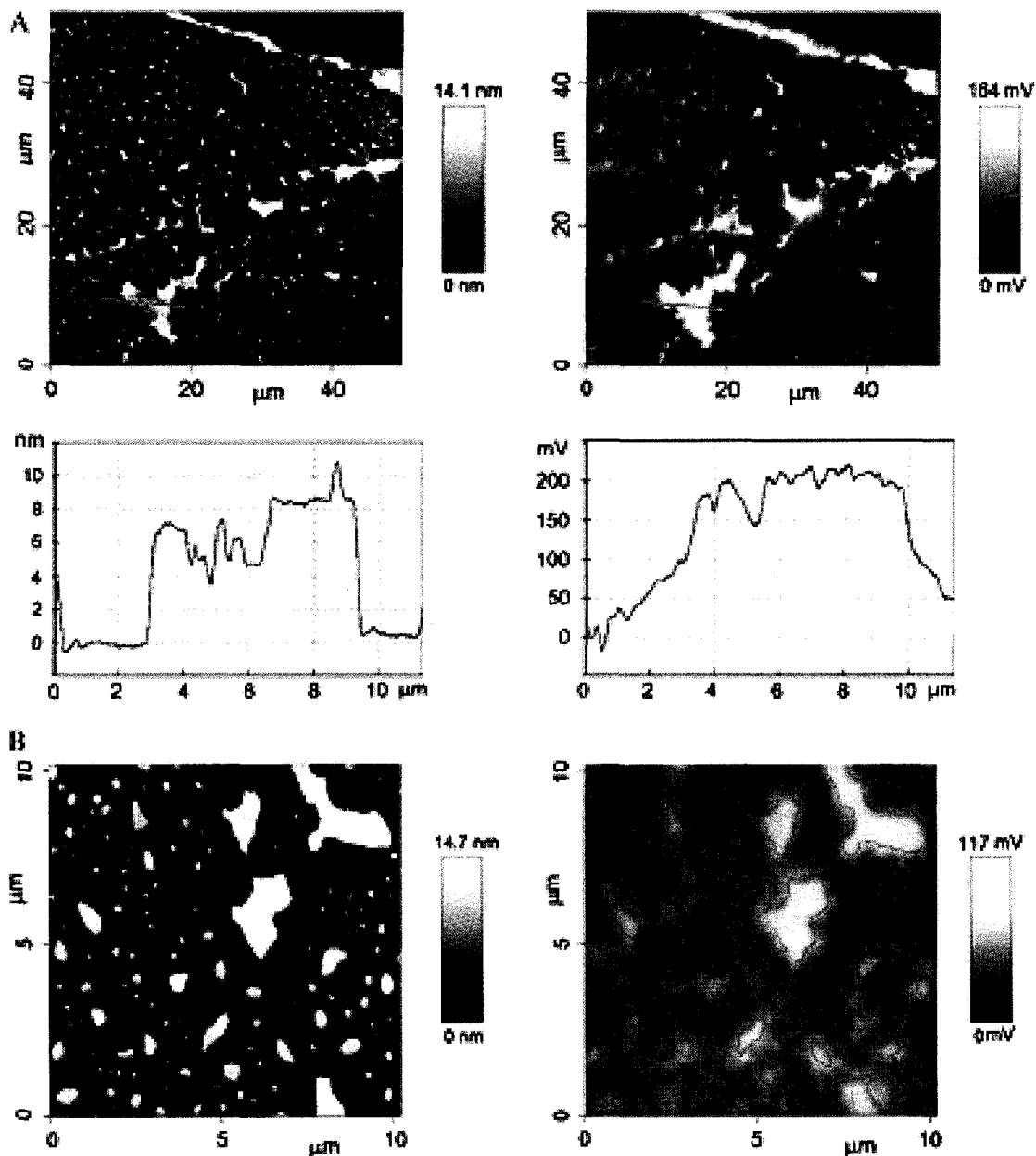


Figure 5.5 (A) Overview of a film of BLES that contains no cholesterol. The topographical image (left, and cross-section below) shows a pattern of monolayer and scattered multilayer regions. In the potential map (right, and cross-section below) large stacks of bilayer patches are at a potential of up to 200 mV above the monolayer. The arrows in the topographical image and in the potential map point to a region, where the topographical height does not change but the potential shows two distinct levels. (B) BLES film at higher magnification. The outer perimeters of the bilayer stacks from the topological image (left) are overlaid in red in the potential map (right). The larger of the bilayer stacks are at positive potential with respect to the monolayer. Small stacks are up to ~ 100 mV lower in the electrical potential than average.

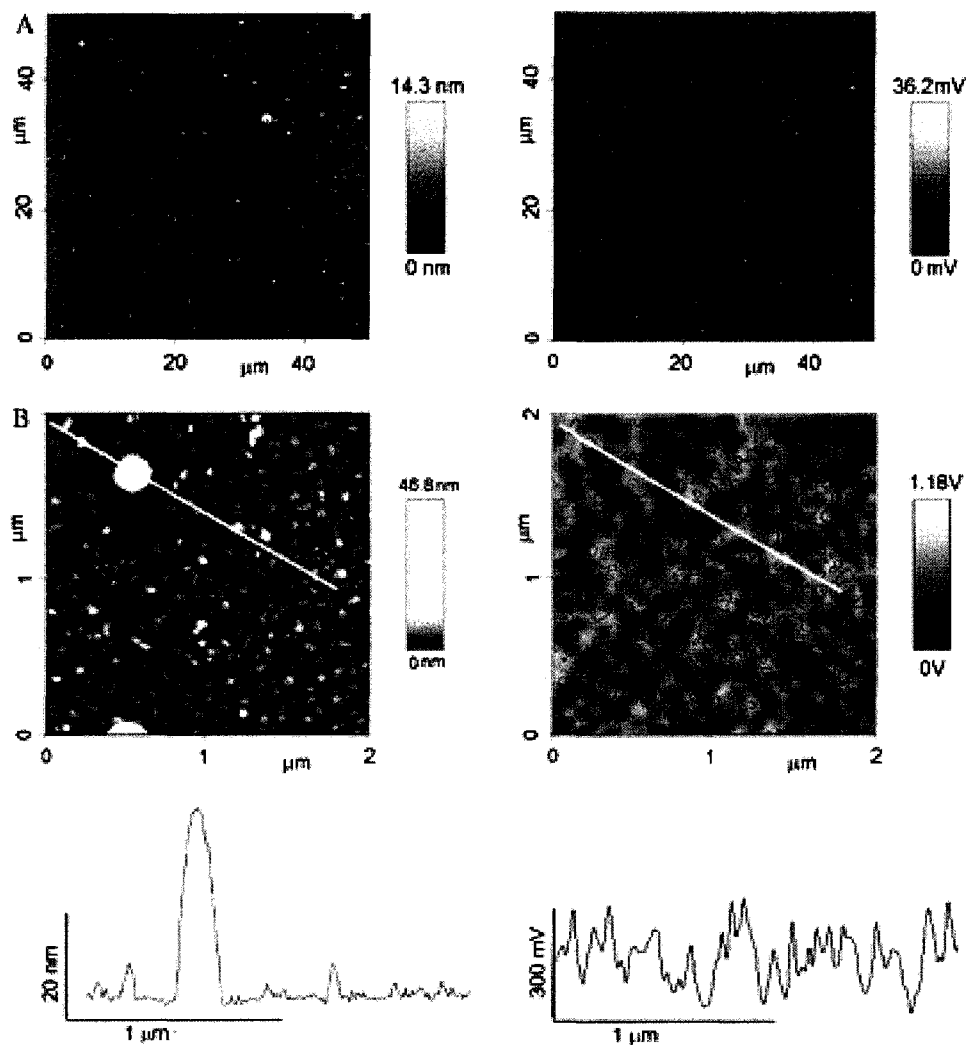


Figure 5.6 (A) Overview of a film of BLES that contains 20% cholesterol by weight. Protrusions in the topographical image (left) are not different in the potential map (right). (B) A high-resolution map of the topography (left) and potential (right) of the film containing 20% cholesterol. The perimeter of the small topographical features were computed from the topographical image and overlaid in red on the potential map. The monolayer is strongly electrically structured with a dynamic range of up to 300 mV. The length scale of the electrical domains is ~ 100 nm. The perimeters shown in the overlay are enclosing an area of larger topographical height (i.e., larger film thickness). In the potential map, these areas coincide with the regions at a more positive surface potential.

For the films shown in Figure 5.4 or discussed in the Results section, a first sample of each film was deposited onto mica upon the film contraction at a surface tension of $\gamma = 34$ mN/m (denoted by 1 in Fig. 5.1; denoted expanded in Fig. 5.4). A second sample was collected at $\gamma = 26$ mN/m in a similar way (denoted by 2 in Fig. 5.1; denoted contracted in Fig. 5.4). A third sample was collected at $\gamma = 34$ mN/m (denoted by 3 in Fig. 5.1; denoted re-expanded in Fig. 5.4) after the film area had been re-expanded. The collection points were chosen such that upon area reduction, the first sample was taken before the onset of a shoulder in area-surface tension isotherm, the second sample at the end of the shoulder, and the third sample after a partial re-expansion of the film (Fig. 5.1). For the results shown in Figures 5.5 and 5.6, films were obtained similar to collection point 2 (after ~50% area reduction from the onset of the shoulder in surface tension isotherm).

5.3.3 Microscopy

AFM topographical images were collected in air with a NanoWizard AFM (JPK Instruments, Berlin, Germany) using noncontact mode silicon cantilevers (NCH-20 from NanoWorld) with typical spring constants of 21-78 N/m, and resonance frequencies of 260-460 kHz.

Surface potential maps and corresponding topographical images were acquired on two different instruments employing two different methods of measuring the electrical surface potential. Both methods revealed similar potentials for corresponding film areas. The data displayed in Figures 5.5A and B, and Figure 5.6A were collected in air with a NanoWizard AFM. The images were acquired by tracing the sample areas line by line.

On tracing, the sample topography was measured in intermittent contact mode. Upon the return pass (retrace), the height information was used to maintain the cantilever at a constant offset height above the surface and the electrical surface potential measured as described (351). Conductive cantilevers (Type BS-ElectriTap300, BudgetSensors, Sofia, Bulgaria) were used and connected to an external circuit to control the tip potential. The high magnification image of Figure 5.6B was acquired, using a laboratory-built setup described in the literature (352,353). With this setup, potential and topography were measured simultaneously, using the frequency modulation technique (FM-KPFM). This method derives a surface potential by measuring the gradient of the electrostatic force rather than the force itself and is largely insensitive to the geometry of the tip.

The potential maps in this study show relative values. A value of 0 V was assigned to the most negative value in each of the maps displayed. The absolute potentials are measured by the instruments, but carry an offset due to a contact potential, brought about by the sample support to which the measured potential is referred. This is discussed in Leonenko et al. (354).

5.3.4 Quantitative image analysis

The total area of lipid leaflets within bilayer stacks in the AFM micrographs was computed to determine the extent by which the surfactant monolayer folded into stacks of bilayers upon the area reduction between collection points 1 and 2. For the analysis, it was assumed that the lowest topographical level in each micrograph represented a lipid monolayer. Hence, the image size equalled the monolayer area. A plateau ~5 nm above the monolayer was considered a lipid bilayer (i.e., two leaflets of lipid monolayer) on top

of the monolayer; a plateau of 10 nm in height was considered a monolayer with two bilayers on top of each other; etc. The total amount of lipid leaflets within bilayer stacks was then related to the area change, which occurred within the shoulder of the area-surface tension isotherm. For example, if the film area had been reduced by half between collection points 1 and 2, and the area of lipid leaflets within bilayer stacks summed up to be similar to the image size, the monolayer-bilayer conversion was considered to be 100%. For each concentration of cholesterol in BLES and each of the three collection points, four micrographs from two independent experiments were analyzed.

5.4 Results

5.4.1 Structure-function relationship of the surfactant films

The structures formed by surfactant films containing 0%, 5%, or 20% w/w cholesterol were related to our earlier functional study on these films (264). Films containing 0% or 5% reduce the surface tension close to zero mN/m and are considered functional. Films containing 20% cholesterol are unable to lower the surface tension below ~ 16 mN/m. A surface tension of 16 mN/m is not sufficiently low for proper lung function.

The functional surfactants show lamellar structures scattered over the monolayer surface (Fig. 5.3). Each step in a stack is 5 nm high, indicative of a single lipid bilayer. The bilayer stacks form from the monolayer upon contraction. This monolayer-multilayer conversion corresponds to a shoulder in the area-surface tension isotherm (Fig. 5.1, see also (264)), where the surface tension changes little upon a change of ~ 25 -50% in surface area. Before the shoulder, the films show none or only a few lamellar structures (Fig.

5.4A and B, expanded). At the end of the shoulder, the bilayer stacks have fully established (Fig. 5.4A and B, contracted). Our earlier functional study of these samples show that, at this point, the films have become incompressible and the surface tension drops steeply, often to <1 mN/m upon further film contraction (264). Formation of lamellar structures is reversible: the lamellar structures unfold into the monolayer (Fig. 5.4A and B, re-expanded).

The amount of area reduction required to reach a surface tension of 26 mN/m varied between $\sim 40\%$ and 50% of the area after the first sample was collected. The amount of re-expansion required to reach a surface tension of 34 mN/m was also different for each film and varied from $\sim 50\text{-}30\%$ of the area change that had occurred previously between collection points 1 and 2. The amount of re-expansion was less than the previous contraction because of a hysteresis between the contraction and expansion trace (Fig. 5.1; i.e., the surface tension rose faster on the expansion as it had previously dropped on contraction). For the film shown in Figure 5.4A, the area between sample collections has been reduced from the expanded state (100%) to $\sim 50\%$ and was then re-expanded to $\sim 75\%$ for collection of the film denoted "re-expanded." The variability between isotherms of similar samples is discussed in Gunasekara et al. (264).

For films containing 20% cholesterol, the AFM micrographs reveal almost no lamellar structures (Fig. 5.4C). Lack of lamellar structures is consistent with a continuous, irreversible collapse of monolayer matter into the aqueous phase upon the film contraction. The area reduction required to reach 26 mN/m was only $\sim 20\%$ for the films containing 20% cholesterol. We therefore also collected after $\sim 50\%$ area reduction,

at which point the surface tension had dropped to ~ 20 mN/m. These films too were devoid of bilayer stacks (not shown).

Quantitative analysis of the micrographs from expanded and contracted films allowed for an estimate of the proportion of lipids that underwent a monolayer-bilayer conversion over the lipids that were lost to the aqueous phase upon film contraction (Fig. 5.2; and see Materials and Methods). The estimate was based on the analysis of four micrographs such as shown in Figure 5.4 for each condition. According to this analysis, for surfactant containing no cholesterol, 100% of the lipids in the monolayer displaced from the interface were recovered in bilayer stacks. Individual micrographs ranged from 100% to 103% recovery. For films containing 5% w/w cholesterol, $\sim 12\%$ of the squeezed lipids were lost to the subphase and, hence, $\sim 88\%$ converted into stacks of bilayers after the film area had been reduced by half. Individual micrographs ranged from 5% to 18% loss. For films containing 20% w/w cholesterol, $>90\%$ of the lipids were lost to the aqueous phase upon contraction.

5.4.2 The structure of the bilayer stacks as revealed by Kelvin probe force microscopy

Figure 5.5 shows the topography (left) and local electrical surface potential (right) of films containing no cholesterol. Both the topographical map and the electrical surface potential map (right) are highly structured for these films, and the dynamic range of the electrical signal is 300-400 mV. Large stacks of bilayer patches are at a potential of up to 200 mV above the monolayer. Upon close inspection of Figure 5.5A, including the cross-sections below the respective images, the potential is not strictly correlated with

topographical height (i.e., film thickness). Sometimes the potential even drops to a lower level within an area of constant topographical height (arrows in Fig. 5.5A).

Figure 5.5B shows the film at higher magnification. To allow for easy correlation between topology and potential, the outer perimeters of the bilayer stacks were computed from the AFM topographical image (Fig. 5.5B, left) and overlaid in red in the potential map (Fig. 5.5B, right). Interestingly, only the larger, irregularly shaped bilayer-stacks are consistently at a more positive voltage with respect to the average potential. Smaller stacks have an almost spherical perimeter. The stacks between 200 and 400 nm in diameter are either at a more negative or more positive potential. Smaller stacks are up to ~100 mV below average potential.

The most striking feature in the surface potential maps is the either positive or negative surface potential of the stacks of lipid bilayers with respect to the monolayer areas. The large contributions of the stacks to the surface potential may not likely be ascribed to lipids. The lipids of the two leaflets of a bilayer are of opposite orientation with respect to the sample plane such that the contribution to the surface potential cancels out. Rather, the surface potential difference to the monolayer observed for most of the stacks may find its explanation by the presence of the small hydrophobic surfactant-associated protein SP-C. SP-C consists mostly of an α -helical segment that spans lipid bilayers (205,355). Alpha-helices exhibit a strong molecular dipole moment along the helix axis, which, in the case of SP-C, may be accentuated by positive charges near its N-terminus. Residing in these multilamellar regions of the surfactant films (356), SP-C promotes the formation of lipid bilayer patches. Note that the absolute contribution of the

SP-C to the surface potential of the lipid stacks will be reduced by the screening of the helical dipole in the lipid environment (357).

If SP-C is indeed the cause for the observed surface potential of the bilayer stacks, it is not randomly oriented. A positive surface potential such as that observed for the large stacks is caused when a majority or all SP-C molecules in a designated area span the lipid bilayers in a stack with the N-terminus pointing toward the air. If SP-C is arranged with its C-terminal end toward the air, the bilayer stacks will be at a more negative potential than the monolayer such as that observed with the small stacks. The extended irregularly shaped bilayer stacks shown in Figure 5.5A may have arisen from multiple folding events and/or the fusion of smaller stacks. This would explain why, in a region of constant topographical height, the electrical surface potential sometimes changes in stepwise fashion, as outlined by the arrows in Figure 5.5A.

SP-B is also present in BLES and also promotes the formation of lamellar structures (358,228). SP-B is likely composed of four to five amphipathic helices (i.e., helices with a highly hydrophobic face on the one side of the helix-axis and a hydrophilic face on the opposite side; for reviews, see 36, 230). It is proposed that the helices are aligned partially immersed in the lipid layer with the axis parallel to the interface (106) and act as a cross-linker between monolayer and bilayer patches. Since the helix-dipoles in this case are parallel to the interface, they should not contribute to the surface potential. However, being immersed only in one of the two leaflets of a bilayer might introduce sufficient asymmetry for a bilayer to show a net surface potential.

The elevated surface potential of the large bilayer stacks immediately drops by ~100 mV outside the perimeter of the large bilayer stacks (cross-sections, Fig. 5.5A).

Further reduction of the potential by ~50-100 mV gradually occurs over a distance of ~1 μm , indicating that the molecular composition and order of the monolayer gradually changes toward the stacks. It was shown earlier that SP-C becomes gradually inserted from the monolayer into the bilayer stacks upon area reduction (356,218,316). Hence, SP-C may also still be present in the monolayer close to the stacks in Figure 5.5 and induce an elevated surface potential. SP-B appears to become gradually integrated in bilayer stacks upon film contraction (228) and could have a similar effect. The monolayer close to the stacks may also have a different lipid composition.

For the films containing 20% cholesterol (Fig. 5.6), the occasional protrusions are not at an elevated electrical potential with respect to the monolayer. The absence of a contrast in the Kelvin signal in this case may either reflect a disordered molecular arrangement where molecular dipoles cancel out or bilayers devoid of protein. This indicates that cholesterol inhibits the ordered monolayer-bilayer conversion promoted by SP-B and/or SP-C. Furthermore, unlike in the absence of cholesterol, the surface potential is also not altered in the monolayer in proximity to the (rare) protrusions. Hence, given the role ascribed to SP-B and/or SP-C in shaping the surface potential maps of films devoid of cholesterol, these proteins may have been lost early on upon contraction for the films containing 20% cholesterol.

At high resolution of the films containing 20% cholesterol (Fig. 5.6B), electrical domains in the monolayer region become visible. The domains are ~100 nm across and are therefore too small to be resolved in the low-magnification map shown in Figure 5.6A. The dynamic range of the potential of the domains is ~300 mV. On close inspection, regions of slightly greater film thickness are found to coincide with regions at

a more positive surface potential. Electrical domains of this size are not present in films containing no cholesterol. Hence, cholesterol causes the lipids in the monolayer to become differently arranged as well. In fluorescence light microscopy, surfactant containing no cholesterol segregates into domains. Condensed domains, typically several micrometers across, are surrounded by the more fluid components in the film (e.g., 316,359,360,361,318). Surfactants containing cholesterol, on the other hand, appear homogenous by light microscopy (361,362). This study now shows that these films still form domains, but they are too small to be resolved in a light microscope. Areas of higher potential are always found in topographically elevated areas. Cholesterol promotes a more positive surface potential in phospholipid films (362) and may therefore reside in the elevated (thicker) film areas.

5.5 Discussion

Our experimental findings indicate that the function of pulmonary surfactant films depends on the presence of bilayer stacks. The stacks are reversibly formed from the monolayer during film contraction and reinsert into the monolayer upon re-expansion. An elevated level of cholesterol inhibits the monolayer-bilayer conversion and results in dysfunctional films. In this Discussion, we will attribute the unique mechanical properties observed with the functional surfactant partially to sorting of the surfactant components between the monolayer and adjacent bilayer patches and partially to mechanical reinforcement of the film by the bilayer stacks.

5.5.1 Sorting

The minimum surface tension achievable by unsaturated phospholipids is ~20-30 mN/m. DPPC films, on the other hand, can attain near-zero surface tension. During monolayer-bilayer conversion, unsaturated lipids may be transferred from the monolayer to the adjacent bilayer patches. The monolayer may therefore become enriched in DPPC, which allows for low surface tension. If the monolayer-bilayer conversion is inhibited by an excess amount of cholesterol, the unsaturated lipids remain in the monolayer and a low surface tension cannot be achieved. Instead, the film continuously collapses upon contraction.

The notion of a monolayer-bilayer conversion that also involves sorting of lipids is supported by the unique properties of SP-C in conjunction with our experimental finding of a defined orientation and polarity of SP-C within the stacks. Figure 5.7 depicts how the orientation of SP-C may become defined by the two palmitoyl groups close to the N-terminus during film contraction. In this model, the palmitoyl groups remain anchored in the monolayer while the helix moves together with the lipids into a newly formed bilayer toward the aqueous phase. An inverted bilayer patch, formed toward the air, causes the opposite orientation of the SP-C molecule. The palmitoyl groups tend to remain anchored to the monolayer because of their strong affinity to domains of condensed, saturated lipids (363). Condensed DPPC domains are common for both model and natural surfactant films (e.g., 364). In accordance with this proposed role of the palmitoyl anchor, it was found that in a model surfactant containing SP-C the bilayer stacks were always associated with condensed regions of a phase-separated monolayer and were excluded from the more fluid regions of the film (245). While the palmitoyl-

groups of the SP-C are likely associated with DPPC in the monolayer at the air-water interface, the helical part of the SP-C is known to span lipid bilayers in a fluid state and is excluded from bilayers in the condensed gel phase (205). This suggests that SP-C promotes the formation of bilayer patches of unsaturated lipids.

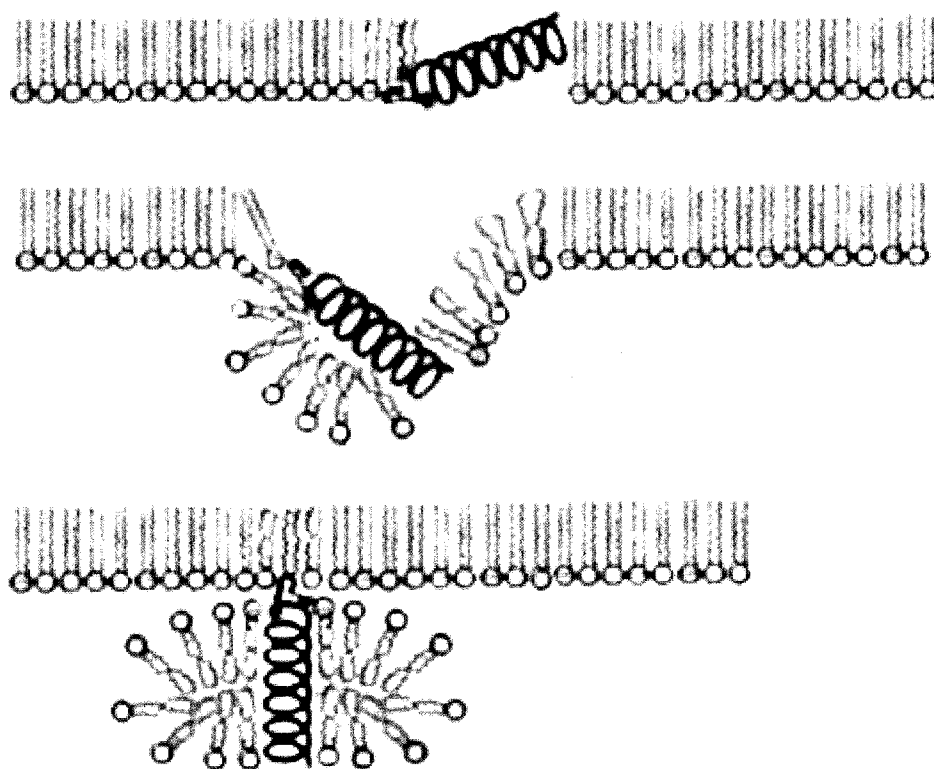


Figure 5.7 Mechanism explaining a positive surface potential on the large bilayer stacks. The helical span of SP-C is oriented in lipid monolayers with $\sim 70^\circ$ to the normal of the interface (51). Upon film contraction, a first bilayer adjacent to the monolayer is formed toward the aqueous subphase. SP-C rotates to span the newly formed bilayer and remains anchored to the monolayer by its two palmitoyl groups near its N-terminal end. SP-C is known to span lipid bilayers (52). As a result, all SP-C molecules face with the N-terminus toward the air, resulting in a positive surface potential. A related mechanism (not shown) may occur for the small bilayer stacks that were found to be at negative electrical surface potential. This time, the bilayer stacks may form toward the air. With the highly hydrophilic N-terminus remaining immersed in the water phase, SP-C may now point with its C-terminus toward the air.

While pulmonary surfactant function may depend on the monolayer-bilayer conversion to remove unsaturated lipids from the monolayer, the monolayer-bilayer conversion does not necessarily depend on the presence of unsaturated lipids. The conversion occurs even in the presence of only saturated lipids (DPPC, dipalmitoyl phosphatidyl glycerol) and SP-C (316) and can be inhibited by an excess amount of cholesterol as well (365).

5.5.2 Reinforcement

Sorting and a pure or enriched DPPC monolayer alone cannot fully account for the mechanical stability of a functional surfactant film by itself. Pure DPPC monolayers, while capable of sustaining a near-zero surface tension, collapse irreversibly when mechanically disturbed or overcompressed after reaching close-to-zero surface tension (314). To understand why the monolayer-bilayer conversion is required for stability at close-to-zero surface tension, the bilayer stacks may be ascribed a mechanical role, similar to the role of reinforcing elements in preventing a thin plate from collapsing under lateral compression (366). In this analogy, the surface tension is equivalent to an external lateral pressure compressing a plate and the molecular film is the continuum plate. The film will buckle above a critical compression. Buckling has been described as a mode of failure for pulmonary surfactant (367). Qualitatively, having lipid bilayer patches on the surface breaks the large areas into smaller patches. According to elastic theory, the compression above which collapse occurs increases strongly with a decrease in size of the elements for a given cross-section (or film thickness) (366). For the bilayer stacks to be mechanically reinforcing, they must be cross-linked to the monolayer. Otherwise, they

will separate from, or glide over, the monolayer upon area reduction and have no mechanical effect. In the mechanism for the formation of stacks proposed above (Fig. 5.7), SP-C acts as the cross-link. We earlier found direct evidence for cross-linkage by SP-C by mechanically manipulating bilayer stacks in a surfactant model containing SP-C (245). SP-B is also acting as a cross-linker, and on its own has led to the formation of bilayer stacks in a model surfactant film of exceptional stability (317). In agreement with this proposed function of SP-C and SP-B, artificial or animal extract surfactants depend on the presence of either one or both hydrophobic proteins to lower the surface tension to a physiological low level.

Cholesterol inhibits the monolayer-bilayer conversion. It thus affect both purification of the monolayer from unsaturated lipid species and reinforcement of the film by the bilayer stacks. Cholesterol does not appear to cause monolayer instability independent of these mechanisms. Our earlier study of surfactant function (264) revealed that BLES films can attain a very low surface tension even in the presence of 20% cholesterol, if the relative amount of DPPC is also increased by the same proportion as the cholesterol. We now found that, under these conditions, the monolayer-bilayer conversion is still mostly inhibited (not shown). Hence, these films may already contain a sufficient proportion of DPPC to allow for a low surface tension and may therefore not depend on the monolayer-bilayer conversion for sorting. However, the functional study (264) also showed that, while attaining a surface tension close to zero, the films were otherwise inferior to a fully functional film. The films required an unphysiologically large amount of area reduction to lower the surface tension close to zero. They also became dysfunctional after repeated expansion and compression (264). Hence, similar to

pure DPPC films, these films lacked stability at near-zero surface tension. We ascribe lack of stability was ascribed to the absence of the reinforcing bilayer stacks.

5.6 Conclusions

An elevated level of cholesterol inhibits the reversible monolayer-bilayer conversion in pulmonary surfactant, thus leading to failure of surfactant function. Cholesterol should therefore become a target for treatment of surfactant impairment in ARDS. To find ways to reverse the effect of excess cholesterol, future studies will have to address the mechanism by which cholesterol inhibits the monolayer-bilayer conversion. An effective treatment, in addition to countering the effect of cholesterol, may also have to target other mechanisms of surfactant inhibition, including oxidation of surfactant through the reactive oxygen species present in the injured lung (232,341,342,343,368) and interference with serum proteins interact with surfactant (e.g., 369).

Chapter 6: A Comparative Study of Mechanisms of Surfactant Inhibition

6.1 Background

6.1.1 Surfactant inhibition and ARDS

Acute respiratory distress syndrome (ARDS) is a common and devastating spectrum of disease that has a high overall mortality rate. Acute lung injury (ALI) and its severe form acute respiratory distress syndrome (ARDS) are characterized by the rapid onset of hypoxemia, dyspnea, respiratory failure, and bilateral infiltrates on a chest radiograph that occur with pulmonary edema (372). The published, population-based incidence of ARDS ranges from 1.5 to 5.3/10⁵ population/year, with a mortality rate of 36% to 60% (328). It is a reflection of acute inflammatory lung injury from multiple pulmonary and extrapulmonary causes (214). The strongest clinical evidence of a cause-and-effect relationship was identified for sepsis, aspiration, trauma, and multiple transfusions (328) and these conditions can affect both adults and children.

A central component of this condition is pulmonary surfactant inhibition and the concomitant elevation of surface tension. In ARDS, inflammation gives rise to excess production of lipases and proteases, radical oxygen species (ROS), and other inflammatory mediators within lung tissue. Damage to the alveolar wall allows these compounds, together with blood-serum components, access to the alveolar space where they can impair pulmonary surfactant. Since surfactant impairment is a major factor in the morbidity and mortality of ARDS, it has been targeted by replacement surfactant therapy. However, success has been minimal (for a review, see 312). This is likely because the exogenous surfactant also becomes inactivated in the affected lung. It is now

generally believed that successful treatment will depend on an in-depth understanding of the mechanisms of impairment.

6.1.2 Pathophysiology of ALI and ARDS

The pathology of lung injury is complex and associated with damage to the alveolar capillary membrane, edema, ventilation-perfusion mismatches, inflammation, oxidant injury, and surfactant dysfunction among its many aspects (214). In ARDS, multiple cell types are affected, which is reflected by a significant elevation in the number of inflammatory mediators, products, enzymes (214).

6.1.3 Cellular molecular mechanisms of injury

6.1.3.1 Endothelial injury

Due to the primary insult to the lung, widespread injury and activation of both the lung and systemic endothelium causes the enhancement of endothelial permeability and the expression of adhesion molecules. A number of the circulatory markers of endothelial cell injury and activation have been identified in ALI/ARDS patients (373,374). In patients with ALI/ARDS, the upregulation of endothelin-1 and von willebrand factor antigen indicates systemic and pulmonary endothelial activation and injury (375,376,377). Microvascular endothelial injury leads to increased permeability and pulmonary edema, which is the pathological hallmark of ALI/ARDS (378). After the initial insult, endothelial injury occurs within minutes to hours. It is characterized by the formation of intercellular gap junctions between endothelial cells, along with variable necrosis and degeneration of the endothelium (379).

6.1.3.2 Epithelial injury

Epithelial injury during ALI/ARDS plays a major role in the development and recovery of this condition. Type I pneumocytes cover 90% of the alveolar surface and are more prone to damage. Type II pneumocytes cover the remaining 10% of the alveolar surface and are more resistant to injury. In addition to surfactant production, type II cells are also responsible for the regeneration of type I cells after injury (380). The epithelial barrier is much tighter than the endothelial barrier. Thus, loss of epithelial integrity during ALI/ARDS leads to the formation of alveolar edema. Pulmonary edema formation is also facilitated by the impairment of normal fluid transport mechanisms of the epithelium (380). Type II cell injury diminishes and alters the synthesis, turnover, and metabolism of surfactant. In doing so, it also alters the protein and lipid components of surfactant. In addition, pulmonary edema due to increased permeability of the epithelium brings some of the inflammatory products, blood proteins and proteolytic enzymes into the alveolar space. These products can also inactivate the surfactant system.

6.1.3.3 Neutrophil-mediated injury

Several studies showed that neutrophils play a very important role in most cases of ALI/ARDS. Histology of early ALI/ARDS lesions demonstrated a marked accumulation of neutrophils in the lungs (383,381). Similar results were obtained from the studies with bronchoalveolar fluid and edema fluid from the lung (382). Although many animal models of ALI/ARDS are neutrophil dependent, rare ALI/ARDS cases have been reported to occur without neutrophils (384).

Once neutrophils are retained in the lung, they release injurious metabolites such as proteolytic enzymes, reactive oxygen species, nitrogen species, cytokines, and growth factors (385). Proteases damage the extracellular matrix of the lung and promote the migration of neutrophils from the capillary into the air space (386). In the air space, proteases can degrade surfactant-associated proteins, which in turn cause surfactant inactivation. Most of the toxic products of neutrophils can be counteracted by a complex of endogenous antiproteases and antioxidants whose production can be upregulated by proinflammatory cytokines (380). A balance of these protective and harmful compounds might be important in minimizing tissue damage in ALI/ARDS (380).

6.1.3.4 Cytokine-mediated inflammation and injury

Proinflammatory molecules and cytokines, which are produced by a variety of cells in the lung, can initiate, enhance, and modulate the inflammatory response in ALI/ARDS. Cells that produce these proinflammatory molecules include fibroblasts, epithelial cells (type I and II cells), and inflammatory cells (387). Direct and indirect insults to the lung, such as through endotoxins and other microbial products, lead to the production of early response cytokines like TNF- α and IL-1 from monocytes and macrophages (388). These mediators act locally on cells such as macrophages, endothelial cells, fibroblasts, and epithelial cells in order to stimulate the synthesis of other cytokines like IL-8 (neutrophil chemotactic factor). High IL-8 concentrations were reported in the alveolar space of ALI/ARDS patients (380). Thus, local releases of these cytokines evoke a series of effects that result in both neutrophil influx and the release of a

number of toxic products. However, a number of anti-inflammatory mediators such as IL-10 and IL-11 may have protective functions against lung injury (380).

6.1.3.5 Oxidant-mediated injury

Activated macrophages, lung endothelial and lung epithelial cells are capable of producing reactive oxygen and nitrogen species in response to inflammatory stimuli. In ALI/ARDS, most cellular damage is done by reactive oxygen (386). Reactive oxygen species oxidize membrane fatty acids and enhance cell membrane permeability, whereas protein oxidation can render them inactive, and oxidation of DNA can arrest protein synthesis (380).

6.1.4 Mechanisms of surfactant alteration in ARDS

A central component of ARDS is pulmonary surfactant inhibition and the concomitant elevation of surface tension. A number of studies were done to investigate the mechanisms of surfactant alteration during acute lung injury. These studies were mainly conducted with animal models of lung injury, as well as with *in vitro* methods. As noted in these experiments, alterations of surfactant systems in ALI/ARDS (312) also can be detected by analysis of bronchoalveolar lavage (BAL) samples obtained from patients with ARDS. These studies confirm that the alteration of endogenous surfactant contributes to lung dysfunction in ARDS (185,389). Changes in lipid profile, alterations in the concentrations of surfactant associated proteins, and changes in the relative amount of large and small aggregate forms within the alveoli are some of the notable alterations that occur during ARDS. According to results of the aforementioned studies, the potential

mechanisms of surfactant inhibition in ARDS can be categorized roughly into three groups.

- 1) Alterations in type II pneumocyte function
- 2) The influence of inflammatory mediators and other products on the surfactant system
- 3) Contributions of therapeutic involvement

During ARDS, the alteration and dysfunction of type II pneumocytes occurs, which affects pathways of surfactant synthesis and/or secretion within type II cells. This is reflected by a reduction in total phosphatidylcholine, as well as a reduction in the DPPC fraction of lung surfactant. Reductions in phosphatidylglycerol and other minor phospholipids are also obvious during ARDS (389,390). Furthermore, ALI/ARDS is associated with the upregulation of proinflammatory mediators such as TNF. TNF decreases the amount of choline incorporated into phosphatidylcholine in type II pneumocytes (391), as well as decreases the synthesis of surfactant-associated proteins (391). In addition, other mediators that can be upregulated in ALI, such as hepatocyte growth factor, can inhibit the synthesis and secretion of PC.

Inflammatory cell infiltration is another key feature of ALI/ARDS. These cells produce a number of inflammatory mediators, enzymes and other products. Such products contribute to the alteration of the surfactant system. For example, an inflammatory product that directly influences surfactant alteration is phospholipase A₂. Several secretory phospholipase A₂ (sPLA₂) isoforms are synthesized mainly by infiltrated leukocytes in inflamed lungs (392,393). Enhanced sPLA₂ activity has been shown in bronchoalveolar lavage (BAL) fluid in animal models of lung inflammation (394,395), and in human studies of ARDS and asthma (396,397,398). sPLA₂ hydrolyzes the sn-2

fatty acid from a phospholipid glycerol backbone, usually without any preference for specific sn-2 fatty acids (399). This gives rise to a free fatty acid and a lysophospholipid. Lysophospholipids can disrupt molecular packing of the surface film at the air-water interface of lung alveoli (400). Also, the reduction of phospholipids due to the action of sPLA₂ leads to an inability to maintain the phospholipid film. Finally, resultant free fatty acids due to the action of sPLA₂ can also interfere with the packing of phospholipid film, and can interrupt the surface tension lowering ability of surfactant (401). Lyso-PC at low concentration does not inhibit surfactant, but can sensitize it to protein inhibition.

Surfactant can also be inactivated by oxidative stress. Superoxide and hydroxyl radicals seem to react with surfactant lipids and surfactant proteins (343,402). Surfactant proteins are also affected by nitration (403). Inflammatory cells in ALI can enhance the activity of inducible nitric oxide synthase (iNOS) (404). Increased activity of this enzyme leads to prolonged production of NO, which can nitrosylate surfactant associated proteins. These proteins then become less functional compared to their normal state. Furthermore, neutrophils that are attracted to inflamed lungs during ARDS can secrete various proteases such as elastase, which reacts and degrades surfactant protein A. Enhancing the activity of proteases increases the conversion of large aggregate fractions to small aggregate fractions in lung alveoli (404,405). This acts to reduce the surface-active large aggregate fraction in the alveolar compartment.

Plasma proteins are considered as another candidate that is believed to cause surfactant inhibition during ALI/ARDS. Acute lung injury occurs due to certain insults that result in the disruption of capillary-endothelium integrity. This in turn leads to leaky capillary membranes that facilitate plasma protein influx into the alveolar space

(406,407). Such enhanced permeability and increased protein oncotic pressure in the alveoli oppose the efforts of the alveolar epithelium to remove fluid from the alveoli, leading to pulmonary edema. There are a number of studies about serum protein (mainly albumin and fibrinogen) mediated surfactant inhibition. Fibrinogen and fibrin monomers can inhibit surfactant by sequestering surfactant constituents such as surfactant-associated proteins. Meconium is also another endogenous inhibitor of lung surfactant (419, 38). Mechanical ventilation is usually a useful treatment strategy to treat patients with ALI, as it helps to maintain blood oxygenation. Unfortunately, mechanical ventilation also contributes to alterations in surfactant (408,409). According to some studies, mechanical ventilation directly contributes to the conversion of large aggregates into small aggregates (410). This is demonstrated both *in vivo* using normal ventilated rabbits (412) and *in vitro* (411). Furthermore, mechanical ventilation can cause damage to the surfactant system through some of the shear forces associated with the opening and closing of the lung under positive pressure, which occurs during the procedure (413). These forces can promote the leakage of plasma proteins and other inhibitory plasma constituents into the alveoli, thus contributing to surfactant inhibition. Also, mechanical ventilation increases the concentration of oxygen in the blood. High levels of oxygenation can disturb the balance between oxidants and antioxidants, which can result in oxidative damage to the surfactant (414).

As we have shown previously, supraphysiological amount of cholesterol can completely abolished surfactant function *in vitro* (264). Very importantly, few animal studies and a human study of acute lung injury clearly confirmed that significantly

increased cholesterol amount in lung surfactant (145,224,302). Therefore, cholesterol also should be considered as a potent inhibitor in surfactant function.

6.1.5 Mechanisms of surfactant inhibition

Inactivation is defined as the reduction in, or loss of, physical attributes when a substance is added to a surfactant. Current understanding of surfactant inhibition has suggested two alternative mechanisms, one being competition for the interface (312,415,311,340). According to this model, blood proteins, inflammation specific proteins, or other surface-active substances adsorb to the air-water interface and compete with the pulmonary surfactant for the interface. A high-surface tension will then result from an absence of surfactant film over significant portions of this interface. The other model of surfactant inhibition attributes high-surface tension to impairment of the surfactant film itself (416,264,337,232,341,342,343). Small amphiphilic molecules such as free fatty acids, supraphysiological amount of cholesterol and lysophospholipids are thought to associate with the surfactant film and render it dysfunctional (416,264,337). The detrimental effect of surfactant lipid and protein oxidation by ROS also falls into this category of surfactant impairment (232,341,342,343).

6.2 Introduction

In the current study, we compared the two alternative mechanisms of surfactant inhibition, competition for the interface versus impairment of the surfactant film itself in vitro under conditions which attempt to more adequately reflect those in the lung than the conditions chosen in earlier studies (see “Discussion”). The captive bubble surfactometer

(CBS) was used for measuring the surface activity, because it comes closest to mimicking lung function as determined *in vivo* from pressure-volume studies (20). The CBS consists of a chamber, filled with buffer, with an air bubble floating against a convex agarose ceiling. Varying the volume in the chamber alters bubble size changing the surface tension. Alterations in γ at the air-liquid interface in the CBS are seen as a flattening of the bubble as γ falls and a rounding as it rises (250). We investigated films formed from clinically used bovine lipid extract surfactant (BLES) (295). BLES contains all lipids of natural surfactant with the exception of cholesterol. We used BLES as is to reflect normal surfactant and after the addition of 20% w/w cholesterol to model the elevated amount found in diseased lungs (224,417). We have found that this level of cholesterol, while not being the only neutral lipid change in diseased lung, produces marked inhibition of surfactant while lower physiological levels do not (264). BLES also contains the two highly hydrophobic surfactant associated proteins SP-B and SP-C in natural proportions. To study the effect of serum proteins, we added either serum albumin or fibrinogen to the aqueous phase. The protein concentrations (40 mg/ml for albumin, 3 mg/ml for fibrinogen) were chosen to reflect what the alveolus might be exposed to in extreme ARDS. Albumin was also tested at 80 mg/ml. The protein was added either before or after a BLES film had been formed at the bubble air-water interface to assess the competing hypotheses. Surfactants were administered to the air-water interface in a small but concentrated (27 mg/ml phospholipids) aqueous bolus of surfactant (264,263). We then observed the change in γ to see how serum proteins affected film formation. Next the bubble size was rapidly increased and changes in γ were followed to monitor the films' ability to incorporate additional material and then accommodate this addition. Thereafter

the bubble size was slowly decreased and increased (quasi-static cycles), followed by rapid cycles (dynamic cycles). A similar experimental protocol was pursued with BLES containing 20% w/w cholesterol. Finally, we also explored whether the addition of PEG to the aqueous phase reversed the inhibition by cholesterol or albumin similar to the published findings for serum protein inhibition.

6.3 Materials and methods

6.3.1 Surface activity assessment

The surface activity of the surfactant was determined using a laboratory-built, fully computer controlled CBS evolved from the apparatus described earlier (314). The chamber of the CBS was filled with a buffer solution (140 mM NaCl, 10 mM HEPES, and 2.5 mM CaCl₂, pH 6.9), with or without protein, as described below and a small (0.035-0.040 ml) bubble was allowed to float up to the chamber's concave agarose ceiling. Then, ~ 0.05 μ l of the surfactant was deposited at the air-buffer interface by means of a transparent capillary. This allowed a precisely defined volume of surfactant to be deposited under visual control. The bubble was imaged by a video camera (Pulnix TM 7 CN) and recorded for later analysis. The chamber was kept at 37°C during the experiment. A 5-minute adsorption (film formation) period followed the introduction of the surfactant into the chamber during which the bubble was not manipulated and the change in γ was monitored. The chamber was then sealed and the bubble was rapidly (1 s) expanded to a volume of 0.13 ml. Five minutes after the bubble was expanded quasi-static cycling commenced. In the quasi-static portion of the experiment the bubble size was first reduced and then enlarged in a stepwise fashion by altering the internal

volume of the chamber. Each step had two components: a 3-second change in volume followed by a 4-second delay when the chamber volume remained unchanged allowing the film to “relax.” There was a 1-minute inter-cycle delay between each of four quasi-static cycles and a further 1-minute delay between the quasi-static and dynamic cycles. In the dynamic cycle portion of the experiment, the bubble volume was smoothly varied over the same range as the last quasi-static cycle for 20 cycles at a rate of 20 cycles/min. Bubble volume, interfacial area, and γ were calculated using height and diameter of the bubble as described (260).

6.3.2 Surfactant

BLES (a kind gift from the manufacturer BLES Biochemicals Inc., London, ON; see Yu et al. (295 and fig. 1.1b) for analysis of BLES composition) in non-buffered normal saline (pH 5-6) with calcium added and at a phospholipid concentration of 27 mg/ml was used as is for the protein-inhibition experiments or after the addition of cholesterol (Sigma Chemicals, St. Louis, MO) for the cholesterol-inhibition experiments. Cholesterol cannot be added reliably and quantitatively to BLES while in aqueous suspension. Therefore, BLES was first taken up in organic solvent, cholesterol added and the mixture returned into an aqueous solution as follows. A 1:1:1 ratio solution of methanol, chloroform, and BLES by volume was first vortexed and then spun at 100 g for 5 min. The chloroform phase contained most of the BLES and was saved. For complete recovery of BLES, the water/methanol phase was extracted a second time with chloroform and the two fractions of BLES in chloroform pooled. To this pool, cholesterol in chloroform was added to a final concentration of 20% w/w with respect to BLES

phospholipids. The solution was dried under N_2 and re-suspended in buffer (140 mM NaCl, 10 mM HEPES and 2.5 mM $CaCl_2$; pH 6.9) to obtain an aqueous suspension of BLES and cholesterol at a phospholipid concentration of 27 mg/ml.

6.3.3 The aqueous phase of the CBS

Sucrose, 10% w/w, was added to the buffer to increase its density so that the surfactant suspension would float to make and remain in contact with the bubble upon injection (see below). Adding sucrose does not affect surface activity of surfactant (264). For the protein-inhibition experiments, proteins were added to the buffer either before, or after the surfactant was placed at the air-buffer interface of the CBS. The proteins remained present throughout all tests. Dry powders of bovine serum albumin (catalogue number A7906) and fibrinogen from human plasma (catalogue number F4883) were purchased from Sigma-Aldrich. Dry serum albumin was dissolved in buffer to a final concentration of 40 mg/ml or 80 mg/ml and fibrinogen to a concentration of 3 mg/ml. In two instances, polyethylene glycol (PEG) was introduced into the chamber, after the surfactant had been injected. PEG (MW 6000, Fluka Chemicals Co., Switzerland) was dissolved in buffer and injected into the sample chamber to a final concentration of 25 mg/ml.

6.3.4 Representation of CBS results

Film formation was plotted as surface tension γ versus time. For quasi-static and dynamic cycles, surface tension (γ)–bubble area (A) isotherms were plotted and the film's

two-dimensional compressibility (β) was also calculated, according to the following equation, to further describe the surfactant films' surface activity.

$$\beta = (1/A) \cdot (\Delta A/\Delta\gamma)$$

In this equation A is the absolute bubble area at a given surface tension γ , and values for β at $\gamma = 10$ mN/m ($\beta_{\gamma 10}$) are given in the results (table 6.1).

6.3.5 Statistical analysis of CBS experiments

Nonparametric tests (SPSS 14.0) of differences in surface tension during film formation and in minimum surface tension attained in bubble cycling were performed with $P < 0.05$ used as the standard for significance in all cases. The Friedman test for multiple related measures was used first to test for main within treatment effects and the Wilcoxon paired related measures test was used for subsequent orthogonal comparisons after overall significance was determined. The Kruskal-Wallis and the Mann-Whitney U tests for independent samples were similarly used to determine overall between treatment effects and to make subsequent specific orthogonal comparisons.

6.3.6 Electron microscopy

Five μ l each of an aqueous suspension of either BLES of 27 mg/ml, BLES at 5 mg/ml, or BLES at 5 mg/ml plus PEG were put down onto a bare electron microscopy grid, excess of the suspension removed by filter paper and the grid injected into liquid ethane. Grids were transferred onto a cryo-holder and imaged in a Tecnai F-20 (FEI) at -100°C without further staining.

6.4 Results

6.4.1 Film formation

Film formation was studied in two ways. As the first step in the experimental protocol, we injected the aqueous suspension of BLES close to the bubble from a transparent capillary (Fig. 6.1a). The surfactant then made contact with the bubble surface and the resultant drop in γ was observed over 5 minutes (Fig. 6.1b). The drop in surface tension after injection of surfactant as a function of time was indicative of the ability of surfactant to form a functional film at a clean or serum protein-covered interface. In the following sections, results are shown for adsorption of BLES onto a serum protein-free buffer and a buffer containing either serum albumin or fibrinogen. Finally, adsorption of BLES with 20% w/w cholesterol onto a serum-free buffer is described. Results on the adsorption of the films for all conditions are summarized in Table 6.1.

For all samples, upon making contact, the surfactant spread over the entire bubble and lowered the surface tension. However, the time course of film formation differed significantly for different treatments (Fig. 6.1b). Spreading BLES onto a protein-free buffer resulted in a drop of γ to between 35.0 and 30.0 mN/m within 0.15 s for all but three samples. Thereafter, γ dropped further to reach a value of 23.5 (\pm 0.05) mN/m within 30 s (e.g., Fig. 6.1b, black curve). The equilibrium surface tension obtained with BLES is \sim 23.5 mN/m (e.g. 264). Reaching this surface tension indicates that the process of film formation is complete. Hence, film formation could be seen as two processes with an initial extremely fast drop in γ reflecting surfactant material spreading from the point of contact to cover the interface. The following slower further drop in γ to equilibrium may reflect alterations in the surfactant film architecture after the surface has been covered.

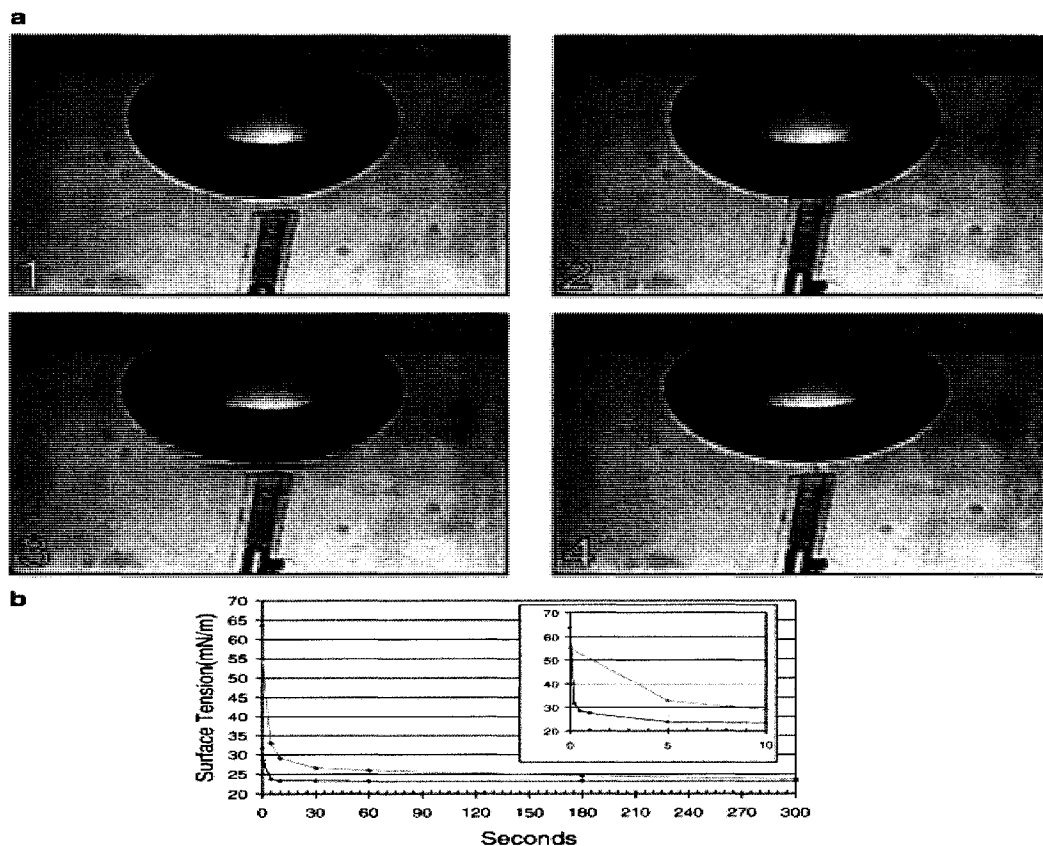


Figure 6.1 Adsorption of surfactant. (a) (1) An air bubble in buffer floats against the agar ceiling of the captive bubble surfactometer chamber (image width 6 mm). (2) A transparent capillary is advanced just to the air-water interface from below and a small amount of surfactant ejected (BLES, 27 mg/ml). This material contacts the bubble surface causing it to flatten (3). Due to interlacing of the video image, the old shape of the bubble is evident in frame 3 field 1 as fine horizontal stripes, whereas the new shape appears solid in the second field of this frame. The time display at the top left of each image indicates a time change of 0.1 s between image frames 3 and 4. This change in shape brings the bubble out of contact from the capillary (4). (b) Two plots of the surface tension over time as calculated from video frames such as shown in (a). The inset represents the initial part of the curve at higher time resolution. The dark curve is an example of BLES being adsorbed to the air-water interface of a bubble in buffer, in the absence of a potential inhibitor. Note the very rapid initial film formation. The plot in grey shows the adsorption of BLES containing 20% w/w cholesterol. Initial film formation is slightly slower under this condition.

	Film spread < 0.15 sec	1st compression		1st dynamic cycles		2nd quasi-static cycles		3rd quasi-static cycles	
		$\gamma_{\min} < 2$ [mN/m]	$\beta_{\gamma 10}$ [m/N]						
Control	100%	93%	11.3	100%	7.2				
80 mg/ml albumin injected after film formation	100%	0%	–	100%	7.6	25%	8.7	100%	6.9
80 mg/ml albumin and PEG injected after film formation	80%	60%	14.2	100%	4.0	100%	4.6	0%	
40 mg/ml albumin injected after film formation	75%	50%	10.0	100%	6.0	100%	6.5	0%	
80 mg/ml albumin in the buffer during film formation	0%	50%	23.9	100%	5.8	100%	7.7		
40 mg/ml albumin in the buffer during film formation	0%	50%	13.7	100%	7.0	100%	5.9		
3 mg/ml fibrinogen in the buffer during film formation	33%	33%	39.2	66%	8.1	100%	8.2		
20% cholesterol added to BLES	0%	0%	–	0%	–	0%	–	–	–
20% cholesterol added to BLES, PEG in the buffer	33%	0%	–	0%	–	0%	–	–	–

Table 6.1 The column headed “film spread < 0.15 s” indicates for each condition the percentage from all individual tests where the surface tension γ fell below 35 mN/m within 0.15 s. This criterion is indicative of whether film formation was slowed by the presence of inhibitors or not. The second column shows the percentages of films that reached very low surface tension ($\gamma_{\min} < 2$ mN/m) for the first compression after film formation (i.e., the first compression of the first quasi-static compression-expansion cycles), and the following columns show the first series of dynamic cycles, the second, and the third of quasi-static cycles respectively. Another measure of function, the median compressibility at a surface tension of 10 mN/m (median $\beta_{\gamma 10}$ [m/N] shown in the second column of each set) indicates whether a film was sufficiently incompressible. In the lung, a low compressibility of the surfactant film is found, as the very low surface tension required at end expiration occurs with a small area change. In the table, “–” denotes incidences where a surface tension of 10 mN/m was not achieved, and, hence, compressibility not measured. Cells with a grey background denote significantly impaired function.

Spreading BLES onto a serum protein containing buffer was chosen to test for the effect of competitive adsorption, by first giving the protein time to adsorb to the interface before injecting surfactant. The initial drop in surface tension was significantly slower under this condition. With serum albumin at the interface, the initial drop in γ to below 35.0 mN/m took longer than 0.15 s irrespective of whether the protein concentration was 40 or 80 mg/ml in the buffer. The results were more varied when the buffer contained fibrinogen. Here one sample dropped below 35.0 mN/m in less than 0.15 s and one took over 7 s to pass this threshold. Despite this initially slower surfactant adsorption, the time for these samples to reach equilibrium was not significantly different from those without protein in the buffer. Hence, surface coverage by surfactant appeared to have been slowed down by the presence of serum proteins, but after an initial coverage, film refinement progressed rapidly enough to obscure the effect by the time equilibrium was reached. Initial film formation was also statistically significantly slower when cholesterol was added to the surfactant, and surface tension took longer than 0.15 s to drop below the 35.0 mN/m criterion in all but one case. This slower initial spreading did not significantly affect the ability to reach equilibrium within 30 s with only one case failing to reach this criterion. The remaining sample then asymptotically approached equilibrium over the allotted 5 min (Fig. 6.1b, grey curve).

Next, the bubble was rapidly expanded to approximately double the size of the air-water interface and γ observed for another 5 minutes. Surfactant not only forms a single layer but spreads to the interface with patches of multiple surface associated layers when prepared as in the current study (264,196). Adsorption of additional surfactant from this surface associated reservoir to the interface was thus observed upon rapid expansion.

For films devoid of cholesterol the surface tension peaked at similar levels after rapid expansion both in the presence and absence of serum proteins while films containing 20% w/w cholesterol reached significantly higher surface tensions. Hence, insertion of new material from the surface associated reservoir was less efficient for films containing excess cholesterol than for films without cholesterol. However, by 60 s after expansion completed, all films had returned to equilibrium with only one surface tension value remaining above 24.0 mN/m. In our experimental protocol, rapid expansion followed by a 5-minute waiting period concluded the assessment of film formation.

6.4.2 Film expansion and compression

After film formation, the bubble volume first was slowly stepwise decreased and increased (quasi-static cycles). Quasi-static cycles reveal whether a surfactant film is able to sustain a low surface tension over time. This is an important parameter of surfactant function. A large proportion of the lung is experiencing minimal or no area change during tidal breathing and these parts of the lung too require stable near-zero surface tension to maintain the alveolar structure. The volume was then cycled dynamically to simulate lung inflation and deflation during normal breathing. Quasi-static and dynamic cycles were repeated to see whether impaired surfactant regained function or functional surfactant became impaired upon further cycling. All results on film expansion and compression are summarized in Table 6.1.

Figure 6.2 shows the compression component of the isotherms for BLES, spread on buffer containing no protein (control, upper row), 80 mg/ml albumin (middle row) or 3 mg/ml fibrinogen (lower row). The individual compression curves for the repeats under

each condition are denoted by different shades of grey. The main results are also summarized in Table 6.1. During the first compression, all films exposed to protein were at least partially dysfunctional in that the surface tension dropped less rapidly than control during size reduction. At $\gamma = 10$ mN/m, median compressibility was 20 mN as compared to 11 mN for the control. Note that at $\gamma = 10$ mN/m a compressibility on the order of 10 mN is consistent with molecules becoming more tightly packed at the interface. Much larger values indicate that some film collapse occurs and molecules are removed from the interface. Some films reached a surface tension near zero ($\gamma_{\min} < 2$ mN/m), others did not. Interestingly, there was not a tight association between compressibility and low γ_{\min} during the first compression of the films.

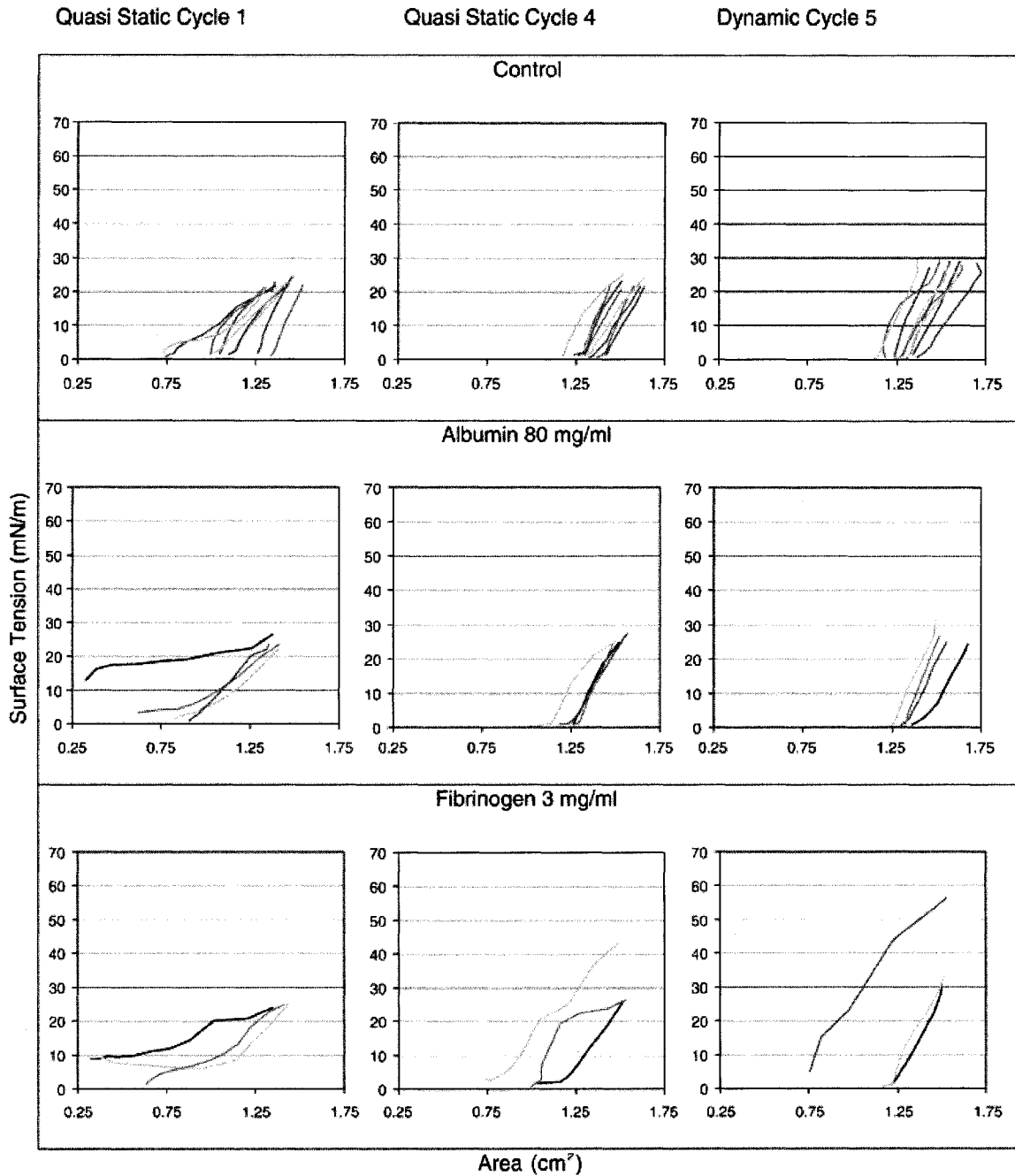


Figure 6.2 Area-surface tension isotherms of BLES films exposed to plasma proteins. The isotherms were acquired during film compression. The films were adsorbed to the air-water interface on unadulterated buffer (upper row) or buffer already containing either albumin (80 mg/ml, middle row) or fibrinogen (3 mg/ml, lower row). For the first, control, condition 14 tests were carried out but only eight representative cases are shown for clarity and for the two experimental conditions, three or four individual tests were carried out, indicated by different shades of grey. Note that under these two conditions, all films showed inhibition in the first compression, but regained full function thereafter.

However, inhibition was not persistent for all films formed with protein present in the buffer during further cycling. All signs of inhibition had virtually disappeared by the fourth quasi-static cycle (median $\beta_{\gamma_{10}}$ 6-7 m/N, similar to control). It is notable that this full recovery of function took place even though the films were continuously exposed to the protein.

Surprisingly, exposure to higher levels of protein *after* film formation resulted in films that failed to show meaningful reductions in surface tension and rarely displayed a surface tension below 15 mN/m from the start to the end of quasi-static testing (Fig. 6.3). In dynamic cycling, surfactant inhibition was all but gone (median $\beta_{\gamma_{10}}$ 8 m/N) but dysfunction showed up again in the following set of quasi-static cycles (median $\beta_{\gamma_{10}}$ 13 m/N). We allowed one of these latter films to rest overnight after at which time it was no longer impaired. In contrast, for films exposed to a lower amount of serum albumin (40 mg/ml) in the buffer after film formation signs of inhibition had all but disappeared by the fourth quasi-static cycle (median $\beta_{\gamma_{10}}$ 8 m/N). In summary, exposure to albumin and fibrinogen had no lasting effect on function under the conditions tested. An effect, when present, was only observed in quasi-static cycling but not in dynamic cycles. Interestingly, 80 mg/ml albumin had only limited effect when present at the time of film formation and the most pronounced inhibitory effect when brought into contact with BLES films after film formation if PEG was not added after the protein. However, even this latter inhibition disappeared over time and area cycling.

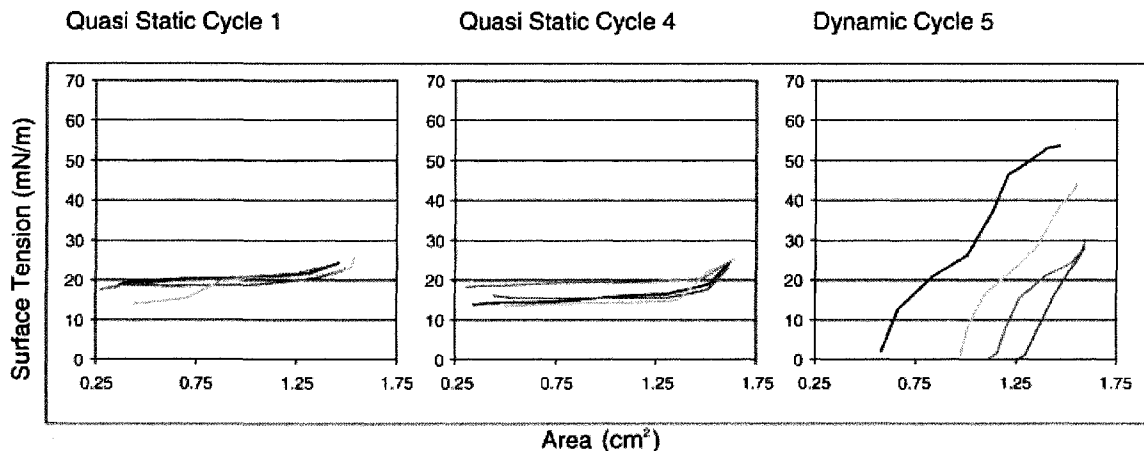


Figure 6.3 Area-surface tension isotherms of BLES films exposed to albumin (80 mg/ml). Unlike in Figure 6.2, the films were adsorbed to clean buffer-air interface first and the albumin injected afterward. Four individual tests were carried out, indicated by different shades of grey. Under this condition, all films showed severe inhibition during the course of four quasi-static cycles, but were functional upon dynamic compressions. These films regained full function upon later series of quasi-static compressions (not shown).

In contrast, 20% cholesterol in surfactant abrogated function with no recovery (Fig. 6.4). γ stayed above 15 mN/m throughout testing. Even a waiting period of 12 h did not lead to recovery of function of BLES containing 20% cholesterol (Table 6.1).

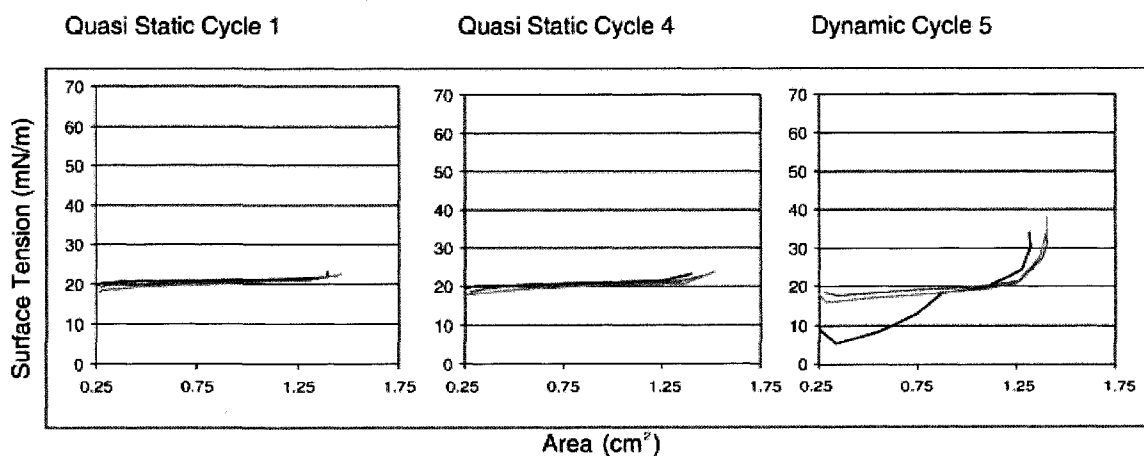


Figure 6.4 Area-surface tension isotherms of BLES films containing 20% w/w cholesterol. Three individual tests were carried out, indicated by different shades of grey. Under this condition, all films showed severe inhibition during the course of all quasi-static and dynamic compression-expansion cycles. Function was also not regained upon later series of compression-expansion cycles (not shown).

Finally, we tested whether inhibition by cholesterol or inhibition brought about by 80 mg/ml albumin after film formation could be reversed by the addition of PEG to the buffer. PEG has been shown to be effective in reversing surfactant inhibition by proteins (e.g., (340) and references therein). This observation was explained by the action of PEG to drive surfactant to the air-water interface by a mechanism called depletion attraction (418,419,420,421,422,423). PEG was thought to specifically counter surfactant inhibition by competitive adsorption by driving the protein off the interface and allowing surfactant to adsorb. As expected, PEG had no effect on cholesterol inhibited surfactant (Table 6.1). However, inhibition by 80 mg/ml albumin on previously formed surfactant films was effectively reversed by adding PEG even with our current experimental protocol. This was surprising as the surfactant film resided at the interface prior to both, exposure to albumin and exposure to PEG. Hence, the inhibition is not likely to have been by competitive adsorption in the first place and PEG improved surfactant function in an as yet unknown way.

6.4.3 Cryo-electron microscopy

Current results on surfactant inhibition by serum proteins differ from results reported earlier on that subject in that our results were not consistent with surfactant inhibition by competitive adsorption. The one difference in experimental procedures that might best account for these divergent results may be the current use of highly concentrated surfactant over the more dilute suspensions used in the earlier studies. We therefore studied the influence of concentration on the structures formed by surfactant in suspension by cryo-electron microscopy of unstained aqueous suspensions (Fig. 6.5). At

high concentration (27 mg/ml) such as used for the CBS studies, BLES formed dense aggregates of vesicular structures (Fig. 6.5, left). Large vesicles were packed with smaller vesicles or other spherical lipid particles. At a lower concentration (5 mg/ml), BLES formed unilamellar vesicles (Fig. 6.5, top right). This or a lower concentration reflects the condition used in earlier studies of surfactant inhibition by serum proteins. Adding PEG to 5 mg/ml of surfactant lead to condensed surfactant aggregates in the buffer (Fig. 6.5, bottom right), similar to those observed with 27 mg/ml of surfactant.

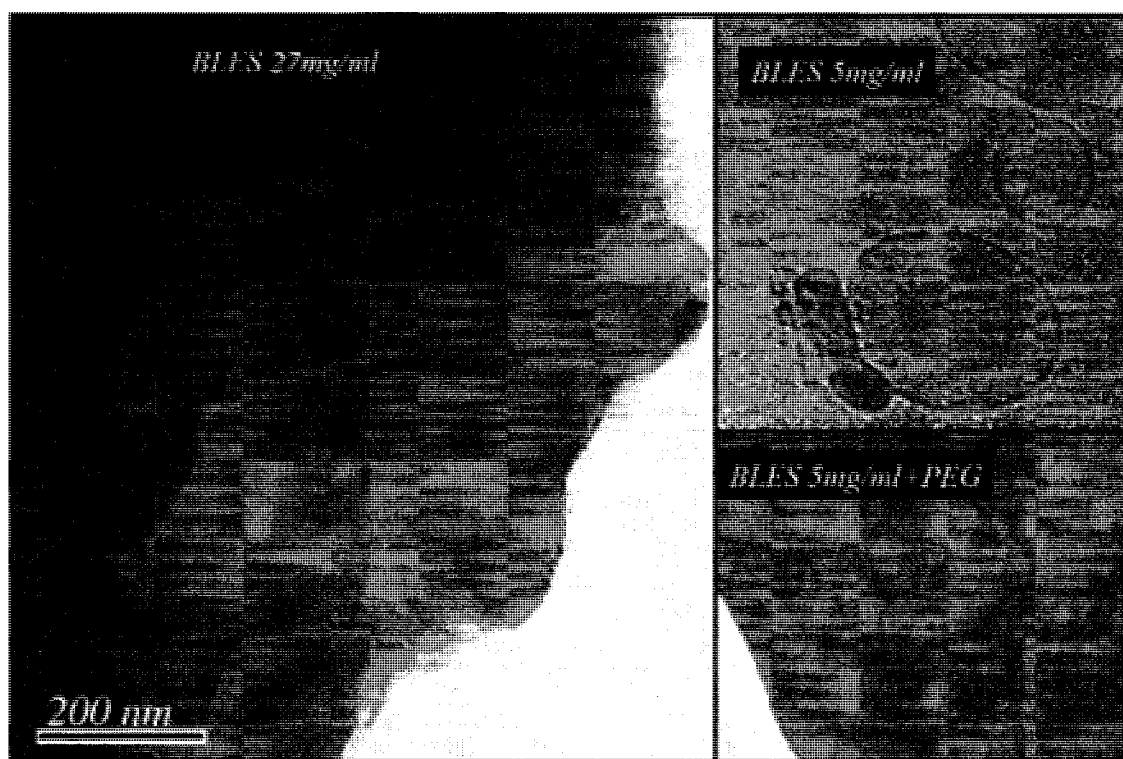


Figure 6.5 (left) Cryo-electron micrographs of an aqueous suspension of BLES of 27 mg/ml such as used in the current study, BLES at 5 mg/ml (top right) and BLES at 5 mg/ml plus PEG (bottom right). At high concentration or at low concentration in the presence of PEG, BLES forms dense aggregates of vesicular structures. At low concentration, BLES forms unilamellar vesicles. For each sample, 5 μ l of the suspension was put down onto a bare electron microscopy grid, excess of the suspension removed by filter paper and the grid injected into liquid ethane. Grids were transferred onto a cryo-holder and imaged in a Tecnai F-20 (FEI) at -100 °C.

6.5 Discussion

The current findings indicate that under the experimental conditions chosen here, surfactant inhibition is likely caused by a dysfunctional film rather than by inhibition via competitive adsorption of plasma proteins to the air-lung interface. This is in contrast to earlier studies that demonstrated competition for the interface by serum proteins such as used in the current study (312,415,311,340). The following sections will first address the experimental differences between the current and the earlier studies that could account for this discrepancy. We will then make the argument why studying surfactant inhibition with highly concentrated surfactant rather than dilute surfactant solutions may better approximate the conditions in the alveolar hypophase and produce results that could be more immediately relevant to the diseased lung.

According to the inhibition via competitive adsorption model, serum proteins form a film at the air-water interface. The layer of serum proteins prevents, or greatly delays, surfactant adsorption by repelling surfactant aggregates approaching the interface from the buffer because of its hydration shell as well as through electrical double layer repulsion (424,425). In agreement with this proposed mechanism of inhibition, the addition of polymers such as polyethylene glycol (PEG) or hyaluronic acid to the buffer reversed this type of surfactant inactivation in these earlier studies. The polymers cause surfactant to flocculate, but also drive it to the interface by a mechanism termed depletion attraction (418,419,420,421,422,423).

In contrast, in the current study film formation was only minimally delayed by the presence of a film of proteins. Despite an initially slower drop in surface tension, the total time required to reach the equilibrium surface tension of 23.5 mN/m was not increased by

plasma proteins in the buffer. In testing after film formation only limited inhibition by protein was observed in the first quasi-static cycle when present at the time of film formation. A high concentration of protein introduced after film formation produced significant and persistent inhibition but if PEG was added after the protein or a lower concentration of protein was used then the observed inhibition was modest and transient like that seen with protein present at the interface at the time of film formation. Hence, while there clearly was an effect of proteins at the interface in our experiments, the effect was transient and so any protein film at the interfaces seems to have been efficiently replaced by a film of surfactant.

The disagreement between earlier studies supporting inhibition by competitive adsorption and the current study is best explained by difference in the concentration of the surfactant applied; 27 mg/ml for the current study as compared to < 2 mg/ml for most of the earlier studies (312,415,311,340) and is consistent with the findings by Holm et al. (416), where serum albumin abolished surfactant function at a surfactant concentration of 1 mg/ml but had no effect at only three times this concentration. The results by Holm and our current findings also show that surfactant inhibition by competitive adsorption is not linearly dependent on surfactant concentration and, hence, not merely subject to mass action. Rather, it appears to be related to the critical concentration, above which surfactant condenses from a dispersed suspension of unilamellar vesicles into extended mesostructures, depending on surfactant and buffer composition. Such transition has been studied experimentally and theoretically for lipids (426) and is evident for BLES in the electron micrographs shown in Figure 6.5. According to this view, surfactant will be susceptible to inhibition by competitive adsorption if in the dispersed form and not be

affected by competing serum proteins if present in condensed form. BLES forms unilamellar vesicles (Fig. 6.5, top right) at 5 mg/ml and dense aggregates at 27 mg/ml (Fig. 6.5, left). Diffusion of the vesicles to the interface and insertion into the interface are slow even in the absence of plasma proteins (e.g., (314)) and so films form over a time period measured in minutes. Under these conditions, the vesicles are apparently unable to effectively overcome a barrier posed by a film of protein. In contrast film formation from dense aggregates is effective even in the presence of a protein film at the interface. Once an aggregate has come into contact with the interface, it might spread over the interface, unaffected by the energy barrier encountered by vesicles. Because each densely packed particle delivers a much larger amount of surfactant to the interface than its unilamellar vesicular counterpart, film formation will be accordingly faster. Interestingly, BLES also forms dense aggregates at low concentration when in the presence of PEG. This would suggest that the earlier described effect of PEG in overcoming surfactant inhibition by serum proteins may not only have been the effect of driving the (dilute) surfactant to the interface (312,415,311,340,418,419,420,421,422, 423) but also due to its effect on flocculating the surfactant and turning it into this physical form which spreads to an air-water interface so much more effectively.

When evaluating the validity of the current over earlier findings for explaining surfactant dysfunction in ARDS, one needs to assess, which of the surfactant concentrations, 27 mg/ml chosen here or the more typical concentrations of <5 mg/ml better approximate the alveolar hypophase in the diseased lungs. The concentration of surfactant has not been directly measured to date, neither in the healthy nor the diseased lung. The best available estimate of the alveolar hypophase surfactant concentration to

our knowledge is that of Clements et al. (189), which they roughly calculate to be 120 mg/ml phospholipids. These authors later, referring to the work of Bray, note that their estimate likely is a conservative one (419,427). Bray (428) proposed that local concentrations of surfactant at the interface could be enhanced by hyaluronic acid or other organizing factor in the surfactant hypophase. Another line of evidence indicating that the surfactant hypophase is an organized “structure” with locally enhanced concentration is that found in EM studies of the lung. None of these studies present any evidence for the existence of a uniform suspension of unilamellar vesicles of surfactant, capped at the air-fluid interface by a phospholipid monolayer. Rather from the earliest studies (429) the surfactant hypophase is seen as containing consistent highly organized osmophilic structures including lamellar bodies, tubular myelin, and a multilamellar superficial layer. Several authors have also noted a tight association between tubular myelin and the superficial lamellar structures (429). It should be remembered that the osmium used to produce the contrast in these images is specifically localized to phospholipids the most abundant constituent of surfactant and so reveal the structured non-homogeneous distribution of surfactant in the hypophase. Subsequent investigations have largely ruled out artifact as a significant factor in these studies and revealed more subtle details of this organization (87,314,430,431). This leads us to conclude that the complex organization in the lung is functionally important for the surface tension altering effects of pulmonary surfactant and that the “self organization” occurring with more concentrated material would be qualitatively different from that formed in more dilute surfactant solutions. In a recent comparative study of BLES and other hydrophobic animal extract surfactants with natural surfactant in vitro showed comparable surface

activities in a CBS but also quite similar structures (with the exception of the lack of tubular myelin for the animal extract surfactants) at the air-water interface as obtained by electron microscopy (432). This is irrespective of the deficiency in the water-soluble surfactant associated proteins A and D (SP-A, SP-D) for the hydrophobic extract surfactants.

However, SP-A and SP-D might play an important role in the injured lung, when surfactant in the alveolar fluid becomes diluted and dispersed by edema. SP-D and SP-A both have been shown to keep surfactant from dispersing in a more dilute suspension (433) and prevent it from becoming more susceptible to inhibition by competitive adsorption. The naturally occurring hyaluronic acid in the alveolar fluid is another substance that keeps surfactant condensed and close to the air-alveolar interface (428). Together, the above *in vitro* and *in vivo* findings lead us to conclude that the approach chosen in the current study over earlier experiments is more likely to reflect the situation in the lung and the choice of BLES at 27 mg/ml is appropriate when assessing surfactant inhibition. As a consequence, competitive adsorption is not likely occurring in the lung as the initial inhibitory mechanism. However, we would not rule out the possibility that when its constituents become degraded by mechanisms discussed below and other disease related-mechanisms, surfactant may no longer maintain a condensed structure and may eventually become susceptible to inhibition by competitive adsorption as well. There are more reasons for surfactant inhibition by competitive adsorption not to occur as the primary inhibition mechanism. Firstly, serum albumin is in the alveolar space even in the healthy lung at relatively high concentrations where it does no damage to the surfactant system. Ishizaka et al. reported 8 mg/ml albumin in the alveolar fluid of a lung

in healthy individuals (434). This is above a buffer concentration beyond which the equilibrium surface tension of serum albumin becomes largely independent of the buffer concentration and competitive adsorption should have reached its maximum level (~ 0.1 mg/ml; (435)). Furthermore, for competitive adsorption to occur, a protein film would need to be in place before surfactant had time to form a film on its own and lower the surface tension to below the equilibrium surface tension value for the respective protein (~ 43 mN/m for albumin and ~ 37 mN/m for fibrinogen, according to the current study). At an equilibrium surface tension of surfactant below 24 mN/m, protein molecules are unlikely to insert into the interface and displace surfactant. On the other hand, surfactant with its higher surface activity, evident from a lower equilibrium surface tension, can drive a protein film from the interface.

While our findings do not support surfactant inhibition by competitive adsorption as the primary inhibitory mechanism, serum proteins still caused functional inhibition of surfactant. The first quasi-static compression of the surfactant films revealed elevated compressibility. The interfacial area needed to be reduced at least by 50% to lower the surface tension from equilibrium to near zero as compared to about 15% in the absence of proteins. For all conditions tested, some films never reached a low surface tension in the presence of proteins in quasi-static cycle 1. Remarkably, the inhibition by proteins was most pronounced when the exposure occurred after the surfactant films had been formed and a high concentration of surfactant was used. This inhibition was transient and all cases, except those where a high concentration of albumin was added after film formation, showed quick and sustained recovery. The latter had slower and somewhat transient recovery.

We have no detailed explanation how serum proteins interfere with surfactant. However, comparison with films inhibited by cholesterol is illustrative. Film adsorption to the equilibrium value was not affected by an excess of cholesterol or exposure to proteins in the buffer but the films could not withstand a film pressure associated with a surface tension below equilibrium. This resulted in an extended plateau in the surface tension-area isotherm for the cholesterol-inhibited films, which was greater than the most extreme cases of protein inhibition. Below equilibrium surface tension, an interfacial film is metastable by definition (i.e., once matter has left the film, it can no longer return). It is a unique mechanical property of a pulmonary surfactant to not collapse under this condition. This property has been associated with specific film architecture of a monolayer and dispersed multilayer patches (316) and (317) and excess cholesterol has been shown to disrupt this structure (337). By analogy, serum protein might also interfere with this film structure. Nag et al. (436) showed that albumin interacts intimately with the lipids of surfactant causing them to redistribute into a phase pattern not present in the absence of the protein.

In dynamic cycling, all protein exposed films achieved near-zero surface tension even when they showed inhibition during quasi-static cycling before and after the dynamic cycles. Film collapse is time dependent and films may remain intact under pressure for a short while but collapse over longer time periods. Dynamic cycling is therefore a less rigorous stability test and reveals the impairment only for the most severely inhibited surfactants. To judge whether surfactant maintains near-zero surface tension in areas of the lung that are not undergoing area change during tidal breathing, quasi-static cycling or other near static surfactant evaluations are therefore required.

A surprising finding of this study was that films allowed to form in absence of serum protein became (transiently) inhibited after exposure to proteins while films formed in the presence of serum protein were already functional after a single compression-expansion cycle. This effect was most pronounced for 80 mg/ml albumin, which resulted in minimal inhibition when present during film formation but was most inhibitory if added to the aqueous phase after film formation and then showed recovery over with successive cycles with proteins present. Hence, pulmonary surfactant appears to possess a mechanism that makes it tolerant to exposure to serum proteins.

6.6 Conclusion

The current study contradicts surfactant inhibition by competitive adsorption by serum albumin and fibrinogen as the primary mechanism of surfactant inhibition. It appears unlikely to us that this mechanism would hold true for any other plasma or inflammatory protein present in the injured lung as long as the surfactant itself is undamaged. Instead, we found that inhibition by proteins appears to occur via interference with the surfactant film itself. Inhibition was transient for the two proteins tested and the surfactant films became insensitive to their continued presence. This is likely important for normal lung function where at least serum albumin is always present in the alveolar space and is just elevated in ARDS. There is good evidence that other serum or inflammatory proteins may cause more lasting surfactant impairment than albumin and fibrinogen (e.g., (369)). We expect this to occur at least initially via interference with the film structure and not through competitive adsorption. However, we note that surfactant inhibition by competitive adsorption might occur, once the surfactant

has become deficient in its composition and become unable to maintain a condensed structure.

Identification of the relevant mechanism of surfactant impairment in ARDS is important for devising new strategies to counter the inhibition and overcome the current lack of success with exogenous surfactant treatment. The current study does not support the rationale for a treatment that primarily addresses competitive adsorption by introducing hydrophilic polymers such as PEG into the alveolar space as proposed (e.g., (340,425)). Our results for cholesterol inhibition show that addition of PEG has no positive effect on surfactant inhibited by cholesterol. An effective treatment may have to specifically counter the effect of cholesterol and other small hydrophobic molecules and also target other mechanisms, including oxidation of surfactant through the reactive oxygen species present in the injured lung (232,341,342,343,368) interference with serum and inflammatory proteins.

Chapter 7: Final Discussion

This thesis explores *in vitro* the role of cholesterol in pulmonary surfactant, reflecting healthy and diseased statuses. Although no detrimental effect of physiological amount of cholesterol has been found, there might be some beneficial surface activity in human lungs that has yet to be discovered. As cholesterol occurs naturally in lung surfactant, it is important to understand the role that it may play. Such functions have already been observed in certain animal studies, including those of bats and dunarts whose body temperatures could fluctuate rapidly (141,321). In these animals the level of cholesterol serves to optimize for the respective body temperature, which may drop to 15°C. Also, in deep diving mammals such as the pinniped, cholesterol helps to maintain the surfactant fluidity during deep diving.

However, in Chapter 3 of our study we observed that an elevated amounts of cholesterol abolished surfactant function *in vitro* (264). Even though the film formation (initial adsorption) was not significantly affected due to excess cholesterol, minimal surface tension values (G min) that were obtained during quasi-static and dynamic compressions were significantly higher than those for normal surfactant. This leads us to conclude that the supraphysiological amount of cholesterol in lung surfactant in states of disease is a strong surfactant inhibitor.

The molecular mechanism behind this inhibition related to the disruption of proper molecular packing of surfactant lipids and proteins. Physiological amounts of cholesterol have been shown to associate with the disaturated lipid species in surfactant (59,318). It appears that if in excess cholesterol will also interact with the unsaturated

lipids. Such interaction appears to be the cause for a disruption of a functional link between the surface film and a surface associated reservoir. We showed that proper surfactant function depends on the link between the reservoir and the surface film (264). Therefore, it is important to investigate the possible mechanisms that can overcome cholesterol-mediated surfactant dysfunction. One possible way is adding DPPC to surfactant films with excess cholesterol, such that the excess cholesterol in surfactant may associate with DPPC. Therefore, we doubled the amount of DPPC in BLES by adding DPPC into BLES that already contained 20% cholesterol. By doubling the amount of DPPC, the surface activity of such films was restored partially and low surface tensions during compressions were achieved. However, continued cycling led to higher minimum surface tension values (higher G min) towards the end of the dynamic cycles. However, adding the same amounts of DOPC (PC with two unsaturated fatty acyl chains) to the surface films of BLES with 20% cholesterol, we observed no recovery effect in terms of the surface activity being evidence of the importance for cholesterol to associate with DPPC. Concretely, there appears to be a stoichiometric relation between DPPC and cholesterol association in lung surfactant that once exceeded causes dysfunction. Saturation appears to be the prerequisite as similar PC with unsaturated fatty acyl chains could not associate with cholesterol in the same way.

A number of studies by others provide the correlation between increase amount of cholesterol and surfactant inhibition in patients with ARDS as well as in the animal model of lung injury. Cholesterol in surfactant is elevated from a physiological level of 5% - 8% w/w to about 20% w/w in animal models of lung injury (145,302) and 16% to 40% w/w in human ARDS (224). All of these studies reported cholesterol levels in

surfactant from lung lavage at or above 20%. Together with our findings these studies confirm that there is a direct association of excess cholesterol and surfactant inhibition. This led us to the question where this cholesterol comes from. According to previous studies, in healthy lung, 98% of the lung cholesterol is acquired through plasma proteins that are taken up into type II cells via receptor-mediated endocytosis. The rest (2%) of the cholesterol in the lung is gained from *de novo* synthesis by type II cells (221). However, to date we do not know the different percentages of the above two sources that can contribute to the surfactant cholesterol compartment. Orgeig and co-workers reported that the cholesterol derived from plasma protein, is subsequently incorporated into the lamellar bodies, mostly into the lamellar body limiting membrane (70%). The rest (30%) is to the core of the lamellar body, which can then be exocytosed out with other surfactant components during secretion (141). Finally, they suggest that there might be different pathways to secrete lung surfactant cholesterol other than the lamellar body mediated pathway (141). This was also suggested by another study with the isolated perfused lung model. They suggested that there is a non-lamellar body mediated, alternate source of cholesterol, which is rapidly mobilized by hyperventilation (301). Another possible source of surfactant cholesterol could be the lipid bodies. Lipid bodies are structurally unique, non-membrane bound cytoplasmic organelles seen in different types of cells. Lipid bodies usually are bounded by an osmiophilic ring instead of a trilaminar limiting membrane. This ring seems to represent a monolayer of amphipathic phospholipids, glycolipids, sterols, and specific proteins that limits the inner hydrophobic core of neutral lipids, mainly cholesterol (438). Presence of lipid bodies even within the normal cells is much common thus, these components may be playing important role in

various aspects of lipid trafficking (438). Recently, Ochs and co-workers reported the presence of lipid bodies in the type II pneumocytes of healthy lungs. An analysis of the composition of isolated lipid bodies showed that they mainly consist of cholesterol (437). Thus, they probably contribute to surfactant cholesterol in healthy lungs. Murphy and co-workers demonstrated that the accumulation of lipid bodies in a leukocyte is a highly inducible process, and they also suggested that this process may play a vital role in the inflammatory response (438). Interestingly, Ochs and co-workers also demonstrated the up-regulation of lipid body production in various inflammatory conditions, and they found a significant increase in lipid body production in the type II pneumocytes of lung injury patients (437). Thus, we suggest that this pathway might play a significant role in providing a massive amount of cholesterol to lung surfactant during inflammatory mediated lung injury. Various inflammatory mediators that are synthesized in ALI/ARDS can possibly induce lipid body production in type II pneumocytes. Increased lipid bodies may then possibly give rise to high cholesterol in the alveolar compartment, which can in turn cause surfactant inhibition. Thus, cholesterol-mediated surfactant dysfunction opens a new avenue to investigate ARDS-related surfactant dysfunction and try new treatment strategies for ARDS.

In Chapter 4 we mainly focused on exploring the recovery mechanisms of cholesterol-mediated lung surfactant dysfunction. Finding novel mechanisms that restore cholesterol-mediated surfactant dysfunction in ARDS/ALI, is bound to reduce both the severity of the disease and finally, to bring down high mortality rates.

Polyethylene glycol (PEG) is well documented as a recovery agent of plasma protein-mediated surfactant dysfunction. It is also known for its effect exerts on

flocculating surfactant and converting it into a physical form that spreads to an air-water interface much more effectively (418,423). Giving PEG to the lung therefore proposed as treatment of surfactant in ARDS patients. Knowing this, we added PEG to the CBS subphase where the surface film was made with BLES (27 mg/mL) and 20% cholesterol. However, there was no recovery of function. On the other hand, we showed that a addition of DPPC to cholesterol inhibited surfactant partially restored function (264). But, the film compressibility that we obtained during compression was beyond physiological parameters and finally, during dynamic cycling surface activity of the film was deteriorated. Moreover, it is not clear, whether DPPC given to the lung would be able to penetrate and mix with the endogenous surfactant.

M β CD has been known to act as a cholesterol-sequestering agent for decades. It is a commonly used agent in cell culture work to remove cholesterol from cell membranes. Thus, we assumed that M β CD would similarly extract cholesterol from surfactant films. Control tests with BLES and M β CD proved that M β CD does not have an effect on the surface tension reduction during quasi-static and dynamic cycling. Fascinatingly, M β CD restored the cholesterol-mediated surfactant dysfunction very effectively in a time-dependent manner. Films readily and consistently achieved low surface tension throughout the all dynamic cycles with very low film compressibility. However, the maximum surface tension values that we obtained during expansion were above 50 mN/m and thus inconsistent with proper lung physiology. However, we consider this observation to be of limited relevance for a potential treatment, as the lung changes area during breathing much less than we expand the interface in the CBS. Hence, M β CD

could be part of a potential treatment for cholesterol mediated surfactant dysfunction. We therefore plan to investigate the recovery effect in an animal model of ALI/ARDS.

Surfactant dysfunction by cholesterol may be relevant to cystic fibrosis too as may be concluded from a preliminary study by us. Cholesterol homeostasis in type II pneumocytes is deregulated in cystic fibrosis and accumulation of cholesterol in lungs of patients with cystic fibrosis is observed (439). Also, surfactant inhibition in cystic fibrosis reported (440). Thus, we suggest that surfactant impairment in cystic fibrosis can be due to excess amounts of cholesterol in the lung alveoli. To explore this, we investigated the surface activity of BAL samples from babies with cystic fibrosis using CBS. Even though most of the samples reached equilibrium surface tension values during initial adsorption, we observed an inhibition of surfactant function during quasi-static and dynamic cycling. Next, we added 20 mM M β CD to the subphase. Surprisingly, a significant number of samples completely recovered surfactant function with respect to low surface tension and low film compressibility during compressions (unpublished data). As with our study using BLES, recovery was time dependent.

Yet another example of cholesterol inhibition of surfactant appears to be high-stretch ventilation. In a collaborative study led by Dr. Ruud Veldhuizen (Lawson Health Research Institute, London, ON), BAL samples of rats with injured lungs due to high-stretch ventilation showed surfactant dysfunction *in vitro*. These samples initially did not reach low surface tension values during quasi-static and dynamic cycling. Previously, analysis of BAL fluid from high stretch ventilator mediated acute lung injured rats showed increase level of cholesterol in lung surfactant (47). We retested these samples in the presence of M β CD in subphase and observed significant surfactant improvement

during cycling. Significant number of these samples reached to very low surface tension values during cycling. These findings suggest that surfactant impairment due to high stretch ventilation mediated lung injury can be recovered by M β CD too.

It is important to determine the structure of BLES films with and without cholesterol in order to understand the structure-function relationship of the surface film in both healthy and diseased lungs. In Chapter 5, we focused on the surface structure of surfactant films (BLES) with different percentages of cholesterol. Here, we used novel techniques such as atomic force microscopy (AFM) and Kelvin probe force microscopy (KPFM). AFM usually gives a nanometer scale resolution of a topographical image of the observed surface film. KPFM is an imaging mode of AFM and produces a map of the local electrical surface potential in addition to a topographical AFM image. For films of amphiphilic molecules, the electrical surface potential is a footprint of the molecular species and/or their molecular order under the tip. Using above techniques, we investigated the structure of functional film and determine how increased levels of cholesterol disrupts the assembly of such functional film. Functional surfactant films underwent a monolayer-bilayer conversion upon contraction and resulted in a film with lipid bilayer stacks that were scattered over a lipid monolayer. Large stacks were at positive electrical potential while small stacks were at negative potential with respect to the surrounding monolayer areas. Dysfunctional films formed only a few stacks. The surface potential of these occasional stacks was also not different from the surrounding monolayer. Thus, elevated levels of cholesterol inhibit the reversible monolayer-bilayer conversion in pulmonary surfactant and thus lead to a failure in surfactant function. Based on film topology and potential distribution, we proposed a mechanism for the formation

of stacked bilayer patches whereby the helical surfactant-associated protein SP-C becomes inserted into bilayers with defined polarity. We discussed the functional role of these stacks as mechanically reinforcing elements, and demonstrated how elevated levels of cholesterol inhibit the formation of the stacks. This offers a simple biophysical explanation for surfactant inhibition in adult respiratory distress syndrome and possible targets for treatment.

Finally, in Chapter 6, we put our finding on surfactant inhibition by cholesterol into perspective of inhibition by plasma proteins. Plasma proteins (mainly albumin and fibrinogen) are considered potent inhibitors of pulmonary surfactant during lung injury. Due to various insults to the lung, blood-capillary barrier can be damaged and as a result, plasma proteins can leak into the lung alveoli and interact with the surface film. Until recently, the mechanism of inhibition due to plasma protein was considered to be competitive inhibition at the interface. We revisited this proposed inhibition mechanism by observing experimental conditions that we deemed more physiologically relevant than those used in earlier studies. Most previous inhibition studies have been done with very low surfactant concentrations and they have observed pronounced inhibition with the plasma proteins. The phospholipid concentration in the surface film at the air water interface of the lung alveoli is not accurately known. However, estimates place this concentration is above 120 mg/mL (189). These concentrations are at least an order of a magnitude higher than what was used in earlier inhibition studies (312,415,311,340). Using a surfactant concentration on the same order as expected in the lung we observed only transient inhibition of surfactant with plasma proteins at the initial cycling. The transient inhibition was more pronounced with fibrinogen than albumin. This inhibition

totally resolved during further cycling. Moreover, our results were not consistent with competitive inhibition. Not even undiluted blood plasma inhibited function in our hands. Thus, we suggest that inhibition by plasma proteins is not a strong candidate of surfactant inhibition during lung injury. We cannot exclude, however, that it contributes to the inhibition of surfactant already affected by excess of cholesterol or other strongly inhibitory agents in the film. Thus, finding the new treatment strategies is essential to reduce high mortality rate of ARDS.

7.1 Conclusions

The current study establishes that cholesterol at physiological proportions has no detrimental effect on the surface activity of pulmonary surfactant, notwithstanding its marked influence on the molecular architecture of the interfacial films formed. A beneficial function of physiological amounts of cholesterol in the human lung, however, has yet to be discovered.

At an elevated level, cholesterol abolishes one of the lung surfactant's most important functions, that is, the ability to reach near zero surface tension. This finding may bring about a change in paradigm how surfactant inhibition is explained and, eventually, treated in the case of acutely injured lungs and possibly in other conditions with impaired surfactant function as well. Until now, surfactant inhibition has largely been attributed to factors other than cholesterol such as plasma proteins. During this study, we were able to show the inhibitory effect of plasma protein is transient and can be reversed during cycling but the inhibition due to excess amount of cholesterol in lung surfactant persists. Using cholesterol-sequestering agent, M β CD we were able to reverse

cholesterol mediated surfactant dysfunction *in vitro*. Cholesterol in surfactant is elevated from a physiological level of 5% to 8% w/w to about 20% w/w in animal models of lung injury (145,302) and 16% to 40% w/w in human ARDS (224). Thus, M β CD can be a potential treatment for cholesterol mediated surfactant dysfunction in ALI/ARDS.

References

1. Schmitz G, Muller G. Structure and function of lamellar bodies, lipidprotein complexes involved in storage and secretion of cellular lipids. *J Lipid Res* 32:1539-1570 (1991).
2. Crapo JD, Barry BE, Gehr P, Bachofen M, Weibel ER. Cell number and cell characteristics of the normal human lung. *Am Rev Respir Dis* 125:332-337 (1982).
3. Johansson MD, Bao HF, Helms MN, Chen XJ, Tigue Z, Jain L, Dobbs LG, Eaton DC. Functional ion channels in pulmonary alveolar type I cells support a role for type I cells in lung ion transport. *Proc Natl Acad Sci USA* 103:4964-4969 (2006).
4. Wright JR, Clements JA. Lung surfactant turnover and factors that affect turnover. In: Massaro D, Ed. *Lung Cell Biology*. New York: Marcel Dekker Inc. 655-699 (1989).
5. Haagsman HP, van Golde LMG. Synthesis and assembly of lung surfactant. *Annu Rev Physiol* 53:441-464 (1991).
6. Goerke J. Pulmonary surfactant: Functions and molecular composition. *Biochim Biophys Acta*, 1408:79-89 (1998).
7. Hallman M, Glumoff V, Ramet M. Surfactant in respiratory distress syndrome and lung injury. *Comp Biochim Physiol* 129:287-294 (2001).
8. Seeger W, Gunther A, Walmrath HD, Grimminger F, Lasch HG. Alveolar surfactant and adult respiratory distress syndrome. Pathogenetic role and therapeutic prospects. *Clin Invest* 71:177-190 (1993).
9. King R. Pulmonary surfactant. *J Appl Physiol* 53:1-8 (1982).

10. Bernard GR, Artigas A, Brigham KL, Carlet J, Falke K, Hudson L, Lamy M, Legall JR, Morris A, Spragg R. The American-European Consensus Conference on ARDS: Definitions, mechanisms, relevant outcomes, and clinical trial coordination. *Am J Crit Care Med* 149:818-824 (1994).
11. Hyers TM. Prediction and survival and mortality in patients with the adult respiratory distress syndrome. *New Horizons* 1:466-470 (1993).
12. Murry JF, Matthay MA, Luce JM, Flick MR. An expanded definition of the adult respiratory distress syndrome. *Am Rev Respir Dis* 138:720-723 (1988).
13. Villar J, Stutsky AS. The incidence of the adult respiratory distress syndrome. *Am Rev Respir Dis* 140:814-816 (1989).
14. Possmayer F. Physiochemical aspects of pulmonary surfactant. In: Polin RA, Fox WW, Eds. *Fetal and Neonatal Physiology*. WB Saunders Company, 1014-1034 (2001).
15. Pattle RE. Properties, function and origin of the alveolar lining layer. *Nature* 175:1125 (1955).
16. Clements JA, Browns ES, Johnson RP. Pulmonary surface tension and the mucous lining of the lungs: Some theoretical considerations. *J Appl Physiol* 12:262 (1958).
17. Avery ME, Mead J. Surface properties in relation to atelectasis and hyaline membrane disease. *Am J Dis Child* 97:517 (1959).
18. Schürch S, Goerke J, Clements JA. Direct determination of surface tension in the lungs. *Proc Natl Acad Sci USA* 73:4698-4702 (1976).
19. Schürch S. Surface tension at low lung volumes: Dependence on time and alveolar size. *Respir Physiol* 48:339-355 (1982).

20. Schürch S, Bachofen H, Weibel ER. Alveolar surface tension in excised rabbit lungs: Effect of temperature. *Respir Physiol* 62:31-45 (1985).
21. Wilson TA. Relation among the recoil pressure, surface area, and surface tension in the lung. *J. Appl Physiol* 50:921-926 (1981).
22. Wilson TA. Surface tension - surface area curves calculated from pressure - volume loops. *J Appl Physiol* 53:1521-1520 (1982).
23. Wilson TA, Bachofen H. A model for mechanical structure of the alveolar duct. *J Appl Physiol* 52:1064-1070 (1982).
24. Bastacky J, Lee CYC, Goerke J, Kaushafen H, Yager D, Kenaga L, Speed TP, Chen Y, Clements JA. Alveolar lining layer is thin and continuous. Low temperature scanning electron microscopy of rat lung. *J Appl Physiol* 79:1615-1628 (1995).
25. Schürch S, Bachofen H. Biophysical aspects in the design of a therapeutic surfactant. In: Robertson B, Taeusch HW, Ed. *Surfactant Therapy for Lung Disease*. New York: Marcel Dekker, 3-32 (1995).
26. Veldhuizen RAW, Nag K, Orgeig S, Possmayer F. The role of lipids in pulmonary surfactant. *Biochim Biophys Acta* 1408:90-108 (1998).
27. Wright JR. Clearance and recycling of pulmonary surfactant. *Am J Physiol* 259:L1-L12 (1990).
28. Daniels CB, Lopatko OV, Orgrig S. Evaluation of surface activity related functions of vertebrate pulmonary surfactant. *Clin Exp Pharmacol Physiol* 25:716-721 (1998).
29. Batenburg JJ. Surfactant phospholipids: Synthesis and storage. *Am J Physiol* 262:367-385 (1992).

30. Goerke J, Clements JA. Alveolar surface tension and lung surfactant. In: Macklem PT, Mead J, Eds. Handbook of Physiology. Section 3: The respiratory system. Vol 3: Mechanics of breathing, Part I. Washington DC: American Physiological Society, 247-260 (1985).
31. Crouch E, Wright JR. Surfactant proteins A and D and pulmonary host defence. *Annu Rev Physiol* 63:521-554 (2001).
32. Haagsman HP, Hawgwood S, Sargeant T, Buckely D, White RT, Drickamer K, Bensen B. The major lung surfactant protein 28-36, is a calcium dependent carbohydrate-binding protein. *J Biol Chem* 262:13877-13880 (1987).
33. Persson A, Chang D, Crough E. Surfactant protein D is a divalent cation-dependent carbohydrate-binding protein. *J Biol Chem* 265:5755-5760 (1990).
34. McCormack FX. Structure, processing and properties of surfactant protein A. *Biochim Biophys Acta* 1408:109-131 (1998).
35. Sullivan LC, Daniels CB, Phillips ID, Orgeig S, Whitsett JA. Conservation of surfactant protein A: Evidence for a single origin for vertebrate pulmonary surfactant. *J Mol Evol* 46:131-138 (1998).
36. Hawgood S, Dirrick M, Poulain F. Structure and properties of surfactant protein B. *Biochim Biophys Acta* 1408:150-160 (1998).
37. Johansson J. Structure and properties of surfactant protein C. *Biochim Biophys Acta* 1408:161-172 (1998).
38. Weaver TE, Conkright JJ. Function of surfactant proteins B and C. *Annu Rev Physiol* 63:555-578 (2001).

39. Weaver TE. Synthesis, processing and secretion of surfactant protein B and C. *Biochim Biophys Acta* 1408:173-179 (1998).
40. Cockshutt A, Possmayer F. Metabolism of surfactant lipids and proteins in the developing lung. In: Robertson B, van Golde LMG, Barenburg JJ, Eds. *Pulmonary surfactant: From molecular biology to clinical practice*. Amsterdam: Elsevier, 339-378 (1992).
41. Creuwels LAJM, van Golde LMG, Haagsman HP. Pulmonary surfactant system: Biochemical and physical aspects. *Lung* 175:1-39 (1997).
42. Hawgood S. Surfactant: Composition, structure and metabolism. In: Crystal RG, West JB, Weibel ER, Barnes PJ, Eds. *The Lung: Scientific Foundation*. 2nd ed. Philadelphia: Lippincott-Raven, 557-571 (1997).
43. King RJ. Isolation and chemical composition of pulmonary surfactant. In: Robertson B, van Golde LMG, Batenburg JJ, Eds. *Pulmonary Surfactant*. Amsterdam: Elsevier, 1-15 (1984).
44. Sanders RL, The composition of pulmonary surfactant. In: Farrel PM, Ed. *Lung Development: Biological and Clinical Perspectives*. New York: Academic Press, 193-219 (1982).
45. van Golde LMG, Batenburg JJ, Robertson B. The pulmonary surfactant system: Biochemical Aspects and Functional Significance. *Physiol Rev* 68:374-455 (1988).
46. Kahn MC, Anderson GJ, Hall SB. Phosphatidylcholine molecular species of calf lung surfactant. *Am J Respir Crit Care Med* 269:567-573 (1995).

47. Maruscak AA, Vockeroth DW, Girardi B, Sheikh T, Possmayer F, Lewis JF, Veldhuizen RAW. Alterations to surfactant precede physiological deterioration during high tidal volume ventilation. *Am J Physiol* 294: 974- 983 (2008).
48. Akino T. Lipid components of the surfactant system. In: Roberson B, van Golde LMG, Battenburg JJ, Eds. *Pulmonary Surfactant: From Molecular Biology to Clinical Practice*. Amsterdam: Elsevier, 19-31 (1992).
49. Gennis RB. *Biomembranes. Molecular Structure and Function*. New York: Springer-Verlag (1989).
50. Shah DO. Surface chemistry of the lipids. *Adv Lipid Res* 8:347-431 (1970).
51. Small DM. *The physical chemistry of lipids: From alkane to phospholipids*. New York: Plenum Press (1986).
52. Chen SC, Sturtevant JM. Thermotropic behaviour of bilayer formed from mixed chain phosphatidylcholine. *Biochemistry* 20:713-718 (1981).
53. Notter RH, Taubold R, Finkelstein J. Comparative adsorption of natural lung surfactant, extracted phospholipids, and synthetic phospholipid mixtures. *Chem Phys Lipids* 33:67-80 (1983).
54. Notter RH, Smith S, Taubold R, Finkelstein JN. Path dependence of adsorption behaviour of mixture containing dipalmitoyl phosphatidylcholine. *Pediatr Res* 16:515-519 (1982).
55. Fleming BD, Keough KMW. Surface respreading after collapse of monolayers containing major lipids of pulmonary surfactant. *Chem Phys Lipids* 49:81-86 (1988).

56. Liu H, Turcotte JG, Notter RH. Dynamic interfacial properties of surface-excess films of phospholipid and phosphonolipids analogs: I. Effects of pH. *J Colloid Interface Sci* 167:378-390 (1994).
57. Liu H, Turcotte JG, Notter RH. Dynamic interfacial properties of surface-excess films of phospholipid and phosphonolipids analogs: II. Effects of chain linkage and headgroup structure. *J Colloid Interface Sci* 167:391-400 (1994).
58. Hawco MW, Davis PJ, Keough KMW. Lipid fluidity in lung surfactant: Monolayers of saturated and unsaturated lecithins. *J Appl Physiol* 51:509-515 (1981).
59. Wang Z, Hall SB, Notter RH. Dynamic surface activity of films of lung surfactant phospholipids, hydrophobic proteins, and neutral lipids. *J Lipid Res* 36:1283-1293 (1995).
60. Wang Z, Hall SB, Notter RH. Roles of different hydrophobic constituents in the adsorption of pulmonary surfactant. *J Lipid Res* 37:790- 98 (1996).
61. Gluck L, Kulovich MV. Lecithin-sphingomyelin ratio in amniotic fluid in normal and abnormal pregnancies. *Am J Obstet Gynecol* 115:539-546 (1973).
62. Hallman M, Feldman BH, Kirkpatrick E, Gluck L. Absence of phosphatidylglycerol (PG) in respiratory distress in newborn. *Pediatr Res* 11:714-720 (1977).
63. Hallman M, Gluck L. Phosphatidylglycerol in lung surfactant. III. Possible modifier of surfactant function. *J Lipid Res* 17:257-262 (1976).
64. Hallman M, Kulovich MV, Kirkpatrick E, Sugerman RG, Gluck L. Phosphatidylinositol and phosphatidylglycerol in amniotic fluid: Indices of lung maturity. *Am J Obstet Gynecol* 125:613-617 (1976).

65. Jobe AH. Lung development. In: Fanaroff A, Martin RJE, Eds. Neonatal-Perinatal Medicine. St. Louis: Mosby-Yearbook, 991-1009 (1997).
66. Rooney SA, Canavan PM, Motoyama EK. The identification of phosphatidylglycerol in the rat, rabbit, monkey and human lung. *Biochim Biophys Acta* 360:56-67 (1976).
67. Treusch HW, Ballard RA. Avery's Disease of the Newborn. 7th ed. Philadelphia: WB Saunders (1998).
68. Taussig LM, Landau LI, Le Souef PN, Morgan WJ, Martinez FD, Sly PDE. Paediatric Respiratory Medicine. St. Louis: Mosby (1999).
69. Johansson J, Curstedt T, Jornvall H. Surfactant protein B: Disulfide bridges, structural properties, and kringle similarities. *Biochemistry* 30:6917-6921 (1991).
70. Keough KMW. Physical chemistry of pulmonary surfactant in the terminal air spaces. In: Robertson B, van Golde LMG, Batenburg JJ, Eds. Pulmonary Surfactant: From Molecular Biology to Clinical Practice. Amsterdam: Elsevier, 109-164 (1992).
71. King RJ, MacBeth MC. Interactions of the lipid and protein components of pulmonary surfactant: Role of phosphatidylglycerol and calcium. *Biochim Biophys Acta* 647:159-168 (1981).
72. Taneva S, Keough KM. Pulmonary surfactant proteins SP-B and SP-C in spread monolayers at the air-water interface: III. Proteins SP-B plus SP-C with phospholipids in spread monolayers. *Biophys J* 66:1158-1166 (1994).
73. Vandenbussche G, Clercx A, Clercx M, Curstedt T, Johansson J, Jornvall H, Ruysschaert JM. Secondary structure and orientation of the surfactant protein SP-B

- in a lipid environment. A Fourier transform infrared spectroscopy study. *Biochimistry* 31:9169-9176 (1992).
74. Wang Z, Gurel O, Weinbach S, Notter RH. Primary importance of zwitterionic over anionic phospholipids in the surface-active function of calf lung surfactant extract. *Am J Respir Crit Care Med* 156:1049-1057 (1997).
75. Frerking I, Gunther A, Seeger W, Pison U: Pulmonary surfactant: Function, abnormalities and therapeutic options. *Intensive Care Med* 27:1699-1717 (2001).
76. Wright JR. Immunoregulatory functions of surfactant proteins. *Nat Rev Immunol* 5:58-68 (2005).
77. Yamada C, Sano H, Shimizu T, Mitsuzawa H, Nishitani C, Himi T, Kuroki Y. Surfactant protein A directly interacts with TLR4 and MD-2 and regulates inflammatory cellular response: Importance of supratrimeric oligomerization. *J Biol Chem* 281:21771-21780, (2006).
78. Haagsman HP, White RT, Schilling J, Lau K, Benson BJ, Golden J, Hawgood S, Clements JA. Studies on the structure of lung surfactant protein SP-A. *Am J Physiol* 257:L421-L429 (1989).
79. King RJ, Simon D, Horowitz PM. Aspects of secondary and quaternary structure of surfactant protein A from canine lung. *Biochim Biophys Acta* 1001:294-301 (1989).
80. McCormack FX, Calvert HM, Watson PA, Smith DL, Mason RJ, Voelker DR. The structure and function of surfactant protein A. *J Biol Chem* 269:5833-5841 (1994).
81. Benson BJ, Williams MC, Sueishi K, Goerke J, Sargent T. Role of calcium ions on the structure and function of pulmonary surfactant. *Biochim Biophys Acta* 793:18-27 (1984).

82. Haagsman HP, Sargent T, Hanschka PV, Benson BJ, Hawgood S. Binding of calcium to SP-A, a surfactant associated protein. *Biochimistry* 29:8894-8900 (1990).
83. Johansson J, Curstedt T, Robertson B. The proteins of the surfactant system. *Eur Respir J* 7:372-391 (1994).
84. Cajal Y, Dodia C, Fisher AB, Jain MK. Calcium-triggered selective intermembrane exchange of phospholipids by the lung surfactant protein SP-A. *Biochemistry* 37:12178-12188 (1998).
85. Poulain FR, Allen L, Williams MC, Hamilton RL, Hawgood S. Effects of surfactant apolipoproteins on liposome structure: Implications for tubular myelin formation. *Am J Physiol Lung Cell Mol Physiol* 262:730-739 (1992).
86. Bachofen H, Schürch S, Urbinelli M, Weibel ER. Relations among alveolar surface tension, surface area, volume and recoil pressure. *J Appl Physiol* 62:1878-1887 (1987).
87. Williams MC. Conversion of lamellar body membranes into tubular myelin in alveoli of fetal rat lungs. *J Cell Biol* 72:260-277 (1977).
88. Bates SR, Dodia C, Fisher AB. Surfactant protein A regulates uptake of pulmonary surfactant by lung type II cells on microporous membranes. *Am J Physiol Lung Cell Mol Physiol* 267:753-760 (1994).
89. Tsuzuki A, Kuroki Y, Akino T. Pulmonary surfactant protein A-mediated uptake of phosphatidylcholine by alveolar type II cells. *Am J Physiol Lung Cell Mol Physiol* 265:193-199 (1993).
90. Dobbs LG, Wright JR, Hawgood S, Gonzalez R, Venstrom K, Nellenbogen J. Pulmonary surfactant and its components inhibit secretion of phosphatidylcholine

- from cultured rat alveolar type II cells. *Proc Natl Acad Sci USA* 84:1010-1014 (1987).
91. Yoshida M, Korfhagen TR, Whitsett JA. Surfactant protein D regulates NF-kappa B and matrix metalloproteinase production in alveolar macrophages via oxidant-sensitive pathways. *J Immunol* 166:7514-7519 (2001).
 92. Korfhagen TR, Bruno MD, Ross GF, Huelsman KM, Ikegami M, Jobe AH, Wert SE, Stripp BR, Morris RE, Glasser SW, Bachurski CJ, Iwamota HS, Whitsett JA. Altered surfactant function and structure in SP-A gene targeted mice. *Proc Natl Acad Sci USA* 93:9594-9599 (1996).
 93. Ikegami M, Korfhagen TR, Whitsett JA, Bruno MD, Wert SE, Wada K, Jobe AH. Characteristics of surfactant from SP-A deficient mice. *Am J Physiol* 275:247-254 (1998).
 94. Cockshutt AM, Weitz J, Possmayer F. Pulmonary surfactant-associated protein A enhances the surface activity of lipid extract surfactant and reverses inhibition by blood proteins in vitro. *Biochemistry* 29:8424-8429 (1990).
 95. Bridges JP, Davis HW, Damodarsamy M, Kuroki Y, Howies G, Hui DY, McCormack FX. Pulmonary surfactant A and D are potent endogenous inhibitors of lipid peroxidation and oxidative cellular injury. *J Biol Chem* 275:38848-38855 (2000).
 96. Persson A, Chang D, Rust K, Moxley M, Longmore W, Crouch E. Purification and biochemical characterization of CP4 (SP-D), a collagenous surfactant associated protein. *Biochemistry* 28:6361-6367 (1989).

97. Crouch E, Chang D, Rust K, Persson A, Heuser J. Recombinant pulmonary surfactant protein D. Post-translational modification and molecular assembly. *J Biol Chem* 269:15808-15813 (1994).
98. Vorhout WF, Veenendaal T, Kuroki Y, Ogasawara Y, van Golde LMG, Geuze HJ. Immunocytochemical localization of surfactant protein D (SP-D) in type II cell, Clara cells and alveolar macrophages of the rat lung. *J Histochem Cytochem* 40:1589-1597 (1992).
99. Crouch EC. Collectins and pulmonary host defence. *Am J Respir Cell Mol Biol* 19:177-201 (1998).
100. Haagsman HP. Surfactant associated protein A and D. *Biochim Soc Trans* 22:100-106 (1994).
101. Ikegami M, Na CL, Korfhagen TR, Whitsett JA. Surfactant protein D influences surfactant ultrastructure and uptake by alveolar type II cells. *Am J Physiol Lung Cell Mol Physiol* 288:552-561 (2005).
102. Wert SE, Yoshida M, LeVine AM, Ikegami M, Jones T, Ross GF, Fisher JH, Korfhagen TR, Whitsett JA. Increased metalloproteinase activity, oxidant production, and emphysema in surfactant protein D gene-inactivated mice. *Proc Natl Acad Sci USA* 97:5972-5977 (2000).
103. Hawgood S, Schiffer K. Structure and properties of the surfactant associated proteins. *Annu Rev Physiol* 53:375-394 (1991).
104. Weaver TE, Whitsett JA. Function and regulation of expression of pulmonary surfactant associated proteins. *Biochim J* 273:249-264 (1991).

105. Wadsworth SJ, Spitzer AR, Chander A. Ionic regulation of proton chemical (pH) and electrical gradients in lung lamellar bodies. *Am J Physiol Lung Cell Mol Physiol* 273:427-436 (1997).
106. Anderson M, Curstedt T, Jornvall H, Johansson J. An amphipathic helical motif common to tumourlytic polypeptide NK-lysin and pulmonary surfactant polypeptide SP-B. *FEBS Lett* 362:328-332 (1995).
107. Liepinsh E, Anderson M, Ruyschaert JM, Otting G. Saposin fold revealed by the NMR structure of NK-lysin. *Nat Struct Biol* 10:793-795 (1997).
108. Perez-Gil J, Keough KM. Structural similarities between myelin and hydrophobic surfactant associated proteins: Protein motifs for interacting with bilayers. *J Theor Biol* 169:221-229 (1994).
109. Hawgood S, Benson BJ, Schilling J, Damm D, Clements JA, White RT. Nucleotide and amino acid sequences of pulmonary surfactant protein SP 18 and evidence for cooperation between SP 18 and SP 28-36 in surfactant lipid adsorption. *Proc Natl Acad Sci USA* 84:66-70 (1987).
110. Nogee LM, Garneir G, Dietz HC, Singer L, Murphy AM, deMello DE, Colten HR. A mutation in the surfactant protein B gene responsible for fatal neonatal respiratory disease in multiple kindreds. *J Clin Invest* 93:1860-1863 (1994).
111. Whitsett JA, Weaver TE. Hydrophobic surfactant proteins in lung function and disease. *N Engl J Med* 347:2141-2148 (2002).
112. Dunbar AE III, Wert SE, Ikegami M, Whitsett JA, Hamvas A, White FV, Piedboeuf B, Jobin C, Guttentag S, Nogee LM. Prolonged survival in hereditary surfactant

- protein B (SP B) deficiency associated with a novel spicing mutation. *Pediatr Res* 48:275-282 (2000).
- 113.** Nogee LM, West SE, Proffit SA, Hull WM, Whitsett JA. Allelic heterogeneity in hereditary surfactant protein B (SP-B) deficiency. *Am J Respir Crit Care Med* 161:973-981 (2000).
- 114.** Tryka AF, Wert SE, Mazursky JE, Arrington RW, Nogee LM. Absence of lamellar bodies with accumulation of dense bodies characterizes a novel form of congenital surfactant defect. *Pediatr Dev Pathol* 3:335-345 (2000).
- 115.** Poulain FR, Nir S, Hawgood S. Kinetics of phospholipid membrane fusion induced by surfactant apoproteins A and B. *Biochim Biophys Acta* 1278:169-175 (1996).
- 116.** Clark JC, Wert SE, Bachurski CJ, Stahlman MT, Stripp BR, Weaver TE, Whitsett JA. Targeted disruption of the surfactant protein B gene disrupts surfactant homeostasis, causing respiratory failure in newborn mice. *Proc Natl Acad Sci USA* 92:7794-7798 (1995).
- 117.** Stahlman MT, Gray MP, Falconieri MW, Whitsett JA, Weaver TE. Lamellar body formation in normal and surfactant protein B-deficient fetal mice. *Lab Invest* 80:395-403 (2000).
- 118.** Nogee LM, de Mello DE, Dehner LP, Colten HR. Brief report: Deficiency of pulmonary surfactant protein B in congenital alveolar proteinosis. *N Engl J Med* 328:406-410 (1993).
- 119.** Beck DC, Ikegami M, Na CL, Zaltash S, Johansson J, Whitsett JA, Weaver TE. The role of homodimers in surfactant protein B function in vivo. *J Biol Chem* 275:3365-3370 (2000).

120. Veldhuizen EJ, Waring AJ, Walther FJ, Barenburg JJ, van Golde LM, Haagsman HP. Dimeric N-terminal segment of human surfactant protein B [dSP-B (1-25)] has enhanced surface properties compared to monomeric SP-B (1-25). *Biophys J* 79:377-384 (2000).
121. Cruz A, Casals C, Plasencia I, Marsh D, Perez-Gil J. Depth profiles of pulmonary surfactant protein B in phosphatidylcholine bilayers, studied by fluorescence and electron spin resonance spectroscopy. *Biochemistry* 37:9488-9496 (1998).
122. Perez-Gil J, Casals C, Marsh D. Interactions of hydrophobic lung surfactant proteins SP-B and SP-C with dipalmitoylphosphatidylcholine and dipalmitoylphosphatidylglycerol bilayers studied by electron spin resonance spectroscopy. *Biochimistry* 34:3964-3971 (1995).
123. Perez-Gil J, Keough KM. Interfacial properties of surfactant proteins. *Biochim Biophys Acta* 1408:203-217 (1998).
124. Rodriguez-Capote K, Nag K, Schürch S, Possmayer F. Surfactant protein interaction with neutral and acidic phospholipid films. *Am J Physiol Lung Cell Mol Physiol* 281:L231-L242 (2001).
125. Schram V, Hall SB. Thermodynamic effects of the hydrophobic surfactant proteins on early adsorption of pulmonary surfactant. *Biophys J* 81:1536-1546 (2001).
126. Veldhuizen EJ, Batenburg JJ, van Golde LM, Haagsman HP. The role of surfactant protein in DPPC enrichment of surfactant films. *Biophys J* 79:3164-3171 (2000).
127. Nag K, Munro JG, Inchley K, Schürch S, Petersen NO, Possmayer F. SP-B refining of pulmonary surfactant phospholipid films. *Am J Physiol* 277:1179-1189 (1999).

128. Brasch F, Johnen G, Winn-Brasch A, Guttenburg SH, Schmiedl A, Kapp N, Suzuki Y, Mullar KM, Hawgood S, Ochs M. Surfactant protein B in type II pneumocytes and intra-alveolar surfactant forms of human lungs. *Am J Respir Cell Mol Biol* 30:449-458 (2004).
129. Vandenbussche G, Clercx A, Curstedt T, Johansson J, Jornvall H, Ruyschaert JM. Structure and orientation of the surfactant associated protein SP-C in a lipid bilayer. *Eur J Biochim* 203:201-209 (1992).
130. Nogee LM, Dunbar AE III, Wert SE, Askin F, Hamvas A, Whitsett JA. Mutation in the surfactant protein C gene associated with familial interstitial lung disease. *N Engl J Med* 344:573-579 (2001).
131. Danlois F, Zaltash S, Johansson J, Robertson B, Haagsman HP, van Eijk M, Beers MF, Rollin F, Ruyschaert JM, Vandenbussche G. Very low surfactant protein C content in newborn Belgian white and blue calves with respiratory distress syndrome. *Biochim J* 351:779-787 (2000).
132. Glasser SW, Burhans MS, Korfhagen TR, Na CL, Sly PD, Ross GF, Ikegami M, Whitsett JA. Altered stability of pulmonary surfactant in SP-C deficient mice. *Proc Natl Acad Sci USA* 98(11):6366- 6371 (2001).
133. Glasser SW, Detmer EA, Ikegami M, Na CL, Stahlman MT, Whitsett JA. Pneumonitis and emphysema in SP-C gene targeted mice. *J Biol Chem* 278:14291-14298 (2003).
134. Nogee LM. Abnormal expression of surfactant protein C and lung disease. *Am J Respir Cell Mol Biol* 26:641-644 (2002).

135. Horowitz AD. Exclusion of SP-C, but not SP-B, by gel phase palmitoyl lipids. *Chem Phys Lipids* 76:27-39 (1995).
136. Creuwels LA, Demel RA, van Golde LMG, Bebson BJ, Haagsman HP. Effects of acylation on structure and function of surfactant protein C (SP-C) at the air-liquid interface. *J Biol Chem* 268:26752-26758 (1993).
137. Oosterlaken-Dijksterhuis MA, van Eijk M, van Golde LMG, Haagsman HP. Lipid mixing is mediated by the hydrophobic surfactant protein SP-B and not by SP-C. *Biochim Biophys Acta* 1110:45-50 (1992).
138. Creuwels LA, Demel RA, van Golde LMG, Haagsman HP. Characterization of a dimeric canine form of surfactant protein C (SP-C). *Biochim Biophys Acta* 1254:326-332 (1995).
139. Oosterlaken-Dijksterhuis MA, Haagsman HP, van Golde LMG, Demel RA. Interaction of lipid vesicles with monomolecular layers containing lung surfactant proteins SP-B or SP-C. *Biochemistry* 30:8276-8281 (1991).
140. Casals C, Arias-Diaz J, Valino F, Saenz A, Garcia C, Balibrea JL, Vara E. Surfactant strengthens the inhibitory effect of C reactive protein on human lung macrophage cytokine release. *Am J Physiol Lung Cell Mol Physiol* 284:466-472 (2001).
141. Orgeig S, Daniels CB. The role of cholesterol in pulmonary surfactant: Insight from comparative and evolutionary studies. *Comp Biochim Physiol A Mol Intergr Physiol* 129:75-89 (2001).
142. Daniels CB, Orgeig S, Smith AW. The evolution of vertebrate pulmonary surfactant. *Physiol Zool* 68:539-566 (1995).

143. Doyle IR, Jones ME, Barr HA, Orgeig S, Crockett AJ, McDonald CF, Nicholas TE. Composition of human pulmonary surfactant varies with exercise and level of fitness. *Am J Respir Crit Care Med* 149:1619-1627 (1994).
144. Codd JR, Slocombe NC, Daniels CB, Wood PG, Orgeig S. Periodic fluctuations in the pulmonary surfactant system in Gould's wattled bat (*Chalinolobus gouldii*). *Physiol Biochim Zool* 73:605-612 (2000).
145. Panda AK, Nag K, Harbottle RR, Rodriguez-Capote K, Veldhuizen RAW, Petersen NO, Possmayer F. Effects of acute lung injury on structure and function of pulmonary surfactant films. *Am J Respir Cell Mol Biol* 30:641-650 (2004).
146. Young SL, Fram EK, Spain CL, Larson EW. Development of type II pneumocytes in rat lung. *Am J Physiol Lung Cell Mol Physiol* 260:113-122 (1991).
147. Yang C, Terada N, Ohno N, Fujii Y, Ohno S. Morphological analysis of lamellar structures in mouse type II pneumocytes by quick-freezing and freeze-drying with osmium tetroxide vapor-fixation. *Med Mol Morphol* 39:88-96 (2006).
148. Froh D, Ballard PL, Williams MC, Gonzales J, Goerke J, Odom MW, Gonzales LW. Lamellar bodies of cultured human fetal lung: Content of surfactant protein A (SP-A), surface film formation and structural transformation in vitro. *Biochim Biophys Acta* 1052:78-89 (1990).
149. Oosterlaken-Dijksterhuis MA, van Eijk M, van Buel BLM, Van Golde LMG, Haagsman HP. Surfactant protein composition of lamellar bodies isolated from rat lung. *Biochim J* 274:115-119 (1992).

150. Walker SR, Williams MC, Benson B. Immunocytochemical localization of the major surfactant proteins in type II cells, Clara cells, and alveolar macrophages of rat lungs. *J Histochem* 34:1137-1148 (1986).
151. Weaver TE, Whitsett JA. Processing of hydrophobic protein B in rat type II cells. *Am J Physiol* 257:100-108 (1989).
152. Rooney SA. The surfactant system and lung phospholipid biochemistry. *Am Rev Respir Dis* 131:439-460 (1985).
153. Rooney SA, Young SL, Mendelson CR. Molecular and cellular processing of lung surfactant. *FASEB J* 8:957-967 (1994).
154. Osanai K, Mason RJ, Voelker DR. Pulmonary surfactant phosphatidylcholine transport bypasses the brefeldin A sensitive compartment of alveolar type II cells. *Biochim Biophys Acta* 1531:222-229 (2001).
155. van Helvoort A, de Brouwer A, Ottenhoff R, Brouwers JF, Wijnholds J, Beijnen JH, Rijneveld A, van der Poll T, van der Valk MA, Majoor D, Voorhout W, Wirtz KW, Elferink RP, Borst P. Mice without phosphatidylcholine transfer protein have no defects in the secretion of phosphatidylcholine into bile or into lung airspaces. *Proc Natl Acad Sci USA* 96:11501-11506 (1999).
156. Dean M, Hamon Y, Chimini G. The human ATP-binding cassette (ABC) transporter superfamily. *J Lipid Res* 42:1007-1017 (2001).
157. Kaminski WE, Piehler A, Wenzel JJ. ABC A-subfamily transporters: Structure, function and disease. *Biochim Biophys Acta* 1762:510-524 (2006).

158. Bates SR, Tao JQ, Collins HL, Francone OL, Rothblat GH. Pulmonary abnormalities due to ABCA1 deficiency in mice. *Am J Physiol Lung Cell Mol Physiol* 289:L980-L989 (2005).
159. Yamano G, Funahashi H, Kawanami O, Zhao LX, Ban N, Uchida Y, Morohoshi T, Ogawa J, Shioda S, Inagaki N. ABCA3 is a lamellar body membrane protein in human lung alveolar type II cells. *FEBS Lett* 508:221-225 (2001).
160. Shulenin S, Nogee LM, Annilo T, Wert SE, Whitsett JA, Dean M. ABCA3 gene mutations in newborns with fatal surfactant deficiency. *N Engl J Med* 350:1296-1303 (2004).
161. Edwards V, Cutz E, Viero S, Moore AM, Nogee L. Ultrastructure of lamellar bodies in congenital surfactant deficiency. *Ultrastruct Pathol* 29:503-509 (2005).
162. Cheong N, Madesh M, Gonzales LW, Zhao M, Yu K, Ballard PL, Shuman H. Functional and trafficking defects in ATP binding cassette A3 mutants associated with respiratory distress syndrome. *J Biol Chem* 281:9791-9800 (2006).
163. Garmany TH, Moxley MA, White FV, Dean M, Hull WM, Whitsett JA, Nogee LM, Hamvas A. Surfactant composition and function in patients with ABCA3 mutations. *Pediatr Res* 59:801-805 (2006).
164. Brasch F, Schimanski S, Muhlfeld C, Barlage S, Langmann T, Aslanidis C, Boettcher A, Dada A, Schroten H, Mildenerger E, Prueter E, Ballmann M, Ochs M, Johnen G, Griese M, Schmitz G. Alteration of the pulmonary surfactant system in full-term infants with hereditary ABCA3 deficiency. *Am J Respir Crit Care Med* 174:571-580 (2006).

165. Nicholas TE, Doyle IR, Bersten AD. Surfactant replacement therapy in ARDS: White knight or noise in the system. *Thorax* 52:195-197 (1997).
166. Oyarzun MJ, Clements JA. Control of lung surfactant by ventilation, adrenergic mediators, and prostaglandin in the rabbit. *Am Rev Respir Dis* 117:879-891 (1978).
167. Massaro D, Clerch L, Massaro GD. Surfactant secretion: Evidence that cholinergic stimulation of secretion is indirect. *Am J Physiol* 243:39-45 (1982).
168. Brown LA, Wood LH. Stimulation of surfactant secretion by vasopressin in primary cultures of the adult rat type II pneumocytes. *J Appl Physiol* 1001:76-81 (1989).
169. Dobbs LG, Gonzales RF, Marinari LA, Mescher EJ, Hawgood S. The role of calcium in the secretion of surfactant by rat alveolar type II epithelial cells. *Biochim Biophys Acta* 877:305-315 (1986).
170. Gilfillan AM, Rooney SA. Purinoceptor agonists stimulate phosphatidylcholine secretion in primary culture of adult rat type II pneumocytes. *Biochim Biophys Acta* 917:18-23 (1987).
171. Pian MS, Dobbs LG, Duzgunes N. Positive correlation between cytosolic free calcium and surfactant secretion in cultured rat alveolar type II cells. *Biochim Biophys Acta* 960:43-53 (1989).
172. Sano K, Voelker DR, Mason R. Involvement of protein kinase C in pulmonary surfactant secretion from alveolar type II cells. *J Biol Chem* 260:12725-12729 (1985).
173. Kuroki Y, Mason RJ, Voelker DR. Pulmonary surfactant apoprotein A structure and modulation of surfactant secretion by rat alveolar type II cells. *J Biol Chem* 263:3388-3394 (1988).

174. Rise WR, Ross GF, Singleton FM, Dingle S, Whitsett JA. Surfactant associated protein inhibits phospholipid secretion from type II cells. *J Appl Physiol* 63:692-698 (1987).
175. Hawgood S, Clements JA. Pulmonary surfactant and its apoproteins. *J Clin Invest* 86:1-6 (1990).
176. Jobe A. Metabolism of endogenous surfactant and exogenous surfactant for replacement therapy. *Semin Perinatol* 12:231-244 (1988).
177. Jobe AH, Ikegami M. Surfactant metabolism. *Clin Perinatol* 20:683-696 (1993).
178. Ryan RM, Morris RE, Rise WR, Ciruolo G, Whitsett JA. Binding and uptake of pulmonary surfactant protein A (SP-A) by pulmonary type II cells. *J Histochem Cytochem* 37:429-440 (1989).
179. Wissel H, Lehfeldt A, Klein P, Muller T, Stevens PA. Endocytosed SP-A and surfactant lipids are sorted to different organelles in rat type II pneumocytes. *Am J Physiol Lung Cell Mol Physiol* 281:345-360 (2001).
180. Guttentag SH, Akhtar A, Tao JQ, Atochina E, Rusiniak ME, Swank RT, Bates SR. Defective surfactant secretion in a mouse model of Hermansky-Pudlak syndrome. *Am J Respir Cell Mol Biol* 33:14-21 (2005).
181. Nicholas TE. Pulmonary surfactant: No mere paint on the alveolar wall. *Respirology* 1:247-257 (1996).
182. Bangham AD, Hill MW, Miller NGA. Preparation and use of liposome as models of biological membranes. In: EDE Korm, Ed. *Methods in Membrane Biology*. New York: Plenum Press, 1-68 (1974).

183. Gross NJ, Schultz RM. Serine protease requirement of the extra-cellular metabolism of rabbit alveolar surfactant subfractions. *Biochim Biophys Acta* 1044:222-230 (1990).
184. Hall SB, Hyde RW, Notter RH. Changes in subphase surfactant aggregates in rabbits injured by free fatty acids. *Am J Respir Crit Care Med* 149:1099-1106 (1994).
185. Veldhuizen R, McCaig L, Akino T, Lewis J. Pulmonary surfactant subfractions in patient with the acute respiratory distress syndrome. *Am J Respir Crit Care Med* 152:1867-1871 (1995).
186. Gross NJ, Narine KR. Surfactant subtypes in mice: Characterization and quantitation. *J Appl Physiol* 66:342-349 (1989).
187. Magoon MW, Wright JR, Baritussio A, Williams MC, Goerke J, Benson BJ, Hamilton RL, Clements JA. Subfractionation of lung surfactant. Implication for metabolism and surface activity. *Biochim Biophys Acta* 750:18-31 (1983).
188. Putman E, Creuwels LAJM, van Golde LMG, Haahsman HP. Surface properties, morphology and protein composition of pulmonary surfactant subtypes. *Biochim J* 320:499-505 (1996).
189. Putz G, Goerke J, Clements JA. Surface activity of rabbit pulmonary surfactant subfractions at different concentration in captive bubble. *J Appl Physiol* 77:597-605 (1994).
190. Veldhuizen RAW, Hearn SA, Lewis JF, Possmayer F. Surface-area cycling of different surfactant preparation: SP-A and SP-B are essential for large aggregate integrity. *Biochim J* 300:519-524 (1994).

191. Wright JR, Benson BJ, Williams MC, Goerke J, Clements JA. Protein composition of rabbit alveolar surfactant subfractions. *Biochim Biophys Acta* 791:320-332 (1984).
192. Gross NJ. Inhibition of surfactant subtype convertase in radiation model of adult respiratory distress syndrome. *Am J Physiol* 4:L311-L317 (1991).
193. Lewis JF, Ikegami M, Jobe AH. Altered surfactant function and metabolism in rabbits with acute lung injury. *J Appl Physiol* 69:2303-2310 (1990).
194. Notter RH, Penney DP, Finkelstein JN, Shapiro DL. Adsorption of natural lung surfactant and phospholipid extracts related to tubular myelin formation. *Pediatr Res* 20:97-101 (1986).
195. Johansson J, Curstedt T. Molecular structure and interaction of pulmonary surfactant components. *Eur J Biochim* 244:675-693 (1997).
196. Schürch S, Qanbar R, Bachofen H, Possmayer F. The surface associated surfactant reservoir in the alveolar lining. *Biol Neonate* 67(suppl):61-76 (1995).
197. Kuroki Y, Voelker DR. Pulmonary surfactant protein. *J Biol Chem* 269:25943-25946 (1994).
198. Eijk MV, DeHass CGM, Haagsman HP. Quantitative analysis of pulmonary surfactant protein B and C. *Ann Biochim* 232:231-237 (1995).
199. Pilot-Matias TJ. Structure and organization of the gene encoding human pulmonary surfactant proteolipids SP-B. *DNA*:8:75 (1989).
200. Jacobs KA. Isolation of cDNA clone encoding a high molecular weight precursor to a 6-kDa pulmonary surfactant-associated protein. *J Biol Chem* 262:9808 (1987).

201. Rise WR. Surfactant peptide stimulate uptake of phosphatidylcholine by isolated cells. *Biochim Biophys Acta* 1006:237 (1989).
202. Weaver TE. Pulmonary surfactant associated proteins. *Gen Pharmacol* 19:361 (1988).
203. Johansson J. Hydrophobic 3.7 kDa surfactant polypeptide: Structural characterization of the human and the bovine forms. *FEBS Lett* 232:61 (1988).
204. Harwood JL. Lung surfactant. *Prog Lipid Res* 26:211 (1987).
205. Johansson J, Szyperski T, Curstedt T, Wuthrich K. Then MNR structure of the pulmonary surfactant associated polypeptide SP-C in an apolar solvent contains a valyl-rich alpha helix. *Biochemistry* 33:6015-6023 (1994).
206. Curstedt T, Johansson J, Persson P, Eklund A, Robertson B, Lowenadler B, Jornvall H. Hydrophobic surfactant associated polypeptides: SP-C is a lipopeptide with two palmitoylated cysteine residues, whereas SP-B lacks covalently linked fatty acyl groups. *Proc Natl Acad Sci USA* 87:2985-2989 (1990).
207. Bi X, Flach CR, Perez-Gil J, Plasencia I, Andreu D, Oliveria E, Mendelsohn R. Secondary structure and lipid interaction of the N-terminal segment of pulmonary surfactant SP-C. In *Langmuir Films: IR reflection- adsorption spectroscopy and surface pressure studies*. *Biochemistry* 41:8385-8395 (2002).
208. Jobe A. The labeling and biological half-life of phosphatidylcholine in subcellular fraction of rabbit lung. *Biochim Biophys Acta* 489:440-453 (1977).
209. King RJ, Martin H, Mitts D, Holmstrom FM. Metabolism of the apoproteins in pulmonary surfactant. *J Appl Physiol* 42:483-491 (1977).

210. Dietl P, Haller T. Exocytosis of lung surfactant: From the secretory vesicle to the air-liquid interface. *Annu Rev Physiol* 67:595-621 (2005).
211. Sen A, Hui SW, Mosgrober AM, Holm BA, Egan J. Localization of lipid exchange sites between bulk lung surfactants and surface monolayer: freeze fracture study. *Colloid Interface Sci* 126:355-360 (1988).
212. Sanders DL, Hassett RJ, Vatter AE. Isolation of lung lamellar bodies and their conversion into tubular myelin figures in vitro. *Anat Rec* 198:485-501 (1980).
213. Postle AD, Heeley EL, Wilton DC. A comparison of the molecular species composition of mammalian lung surfactant phospholipids. *Comp Biochim Physiol A Mol Integr Physiol* 129:65-73 (2001).
214. Notter RH. *Lung Surfactant: Basic Science and Clinical Applications*. New York: Marcel Dekker, Inc. (2000).
215. Lang CJ, Daniels CB, Orgeig S. New insights into the thermal dynamics of the surfactant system from warm and cold animals. In: Nag K, Ed. *Lung Surfactant: Function and Disorder*. Boca Raton: Taylor and Francis, 17-57 (2005).
216. Andreeva AV, Kutuzov MA, Voyno-Yasenetskaya TA. Regulation of surfactant secretion in alveolar type II cells. *Am J Physiol Lung Cell Mol Physiol* 293:259-271 (2007).
217. Perez-Gil J. Molecular interactions in pulmonary surfactant films. *Biol Neonate* 81:6-15 (2002).
218. Amrein M, Nahmen AV, Sieber M. A scanning force- and fluorescence light microscopy study of the structure and function of a model surfactant system. *Eur Biophys J* 26:349-357 (1997).

219. Leonenko Z, Finot E, Vassiliev V, Amrein M. Effect of cholesterol on the physical properties of pulmonary surfactant films: Atomic force measurements study. *Ultramicroscopy* 106:687-694 (2006).
220. Bowden DH. Alveolar response to injury. *Thorax* 2:357-375 (1981).
221. Hass MA, Longmore WJ. Surfactant cholesterol metabolism of the isolated perfused rat lung. *Biochim Biophys Acta* 573(1):166-174 (1979).
222. Guthmann F, Harrach-Ruprecht B, Looman AC, Stevens PA, Robeneck H, Rustow B. Interaction of lipoproteins with type II pneumocytes in vitro: Morphological studies, uptake kinetics and secretion rate of cholesterol. *Eur J Cell Biol* 74(2):197-207 (1997).
223. Perez-Gil J, Cruz A, Plasencia I. Structure-function relationship of hydrophobic proteins SP-B and SP-C in pulmonary surfactant. In: Nag K, Ed. *Lung Surfactant: Function and Disorder*. Boca Raton, FL: Taylor and Francis, 125-142 (2005).
224. Karagiorga G, Nakos G, Galiatsou E, Lekka ME. Biochemical parameters of bronchoalveolar lavage fluid in fat embolism. *Intensive Care Med* 32:116-123 (2006).
225. Cruz A, Worthman LA, Serrano AG, Casals C, Keough KM, Perez-Gil J. Microstructure and dynamic surface properties of surfactant protein SP-B/dipalmitoylphosphatidylcholine interfacial films spread from lipid-protein bilayers. *Eur Biophys J* 29:204-213 (2000).
226. Serrano AG, Cruz A, Rodriguez-Capote K, Possmayer F, Perez-Gil J. Intrinsic structural and functional determinants within the amino acid sequence of mature pulmonary surfactant protein SP-B. *Biochemistry* 44:417-430 (2005).

227. Oosterlaken-Dijksterhuis MA., Haagsman, HP, van Golde LM, Demel RA. Characterization of lipid insertion into monomolecular layers mediated by lung surfactant proteins SPB and SP-C. *Biochemistry* 30:10965-10971 (1991).
228. Krol S, Ross M, Sieber M, Kunneke S, Galla HJ, Janshoff A. Formation of three-dimensional protein-lipid aggregates in monolayer films induced by surfactant protein B. *Biophys J* 79:904-918 (2000).
229. Zaltash S, Palmblad M, Curstedt T, Johansson, J, Persson B. Pulmonary surfactant protein B: A structural model and a functional analogue. *Biochim Biophys Acta* 1466:179-186 (2000).
230. Serrano AG, Perez-Gil J. Protein-lipid interactions and surface activity in the pulmonary surfactant system. *Chemistry and Physics of Lipids* 141:105-118 (2006).
231. Lipp MM, Lee KY, Zasadzinski JA, Waring AJ. Phase and morphology changes in lipid monolayers induced by SP-B protein and its amino-terminal peptide. *Science* 273:1196-1199 (1996).
232. Rodriguez-Capote K, Manzanares D, Haines T, Possmayer F. Reactive oxygen species inactivation of surfactant involves structural and functional alterations to surfactant proteins SP-B and SP-C. *Biophys J* 90:2808-2821 (2006).
233. Thomas AQ, Lane K, Phillips J, Johnson J, Roberts R, Stahlman M, Loyd JE. Heterozygosity for a surfactant protein C gene mutation associated with usual interstitial pneumonitis and cellular nonspecific interstitial pneumonitis in one kindred. *Am J Respir Crit Care Med* 165:1322: 259-271(2002).

234. Suzuki Y. Effect of protein, cholesterol and phosphatidylglycerol on the surface activity of the lipid-protein complex reconstituted from pig pulmonary surfactant. *J Lipid Res* 23:62-69 (1982).
235. Takahashi A, Fujiwara T. Proteilipid in bovine lung surfactant: Its role in surfactant function. *Biochim Biophys Res Commun* 135:527-532 (1986).
236. Yu SH, Possmayer F. Comparative studies on the biophysical activities of the low-molecular weight hydrophobic proteins purified from bovine lipid extract surfactant. *Biochim Biophys Acta* 961:337-350 (1988).
237. Yu SH, Possmayer F. Role of bovine pulmonary surfactant-associated proteins in the surface-active property of phospholipid mixtures. *Biochim Biophys Acta* 1046:233-241 (1990).
238. Possmayer F, Yu SH. Role of the low molecular weight proteins in pulmonary surfactant. *Prog Respir Res* 25:54-63 (1990).
239. Clements JA. Functions of the alveolar lining. *Am Rev Respir Dis.* 115:67-71 (1977).
240. Bangham AD. The physical properties of an effective lung surfactant. *Biochim Biophys Acta* 573:552-556 (1979).
241. Veldhuizen EJ, Haagsman HP. Role of pulmonary surfactant components in surface film formation and dynamics. *Biochim Biophys Acta* 1467:255-260 (2000).
242. Ilangumaran S, Hoessli DC. Effects of cholesterol depletion by cyclodextrin on the sphingolipid microdomains of the plasma membrane. *Biochim J.* 335:433-440 (1998).

243. Schürch S, Bachofen H, Possmayer F. Surface activity in situ, in vivo, and in the captive bubble surfactometer. *Comp Biochim Physiol A*, 129:195-207 (2001).
244. Schürch S. Formation and structure of surface film: Captive bubble surfactometry. *Biochim Biophys Acta* 1408:180-202(1998).
245. Amrein M, Haufs MG, Knebel D. Structure and function of the molecular film of pulmonary surfactant at the air-water interface: The role of SP-C. In: Nag B, Ed. *Lung Surfactant Function and Disorder*. Boca Raton FL: Taylor and Francis Group (2005).
246. Notter RH, Wang Z. Pulmonary surfactant: Physical chemistry, physiology and replacement. *Rev Chem Engineering* 13:1-118 (1997).
247. Tanaka Y. Development of synthetic lung surfactant. *J Lipid Res* 27:475-485 (1986).
248. Schürch S. Surface activity of lipid extract surfactant in relation to film area, compression and collapse. *J Appl Physiol* 77:974-986 (1994).
249. Schürch S, Robertson B. Assessment of surfactant function: Methods in pulmonary research. In: Uhlig S, Taylor AE, Eds. *Birkhauser Verlag Basel*, Chapter 14: 349-383 (1998).
250. Schürch S. A captive bubble method reproduces the in situ behavior of lung surfactant monolayer. *J Appl Physiol* 67:2389-2396 (1989).
251. Zuo Yi Y, Veldhuizen RAW, Neumann AW, Petersen NO, Possmayer F. Current perspectives in pulmonary surfactant-inhibition, enhancement and evaluation. *Biochim Biophys Acta* (2008) (in press).
252. Goerke J, Gonzales J. Temperature dependence of dipalmitoylphosphatidylcholine monolayer stability. *J Appl Physiol* 51:1108-1114 (1981).

253. Adams FH, Enhorning GA. Surface properties of lung extracts I: A dynamic alveolar model. *Acta Physiol Scand* 68:23-27 (1966).
254. Enhorning GA. Pulsating bubble technique for evaluation of pulmonary surfactant. *J Appl Physiol* 43:198-203 (1977).
255. Putz G, Goerke J, Taeusch HW, Clements JA. Comparison of captive and pulsating bubble surfactometers with use of lung surfactant. *J Appl Physiol* 76:1425-1431 (1994).
256. Hall SB. Approximation in the measurement of surface tension on the oscillating bubble surfactometer. *J Appl Physiol* 75:468- 477 (1993).
257. Schürch S. Surface tension at low lung volumes: dependence on time and alveolar size. *Respir Physiol* 48:339-355 (1982).
258. Ohvo H, Slotte JP. Cyclodextrin-mediated removal of sterol from monolayers: Effects of sterol structure and phospholipids on desorption rate. *Biochemistry*. 35: 8018-8024 (1996).
259. Christian AE, Haynes MP, Phillips MC, Rothblat GH. Use of cyclodextrins for manipulating cellular cholesterol content. *J Lipid Res*. 38:2264-2272 (1997).
260. Schoel WM, Schürch S, Goerke J. The captive bubble method for the evaluation of pulmonary surfactant: Surface tension, area and volume calculations. *Biochim Biophys Acta* 1200:281-290 (1994).
261. Malcolm JD, Elliott CD. Interfacial tension from height and diameter of a single profile drop of captive bubble. *Can J Chem Eng* 58:151-153 (1980).

262. Rotenberg YL, Boruvka L, Neumann AW. Determination of surface tension and contact angle from the shape of the axisymmetric fluid interfaces. *J Colloid Interface Sci* 93:169-183 (1983).
263. Codd JR, Schürch S, Daniels CB, Orgeis S. Torpor-associated fluctuations in surfactant activity in Gould's wattled bat. *Biochim Biophys Acta* 1580:57-66 (2002).
264. Gunasekara L, Schürch S, Schoel WM, Nag K, Leonenko S, Amrein M. Pulmonary surfactant function is abolished by an elevated proportion of cholesterol. *Biochim Biophys Acta* 1737:27-35 (2005).
265. Schürch S, Bachofen H, Goerke J, Green F. Surface properties of rat pulmonary surfactant studied with the captive bubble method: Adsorption, hysteresis, stability. *Biochim Biophys Acta* 1103:127-136 (1992).
266. Pattle RE, Kratzing CC, Parkinson CE, Graves L, Robertson RD, Robards GJ. Maturity of fetal lungs tested by production of stable microbubbles in amniotic fluid. *Br J Obstet Gynaecol* 86:615-622 (1979).
267. Chida S, Fujiwara T. Stable microbubble test for predicting the risk of respiratory distress syndrome: I. Comparisons with other predictors of fetal lung maturity in amniotic fluid. *Eur J Pediatr* 152:148-151 (1993).
268. Berggren P, Eklind J, Linderholm B, Robertson B. Bubbles and computer-aided image analysis for evaluation of surfactant inhibition. *Biol Neonate* 61(Suppl 1):15-20 (1992).
269. Fiori HH, Henn R, Bica IGO, Fiori RM. Evaluation of surfactant function at birth determined by the stable microbubble test in term and near term infants with respiratory distress. *Eur J Pediatr* 163:443-448 (2004).

270. Fiori HH, Linderholm B, Fiori RM, Robertson B. Computerized image analysis of bubbles in gastric aspirate for prediction of respiratory distress syndrome. *Acta Paediatr* 90:1402-1404 (2001).
271. Fiori HH, Varela I, Justo AL, Fiori RM. Stable microbubble test and click test to predict respiratory distress syndrome in preterm infants not requiring ventilation at birth. *J Perinat Med* 31:509-514 (2003).
272. Yokoyama S. Release of cellular cholesterol: Mechanism for cholesterol homeostasis in cells and in the body. *Biochim Biophys Acta* 1529:231-244 (2000).
273. Acton S, Rigotti A, Landschulz KT, Xu S, Hobbs HH, Krieger M. Identification of scavenger receptors SR-BI as a high density lipoprotein receptor. *Science* 271:518-520 (1996).
274. Daniels CB, Barr HA, Power JHT, Nicholas TE. Body temperature alters the lipid composition of pulmonary surfactant in the lizard *Ctenophorus nuchalis*. *Exp Lung Res* 16:435-449 (1990).
275. Daniels CB, Smiths AW, Orgeig S. Pulmonary surfactant lipids in the faveolar and saccular lung regions of snakes. *Physiol Zool* 68:812-830 (1995).
276. Davidson KG, Acton SM, Barr HA, Nicholas TE. Effect of lowering serum cholesterol on the composition of surfactant in adult rat lung. *Am J Physiol* 272(1 Pt 1):106-114 (1997).
277. Hass MA, Longmore WJ. Regulation of lung surfactant cholesterol metabolism by serum lipoproteins. *Lipids* 15:401-406 (1980).

278. Voyno-Yasenetskaya TA, Dobbs TALG, Erickson SK, Hamilton RL. Low density lipoprotein and high density lipoprotein mediated signal transduction and exocytosis in alveolar type II cells. *Proc Natl Sci USA* 90:4256-4260 (1993).
279. King RJ, Clements JA. Lipid synthesis and surfactant turnover in the lungs. In: *Handbook of Physiology: The Respiratory System: Circulation and Nonrespiratory Function*. Bethesda, MD: Amer Physiol Soc, 309-336 (1985).
280. Brown MS, Goldstein JL. A receptor mediated pathway for cholesterol homeostasis. *Science* 323:34-47 (1986).
281. Balasubramanian S, Goldstein JL, Faust JR, Brown MS. Evidence for regulation of 3-hydroxy-3-methylglutaryl coenzyme A reductase activity and cholesterol synthesis in nonhepatic tissues of rat. *Proc Natl Acad Sci USA* 73:2564-2568 (1976).
282. Suzuki Y, Tabata R. Selective reduction of phosphatidylglycerol and phosphatidylcholine in pulmonary surfactant by 4-aminopyrazolo(3,4d)pyrimidine in the rat. *J Lipid Res* 21:1090-1096 (1980).
283. Pettenzzo A, Jobe A, Ikegami M, Abra R, Hogue E, Mihalko P. Clearance of phosphatidylcholine and cholesterol from liposomes, liposomes loaded with metaproterenol, and rabbit surfactant from adult rabbit lungs. *Am Rev Respir Dis* 139:752-758 (1989).
284. Jones ME, Barr HA, Nicholas TE. Turnover of cholesterol and dipalmitoylphosphatidylcholine in surfactant of adult lung. *Lipids* 28:173-179 (1993).

285. Orgeig S. The relationship between cholesterol and phospholipids in vertebrate pulmonary surfactant. Ph D. Department of Human Physiology, Flinders University of South Australia. Bedford Park, 319.
286. Presti FT. The role of cholesterol in regulating membrane fluidity. In: Aloia RC, Boggs J, Eds. Membrane Fluidity in Biology, Vol 4, Cellular Aspects. Orlando: Academic Press, 97-141 (1985).
287. Presti FT, Pace RJ, Chan SI. Cholesterol phospholipid interaction in membrane. 2. Stoichiometry and molecular packing of cholesterol rich domains. *Biochimistry* 21:3831-3835 (1982).
288. Hardley NF. The adaptive role of lipids in biological systems. New York: J. Wiley and Sons (1985).
289. Morrow MR, Davis PJ, Jackman CS, Keough KMW. Thermal history alters cholesterol effect on transition of 1- palmitoyl- 2- linoleoyl- phosphatidylcholine. *J Colloid Interf Sci* 71:3207-3214 (1996).
290. Ladbrook BD, Williams RM, Chapman D. Studies on lecithin- cholesterol- water interactions by differential scanning calorimetry and X-ray diffraction. *Biochim Biophys Acta* 150:333-340 (1968).
291. Notter RH, Holcomb RD, Mavis RD. Dynamic surface properties of phosphatidylglycerol- dipalmitoyl phosphatidylechiline mixed films. *Chem Phys Lipids* 27:305-319 (1980).
292. Yu SH, Possmayer F. Effect of pulmonary surfactant protein A and neutral lipid on accretion and organization of dipalmitoylphosphatidylcholine in surface films. *J Lipid Res* 37:1278-1288 (1996).

293. Yu SH, Possmayer F. Interaction of pulmonary surfactant protein A with dipalmitoylphosphatidylcholine and cholesterol at the air/water interface. *J Lipid Res* 39:555-568 (1998).
294. Taneva SG, Keough KMW. Cholesterol modifies the properties of surface films of dipalmitoylphosphatidylcholine plus pulmonary surfactant-associated protein B or C spread or adsorbed at the air-water interface. *Biochimistry* 36:912-922 (1997).
295. Yu SH, Harding PG, Smith N, Possmayer F. Bovine pulmonary surfactant: Chemical composition and physical properties. *Lipids* 18:522-529 (1983).
296. Palmer D, Cheng S, Green F, Schürch S. The role of cholesterol in surfactant. *Am J Respir Crit Care Med* 155:244 (1997).
297. Diemel RV, Snel MME, van Golde LMG, Putz G, Haagsman HP, Batenburg JJ. Effects of cholesterol on surface activity and surface topography of spread surfactant films. *Biochimistry* 41:15007-15016 (2002).
298. de la Serna JB., Pérez-Gil J, Simonsen AC, Bagatolli LA. Cholesterol rules: Direct observation of the coexistence of two fluid phases in native pulmonary surfactant membranes at physiological temperatures. *J Biol Chem* 279:40715-40722 (2004).
299. Langman C, Orgeig S, Daniels CB. Alteration in composition and function of surfactant associated with torpor in *Sminthopsis crassicaudata*, *Am J Physiol* 271:437-445 (1996).
300. Daniels CB, Barr HA, Power JHT, Nicholas TE. Body temperature alters the lipid composition of pulmonary surfactant in the lizard *Ctenophorus nuchalis*. *Exp Lung Res* 16:435-449 (1990).

301. Orgeig S, Barr HA, Nicholas TE. Effect of hyperpnea on the cholesterol to disaturated phospholipid ratio in alveolar surfactant of rats. *Exp Lung Res* 21:157-174 (1995).
302. Davidson KG, Bersten AD, Barr HA, Dowling KD, Nicholas TE, Doyal IR. Lung function, permeability, and surfactant composition in oleic acid-induced acute lung injury in rats. *Am J Physiol* 729:1091-1102 (2000).
303. Notter R H, Tabak SA, Mavis R.D. Surface properties of binary mixtures of some pulmonary surfactant components. *J Lipid Res* 21:10-22 (1980).
304. Hildebran JN, Goerke J, Clements JA. Pulmonary surface film stability and composition, *J Appl Physiol* 47:604-611 (1979).
305. Pitha J, Irie T, Sklar PB, Nye JS. Drug solubilizers to aid pharmacologists: Amorphous cyclodextrin derivatives. *Life Sci* 43:493-502 (1988).
306. Yu SH, Possmayer F. Effect of pulmonary surfactant protein A (SP-A) and calcium on the adsorption of cholesterol and film stability. *Biochim Biophys Acta*, 1211:350-358 (1994).
307. Yu SH, Possmayer F. Effect of pulmonary surfactant protein A and neutral lipid on accretion and organization of dipalmitoylphosphatidylcholine in surface films. *J Lipid Res* 37:1278-1288 (1996).
308. Yu SH, Possmayer F. Interaction of pulmonary surfactant protein A with dipalmitoylphosphatidylcholine and cholesterol at the air/water interface. *J Lipid Res* 39:555-568 (1998).

309. Bender H. Cyclodextrin gluconotransferase from *Klebsiella pneumoniae*. 1. Formmarion, purification and properties of the enzymes from *Klebsiella pneumoniae* M 5 al (author's transl). *Arch Microbiol.* 111: 271-282 (1977).
310. Marzan Y, Mora R, Butler A, Butler M, Ingenito EP. Effects of simultaneous exposure of surfactants to serum proteins and free radicals. *Exp Lung Res* 28:99-121 (2002).
311. Tausch HW, Keough KMW. Inactivation of pulmonary surfactant and the treatment of acute lung injuries. *Pediatr Pathol Mol Med* 20:519-536 (2001).
312. Lewis JF, Veldhuizen R. The role of exogenous surfactant in the treatment of acute lung injury. *Annu Rev Physiol* 65:613-642 (2003).
313. Lee MM, Green FHY, Schürch S, Cheng S, Bjarnason SG, Leonard S, Wallace W, Possmayer F, Vallyathan V. Comparison of inhibitory effects of oxygen radicals and calf serum protein on surfactant activity. *Mol Cell Biochim* 259:15-22 (2004).
314. Schürch S, Green FHY, Bachofen H. Formation and structure of surface films: Captive bubble surfactometry. *Biochim Biophys Acta* 1408:180-202 (1998).
315. Knebel D, Sieber M, Reichelt R, Galla H-J, Amrein M. Fluorescence light microscopy of pulmonary surfactant at the air-water interface of an air bubble of adjustable size. *Biophys J* 83:547-555 (2002).
316. von Nahmen A, Schenk M, Sieber M, Amrein M. The structure of a model pulmonary surfactant as revealed by scanning force microscopy. *Biophys J* 72:463-469 (1997).
317. Lipp MM., Lee KYC, Takamoto DY, Zasadzinski JA, Waring AJ. Coexistence of buckled and flat monolayers. *Phys Rev Lett* 81:1650-1653 (1998).

318. Discher BM, Maloney KM, Grainger DW, Hall SB. Effect of neutral lipids on coexisting phases in monolayers of pulmonary surfactant. *Biophys Chem* 101-102:333-345 (2002).
319. Worthman LA, Nag K, Davis PJ, Keough KM. Cholesterol in condensed and fluid phosphatidylcholine monolayers studied by epifluorescence microscopy. *Biophys J* 72:2569-2580 (1997).
320. Lopatko OV, Orgeig S, Palmer D, Schürch S, Daniels C.B. Alterations in pulmonary surfactant after rapid arousal from torpor in the marsupial *Sminthopsis crassicaudata*, *J Appl Physiol* 86:1959-1970 (1999).
321. Codd JR, Orgeig S, Daniels CB, Schürch S. Alterations in surface activity of pulmonary surfactant in Gould's wattled bat during rapid arousal from torpor. *Biochim Biophys Res Commun* 308:463-468 (2003).
322. Miller NJ, Postle AD, Schürch S, Schoel WM, Daniels CB, Orgeig S. The development of the pulmonary surfactant system in California sea lions. *Comp Biochim Physiol* 141:191-199 (2005).
323. Lang CJ, Postle AD, Orgeig S, Possmayer F, Bernhard W, Panda AK, Jürgens KD, Milsom WK, Kaushik N, Daniels CB. Dipalmitoylphosphatidylcholine is not the major surfactant phospholipid species in all mammals. *Am J Physiol Regul Integr Comp Physiol* 289:1426-1439 (2005).
324. Loftsson T, Duchene D. Cyclodextrins and their pharmaceutical applications. *Int J Pharm* 1 329:1-11 (2007).
325. Stella VJ, He Q. Cyclodextrins. *Toxicol Pathol* 36(1):30-42 (2008).

326. Szejtli J, Osa T. Cyclodextrins. In: JL Atwood, JED Davies, DD Macnicol, F Vogtle, Eds. *Comprehensive Supramolecular Chemistry*, Vol 3 (2000).
327. Ohtani Y, Irie T, Uekama K, Fukunaga K, Pitha J. Differential effects of alpha-, beta- and gamma-cyclodextrins on human erythrocytes. *Eur J Biochim* 186:17-22 (1989).
328. Garber BG, Herbert PC, Yelle JD, Hodder RV, McGowan J. Adult respiratory distress syndrome: A systemic overview of incidence and risk factors. *Crit Care Med* 24:687-695 (1996).
329. Leaver SK, Evans TW. Acute respiratory distress syndrome. *BMJ* 25:389-394 (2007).
330. Rubenfeld GD, Caldwell E, Peabody E, Weaver J, Martin DP, Neff M, Stern EJ, Hudson LD. Incidence and outcomes of acute lung injury. *N Engl J Med* 20:1685-93 (2005).
331. J Wind, Versteegt J, Twisk J, van der Werf T, Bindels A, Spijkstra J, Girbes A, Groeneveld A. Epidemiology of acute lung injury and acute respiratory distress syndrome in The Netherlands: A survey. *Respir Med*. 101:2091-2098 (2007).
332. Fromming KH, Szejtli J. *Cyclodextrins in pharmacy*. Dordrecht: Kluwer Academic Publishers (1994).
333. Riley CM, Rytting JH, Kral MA, Eds. *Takeru Higuchi: A Memorial tribute. Vol 3: Equilibria and Thermodynamics*. Lawrence: Allen Press (1991).
334. Loftsson T, Brewster ME. *Pharmaceutical applications of cyclodextrins. 1. Drug solubilization and stabilization*. *J Pharm Sci* 85:1017-1025 (1996).

335. Gabelica V, Galic N, De Pauw E. On the specificity of cyclodextrin complexes detected by electrospray mass spectrometry. *J Am Soc Mass Spectrom* 13:946-953 (2002).
336. Loftsson T, Magnusdottir A, Masson M, Sigurjonsdottir JF. Self-association and cyclodextrin solubilization of drugs. *J Drug Deliv Sci* 91:2307-2316 (2002).
337. Leonenko Z, Gill S, Baoukina S, Monticelli L, Doehner J, Gunasekara L, Felderer F, Rodenstein M, Eng LM, Amrein M. An elevated level of cholesterol impairs self-assembly of pulmonary surfactant into a functional film. *Biophys J* 93:674-683 (2007).
338. von Neergard, K. New views on a subject of the mechanics of breathing: The retractive force of the lung in dependence of the surface tension in the alveoli. *Z Ges Exp Med* 66:373-381 (1929).
339. Bachofen H, Schürch S. Alveolar surface forces and lung architecture. *Comp Biochim Physiol* 129:183-193 (2001).
340. Taeusch HW, de la Serna JB, Perez-Gil J, Alonso C, Zasadzinski JA. Inactivation of pulmonary surfactant due to serum-inhibited adsorption and reversal by hydrophilic polymers: Experimental. *Biophys J* 89:1769-1779 (2005).
341. Andersson S, Kheiter A, Merritt TA. Oxidative inactivation of surfactants. *Lung* 177:179-189 (1999).
342. Mark L, Ingenito EP. Surfactant function and composition after free radical exposure generated by transition metals. *Am J Physiol Lung Cell Mol Physiol* 276:491 (1999).

343. Gilliard N, Heldt GP, Loredó J, Gasser H, Redl H, Merritt TA, Spragg RG. Exposure of the hydrophobic components of porcine lung surfactant to oxidant stress alters surface-tension properties. *J Clin Invest* 93:2608-2615 (1994).
344. Chi LF, Jacobi S, Fuchs H. Chemical identification of differing amphiphiles in mixed Langmuir-Blodgett films by scanning surface potential microscopy. *Thin Solid Films* 284-285:403-407 (1996).
345. Jacobi S, Chi LF, Fuchs H. Combined scanning force, lateral force, and scanning surface potential microscopy on phase-separated Langmuir-Blodgett films. *J Vac Sci Technol B* 14:1503-1508 (1996).
346. Lu J, Delamarche E, Eng L, Bennewitz R, Meyer E, Guntherodt HJ. Kelvin probe force microscopy on surfaces: Investigation of the surface potential of self-assembled monolayers on gold. *Langmuir* 15:8184-8188 (1999).
347. Knapp HF, Mesquida P, Stemmer A. Imaging the surface potential of active purple membrane. *Surf Interface Anal* 33:108-112 (2002).
348. Dynarowicz-Latka P, Dhanabalan A, Oliveira ON Jr. Modern physicochemical research on Langmuir monolayers. *Adv Colloid Interf Sci* 91:221-293 (2001).
349. Brockman H. Dipole potential of lipid membranes. *Chem Phys Lipids* 73:57-79 (1994).
350. Yu SH, Possmayer F. Lipid compositional analysis of pulmonary surfactant monolayers and monolayer-associated reservoirs. *J Lipid Res* 44:621-629 (2003).
351. Nonnenmacher M, O'Boyle MP, Wickramasinghe HK. Kelvin probe force microscopy. *Appl Phys Lett* 58:2921-2923 (1991).

352. Zerweck U, Loppacher C, Otto T, Grafstrom S, Eng LM. Accuracy and resolution limits of Kelvin probe force microscopy. *Phys Rev B* 71:125424-125433 (2005).
353. Loppacher C, Zerweck U, Teich S, Beyreuther E, Otto T, Grafstrom S, Eng LM. FM demodulated Kelvin probe force microscopy for surface photovoltage tracking. *Nanotechnology* 16:S1-S6 (2005).
354. Leonenko Z, Rodenstein V, Dohner J, Eng LM, Amrein M. Electrical surface potential of pulmonary surfactant. *Langmuir* 22:10135-10139 (2006).
355. Johansson J, Szyperski T, Wüthrich K. Pulmonary surfactant-associated polypeptide SP-C in lipid micelles: CD studies of intact SP-C and NMR secondary structure determination of dipalmitoyl-SP-C (1-17). *FEBS Lett* 362:261-265 (1995).
356. Kramer A, Wintergalen A, Sieber M, Galla HJ, Amrein M, Guckenberger R. Distribution of the surfactant-associated protein C within a lung surfactant model film investigated by near-field optical microscopy. *Biophys J* 78:458-465 (2000).
357. Sengupta D, Behera RN, Smith JC, Ullmann GM. The alpha helix dipole: Screened out? *Structure* 13:849-855 (2005).
358. Lipp MM, Lee KY, Zasadzinski JA, Waring AJ. Phase and morphology changes in lipid monolayers induced by SP-B protein and its amino-terminal peptide. *Science* 273:1196-1199 (1996).
359. Post A, Nahmen AV, Schmitt M, Ruths J, Riegler H, Sieber M, Galla HJ. Pulmonary surfactant protein C containing lipid films at the air-water interface as a model for the surface of lung alveoli. *Mol Membr Biol* 12:93-99 (1995).

360. von Nahmen A, Post A, Galla HJ, Sieber M. The phase behavior of lipid monolayers containing pulmonary surfactant protein C studied by fluorescence light microscopy. *Eur Biophys J* 26:359-369 (1997).
361. Panda AK, Hune A, Nag K, Harbottle RR, Petersen NO. Structural alterations of phospholipid film domain morphology induced by cholesterol. *Indian J Biochim Biophys* 40:114-121 (2003).
362. Mozaffary H. Cholesterol-phospholipid interaction: A monolayer study. *Thin Solid Films* 244:874-877 (1994).
363. Simons K, Toomre D. Lipid rafts and signal transduction. *Nat Rev Mol Cell Biol* 1:31-39 (2000).
364. Nag K, Perez-Gil J, Ruano ML, Worthman LA, Stewart J, Casals C, Keough KM. Phase transitions in films of lung surfactant at the air-water interface. *Biophys J* 74:2983-2995 (1998).
365. Malcharek S, Hinz A, Hilterhaus L, Galla HJ. Multilayer structures in lipid monolayer films containing surfactant protein C: Effects of cholesterol and POPE. *Biophys J* 88:2638-2649 (2005).
366. Fenster SK, Ugural AC. *Advanced Strength and Applied Elasticity*. Englewood Cliffs, NJ: Prentice Hall (2003).
367. Gopal A, Lee KYC. Morphology and collapse transitions in binary phospholipid monolayers. *J Phys Chem B* 105:10348-10354 (2001).
368. Manzanares, D, Rodriguez-Capote K, Liu S, Haines T, Ramos Y, Zhao L, Doherty-Kirby A, Lajoie G, Possmayer F. Modification of tryptophan and methionine

- residues is implicated in the oxidative inactivation of surfactant protein-B (SP-B). *Biochemistry* 46:5604-5615 (2007).
369. Nag, K, Rodriguez-Capote K, Panda AK, Frederick L, Hearn SA, Petersen NO, Schürch S, Possmayer F. Disparate effects of two phosphatidylcholine binding proteins, C-reactive protein and surfactant protein A, on pulmonary surfactant structure and function. *Am J Physiol Lung Cell Mol Physiol* 287:1145-1153 (2004).
370. Gericke A, Flach CR, Mendelsohn R. Structure and orientation of lung surfactant SP-C and L- α -dipalmitoylphosphatidylcholine in aqueous monolayers. *Biophys J* 73:492-499 (1997).
371. Johansson J. Membrane properties and amyloid fibril formation of lung surfactant protein C. *Biochim Soc Trans* 29:601-606 (2001).
372. Ware LB, Matthay MA. Medical progress: The acute respiratory distress syndrome. *N Engl J Med*. 342:1334-1349 (2000).
373. Ware LB, Matthay MA. Alveolar fluid clearance is impaired in the majority of patients with acute lung injury and the acute respiratory distress syndrome. *Am J Respir Crit Care Med* 163:1376-1383 (2001).
374. Fein A, Grossman RF, Jones JG. The value of edema protein measurement in patients with pulmonary edema. *Am J Med* 67:32-39 (1979).
375. Fagan KA, McMurtry IF, Rodman DM. Role of endothelin-1 in lung disease. *Respir Res* 2:90-101 (2001).
376. Pittet JF, Morel DR, Hemsén A. Elevated plasma endothelin-1 concentrations are associated with the severity of illness in patients with sepsis. *Ann Surg* 213:261-264 (1991).

377. Ware LB, Conner ER, Matthay MA, von Willebrand. Factor antigen is an independent marker of poor outcome in patients with early acute lung injury. *Crit Care Med* 29:2325-2331 (2001).
378. Ware LB, Matthay MA. Clinical practice: Acute pulmonary edema. *N Engl J Med* 353:2788-2796 (2005).
379. Hurley JV. Types of pulmonary microvascular injury. *Ann NY Acad Sci* 384:269-286 (1982).
380. Ware LB. Pathophysiology of acute lung injury and the acute respiratory distress syndrome. *Semin Respir Crit Care Med* 27:337-349 (2006).
381. Bachofen M, Weibel ER. Structural alterations of lung parenchyma in the adult respiratory distress syndrome. *Clin Chest Med* 3:35-56 (1982).
382. Prescott SM, McIntyre TM, Zimmerman G. Two of the usual suspects, platelet-activating factor and its receptor, implicated in acute lung injury. *J Clin Invest* 104:1019-1020 (1999).
383. Bachofen M, Weibel ER. Alteration of the gas exchange apparatus in adult respiratory insufficiency associated with septicemia. *Am Rev Respir Dis* 116:589-615 (1977).
384. Lafe MD, Simon RH, Flint A. Adult respiratory distress syndrome in neutropenic patients. *Am J Med* 80:1022-1026.
385. Moraes TJ, Zurawska JH, Downey GP. Neutrophil granule contents in the pathogenesis of lung injury. *Curr Opin Hematol* 13:21-27 (2006).

- 386.** Pitter JF, MacKersie RC, Martin TR. Biological markers of acute lung injury: Prognostic and pathogenetic significance. *Am J Respir Crit Care Med.* 155:1187-1205 (1997).
- 387.** Goodman R, Pugin J, Lees JS. Cytokine mediated inflammation in acute lung injury: Cytokine growth factor. *Rev* 14:523-535 (2003).
- 388.** Nathan CF. Secretory products of macrophages. *J Clin Invest* 79:319-326 (1987).
- 389.** Gunther A, Siebert C, Schmidt R, Ziegler S, Grimminger F. Surfactant alterations in severe pneumonia, acute respiratory distress syndrome, and cardiogenic lung edema. *Am J Respir Crit Care Med* 153:176-184 (1996).
- 390.** Pison U, Gono E, Jika T, Obertacke U. Phospholipid lung profile in adult respiratory distress syndrome-evidence for surfactant abnormality. *Prog Clin Biol Res* 236A:517-523 (1987).
- 391.** Vara E, Arias-Diaz J, Garcia C, Hernandez J, Balibrea JL. TNF-Alpha-induced inhibition of PC synthesis by human type 2 pneumocytes is sequentially mediated by PEG2 and NO. *Am J Physiol* 271:359-365 (1996).
- 392.** Franson R, Weiss J, Martin L, Spitznagel JK, Elsbach P. Phospholipase A activity associated with membranes of human polymorphonuclear leucocytes. *Biochim J* 167:839-841(1977).
- 393.** Seeds MC, Bowton DL, Hite RD, Gyves JI, Bass DA. Human eosinophil group IID secretory phospholipase A2 causes surfactant dysfunction. *Chest* 123:376S-377S (2003).

394. Bowton DL, Seeds MC, Fasano MB, Goldsmith B, Bass DA. Phospholipase A2 and arachidonate increase in bronchoalveolar lavage fluid after inhaled antigen challenge in asthmatics. *Am J Respir Crit Care Med* 155:421-425 (1997).
395. Chilton FH, Averill FJ, Hubbard WC, Fonteh AN, Triggiani M, Liu MC. Antigen-induced generation of lyso-phospholipids in human airways. *J Exp Med* 183:2235-2245 (1996).
396. Hite RD, Bowton DL, Seeds MC, Safta AM, Waite BM, Bass DA. Phospholipase A2-mediated phosphatidylglycerol deficiency predicts surfactant dysfunction in asthma. *Am J Respir Crit Care Med* 163:733 (2001).
397. Kim DK, Fukuda T, Thompson BT, Cockrill B, Hales C, Bonventre JV. Bronchoalveolar lavage fluid phospholipase A2 activities are increased in human adult respiratory distress syndrome. *Am J Physiol* 269:109-118 (1995).
398. Hallman M, Spragg R, Harrell JH, Moser KM, Gluck L. Evidence of lung surfactant abnormality in respiratory failure. Study of bronchoalveolar lavage phospholipids, surface activity, phospholipase activity, and plasma myoinositol. *J Clin Invest* 70:673-683 (1982).
399. Waite BM. *The Phospholipases: Handbook of Lipid Research*. New York: Plenum Publishing Corp. (1987).
400. Holm BA, Keicher L, Liu MY, Sokolowski J, Enhorning G. Inhibition of pulmonary surfactant function by phospholipases. *J Appl Physiol* 71:317-321 (1991).
401. Hite R, Seeds MC, Safta AM, Jacinto RB, Gyves JI, Bass DA, Waite BM. Lysophospholipid generation and phosphatidylglycerol depletion in phospholipase

- A2-mediated surfactant dysfunction. *Am J Physiol. Lung Cell Mol Physiol* 288:618-624 (2005).
- 402.** Cifuentes J. Interaction of surfactant mixtures with reactive oxygen and nitrogen species. *J Appl Physiol* 78:1800-1805 (1995).
- 403.** Zhu S. Carbon dioxide enhances nitration of surfactant protein A by activated alveolar macrophages. *Am J Physiol Lung Cell Mol Physiol* 278:1025-1031.
- 404.** Sittipunt C, Steinberg KP, Ruzinski JT, Myles C, Zhu S, Goodman RB, Hudson LD, Matalon S, Martin TR. Nitric oxide and nitrotyrosine in the lungs of patients with acute respiratory distress syndrome. *Am J Respir Crit Care Med* 163:503-510 (2001).
- 405.** Veldhuizen RA, Inchley K, Hearn SA, Lewis JF, Possmayer F. Degradation of surfactant-associated protein B (SP-B) during in vitro conversion of large to small surfactant aggregates. *Biochim J* 295:141-147 (1993).
- 406.** Gunther A. Surfactant alteration and replacement in acute respiratory distress syndrome. *Respir Res* 2:353-364 (2001).
- 407.** Holm BA. Surfactant inactivation in adult respiratory distress syndrome. In Robertson B et al, Eds. *Pulmonary Surfactant: From Molecular Biology to Clinical Practice*. Amsterdam: Elsevier, 665-684 (1992).
- 408.** Veldhuizen RAW, Slutsky AS, Joseph M, McCaig L. Effects of mechanical ventilation of isolated mouse lungs on pulmonary surfactant and inflammatory cytokines. *Eur Respir J* 17:488-494 (2001).

409. Veldhuizen RA, Welk B, Harbottle R, Hearn S, Nag K, Petersen N, Possmayer F. Mechanical ventilation of isolated rat lungs changes the structure and biophysical properties of surfactant. *A Appl Physiol* 92:1169-1175 (2002).
410. Veldhuizen RAW, Ito Y, Marcou J, Yao LJ, McCaig L, Lewis JF. Effects of lung injury on pulmonary surfactant aggregate conversion in vivo and in vitro. *Am J Physiol* 16:872-878 (1997).
411. Veldhuizen RA, Yao LJ, Lewis JF. An examination of the different variables affecting surfactant aggregate conversion in vitro. *Exp Lung Res* 25:127-141 (1999).
412. Veldhuizen RAW, Marcou J, Yao LJ, McCaig L, Ito Y, Lewis JF. Alveolar surfactant aggregate conversion in ventilated normal and injured rabbits. *Am J Physiol* 270:152-158 (1996).
413. Dreyfuss D, Saumon G. Ventilator-induced lung injury: Lessons from experimental studies. *Am J Respir Crit Care Med* 157:294-323 (1998).
414. Matalon S, Holm BA, Loewen GM, Baker RR, Notter RH. Sublethal hyperoxic injury to the alveolar epithelium and the pulmonary surfactant system. *Exp Lung Res* 14(suppl):1021-1033 (1988).
415. Holm BA, Enhorning G, Notter RH. A biophysical mechanism by which plasma proteins inhibit lung surfactant activity. *Chem Phys Lipids* 49:49-55 (1988).
416. Holm BA, Wang Z, Notter RH. Multiple mechanisms of lung surfactant inhibition. *Pediatr Res* 46:85-93 (1999).
417. Markart P, Ruppert C, Wygrecka M, Colaris T, Dahal B, Walmrath D, Harbach H, Wilhelm J, Seeger W, Schmidt R, Guenther A. Patients with ARDS show

- improvement but not normalisation of alveolar surface activity with surfactant treatment: Putative role of neutral lipids. *Thorax* 62:588-594 (2007).
- 418.** Lu JJ, Yu LMY, Cheung WWY, Goldthorpe IA, Zuo YY, Policova Z, Cox PN, Neumann AW. Poly(ethylene glycol) (PEG) enhances dynamic surface activity of a bovine lipid extract surfactant (BLES). *Colloids Surf B-Biointerfaces* 41:145-151 (2005).
- 419.** Lu KW, Goerke J, Clements JA, Taeusch HW. Hyaluronan reduces surfactant inhibition and improves rat lung function after meconium injury. *Pediatr Res* 58:206-210 (2005).
- 420.** Zuo YY, Alolabi H, Shafiei A, Kang NX, Policova Z, Cox PN, Acosta E, Hair ML, Neumann AW. Chitosan enhances the in vitro surface activity of dilute lung surfactant preparations and resists albumin-induced inactivation. *Pediatr Res* 60:125-130 (2006).
- 421.** Lu JJ, Yu LMY, Cheung WWY, Policova Z, Li D, Hair ML, Neumann AW. The effect of concentration on the bulk adsorption of bovine, lipid extract surfactant. *Colloids Surf B-Biointerfaces* 29:119-130 (2003).
- 422.** Lu JJ, Cheung WWY, Yu LMY, Policova Z, Li D, Hair ML, Neumann AW. The effect of dextran to restore the activity of pulmonary surfactant inhibited by albumin. *Respir Physiol Neuro* 130:169-179 (2002).
- 423.** Lu KW, Taeusch HW, Robertson B, Goerke J, Clements JA. Polyethylene glycol/surfactant mixtures improve lung function after HCl and endotoxin lung injuries. *Am J Respir Crit Care Med* 164:1531-1536 (2001).

424. Israelachvili JN. *Intermolecular and Surface Forces*. London: Academic Press (1997).
425. Zasadzinski JA, Alig TF, Alonso C, de la Serna JB, Perez-Gil J, Taesch HW. Inhibition of pulmonary surfactant adsorption by serum and the mechanisms of reversal by hydrophilic polymers: Theory. *Biophys J* 89:1621-1629 (2005).
426. Israelachvili J. *Intermolecular & Surface Forces (Second Edition)*, London: Academic Press (1991).
427. Lu K, Goerke J, Clements JA, Taesch HW. Hyaluronan decreases surfactant inactivation in vitro. *Pediatr Res* 57:237-241 (2005).
428. Bray BA. The role of hyaluronan in the pulmonary alveolus. *J Theor Biol* 210:121-130 (2001).
429. Weibel ER, Gil J. Electron microscopic demonstration of an extracellular duplex lining layer of alveoli. *Respir Physiol* 4:42-57 (1968).
430. Williams MC. Freeze-fracture studies of tubular myelin and lamellar bodies in fetal and adult rat lungs. *J Ultrastruct Res* 64:352-361 (1978).
431. Manabe T. Freeze-fracture study of alveolar lining layer in adult rat lungs. *J Ultrastruct Res* 69:86-97 (1979).
432. Bachofen H, Gerber U, Gehr P, Amrein M, Schürch S. Structures of pulmonary surfactant films adsorbed to an air-liquid interface in vitro. *Biochim Biophys Acta* 1720:59-72 (2005).
433. Ochs M, Johnen G, Muller KM, Wahlers T, Hawgood S, Richter J, Brasch F. Intracellular and intraalveolar localization of surfactant protein A (SP-A) in the parenchymal region of the human lung. *Am J Respir Cell Mol Biol* 26:91-98 (2002).

434. Ishizaka A, Matsuda T, Albertine KH, Koh H, Tasaka S, Hasegawa N, Kohno N, Kotani T, Morisaki H, Takeda J, Nakamura M, Fang X, Martin TR, Matthay MA, Hashimoto S. Elevation of KL-6, a lung epithelial cell marker, in plasma and epithelial lining fluid in acute respiratory distress syndrome. *Am J Physiol Lung Cell Mol Physiol* 286:1088-1094 (2004).
435. Warriner HE, Ding J, Waring AJ, Zasadzinski JA. A concentration-dependent mechanism by which serum albumin inactivates replacement lung surfactants. *Biophys J* 82:835-842 (2002).
436. Nag K, Keough KM, Morrow MR. Probing perturbation of bovine lung surfactant extracts by albumin using DSC and 2H-NMR. *Biophys J* 90:3632-3642 (2006).
437. Ochs M, Fehrenbach H, Richter J. Occurrence of lipid bodies in canine type II pneumocytes during hypothermic lung ischemia. *Anat Rec Part A* 277A:287-297 (2004).
438. Murphy DJ. The biogenesis and functions of lipid bodies in animals, plants and microorganisms. *Prog Lipid Res* 40:325-438 (2001).
439. White NM, Jiang D, Burgess JD, Bederman IR, Pervis SF, Kelley TJ. Altered cholesterol homeostasis in cultured and in vivo models of cystic fibrosis. *Am J Physiol Lung Cell Mol Physiol* 292:476-486 (2007).
440. Grise M. Pulmonary surfactant in health and human lung diseases: state of the art. *Eur Respir J*. 13: 1455- 1476 (1999).

Apendix

ELSEVIER LICENSE TERMS AND CONDITIONS

Jul 29, 2008

This is a License Agreement between Lasantha C Gunasekara ("You") and Elsevier ("Elsevier"). The license consists of your order details, the terms and conditions provided by Elsevier, and the payment terms and conditions.

Supplier	Elsevier Limited The Boulevard, Langford Lane Kidlington, Oxford, OX5 1GB, UK
Registered Company Number	1982084
Customer name	Lasantha C Gunasekara
Customer address	104 Hidden vale place NW calgary, AB T3A 5C5
License Number	1931461415681
License date	Apr 17, 2008
Licensed content publisher	Elsevier Limited
Licensed content publication	Biochimica et Biophysica Acta (BBA) - Molecular and Cell Biology of Lipids
Licensed content title	Pulmonary surfactant function is abolished by an elevated proportion of cholesterol
Licensed content author	Gunasekara Lasantha, Schürch Samuel, Schoel W. Michael, Nag Kaushik, Leonenko Zoya, Haufs Michael and Amrein Matthias
Licensed content date	15 October 2005
Volume number	1737
Issue number	1

Pages	9
Type of Use	Thesis / Dissertation
Portion	Full article
Format	Both print and electronic
You are an author of the Elsevier article	Yes
Are you translating?	No
Purchase order number	
Expected publication date	Jul 2008
Elsevier VAT number	GB 494 6272 12
Permissions price	0.00 USD
Value added tax 0.0%	0.00 USD
Total	0.00 USD
Terms and Conditions	

INTRODUCTION

The publisher for this copyrighted material is Elsevier. By clicking "accept" in connection with completing this licensing transaction, you agree that the following terms and conditions apply to this transaction (along with the Billing and Payment terms and conditions established by Copyright Clearance Center, Inc. ("CCC"), at the time that you opened your Rightslink account and that are available at any time at <http://myaccount.copyright.com>).

GENERAL TERMS

Elsevier hereby grants you permission to reproduce the aforementioned material subject to the terms and conditions indicated.

Acknowledgement: If any part of the material to be used (for example, figures) has appeared in our publication with credit or acknowledgement to another source, permission must also be sought from that source. If such permission is not obtained then that material may not be included in your publication/copies. Suitable acknowledgement to the source must be made, either as a footnote or in a reference list at the end of your publication, as follows:

"Reprinted from Publication title, Vol number, Author(s), Title of article, Pages No., Copyright (Year), with permission from Elsevier [OR APPLICABLE SOCIETY

COPYRIGHT OWNER]." Also Lancet special credit - "Reprinted from The Lancet, Vol. number, Author(s), Title of article, Pages No., Copyright (Year), with permission from Elsevier."

Reproduction of this material is confined to the purpose and/or media for which permission is hereby given.

Altering/Modifying Material: Not Permitted. However figures and illustrations may be altered/adapted minimally to serve your work. Any other abbreviations, additions, deletions and/or any other alterations shall be made only with prior written authorization of Elsevier Ltd. (Please contact Elsevier at permissions@elsevier.com)

If the permission fee for the requested use of our material is waived in this instance, please be advised that your future requests for Elsevier materials may attract a fee.

Reservation of Rights: Publisher reserves all rights not specifically granted in the combination of (i) the license details provided by you and accepted in the course of this licensing transaction, (ii) these terms and conditions and (iii) CCC's Billing and Payment terms and conditions.

License Contingent Upon Payment: While you may exercise the rights licensed immediately upon issuance of the license at the end of the licensing process for the transaction, provided that you have disclosed complete and accurate details of your proposed use, no license is finally effective unless and until full payment is received from you (either by publisher or by CCC) as provided in CCC's Billing and Payment terms and conditions. If full payment is not received on a timely basis, then any license preliminarily granted shall be deemed automatically revoked and shall be void as if never granted. Further, in the event that you breach any of these terms and conditions or any of CCC's Billing and Payment terms and conditions, the license is automatically revoked and shall be void as if never granted. Use of materials as described in a revoked license, as well as any use of the materials beyond the scope of an unrevoked license, may constitute copyright infringement and publisher reserves the right to take any and all action to protect its copyright in the materials.

Warranties: Publisher makes no representations or warranties with respect to the licensed material.

Indemnity: You hereby indemnify and agree to hold harmless publisher and CCC, and their respective officers, directors, employees and agents, from and against any and all claims arising out of your use of the licensed material other than as specifically authorized pursuant to this license.

No Transfer of License: This license is personal to you and may not be sublicensed, assigned, or transferred by you to any other person without publisher's written permission.

No Amendment Except in Writing: This license may not be amended except in a writing signed by both parties (or, in the case of publisher, by CCC on publisher's behalf).

Objection to Contrary Terms: Publisher hereby objects to any terms contained in any purchase order, acknowledgment, check endorsement or other writing prepared by you, which terms are inconsistent with these terms and conditions or CCC's Billing and Payment terms and conditions. These terms and conditions, together with CCC's Billing and Payment terms and conditions (which are incorporated herein), comprise the entire agreement between you and publisher (and CCC) concerning this licensing transaction. In the event of any conflict between your obligations established by these terms and conditions and those established by CCC's Billing and Payment terms and conditions, these terms and conditions shall control.

Revocation: Elsevier or Copyright Clearance Center may deny the permissions described in this License at their sole discretion, for any reason or no reason, with a full refund payable to you. Notice of such denial will be made using the contact information provided by you. Failure to receive such notice will not alter or invalidate the denial. In no event will Elsevier or Copyright Clearance Center be responsible or liable for any costs, expenses or damage incurred by you as a result of a denial of your permission request, other than a refund of the amount(s) paid by you to Elsevier and/or Copyright Clearance Center for denied permissions.

LIMITED LICENSE

The following terms and conditions apply to specific license types:

Translation: This permission is granted for non-exclusive world **English** rights only unless your license was granted for translation rights. If you licensed translation rights you may only translate this content into the languages you requested. A professional translator must perform all translations and reproduce the content word for word preserving the integrity of the article. If this license is to re-use 1 or 2 figures then permission is granted for non-exclusive world rights in all languages.

Website: The following terms and conditions apply to electronic reserve and author websites:

Electronic reserve: If licensed material is to be posted to website, the web site is to be password-protected and made available only to bona fide students registered on a relevant course if:

This license was made in connection with a course,

This permission is granted for 1 year only. You may obtain a license for future website posting,

All content posted to the web site must maintain the copyright information line on the bottom of each image,

A hyper-text must be included to the Homepage of the journal from which you are licensing at <http://www.sciencedirect.com/science/journal/xxxxx> , and

Central Storage: This license does not include permission for a scanned version of the material to be stored in a central repository such as that provided by Heron/XanEdu.

Author website with the following additional clauses: This permission is granted for 1 year only. You may obtain a license for future website posting,

All content posted to the web site must maintain the copyright information line on the bottom of each image, and

The permission granted is limited to the personal version of your paper. You are not allowed to download and post the published electronic version of your article (whether PDF or HTML, proof or final version), nor may you scan the printed edition to create an electronic version,

A hyper-text must be included to the Homepage of the journal from which you are licensing at <http://www.sciencedirect.com/science/journal/xxxxx> , and

Central Storage: This license does not include permission for a scanned version of the material to be stored in a central repository such as that provided by Heron/XanEdu.

Website (regular and for author): "A hyper-text must be included to the Homepage of the journal from which you are licensing at <http://www.sciencedirect.com/science/journal/xxxxx>."

Thesis/Dissertation: If your license is for use in a thesis/dissertation your thesis may be submitted to your institution in either print or electronic form. Should your thesis be published commercially, please reapply for permission. These requirements include permission for the Library and Archives of Canada to supply single copies, on demand, of the complete thesis and include permission for UMI to supply single copies, on demand, of the complete thesis. Should your thesis be published commercially, please reapply for permission.

Other Terms and Conditions: None

**ELSEVIER LICENSE
TERMS AND CONDITIONS**

Jul 29, 2008

This is a License Agreement between Lasantha C Gunasekara ("You") and Elsevier ("Elsevier"). The license consists of your order details, the terms and conditions provided by Elsevier, and the payment terms and conditions.

Supplier	Elsevier Limited The Boulevard, Langford Lane Kidlington, Oxford, OX5 1GB, UK
Registered Company Number	1982084
Customer name	Lasantha C Gunasekara
Customer address	104 Hidden vale place NW calgary, AB T3A 5C5
License Number	1931461229009
License date	Apr 17, 2008
Licensed content publisher	Elsevier Limited
Licensed content publication	Biochimica et Biophysica Acta (BBA) - Biomembranes
Licensed content title	A comparative study of mechanisms of surfactant inhibition
Licensed content author	Gunasekara Lasantha, Schoel W. Michael, Schürch Samuel and Amrein Matthias W.
Licensed content date	February 2008
Volume number	1778
Issue number	2
Pages	12
Type of Use	Thesis / Dissertation
Portion	Full article
Format	Electronic

You are an author of the Elsevier article	Yes
Are you translating?	No
Purchase order number	
Expected publication date	Jul 2008
Elsevier VAT number	GB 494 6272 12
Permissions price	0.00 USD
Value added tax 0.0%	0.00 USD
Total	0.00 USD
Terms and Conditions	

INTRODUCTION

The publisher for this copyrighted material is Elsevier. By clicking "accept" in connection with completing this licensing transaction, you agree that the following terms and conditions apply to this transaction (along with the Billing and Payment terms and conditions established by Copyright Clearance Center, Inc. ("CCC"), at the time that you opened your Rightslink account and that are available at any time at <http://myaccount.copyright.com>).

GENERAL TERMS

Elsevier hereby grants you permission to reproduce the aforementioned material subject to the terms and conditions indicated.

Acknowledgement: If any part of the material to be used (for example, figures) has appeared in our publication with credit or acknowledgement to another source, permission must also be sought from that source. If such permission is not obtained then that material may not be included in your publication/copies. Suitable acknowledgement to the source must be made, either as a footnote or in a reference list at the end of your publication, as follows:

"Reprinted from Publication title, Vol number, Author(s), Title of article, Pages No., Copyright (Year), with permission from Elsevier [OR APPLICABLE SOCIETY COPYRIGHT OWNER]." Also Lancet special credit - "Reprinted from The Lancet, Vol. number, Author(s), Title of article, Pages No., Copyright (Year), with permission from Elsevier."

Reproduction of this material is confined to the purpose and/or media for which permission

is hereby given.

Altering/Modifying Material: Not Permitted. However figures and illustrations may be altered/adapted minimally to serve your work. Any other abbreviations, additions, deletions and/or any other alterations shall be made only with prior written authorization of Elsevier Ltd. (Please contact Elsevier at permissions@elsevier.com)

If the permission fee for the requested use of our material is waived in this instance, please be advised that your future requests for Elsevier materials may attract a fee.

Reservation of Rights: Publisher reserves all rights not specifically granted in the combination of (i) the license details provided by you and accepted in the course of this licensing transaction, (ii) these terms and conditions and (iii) CCC's Billing and Payment terms and conditions.

License Contingent Upon Payment: While you may exercise the rights licensed immediately upon issuance of the license at the end of the licensing process for the transaction, provided that you have disclosed complete and accurate details of your proposed use, no license is finally effective unless and until full payment is received from you (either by publisher or by CCC) as provided in CCC's Billing and Payment terms and conditions. If full payment is not received on a timely basis, then any license preliminarily granted shall be deemed automatically revoked and shall be void as if never granted. Further, in the event that you breach any of these terms and conditions or any of CCC's Billing and Payment terms and conditions, the license is automatically revoked and shall be void as if never granted. Use of materials as described in a revoked license, as well as any use of the materials beyond the scope of an unrevoked license, may constitute copyright infringement and publisher reserves the right to take any and all action to protect its copyright in the materials.

Warranties: Publisher makes no representations or warranties with respect to the licensed material.

Indemnity: You hereby indemnify and agree to hold harmless publisher and CCC, and their respective officers, directors, employees and agents, from and against any and all claims arising out of your use of the licensed material other than as specifically authorized pursuant to this license.

No Transfer of License: This license is personal to you and may not be sublicensed, assigned, or transferred by you to any other person without publisher's written permission.

No Amendment Except in Writing: This license may not be amended except in a writing signed by both parties (or, in the case of publisher, by CCC on publisher's behalf).

Objection to Contrary Terms: Publisher hereby objects to any terms contained in any purchase order, acknowledgment, check endorsement or other writing prepared by you,

which terms are inconsistent with these terms and conditions or CCC's Billing and Payment terms and conditions. These terms and conditions, together with CCC's Billing and Payment terms and conditions (which are incorporated herein), comprise the entire agreement between you and publisher (and CCC) concerning this licensing transaction. In the event of any conflict between your obligations established by these terms and conditions and those established by CCC's Billing and Payment terms and conditions, these terms and conditions shall control.

Revocation: Elsevier or Copyright Clearance Center may deny the permissions described in this License at their sole discretion, for any reason or no reason, with a full refund payable to you. Notice of such denial will be made using the contact information provided by you. Failure to receive such notice will not alter or invalidate the denial. In no event will Elsevier or Copyright Clearance Center be responsible or liable for any costs, expenses or damage incurred by you as a result of a denial of your permission request, other than a refund of the amount(s) paid by you to Elsevier and/or Copyright Clearance Center for denied permissions.

LIMITED LICENSE

The following terms and conditions apply to specific license types:

Translation: This permission is granted for non-exclusive world **English** rights only unless your license was granted for translation rights. If you licensed translation rights you may only translate this content into the languages you requested. A professional translator must perform all translations and reproduce the content word for word preserving the integrity of the article. If this license is to re-use 1 or 2 figures then permission is granted for non-exclusive world rights in all languages.

Website: The following terms and conditions apply to electronic reserve and author websites:

Electronic reserve: If licensed material is to be posted to website, the web site is to be password-protected and made available only to bona fide students registered on a relevant course if:

This license was made in connection with a course,

This permission is granted for 1 year only. You may obtain a license for future website posting,

All content posted to the web site must maintain the copyright information line on the bottom of each image,

A hyper-text must be included to the Homepage of the journal from which you are licensing at <http://www.sciencedirect.com/science/journal/xxxxx> , and

Central Storage: This license does not include permission for a scanned version of the material to be stored in a central repository such as that provided by Heron/XanEdu.

Author website with the following additional clauses: This permission is granted for 1 year only. You may obtain a license for future website posting,

All content posted to the web site must maintain the copyright information line on the bottom of each image, and

The permission granted is limited to the personal version of your paper. You are not allowed to download and post the published electronic version of your article (whether PDF or HTML, proof or final version), nor may you scan the printed edition to create an electronic version,

A hyper-text must be included to the Homepage of the journal from which you are licensing at <http://www.sciencedirect.com/science/journal/xxxxx> , and

Central Storage: This license does not include permission for a scanned version of the material to be stored in a central repository such as that provided by Heron/XanEdu.

Website (regular and for author): "A hyper-text must be included to the Homepage of the journal from which you are licensing at <http://www.sciencedirect.com/science/journal/xxxxx>."

Thesis/Dissertation: If your license is for use in a thesis/dissertation your thesis may be submitted to your institution in either print or electronic form. Should your thesis be published commercially, please reapply for permission. These requirements include permission for the Library and Archives of Canada to supply single copies, on demand, of the complete thesis and include permission for UMI to supply single copies, on demand, of the complete thesis. Should your thesis be published commercially, please reapply for permission.

Other Terms and Conditions: None

Biophysical Society



Biophysical Journal
Copyright Permission Form

In order to obtain copyright permission, please answer the questions below. When you have completed the form you may fax it to (301) 634-7267 or email it as an attachment to bj@biophysics.org. Once your request is processed, it will be sent back to you for your records.

Name: Lasantha Gunasekara

Address: 104, Hidden Vale Place NW
Calgary, Alberta T3A 5C5
Canada

Phone: 403 730-4920

Fax: _____

Email: lgunase@ucalgary.ca

I am requesting permission to reprint Figure(s) 2,3,4,5,6,7 by Leonenko Z, Gil S, Babukin S.
(figure numbers) (author names)

EngLM
Rodenstein M

Federer F, Gunasekara L, Amrein M. from the article An Elevated Level of cholesterol
Doehner J, Monticelli L impairs self-assembly of pulmonary surfactant into a functional film
(title)
in Biophys. J. 2007 93 July 674-683. I understand that I am obligated to
(year) (vol.) (issue) (page numbers)

notify the original author(s) and will provide appropriate attribution to the Biophysical Society and said author(s) for use of these materials.

OFFICE USE ONLY

Permission granted _____ Date 4/21/08